

Waste Isolation Pilot Plant
Compliance Certification Application
Reference 158

Davies, P.B., 1989.

Variable-Density Ground-Water Flow and Paleohydrology in the Waste Isolation Pilot Plant (WIPP) Region, Southeastern New Mexico, U. S. Geological Survey Open-File Report 88-490, Albuquerque, NM, U. S. Geological Survey.

Waste Reduction Pilot Program

Compliance Certification Application

Reference 158

Dear Sir/Madam:

I am writing to you regarding the Waste Reduction Pilot Program. I have reviewed the terms and conditions of the program and I am pleased to inform you that I am in full compliance with all the requirements. I have implemented the necessary measures to reduce waste and I am confident that I will continue to do so in the future.

I am sure that your organization will find this information helpful and I am happy to provide any further details you may require.

Yours faithfully,

VARIABLE-DENSITY GROUND-WATER FLOW AND PALEOHYDROLOGY
IN THE WASTE ISOLATION PILOT PLANT (WIPP) REGION,
SOUTHEASTERN NEW MEXICO

By Peter B. Davies

U.S. GEOLOGICAL SURVEY
Open-File Report 88-490

Prepared in cooperation with the
U.S. DEPARTMENT OF ENERGY



Albuquerque, New Mexico
1989

DEPARTMENT OF THE INTERIOR
MANUEL LUJAN, JR., Secretary
U.S. GEOLOGICAL SURVEY
Dallas L. Peck, Director

For additional information
write to:

District Chief
U.S. Geological Survey
4501 Indian School Road NE, Suite 200
Albuquerque, New Mexico 87110

Copies of this report can
be obtained from:

U.S. Geological Survey
Books and Open-File Reports
Federal Center, Bldg. 810
Box 25425
Denver, Colorado 80225

CONTENTS

	Page
Abstract	1
Introduction	3
Purpose and scope	6
Previous ground-water models	7
Hydrogeology of the Salado Formation and overlying rock units	11
Stratigraphy and hydraulic characteristics	11
Salado Formation	11
Rustler Formation	13
Dewey Lake Red Beds	16
Undifferentiated Triassic rocks	16
Halite dissolution and related secondary processes	16
Evidence for halite dissolution	16
Description of dissolution process	17
Age of dissolution activity	20
Hydrologic implications	23
Analysis of fluid-density effects on ground-water flow	24
Driving-force theory	25
Driving-force analysis of the model area of Barr and others (1983)	30
Comparison of freshwater-head and variable-density flow simulations	35
Summary and conclusions	38
Analysis of the regional-scale flow system in the Culebra Dolomite Member of the Rustler Formation	39
Regional driving-force analysis	40
Regional structure of the Culebra Dolomite Member of the Rustler Formation	41
Regional fluid-density distribution	41
Regional equivalent-freshwater-head distribution	43
Evaluation of potential errors in the estimation of equivalent-freshwater head	49
Results of the regional driving-force analysis	50

CONTENTS - Concluded

	Page
Regional variable-density ground-water flow model	53
Model implementation	53
Boundary conditions	53
Hydraulic-conductivity distribution	56
Other model input	64
Baseline approximate steady-state simulation	67
Sensitivity analyses and alternative system conceptualizations	72
Density effects	72
Steady-state variable-density assumptions	75
Long-term brine transport patterns	77
Sensitivity to dispersivity	82
Northern and eastern boundaries	82
Pecos River boundary	90
Vertical flux	95
Summary and conclusions	97
Analysis of long-term system response to paleohydrologic conditions	103
Geohydrology and paleohydrology of the model section	103
Transient cross-sectional flow model	107
Model implementation	107
Hydraulic-conductivity distribution	110
Storage parameters	110
Boundary and initial conditions	112
Model results	112
Standard simulation	112
Alternative hydraulic-conductivity distributions	115
Summary and conclusions	119
Summary	123
References	126
Supplemental information	134

FIGURES

		Page
Figure	1. Map showing location of the Waste Isolation Pilot Plant (WIPP) site and the Capitan reef, which forms the northern margin of the Delaware Basin	4
	2. Diagrammatic section showing stratigraphic relations in the northern Delaware Basin and the stratigraphic position of the Waste Isolation Pilot Plant (WIPP) repository	5
	3. Map showing approximate boundaries of ground-water models in the region surrounding the Waste Isolation Pilot Plant	8
	4. Schematic diagram showing stratigraphy and lithology of the uppermost Salado Formation and overlying rock units	12
	5. Map showing thickness of the Rustler Formation in the vicinity of the WIPP site and areal distribution of halite in the Rustler Formation	18
	6. Columnar geologic section across the WIPP site showing correlation of lithologic units in the Rustler Formation	19
	7. Schematic perspective diagram of vertically exaggerated topography in the WIPP region and the spatial relation between Nash Draw and the WIPP site	21
	8. Map showing distribution of the Gatuna Formation and inferred course of streams during the middle Pleistocene	22
	9. Diagram showing relation between pressure-related driving-force component, density-related driving-force component, and the total driving force	29
	10. Map showing equivalent-freshwater head for wells completed in the Culebra Dolomite Member of the Rustler Formation	31

FIGURES - Continued

	Page
Figure 11. Map showing fluid density in wells completed in the Culebra Dolomite Member of the Rustler Formation	32
12. Map showing areal distribution of the dimensionless driving-force ratio in the model area of Barr and others (1983)	33
13. Map showing relative magnitude and direction of density-related and pressure-related driving-force vector components in the model area of Barr and others (1983)	34
14. Map showing comparison of flow velocities and directions computed by the equivalent-freshwater-head simulation and by the variable-density simulation in the model area of Barr and others (1983)	37
15. Structure contour map of the base of the Culebra Dolomite Member of the Rustler Formation	42
16. Graph showing relation between fluid density and specific conductance for ground water in the Rustler Formation in the WIPP region	44
17. Map showing location of wells with hydrologic data in the WIPP region	45
18. Map showing distribution of approximate fluid density in the Culebra Dolomite Member of the Rustler Formation	46
19. Map showing estimated equivalent-freshwater head in the Culebra Dolomite Member of the Rustler Formation prior to shaft excavation at the WIPP site in 1981	48
20. Map showing areal distribution of the dimensionless driving-force ratio in the WIPP region	51

FIGURES - Continued

		Page
Figure 21.	Map showing relative magnitude and direction of density-related and pressure-related driving-force vector components at the WIPP site and in the area to the south	52
22.	Map showing location of regional model boundary and significant hydrologic features	54
23.	Map showing areal distribution of halite in the Rustler Formation in the model region	57
24.	Map showing depth to the top of the Culebra Dolomite Member of the Rustler Formation in the model region	58
25.	Map showing hydraulic conductivity at wells and test holes in the model region	60
26.	Map showing regional hydraulic-conductivity trends and location of model area of Haug and others (1987)	61
27.	Map showing hydraulic-conductivity distribution in model area of Haug and others (1987)	62
28.	Map showing hydraulic-conductivity distribution that incorporates both regional-scale trends and local-scale features	63
29.	Map showing finite-element mesh for the regional model	65
30.	Histogram showing thickness distribution of the Culebra Dolomite Member of the Rustler Formation in 725 drill holes in the northern Delaware Basin	66
31.	Map showing hydraulic-conductivity distribution for the baseline simulation	68

FIGURES - Continued

		Page
Figure 32.	Map showing simulated equivalent-freshwater-head surface from the baseline simulation	70
33.	Map showing difference between equivalent-freshwater heads from the baseline simulation and equivalent-freshwater heads calculated from field measurements	71
34.	Map showing simulated direction and magnitude of ground-water flow produced by the baseline simulation	73
35.	Map showing the magnitude of the deviation angle between the flow direction produced by the equivalent-freshwater-head simulation and the flow direction produced by the baseline (variable-density) simulation	74
36.	Map showing comparison of the flow direction produced by the equivalent-freshwater-head simulation and the flow direction produced by the baseline (variable-density) simulation for the area just south of the WIPP site	76
37-39.	Maps showing magnitude of the deviation angle between the flow direction produced by the baseline simulation and the flow direction after:	
	37. 50 years of transient flow and transport	78
	38. 100 years of transient flow and transport	79
	39. 1,000 years of transient flow and transport	80
40.	Map showing fluid-density distribution after 1,000 years of transient flow and transport superimposed on the initial (present-day) fluid-density distribution	31

FIGURES - Continued

Page

Figure 41. Graph showing pressure distributions (expressed as equivalent-freshwater head) that were specified as boundary conditions along the eastern boundary	84
42. Graph showing pressure distributions (expressed as equivalent-freshwater head) that were specified as boundary conditions along the northern boundary	85
43-46. Maps showing magnitude of the deviation angle between the flow direction produced by the baseline simulation and the flow direction produced by the:	
43. Intermediate-high northern and eastern boundary simulation	86
44. Intermediate-low northern and eastern boundary simulation	87
45. Extreme-high northern and eastern boundary simulation	88
46. Extreme-low northern and eastern boundary simulation	89
47. Map showing difference between equivalent-freshwater heads produced by the baseline simulation and equivalent-freshwater heads produced by a steady-state simulation in which Pecos boundary heads were increased by 5 meters	91
48. Graph showing change in equivalent-freshwater head at the center of the WIPP site caused by a 5-meter head increase at the Pecos River boundary	93
49. Map showing magnitude of the deviation angle between the flow direction produced by the baseline simulation and the flow direction produced by a simulation of conditions 10 years after an instantaneous 5-meter head increase at the Pecos River boundary	94
50. Map showing equivalent-freshwater-head surface produced by the vertical-flux simulation	96

FIGURES - Continued

	Page
Figure 51. Map showing distribution of specified vertical flux used in the vertical-flux simulation	98
52. Map showing simulated direction and magnitude of ground-water flow produced by the vertical-flux simulation	99
53. Section showing approximate distribution of deformation associated with halite dissolution and other secondary processes	104
54. Section showing spring deposits of late Pleistocene age on the eastern margin of Nash Draw and inferred water table	106
55. Section showing equivalent-freshwater heads of the Magenta and Culebra Dolomite Members of the Rustler Formation	108
56. Section showing finite-difference grid for cross-sectional flow model	109
57. Section showing hydraulic-conductivity distribution for the standard simulation	111
58. Section showing the boundary and initial conditions for the cross-sectional model	113
59. Section showing initial water table and the configuration of the water table produced by the standard simulation after 1,000, 4,000, 10,000, and 20,000 years of drainage	114
60. Section showing comparison of simulated heads in the Magenta and Culebra Dolomite Members of the Rustler Formation produced by the standard simulation after 1,000, 4,000, 10,000, and 20,000 years of drainage	116

FIGURES - Concluded

Page

Figure 61. Section showing direction (corrected for vertical exaggeration) and magnitude of ground-water flow produced by the standard simulation after 1,000 years of drainage	117
62. Section showing comparison of heads in the Magenta and Culebra Dolomite Members of the Rustler Formation (after 1,000, 4,000, 10,000, and 20,000 years of drainage) produced by a simulation in which the hydraulic conductivity of the Tamarisk confining unit was one order of magnitude greater than that used in the standard simulation	118
63. Section showing head in the Culebra Dolomite Member of the Rustler Formation (after 1,000, 4,000, 10,000, and 20,000 years of drainage) produced by a simulation in which the hydraulic conductivity of the Tamarisk confining unit was set equal to zero, effectively isolating the Culebra from recharge from overlying units	120
64. Section showing comparison of heads in the Magenta and Culebra Dolomite Members of the Rustler Formation (after 1,000, 4,000, 10,000, and 20,000 years of drainage) produced by a simulation in which vertical flow through the Tamarisk confining unit was allowed only in the westernmost part of the transition zone	121
65. Diagram showing system for locating WIPP-related wells	138
66. Diagram showing system for locating non-WIPP wells	139

TABLE

Table 1. Hydrologic data for wells in the Waste Isolation Pilot Plant (WIPP) region	135
---	-----

CONVERSION FACTORS

<u>Parameter</u>	<u>Dimensional formula</u>	<u>Multiply metric unit</u>	<u>by</u>	<u>To obtain inch-pound unit</u>
Discharge	$[L^3/T]$	cubic meter per second (m^3/s)	2.559×10^4	acre-foot per year (acre-ft/yr)
Compressibility	$[M/LT^2]^{-1}$	meter second squared per kilogram ($kg/m \cdot s^2$) ⁻¹ or square meter per Neuton (N/m^2) ⁻¹	6.895×10^3	per pound per square inch (lb/in^2) ⁻¹
Density	$[M/L^3]$	kilogram per cubic meter (kg/m^3)	6.243×10^{-2}	pound per cubic foot (lb/ft^3)
Dispersivity	$[L]$	meter (m)	3.281	foot (ft)
Gravitational acceleration	$[L/T^2]$	meter per second squared (m/s^2)	3.281	foot per second squared (ft/s^2)
Hydraulic conductivity	$[L/T]$	meter per second (m/s)	2.835×10^5	foot per day (ft/d)
Length	$[L]$	meter (m)	3.281	foot (ft)
		kilometer (km)	6.214×10^{-1}	mile (mi)
Permeability	$[L^2]$	meter squared (m^2)	1.076×10^1	foot squared (ft^2)
		meter squared (m^2)	1.013×10^{12}	darcy
Porosity	$[1]$	---	1.000	---
Pressure	$[M/LT^2]$	kilogram per meter second squared ($kg/m \cdot s^2$) or Neuton per meter squared (N/m^2)	1.450×10^{-4}	pound per square inch (lb/in^2)
Specific yield	$[1]$	---	1.000	---
Specific storage	$[1/L]$	per meter (1/m)	3.048×10^{-1}	per foot (1/ft)
Storage coefficient	$[1]$	---	1.000	---
Transmissivity	$[L^2/T]$	meter squared per second (m^2/s)	9.320×10^5	foot squared per day (ft^2/d)
Velocity	$[L/T]$	meter per second (m/s)	2.835×10^5	foot per day (ft/d)
Weight	$[ML/T^2]$	kilogram (kg)	1.102×10^{-3}	ton

Sea level: In this report, "sea level" refers to the National Geodetic Vertical Datum of 1929 (NGVD of 1929)-- a geodetic datum derived from a general adjustment of the first-order level nets of both the United States and Canada, formerly called "Sea Level Datum of 1929."

VARIABLE-DENSITY GROUND-WATER FLOW AND PALEOHYDROLOGY
IN THE WASTE ISOLATION PILOT PLANT (WIPP) REGION,
SOUTHEASTERN NEW MEXICO

By Peter B. Davies

ABSTRACT

A series of analyses, including variable-density flow simulations, was used to examine ground-water flow in the vicinity of the Waste Isolation Pilot Plant (WIPP) in the context of the regional flow system. WIPP is an underground repository mined from a thick bedded-salt unit to provide a facility for the disposal of radioactive waste. WIPP is located in southeastern New Mexico. The analyses primarily examined the Culebra Dolomite Member of the Rustler Formation, which is a potential pathway for the transport of radionuclides to the biosphere in the event of a breach of the WIPP repository.

An analysis of the relative magnitude of pressure-related and density-related flow-driving forces indicates that density-related forces are not significant at the WIPP site and to the west but are significant in areas to the north, northeast, and south of the site. The area to the south is important because it lies along potential transport pathways from the site. In this area, ground-water flow simulations based on equivalent-freshwater head produce very misleading information on predicted flow directions and velocity magnitudes.

A regional-scale, variable-density model of ground-water flow in the Culebra Dolomite Member was developed in which a baseline, approximate steady-state simulation was calibrated to the distribution of equivalent-freshwater heads. The flow field from the baseline simulation, along with long-term brine transport patterns, indicates that flow velocities are relatively fast west of the site and extremely slow east and northeast of the site. In the transition zone between these two extremes, which includes the WIPP site, velocities are highly variable.

A series of sensitivity simulations was used to analyze boundary effects and vertical flux. These simulations indicate that if the Culebra is as impermeable to the east and northeast of the WIPP site as geologic conditions indicate, the central and western parts of the region, including the WIPP site, are fairly well insulated from the eastern and northeastern boundaries and are insensitive to whatever conditions are assumed to be present along these boundaries. A simulation of a 5-meter head increase along the Pecos River boundary indicates that if the Culebra were tightly confined throughout the entire region, approximately 50 percent of any change in river elevation would eventually reach the WIPP site. Uncertainty in the regional distribution of storage characteristics in the Culebra makes it difficult to accurately predict how long it would take for Pecos-related stresses to propagate through the WIPP region. A series of vertical-flux simulations indicates that as much as 25 percent of total inflow to the Culebra could be entering as vertical flux.

These simulations also indicate that if significant volumes of water enter the Culebra vertically, most of the influx must be occurring in the westernmost part of the transition zone adjacent to Nash Draw.

Motivated by recent isotopic and geochemical analyses, a simple cross-sectional model was developed to provide a physically based analysis of the flow system as it may have drained through time following recharge during a past glacial pluvial. Drainage for 20,000 years was simulated using a variety of hydraulic-conductivity distributions for rock units overlying the Culebra. These simulations indicate that the system as a whole drains very slowly and that it apparently could sustain flow from purely transient drainage following recharge of the system during the Pleistocene. Although these simulations do not prove that this has been the case, they do show that such long-term transient drainage is physically possible. The simulations also indicate that the observed underpressuring of the Culebra in the vicinity of the WIPP site is most likely the hydrodynamic result of the Culebra having a relatively high hydraulic conductivity and being well connected to its discharge area but poorly connected to sources of recharge.

INTRODUCTION

The Waste Isolation Pilot Plant (WIPP) is a U.S. Department of Energy (DOE) project designed to provide a research and development facility to demonstrate the safe disposal of transuranic waste from defense-related activities. If the demonstration phase of the project is successful, then the repository will be used for the permanent disposal of approximately 170,000 cubic meters of transuranic waste. The WIPP consists of an underground repository mined from a thick bedded-salt unit and associated waste-handling facilities at land surface. The facility is located in southeastern New Mexico in an evaporite-bearing sedimentary basin known as the Delaware Basin (fig. 1). A key component in the assessment of the long-term performance of the facility is evaluating the potential for radionuclide transport from the underground repository to the biosphere by ground water.

Following initial site-selection studies in the early 1970's, field investigations began in 1974. In 1975, the third exploration borehole at the proposed site (ERDA-6) penetrated highly pressurized brine and strongly deformed rock in the lower part of the evaporite section. Because of the unexpected conditions at ERDA-6, the site was relocated approximately 11 kilometers southwest to its current location. Exploration of this new site began in 1976 with the drilling of ERDA-9. Site-characterization studies between 1976 and 1983 included mapping the geology, drilling 78 holes to acquire geologic and hydrologic data, and conducting numerous geophysical surveys. From 1981 to 1983, two shafts and approximately 3 kilometers of exploratory drifts were excavated.

In 1983, the decision was reached that the site fully met all geotechnical qualification factors, and the project should continue with full-scale facility construction (Weart, 1983). Independent technical reviews of the site-characterization studies by the National Academy of Sciences and by the State of New Mexico's Environmental Evaluation Group concurred with the decision to proceed with full construction but recommended that a number of geotechnical issues be further studied and resolved prior to the receipt of waste (Neill and others, 1983; National Academy of Sciences, 1984). One of the main topics recommended for further study was clarifying uncertainties about the ground-water flow system in the rock units that overlie the evaporite section.

The WIPP repository is located approximately 650 meters below the land surface in the lower part of the predominantly halite Permian Salado Formation (fig. 2). Overlying the Salado is the Permian Rustler Formation, which is composed of interbedded halite, anhydrite, fine-grained clastics, and two dolomite members. The Rustler is overlain by fine-grained clastics of the Permian Dewey Lake Red Beds. Three laterally persistent, water-bearing units have been identified in the post-Salado rock units, the Magenta Dolomite and Culebra Dolomite Members of the Rustler Formation, and the rocks of the contact zone between the Rustler and Salado Formations (Mercer, 1983). Of these three zones, the Culebra Dolomite Member has been identified as being the most transmissive zone; therefore, it is considered an important potential pathway for the transport of radionuclides to the biosphere in the event of a breach of the repository (U.S. Department of Energy, 1980a; Gonzalez, 1983a).

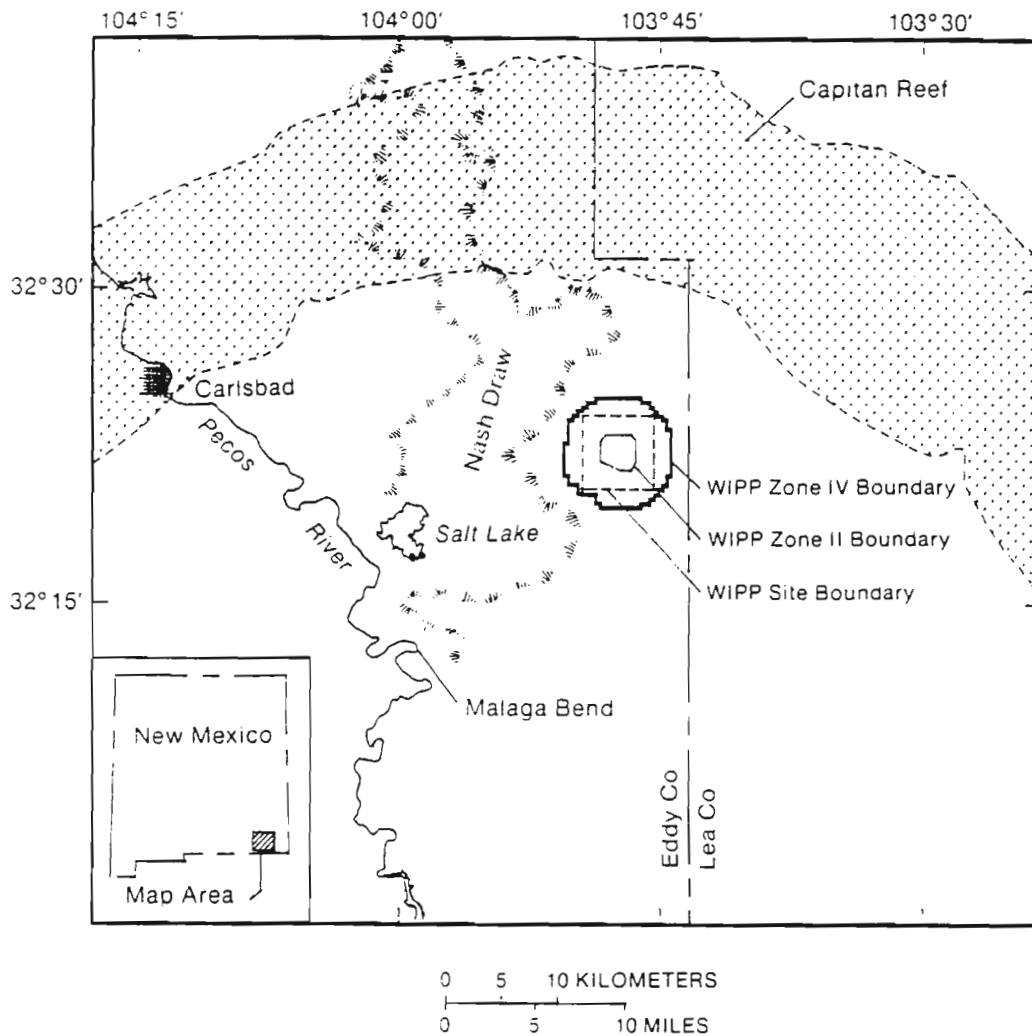
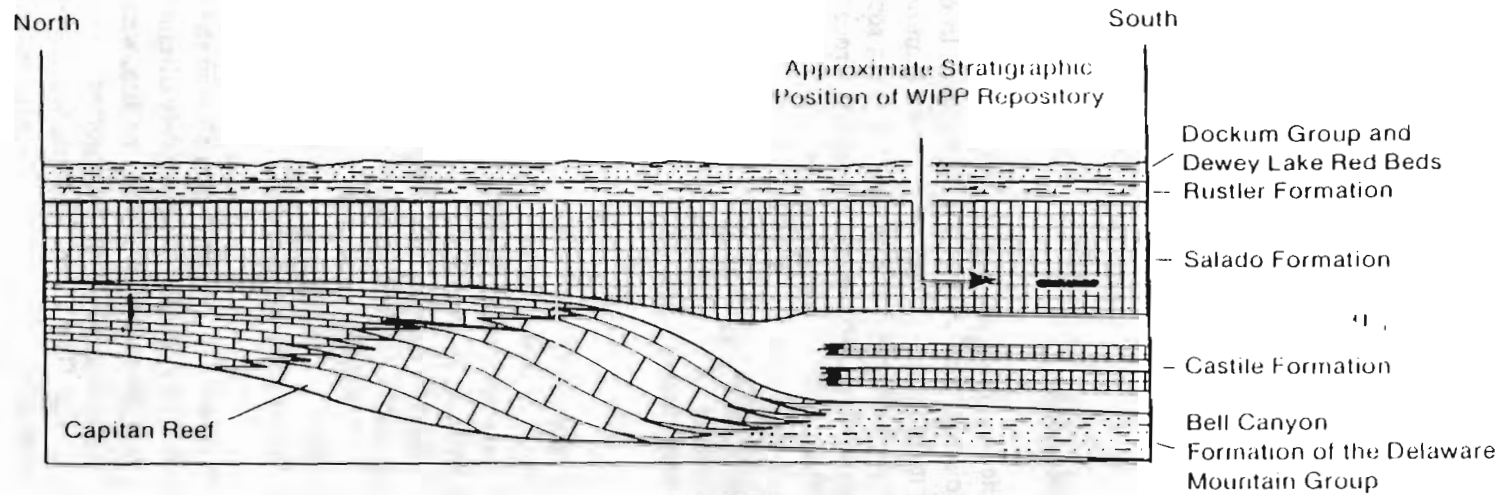


Figure 1.-- Location of the Waste Isolation Pilot Plant (WIPP) site and the Capitan reef, which forms the northern margin of the Delaware Basin.



EXPLANATION



Figure 2.-- Stratigraphic relations in the northern Delaware Basin and the stratigraphic position of the Waste Isolation Pilot Plant (WIPP) repository. (Modified from Davies, 1984, fig. 2-1).

Secondary processes of halite dissolution, subsidence, and calcium sulfate hydration have produced complex hydrologic conditions. Complexities include spatial variation in permeability of several orders of magnitude within the same rock unit, local areas of fracture-dominated flow, and variation in fluid density ranging from freshwater to saturated brine, with associated variations in fluid chemistry. These secondary processes along with gypsum dissolution have been most active in an area west of WIPP, producing a pronounced valley called Nash Draw, which trends north-south (fig. 1). East of Nash Draw, halite dissolution and other secondary processes have been less active, and there is a transition to intact rock with much lower permeabilities. The WIPP site is located within the transition zone, which generally is characterized by large spatial variations in permeability and fluid density.

Purpose and Scope

The purpose of this report is to describe the ground-water flow system in the rock units that overlie the Salado Formation in the Waste Isolation Pilot Plant (WIPP) region. In order to meet that objective, the report is divided into four main sections. The first section is an overview of the stratigraphy and hydraulic characteristics of the Salado Formation and overlying rock units. This section also contains a description of halite dissolution and related secondary processes that have had a significant effect on the development of the current ground-water flow system. Each of the remaining three sections contains discussion of one of the three major topics summarized in the following paragraphs. The discussion of each major topic includes specific objectives, pertinent field data, model implementation, and simulation results. The scope of this report is limited to analyzing data available as of 1987. This study was carried out in cooperation with the U.S. Department of Energy.

The first major topic addressed is whether fluid-density effects have a significant effect on flow patterns in the WIPP region. All previous ground-water models of the WIPP area have used the concept of equivalent-freshwater head as a mechanism to account for density effects. However, the assumptions inherent in that concept are quite restrictive, and it is not clear that the assumptions are valid in the WIPP region. Two approaches were taken to address this question. One approach was to develop an analytic technique, based on dimensional analysis of the variable-density flow equation, that produces a dimensionless parameter whose magnitude is proportional to the relative magnitude of density-related effects at a given location. The second approach was to directly compare equivalent-freshwater-head and variable-density flow simulations.

The second major topic addressed is the relation between ground-water flow in the vicinity of the WIPP site and in the larger regional flow system. What effects do relatively distant stresses have on flow in the site area? If radionuclides were to be transported beyond the site, what do the regional flow patterns indicate about where the radionuclides would be transported? In order to address these questions, a regional model of ground-water flow in the Culebra was constructed. Previous regional models had utilized somewhat arbitrary boundary conditions consisting of a single set of specified head or flux conditions at the perimeter of a rectangular area. Although this approach is acceptable for the simulation of internal short-term stresses that do not affect the

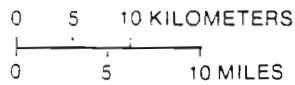
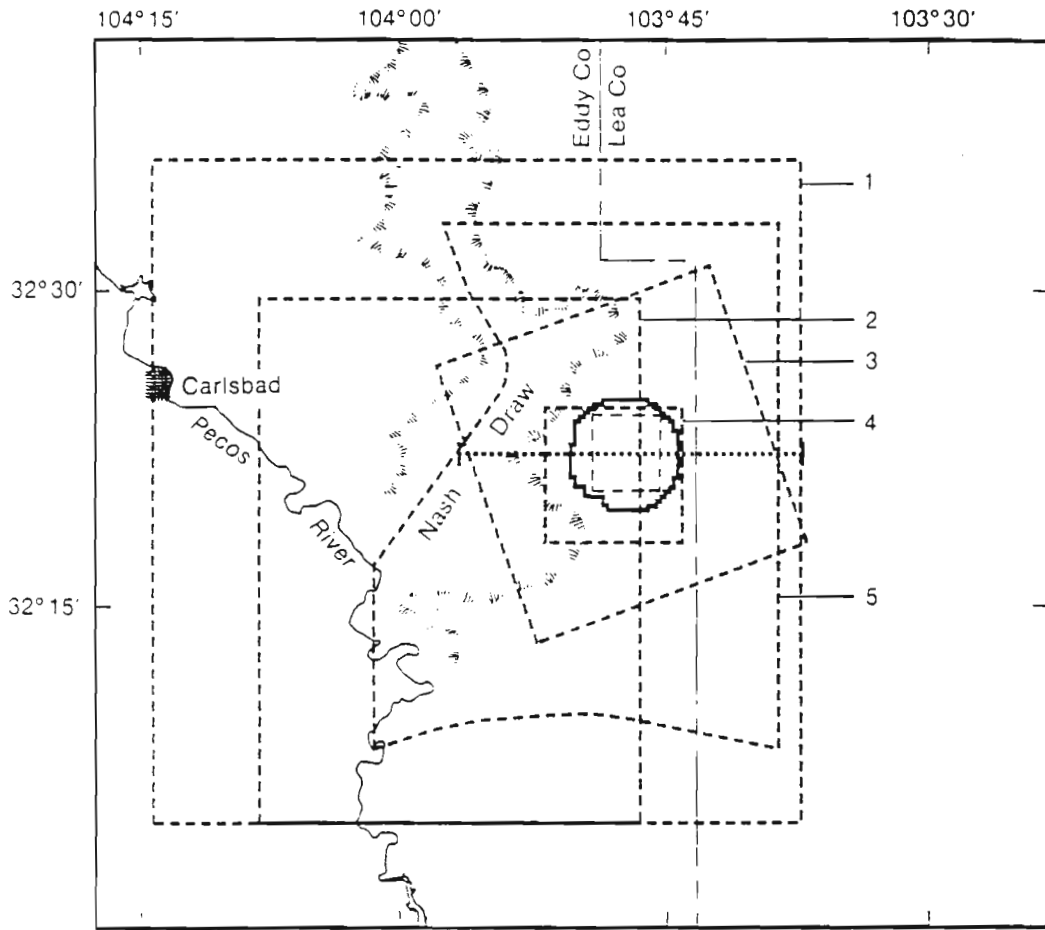
boundaries, the use of such boundaries is less desirable for making long-term predictions. Therefore, in the model of regional flow in the Culebra developed for this study, boundaries were located at well-defined hydrologic features. Where this was not possible, a range of different boundary conditions was examined.

The third major topic addressed concerns the source of recharge to the Culebra. The generally accepted flow-system conceptualization envisions the rock units of the Rustler Formation as relatively isolated vertically, with recharge coming from an area somewhere to the north (Mercer, 1983). However, recent isotopic data from Rustler Formation waters and other geochemical analyses have raised new questions regarding the nature of recharge to and vertical flow within the Rustler Formation. An analysis of isotope data in the Rustler by Chapman (1986) suggests that the Rustler receives recharge by the downward percolation of local meteoric water. In a somewhat different interpretation of the Rustler isotope data, Lambert (1987) and Lambert and Harvey (1988) suggest that the Rustler was recharged during a past glacial pluvial period, has been draining since that time, and has received no significant input of modern meteoric water. In order to address some of these questions about recharge, a transient cross-sectional model was developed to examine the physical feasibility of long-term drainage in the Rustler and to examine, to a limited extent, the role of vertical flow within the Rustler Formation.

Previous Ground-Water Models

Several numerical models simulating ground-water flow in the WIPP region were constructed between 1977 and 1983. These models were developed to address a variety of different questions and were based on data sets that evolved through time as ongoing field investigations produced additional data. Therefore, these models are based on different flow-system conceptualizations and different numerical implementations of those conceptualizations. The following paragraphs are a brief summary of the model objectives, implementation, and conclusions from each of these studies. The approximate boundaries of these models are shown in figure 3.

The first ground-water flow model of the WIPP region, which encompassed a square 58-by 58-kilometer area, was developed by INTERA Technologies for the Safety Analysis Report and for the WIPP Environmental Impact Statement (U.S. Department of Energy, 1980a, b). The water-bearing zones simulated by this model included the Rustler Formation (simulated as a single unit), the Rustler-Salado contact zone, the Permian Delaware Mountain Group, and the Permian Capitan Limestone referred to locally as the Capitan reef. The objectives of the study were to verify the degree of consistency between various sets of hydrologic data, to calculate the extent of vertical hydraulic connection between various hydrologic units, to delineate spatial variations in hydraulic conductivity, to calculate potentials and hydraulic conductivity in areas where data were lacking, and to calculate boundary conditions for local repository-breach simulations. Simulations were carried out using the three-dimensional, finite-difference SWIFT (Sandia Waste-Isolation Flow and Transport) code (Dillon and others, 1978).



EXPLANATION

- BOUNDARY OF WIPP ZONE IV
- WIPP SITE BOUNDARY
- BOUNDARY OF MODELED AREA--Number indicates study:
 - 1 U.S. Department of Energy (1980a, b); Cole and Bond (1980)
 - 2 D'Appolonia Consulting Engineers (1981)
 - 3 Barr and others (1983); this report
 - 4 Haug and others (1987)
 - 5 This report
- LINE OF CROSS-SECTIONAL MODEL OF THIS REPORT

Figure 3.-- Approximate boundaries of ground-water models in the region surrounding the Waste Isolation Pilot Plant (WIPP).

The early INTERA model was reworked by Cole and Bond (1980) using the same system conceptualization but a different simulation code known as VTT (Variable Thickness Transient), which is a two-dimensional, finite-difference code in which multiple aquifers are simulated using interaquifer transfer coefficients (Reisenauer, 1979). The study was done to provide a benchmark comparison between the SWIFT and VTT codes. The data set for the Cole and Bond (1980) study was quite similar to that used in the INTERA study. The model results were, therefore, quite similar.

D'Appolonia Consulting Engineers (1981) constructed a model of the WIPP region with the primary objective of verifying the calculation procedures used by the early INTERA model (U.S. Department of Energy, 1980a,b) for the analysis of liquid breach and transport scenarios. D'Appolonia (1981) modeled the Rustler Formation, simulated as a single unit, in a rectangular 34- by 46-kilometer area, located with the WIPP site along the eastern margin (fig. 3). In a separate simulation, the Permian Bell Canyon Formation (the uppermost formation in the Delaware Mountain Group) was modeled over a somewhat larger area. The D'Appolonia (1981) model study used an inhouse two-dimensional, finite-element code known as GEOFLOW. The results of the D'Appolonia study generally were similar to the earlier INTERA study. These two studies had different interpretations of flow conditions in the Rustler in southern Nash Draw. The INTERA study hypothesized a trough in the potentiometric surface of the Rustler in southern Nash Draw as being produced by downward leakage to the Rustler-Salado contact zone. The D'Appolonia study hypothesized the same trough as being caused by higher hydraulic conductivity in the Rustler in the Nash Draw area due to more extensive fracturing in the area. Perhaps related to this difference in flow-system conceptualizations, the D'Appolonia study computed travel times between the site and the Pecos River that were 2.2 times shorter than those computed by the INTERA study.

Using new, more detailed data on the Rustler Formation, Barr and others (1983) constructed a model that explicitly simulated the Magenta and Culebra Dolomite Members of the Rustler Formation as separate units within a square 26- by 26-kilometer area, centered on the WIPP site (fig. 3). In order to incorporate anisotropy in the model, the model mesh was rotated 25 degrees west of north. After construction of a flow model, the study examined transport of an ideally nonsorbing contaminant from the center of the WIPP site. These simulations indicated that contaminant travel times may be significantly longer than those computed in previous modeling studies. For numerical simulations, the study used ISOQUAD, a two-dimensional, finite-element code that solves both the flow and transport equations (Pinder, 1974).

The models described in the preceding paragraphs provided a foundation for the regional modeling study that is the subject of this report. Insights gained from these previous models and questions raised about their limitations were instrumental in formulating the objectives of this study, which was carried out between 1985 and 1987. Also during this time period, Haug and others (1987) and Niou and Pietz (1987) developed detailed models of the WIPP-site vicinity. The primary objective of the model of Haug and others (1987) was to use the hydraulic stresses created by the excavation of the WIPP shafts and by multiple-well aquifer tests to develop a detailed understanding of the flow system in the Culebra in the vicinity of the WIPP site. The study has provided valuable information on the hydraulic conductivity of the Culebra in the site area, and it will be described in more detail in the regional model simulations section of this report. The primary objective of the model of Niou and Pietz (1987) was to corroborate values of transmissivity

and storativity in the Culebra by calculating these parameters from the H-3 multiple-well pumping test using a statistical inverting code (Niou and Pietz, 1987, p. 1-2).

HYDROGEOLOGY OF THE SALADO FORMATION AND OVERLYING ROCK UNITS

The purpose of this section is to provide a brief review and description of the hydrogeology of the WIPP region that is pertinent to the ground-water flow-system conceptualization that was used in the construction of numerical simulations. This section is divided into one section describing stratigraphy and hydraulic characteristics and a second section describing near-surface secondary processes that have had significant structural and hydrologic impact.

Stratigraphy and Hydraulic Characteristics

The stratigraphic section from undifferentiated Triassic rocks down to the contact zone between the Rustler and Salado Formations comprises the framework of the post-Salado ground-water flow system. A schematic diagram of the stratigraphy and lithology of these rocks is shown in figure 4. A number of Quaternary deposits have indirect hydrologic significance. These deposits will be discussed where pertinent in later sections of this report.

Salado Formation

The Permian Salado Formation consists of 85 to 90 percent thickly bedded halite that contains thin interbeds of anhydrite and polyhalite (Jones, 1973, p. 10-13; Powers and others, 1978, p. 4-29 to 4-39). The halite commonly is interspersed with clay and trace amounts of anhydrite, polyhalite, or hematite. Jones (1973, p. 11) reported that the thickness of the Salado averages between 1,700 and 1,900 feet (520 and 580 meters) but reaches as much as 2,310 feet (700 meters) in deformationally thickened masses. The halite of the Salado Formation is relatively impermeable. Most drill-stem tests in the Salado yield permeability values of less than 0.1 microdarcy, hydraulic conductivities of less than 10^{-12} m/s (meters per second), which is the sensitivity of the drill-stem test procedures used (Beauheim, 1986, p. 57-60; Mercer, 1987, p. 26). A few of the tests in the Salado have yielded measurable permeability values of as much as 25 microdarcies (2.4×10^{-10} m/s). These tests, coupled with observations of the stratigraphic locations of water leakage in the WIPP mine (Nowak, 1986; Nowak and McTigue, 1987), indicate that higher permeabilities in the Salado are associated with the anhydrite and polyhalite interbeds and with discrete clay seams. Relative to the overlying rock units, permeability in the undisturbed Salado is so low that it forms the effective base for the ground-water flow system in the overlying rock.

As a result of eastward tilting of the Delaware Basin during the late Cenozoic, bedding in the WIPP region has a regional eastward dip of not more than 2 degrees (Brokaw and others, 1972, p. 28). In the western, updip part of the WIPP region, the upper part of the Salado Formation is characterized by a zone in which halite has been removed by circulating ground water, leaving behind a residue of unconsolidated silt and clay with varying amounts of brecciated gypsum (Vine, 1963, p. B3). The residuum, which is as much as 45 meters thick, is estimated to represent only

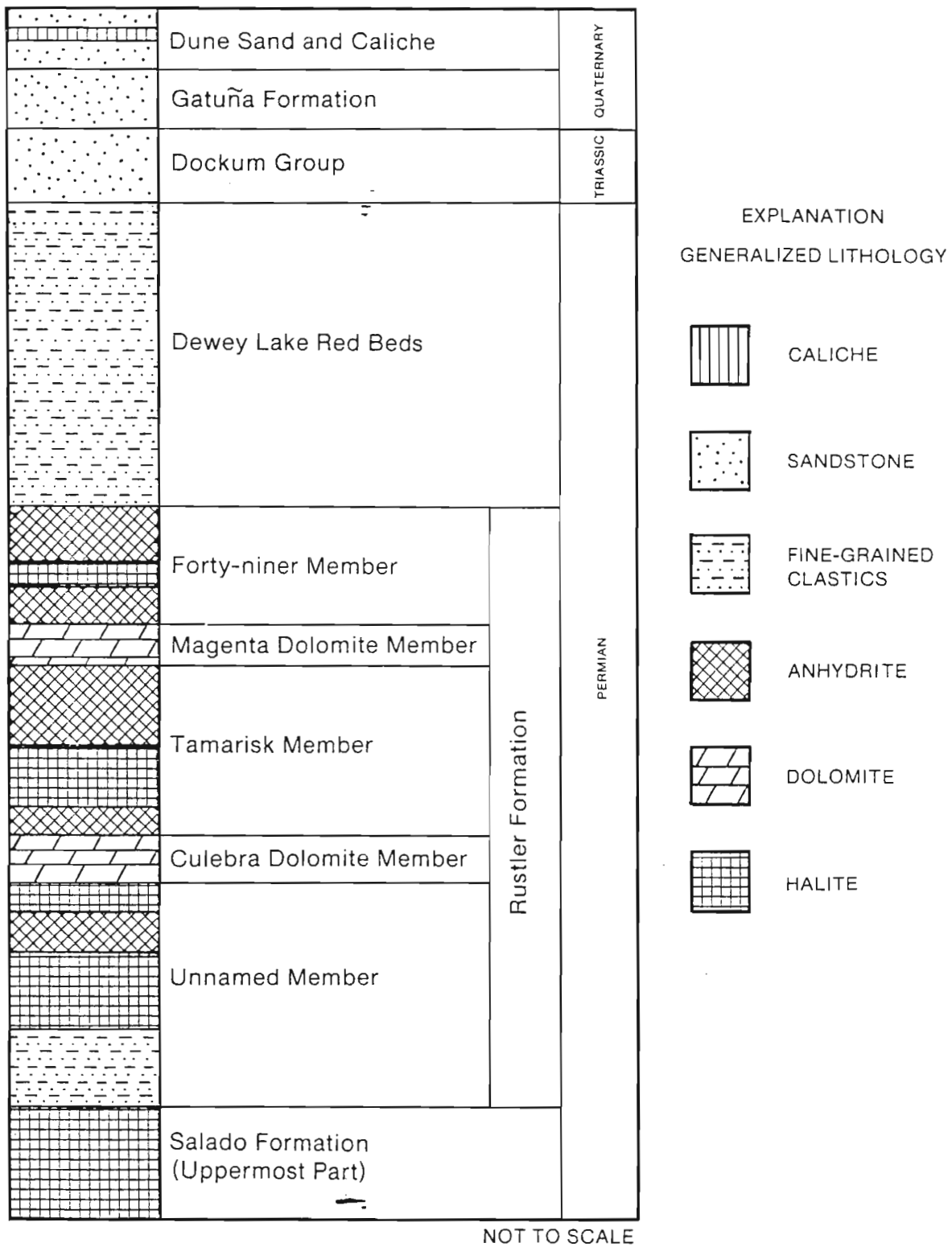


Figure 4.-- Stratigraphy and lithology of the uppermost Salado Formation and overlying rock units.

one-third to one-tenth of the original rock thickness (Jones, 1959, p. 13; Vine, 1963, p. B7). The residuum is difficult to distinguish in drill cuttings and geophysical logs from the lower Rustler Formation; therefore, there has been some disagreement as to whether this residuum should be considered to be part of the Salado Formation or grouped with the overlying Rustler Formation (Cooper, 1962, p. 23; Vine, 1963, p. B7; Cooper and Glanzman, 1971, p. A6; Mercer, 1983, p. 16). In this report, the Salado residuum, along with the lowermost part of the Rustler Formation, is referred to as the Rustler-Salado contact zone.

The Rustler-Salado contact zone is the lowest water-bearing unit in the post-Salado flow system. Early studies of this unit (Robinson and Lang, 1938; Theis and Sayre, 1942; and Hale and others, 1954) primarily focused on southernmost Nash Draw because large quantities of brine were discharging from this unit into the Pecos River. Theis and Sayre (1942, p. 69) reported that approximately 342 tons (3.1×10^5 kilograms) of sodium chloride per day discharged into the Pecos River in the Malaga Bend area. These studies found that brine in the Rustler-Salado contact zone is under artesian conditions (Robinson and Lang, 1938, p. 86-90). Hale and others (1954, p. 29) reported a transmissivity value of 8×10^3 ft²/d (feet squared per day) (1×10^{-2} m²/s (meters squared per second)) from aquifer tests of the Rustler-Salado contact zone in the southern Nash Draw area.

Mercer (1983, p. 48-56, table 6) reported that drilling and testing associated with the WIPP project have confirmed the presence of a well-developed Rustler-Salado contact zone and brine under artesian conditions in the central and northern parts of Nash Draw. In this area, thickness of the Rustler-Salado contact zone ranges from 11 to 108 feet (3 to 33 meters), and transmissivities range from 2×10^{-4} to 8 ft²/d (2×10^{-10} to 9×10^{-6} m²/s). Drilling and testing associated with the WIPP project also have revealed that the Rustler-Salado contact zone locally extends eastward from the geographic limits of Nash Draw, although it is not as well developed (Mercer, 1983, p. 51, 54-56). Aquifer tests east of Nash Draw yielded transmissivity ranging from 3×10^{-5} to 5×10^{-2} ft²/d (3×10^{-11} to 5×10^{-8} m²/s). Mercer (1983, p. 51) concluded that the Rustler-Salado contact zone is characterized by two areas of considerably different permeability. The area of greater permeability is associated with the residuum in the Nash Draw area, where flow primarily is through fractures and intergranular pore spaces. The area of lower permeability occurs east of Nash Draw in the vicinity of the WIPP site, where flow primarily is along bedding planes at the contact between the Rustler and Salado Formations and in the lowermost part of the Rustler.

Rustler Formation

The Permian Rustler Formation is the youngest salt-bearing formation in the Delaware Basin. The Rustler consists of anhydrite interbedded with dolomitic limestone, interlaminated dolomite and anhydrite, muddy halite, and clastics ranging from mudstone to fine-grained sandstone (Vine, 1963, p. B13-B18; Powers and others, 1978, p. 4-39 to 4-42; Lowenstein, 1987, p. 7-28). The lithologic, structural, and hydrologic characteristics of the Rustler have been affected by secondary processes related to the circulation of ground water. Due to these secondary processes and depositional variations, the thickness of the Rustler is variable, ranging from approximately 200 to 500 feet (60 to 150 meters) (Vine, 1963, p. B14; Jones, 1973, p. 23). Secondary processes

affecting the Rustler Formation will be discussed in more detail following the description of the remainder of the stratigraphic column.

The Rustler Formation has been divided into five members (fig. 4). Where unaltered by circulating ground water, the lower unnamed member consists of a basal, fine-grained sandstone and mudstone overlain by interbeds of anhydrite, halite, and mudstone. Bachman (1980, p. 21) reported that the thickness of the lower unnamed member averages about 27 meters (90 ft) in eastern Nash Draw and is about 37 meters (120 ft) at the WIPP site. The basal, fine-grained sandstone of the lower unnamed member is the upper part of the Rustler-Salado contact zone described in the previous section. The anhydrite, halite (where present), and mudstone in the upper part of the lower unnamed member are relatively impermeable and apparently act as confining beds for the brine in the Rustler-Salado contact zone. The brine is under artesian conditions, even in parts of the Malaga Bend area where only 9 meters of the confining beds separate the Rustler-Salado contact zone from the overlying river alluvium (Theis and Sayre, 1942, p. 67).

Overlying the lower unnamed member is a fine-textured, microcrystalline dolomite or dolomitic limestone referred to as the Culebra Dolomite Member (fig. 4). The Culebra is lithologically distinct, areally extensive, and quite uniform in thickness (approximately 8 meters) over a very large area. Where secondary processes have been active, the Culebra is extensively fractured, forming a water-bearing unit with relatively high permeability. Hydrologic field studies first focused on the Culebra during preparations for the 1961 Project Gnome underground nuclear detonation approximately 12 kilometers southeast of the WIPP site (Cooper, 1962; Cooper and Glanzman, 1971). Because of its relatively high permeability in the vicinity of the WIPP site, the Culebra is considered an important potential pathway for the transport of radionuclides in the event of a repository breach (U.S. Department of Energy, 1980a, sec. 8.3; Gonzalez, 1983a, p. 3-10). Therefore, the Culebra has been the primary focus of hydrologic studies for the WIPP project. Mercer (1983, p. 58) reported transmissivity of the Culebra ranging from 1.8×10^2 to 1.25×10^3 ft²/d (1.9×10^{-4} to 1.3×10^{-3} m²/s) in Nash Draw and from 1×10^{-3} to 1.4×10^2 ft²/d (1×10^{-9} to 1.5×10^{-4} m²/s) in the vicinity of the WIPP site. A more detailed description of data characterizing Culebra hydrology is presented in the section titled "Analysis of the Regional-Scale Flow System in the Culebra Dolomite Member."

Overlying the Culebra Dolomite Member is the Tamarisk Member (fig. 4). East of the WIPP site, where it is not altered by circulating ground water, the Tamarisk consists of approximately 55 meters (180 ft) of anhydrite and muddy halite (Lowenstein, 1987, fig. 5a). In the vicinity of the WIPP site and to the west in Nash Draw, the 20 to 30 meters of Tamarisk halite have been completely removed, leaving behind a 2- to 5-meter-thick residue, consisting of mudstone that locally contains angular clasts of anhydrite and gypsum (Sandia Laboratories and U.S. Geological Survey, 1979a, b, c, d, 1980; Chaturvedi and Channell, 1985, p. 30-31; Lowenstein, 1987, p. 21-25). In the vicinity of the WIPP site, the remainder of the Tamarisk primarily consists of anhydrite. The anhydrite has been affected locally by secondary processes, as indicated by the presence of gypsum-filled fractures, locally contorted beds, small fault offsets, and brecciated anhydrite associated with the dissolution residue. The relative proportion of gypsum increases from east to west (Lambert, 1983, fig. VIII-2; Snyder, 1985, fig. 2).

Hydraulic testing of the Tamarisk only has been attempted in two holes in the vicinity of the WIPP site (Beauheim, 1986, p. 42-43; 1988, p. 34-35). In both cases, Tamarisk permeability was too low to measure during the available test period of a few days. In the vicinity of the WIPP site, strong underpressuring of the Culebra Dolomite Member relative to the Magenta Dolomite Member of the Rustler Formation also shows that the Tamarisk is relatively impermeable in this area (Mercer, 1983, p. 67; Chaturvedi and Channell, 1985, p. 40-43; Davies, 1986, p. 580). Westward toward Nash Draw, the underpressuring of the Culebra gradually dissipates, indicating a gradual increase in Tamarisk permeability, possibly due to fracturing associated with halite dissolution and other secondary processes. The role of vertical ground-water fluxes through the Tamarisk and its role as a confining unit are described in more detail in the section of this report describing vertical cross-sectional flow simulations.

The Tamarisk Member is overlain by the Magenta Dolomite Member (fig. 4), which consists of approximately 7 meters of alternating laminae of dolomite and anhydrite (or gypsum). Like the Culebra, the Magenta is fractured in areas where secondary processes have been active, although permeability in the Magenta tends to be somewhat lower than in the Culebra. As in the Culebra, the intensity of fracturing increases from east to west, and transmissivity generally is correlated with fracture intensity. Mercer (1983, p. 65-67) reported transmissivity of the Magenta ranging from 1×10^{-3} to 3×10^{-1} ft²/d (1×10^{-9} to 3×10^{-7} m²/s) in the vicinity of the WIPP site in contrast to the range from 5×10^1 to 4×10^2 ft²/d (6×10^{-5} to 4×10^{-4} m²/s) to the west in Nash Draw. The Magenta is dry at several locations in central and northern Nash Draw, and it has been completely removed by erosion in southern Nash Draw.

The youngest unit in the Rustler Formation is the Forty-niner Member (fig. 4). Where unaltered by circulating ground water, the Forty-niner consists of approximately 25 meters (80 ft) of anhydrite and muddy halite (Lowenstein, 1987, fig. 6a). In the vicinity of the WIPP site and to the west, the approximately 10 meters of Forty-niner halite have been completely dissolved, leaving behind a 2- to 3-meter-thick residue of mudstone that has contorted bedding and angular fragments of gypsum (Chaturvedi and Channell, 1985, p. 28-30; Lowenstein, 1987, p. 26-28). In the vicinity of the WIPP site, the remainder of the Forty-niner is primarily anhydrite, with secondary gypsum and gypsum-filled fractures. In Nash Draw, most of the anhydrite of the Forty-niner has been hydrated to form gypsum. Where it is exposed at the land surface, the gypsum of the Forty-niner is extensively dissolved, forming small caves, solution-enlarged joints, and sinkholes (Vine, 1963, p. B17).

Hydraulic testing of the Forty-niner has only been attempted in two holes in the vicinity of the WIPP site (Beauheim, 1986, p. 37-39; 1987a, p. 119-128). Tests of sections that include the mudstone layers yielded transmissivity ranging from 2×10^{-3} to 7×10^{-2} ft²/d (3×10^{-9} to 8×10^{-8} m²/s). The anhydrite parts of the Forty-niner were too impermeable to yield test results during the test period of a few days. Although the highly altered Forty-niner at and near the land surface in Nash Draw is unsaturated, it is clearly very permeable, and small caves and sinks may act as point recharge locations during runoff following intense rainfall.

Dewey Lake Red Beds

The Rustler Formation is overlain by the Permian Dewey Lake Red Beds (fig. 4). The Dewey Lake consists of alternating beds of siltstone and fine-grained sandstone (Vine, 1963, p. B19-B25; Powers and others, 1978, p. 4-42 to 4-44). The Dewey Lake also contains approximately 15 to 25 percent clay, which forms the principal rock cement. In the area east of WIPP, the Dewey Lake is 150 to 180 meters thick; it has been thinned and completely removed by erosion to the west. Although the Dewey Lake does not contain any laterally extensive, high permeability units, some of the sandstone layers do yield water locally to domestic and stock wells (Hendrickson and Jones, 1952, p. 75; Vine, 1963, p. B24; Mercer, 1983, p. 75). All but the uppermost part of the Dewey Lake is cut by crisscrossing gypsum-filled fractures, indicating that at some point in the past, sulfate-rich ground water was moving through the formation (Bachman, 1985, p. 11; Snyder, 1985, p. 1).

Undifferentiated Triassic Rocks

East of the center of the WIPP site, the Dewey Lake Red Beds are overlain by undifferentiated Triassic rocks, which include the Dockum Group (fig. 4). The Triassic rocks consist of medium- to coarse-grained sandstone and interbeds of conglomerate, siltstone, and mudstone (Vine, 1963, p. B25-B27; Bachman, 1980, p. 24-27). Like the Dewey Lake, the Triassic rocks are thickest in the east (460 meters) and have been thinned to the west by erosion. Although the Triassic rocks are unsaturated along the erosionally thinned western margin, these rocks are a productive aquifer in the easternmost part of the WIPP region (Nicholson and Clebsch, 1961, p. 56-58).

Halite Dissolution and Related Secondary Processes

In the WIPP region, halite dissolution and related secondary processes have significantly modified the uppermost part of the Salado Formation and the overlying Rustler Formation. The following section summarizes the geologic evidence for halite dissolution, the processes that control halite dissolution, the age of dissolution-related activity, and the hydrologic implications of these processes.

Evidence for Halite Dissolution

In the western, updip part of the WIPP region, soluble evaporite beds in the uppermost part of the Salado Formation and the overlying Rustler Formation have been exposed to circulating ground water, resulting in extensive halite dissolution and related secondary processes. The evidence for halite dissolution in the vicinity of the WIPP site and to the west is the spatial

distribution of halite beds (fig. 5) and the stratigraphic correlation of halite beds at depth in the east with mudstone beds near the land surface in the west (fig. 6) (Jones, 1973, p. 18-23; Powers and others, 1978, p. 6-20 to 6-21, 6-38 to 6-40; Bachman, 1980, p. 55-57; Chaturvedi and Channell, 1985, p. 18-32; Snyder, 1985, p. 3-10; Lowenstein, 1987, p. 7-33). Lithologic and sedimentological core descriptions by Sandia Laboratories and the U.S. Geological Survey (1979a, b, c, d, 1980), Chaturvedi and Channell (1985, p. 28-32), and Lowenstein (1987, p. 7-28) indicate that the mudstone beds in the west represent the insoluble residue resulting from dissolution of impure halite. Geochemical analyses by Lambert (1983, p. 65-73) and by Bodine and Jones (U.S. Geological Survey, written commun., 1988) indicate that the ground water in much of this area has played an active role in dissolving evaporite minerals.

In addition to the geologic evidence for extensive halite dissolution, the spatial correlation between the halite distribution and the permeability distribution in the Rustler Formation has led Mercer (1983, p. 43, 56, 60), Gonzalez (1983, p. 17-18), Chaturvedi and Channell (1985, p. 46-51), and Snyder (1985, p. 10) to suggest that there is a causative link between the deformation associated with halite dissolution and the creation of secondary permeability in the Rustler Formation. These secondary processes, along with rock lithology, appear to be the primary factors controlling the spatial variation of rock permeability in the Rustler Formation.

A recently published study has challenged the concept of halite dissolution in the Rustler Formation on the basis of geophysical logs and cores from the WIPP project (Holt and Powers, 1988). The study concluded that dissolution is not responsible for the majority of lateral variations in Rustler halite beds, but rather, facies changes and syndepositional dissolution are responsible for the observed variability in zones containing halite and, laterally, mudstone. The hydrologic implications of this hypothesis are unclear. Hydraulic testing indicates that permeability in the Culebra in many locations is controlled by fracturing (Beauheim, 1986, 1987a, 1987b), presumably caused by secondary processes of some form. If little or no halite dissolution has occurred in the Rustler Formation, as indicated by Holt and Powers (1988), the mechanism responsible for producing several orders of magnitude of secondary permeability variation in the Culebra is equivocal. Because the relation between dissolution of Rustler halite and permeability in the Rustler is well established in the literature, this concept has been utilized in the flow-system conceptualization that has been incorporated into the model analyses described in this report. If at some point in the future the hydrologic ramifications of the alternative hypothesis of little or no halite dissolution in the Rustler are assessed, and if those ramifications indicate a different interpretation of regional permeability trends, then construction of additional regional simulations that explore this alternative system conceptualization would be very useful.

Description of Dissolution Process

The mechanics and geochemistry of halite dissolution and related secondary processes are complex. The following paragraphs are a brief description of the processes that control halite dissolution in the WIPP region based primarily on the work of Lambert (1983, p. 65-73), Chaturvedi and Channell (1985, p. 46-51), and Snyder (1985, p. 10).

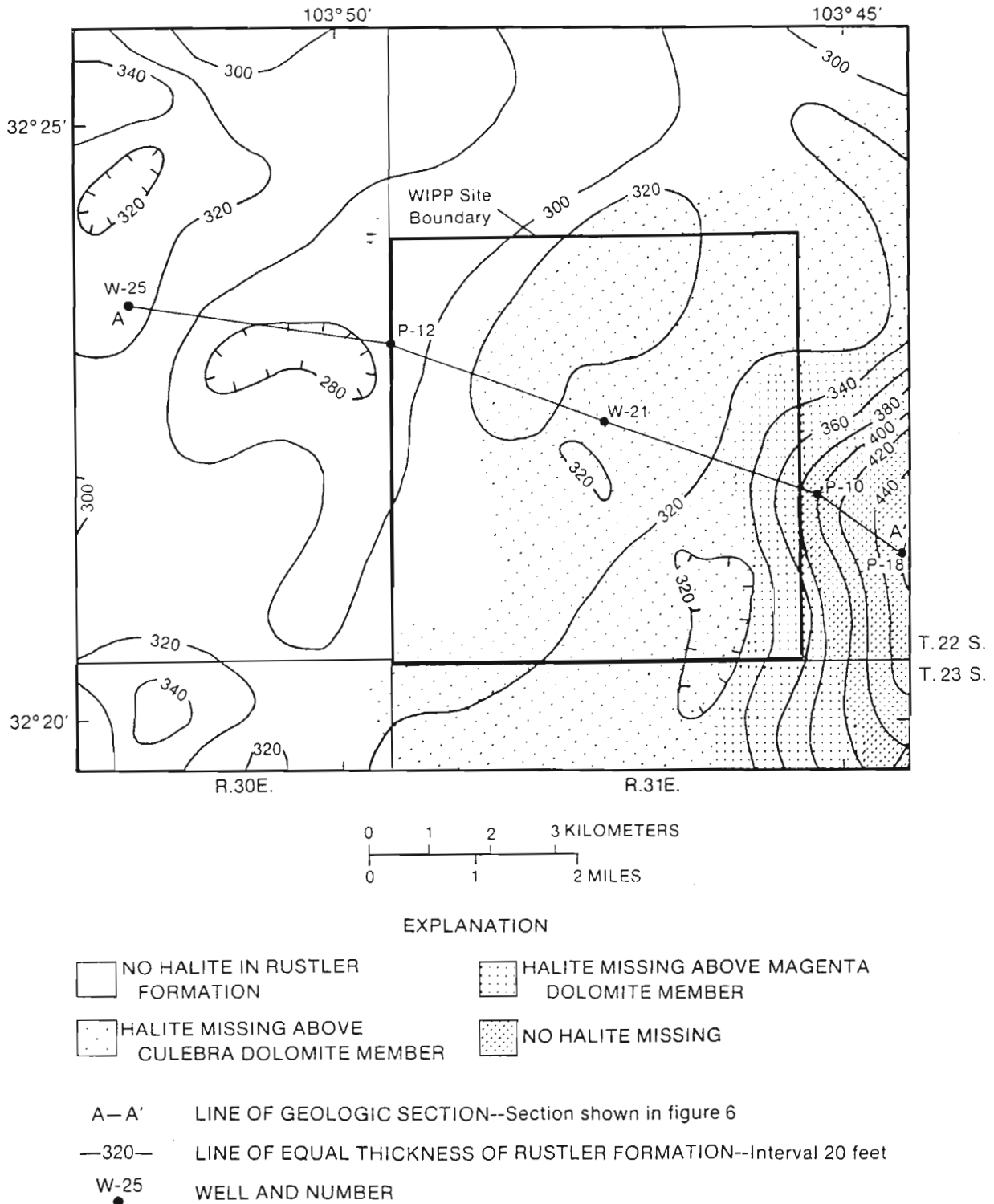


Figure 5.-- Thickness of the Rustler Formation in the vicinity of the WIPP site and areal distribution of halite in the Rustler Formation. (Modified from Snyder, 1985, fig. 4).

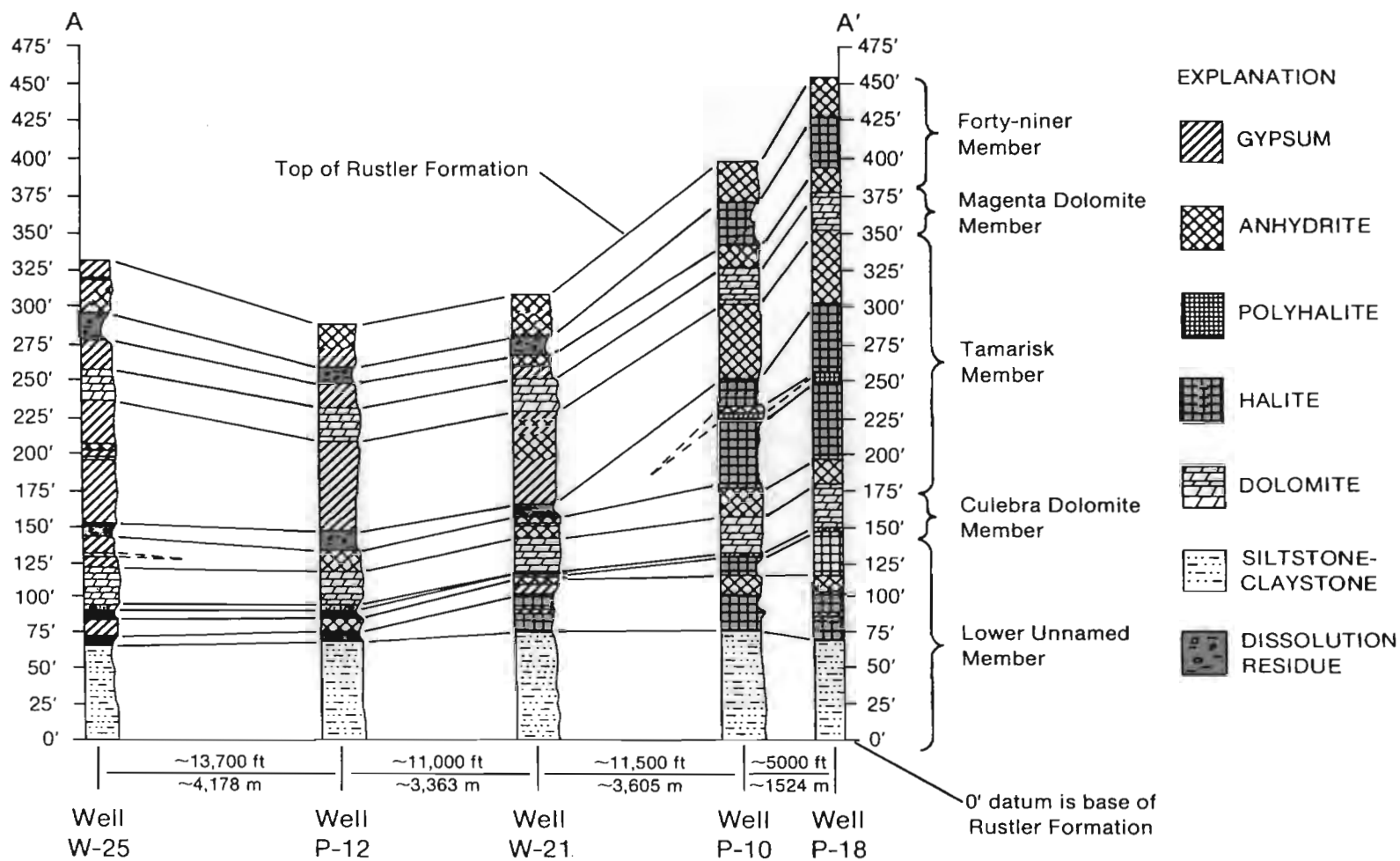
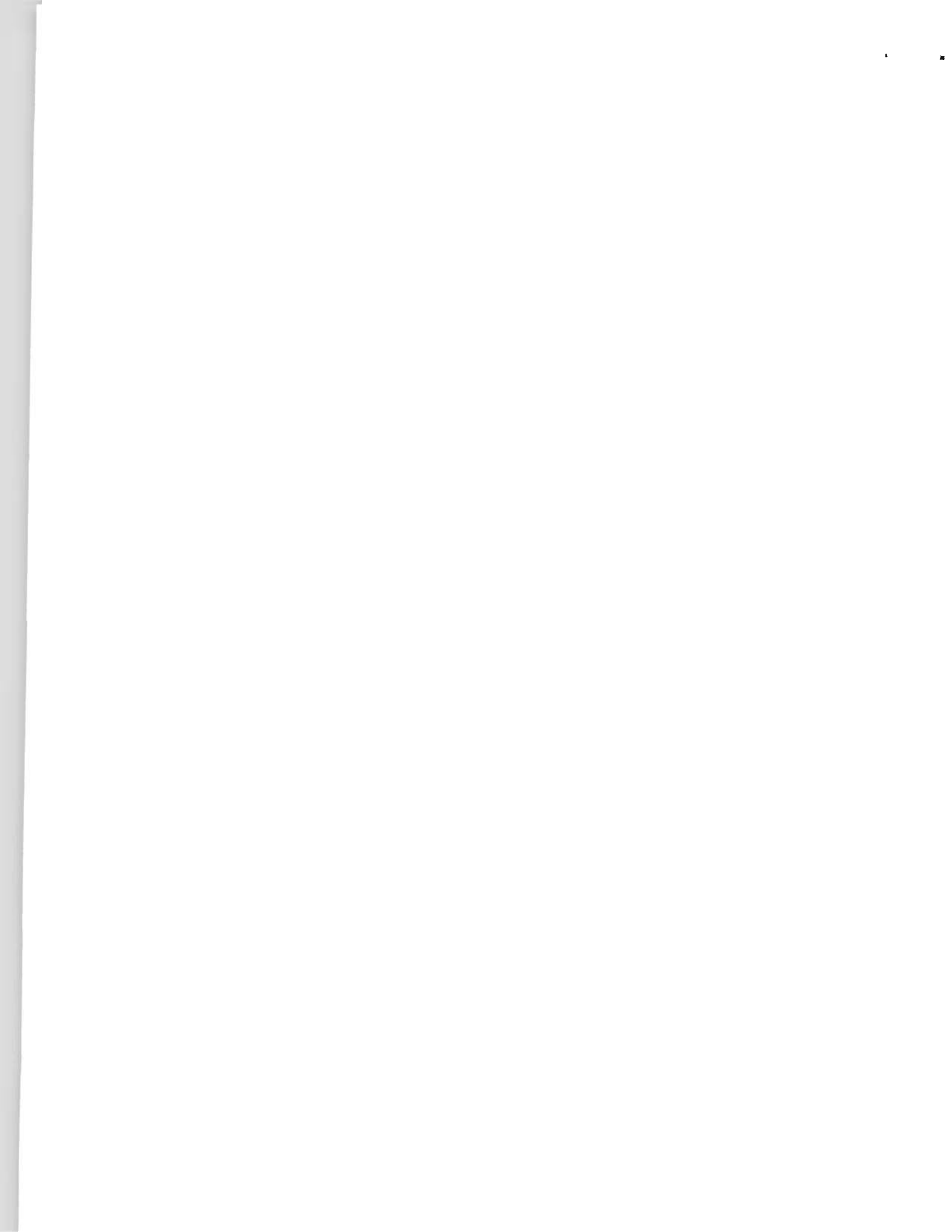


Figure 6.-- Columnar geologic section across the WIPP site showing correlation of lithologic units in the Rustler Formation. See figure 5 for trace of section. (Modified from Snyder, 1985, fig. 2).



Dissolution occurs when undersaturated meteoric water gains access to soluble halite by flow along permeable horizons. On a local scale, halite is dissolved by contact with undersaturated water and is then removed by some combination of convective and diffusive transport. The dissolution process is a "self-feeding" process. Deformation associated with the removal of halite further enhances both the total ground-water flux through a given horizon and localized access between the water-transmitting horizons and the halite beds, which in turn causes further dissolution.

Once the halite in a given area has been removed, solute concentration decreases to a level where the hydration of anhydrite to gypsum can occur. This hydration process produces a substantial volume increase, which, in turn, causes further deformation of the surrounding rock units. Following this hydration process, the gypsum gradually is dissolved and removed.

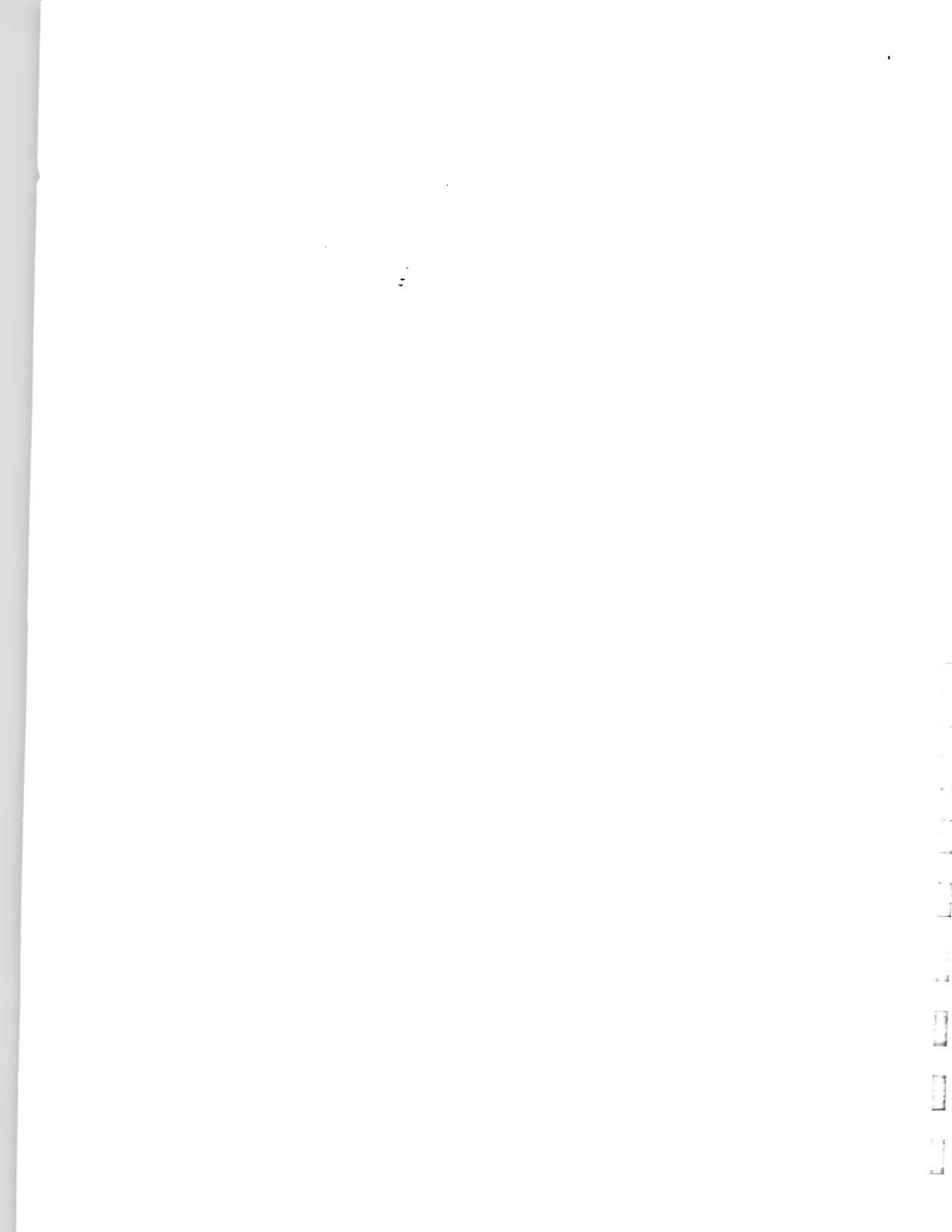
The fracture-enhanced permeability of the relatively brittle Culebra and Magenta Dolomite Members has made these horizons particularly active in the dissolution process. In the Nash Draw area, the fine-grained sandstone at the base of the Rustler is a water-transmitting horizon that also has been particularly active in the dissolution process. Dissolution of the underlying Salado halite has produced a permeable residue and subsidence-related fracturing of the sandstone, which have further enhanced the water-transmitting capabilities of the Rustler-Salado contact zone.

Halite dissolution and related secondary processes have been most active in Nash Draw, causing the removal of all halite beds from the Rustler and from the uppermost Salado. Subsidence associated with this dissolution has produced the 60- to 75-meter-deep valley called Nash Draw, which trends roughly north-south and has two eastwardly trending reentrants, one to the north of the WIPP site and one to the south (fig. 7). In the Nash Draw area, much of the anhydrite in the upper part of the Salado and in the Rustler has been hydrated to gypsum, which has, in turn, been locally dissolved.

Age of Dissolution Activity

Surficial geologic mapping of stream-gravel deposits of the middle Pleistocene Gatuña Formation has shown that Nash Draw was the location of a major stream (fig. 8) during middle Pleistocene time (Bachman, 1985, p. 14-16, 24-27). The Rustler Formation in this area apparently was shallow enough that ground-water circulation associated with this stream caused substantial dissolution-subsidence activity in both the Rustler and upper part of the Salado. This dissolution-subsidence activity was the primary mechanism responsible for the formation of Nash Draw. The earliest phases of dissolution and subsidence may have played an influential role in controlling the location of streamflow during the early phases of channel development.

Calcium sulfate spring deposits of late Pleistocene age on the eastern margin of Nash Draw indicate that by late Pleistocene, Nash Draw was a well developed valley and that dissolution was still active (Bachman, 1981, pl. 2; Bachman, 1985, p. 20, 24). The presence of these spring deposits at an elevation well above the current water table indicates that the late Pleistocene ground-water flow system probably contained more water than is contained in the present-day flow system. The



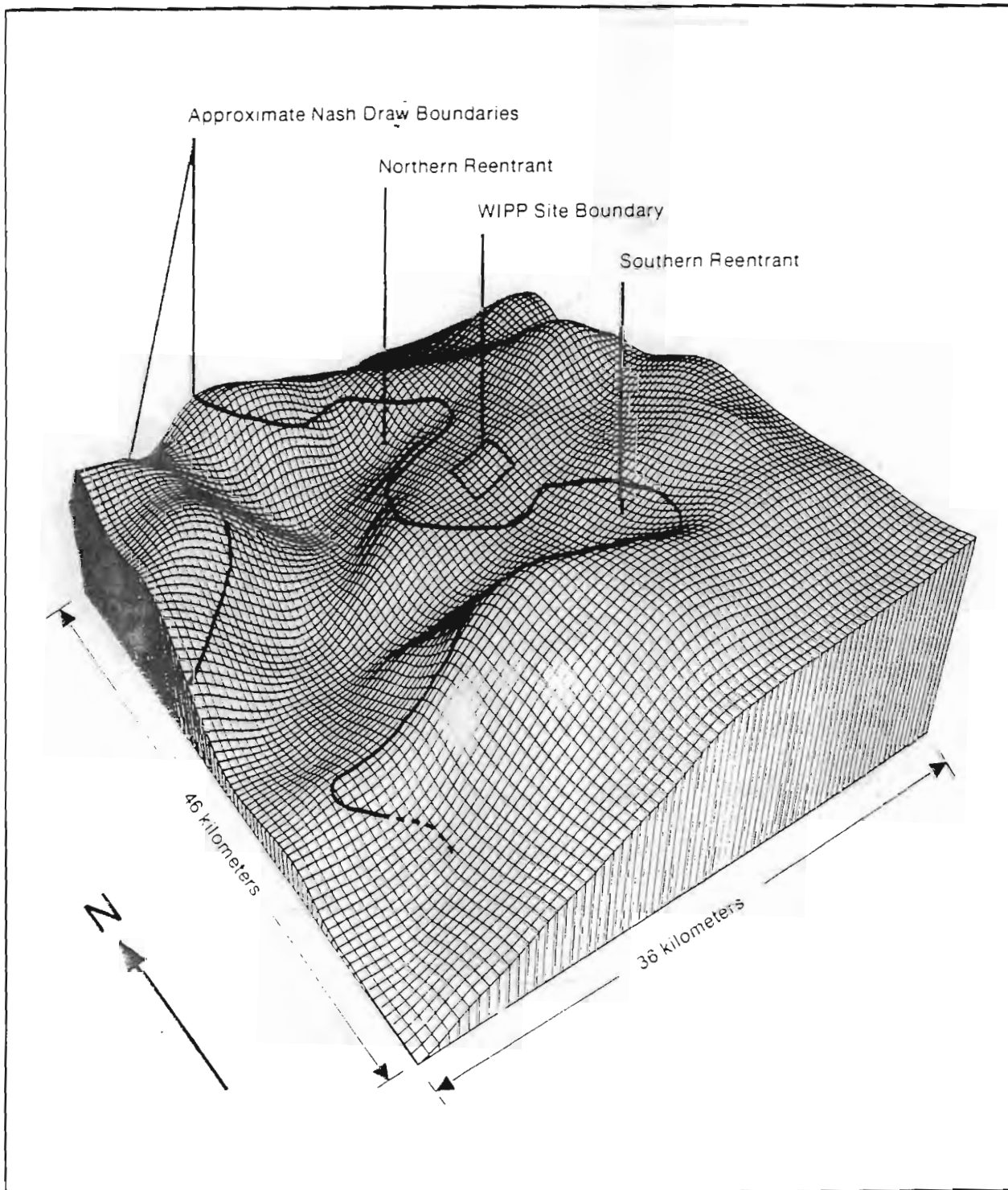
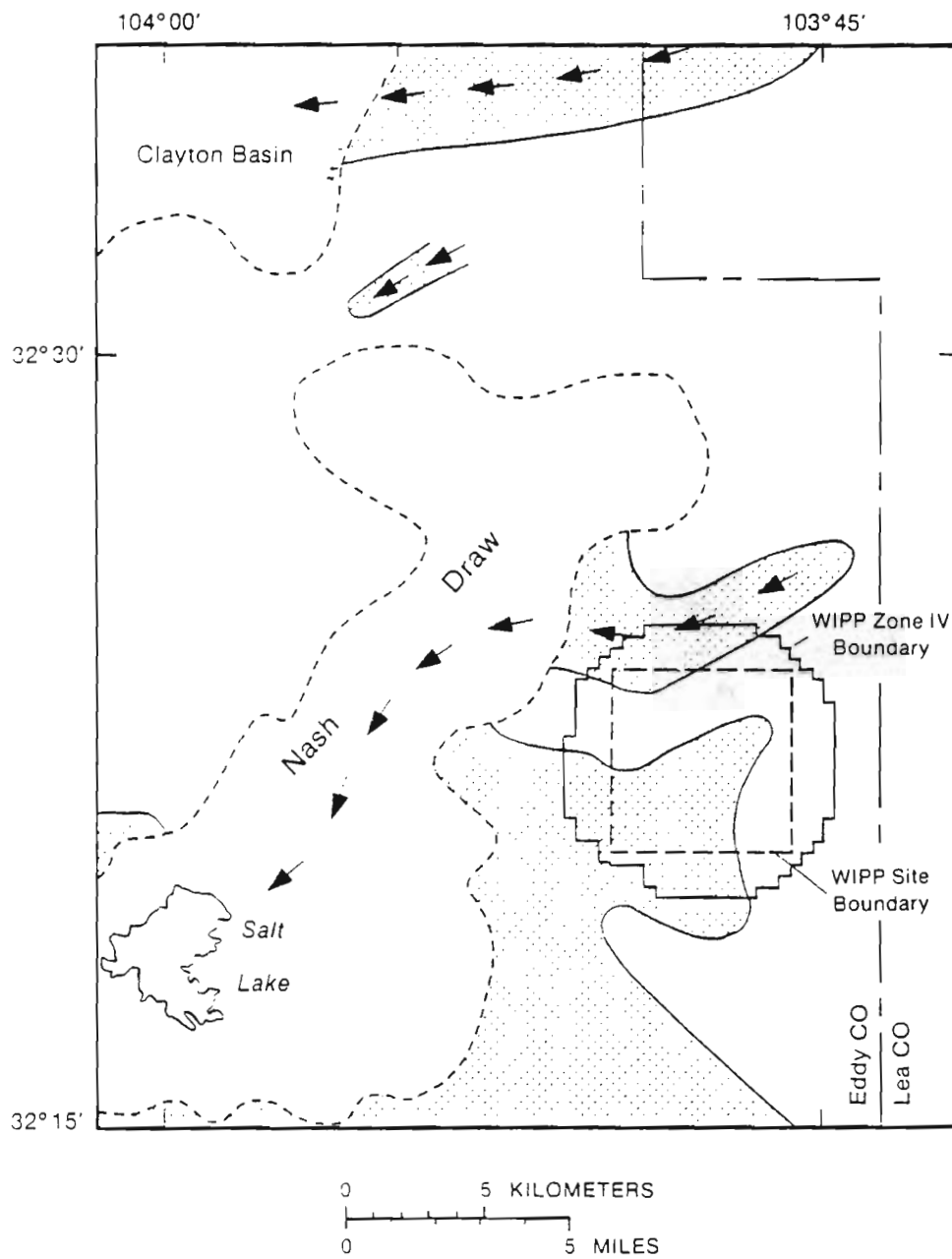


Figure 7.-- Schematic perspective diagram of vertically exaggerated topography in the WIPP region and the spatial relation between Nash Draw and the WIPP site.



EXPLANATION



DISTRIBUTION OF GATUÑA FORMATION



INFERRED COURSE OF STREAMS DURING THE MIDDLE PLEISTOCENE

Figure 8.-- Distribution of the Gatuña Formation and inferred course of streams during the middle Pleistocene. (Modified from Bachman, 1985, fig. 11).

deposits also indicate that dissolution processes were active in the area east of Nash Draw and that in some areas these processes had reached the mature phase of gypsum dissolution.

The present-day climate in the WIPP region is much drier than that during the Pleistocene, and consequently, there is less ground water in circulation than in the past. However, the geochemistry of ground-water samples from the Rustler indicates that halite dissolution and related secondary processes may still be active today (Lowenstein, 1987, p. 36-39), although probably at much slower rates than during the Pleistocene. These processes can be expected to continue into the future at their present relatively slow rate, unless at some time the climate returns to a more humid phase, which would most likely cause an increase in the rate of dissolution.

Hydrologic Implications

Halite dissolution and the related secondary processes described in the previous sections are the primary factors controlling spatial variations in permeability within any given stratigraphic horizon. These processes have also been the primary mechanisms that have controlled the development of Nash Draw, where they have been most active. Nash Draw is a valley (fig. 7) underlain by relatively permeable rock. This combination of low topography and high permeability causes Nash Draw to act as a drain in the regional ground-water flow system. Two reentrants extend eastward from the main north-south-trending body of Nash Draw, extending the low topography and high permeability drain-like conditions to the east.

East of the WIPP site the Rustler Formation is more than 400 meters beneath the land surface. In this area, the Rustler is completely intact, with approximately 50 percent of its thickness comprised of thick, clayey halite beds. The underlying Salado Formation is completely intact as well. Hydrologically, the Rustler is relatively impermeable east of WIPP.

Between the totally intact Rustler east of the WIPP site and the highly altered Rustler in Nash Draw west of the WIPP site is a transition zone. From east to west, the Rustler becomes progressively shallower and thinner, and more halite has been removed from deeper horizons (figs. 5 and 6). Toward the west, mudstone residues occur where muddy halite beds have been removed by dissolution. Also toward the west, progressively more anhydrite has been hydrated to gypsum. This transition zone is characterized by large spatial variability in permeability superimposed on a general trend of increasing permeability toward the west. The WIPP site is located in this transition zone.

ANALYSIS OF FLUID-DENSITY EFFECTS ON GROUND-WATER FLOW

Equivalent-freshwater head is a widely used concept in modeling ground-water flow systems that contain substantial spatial variation in fluid density. Equivalent-freshwater head at a point within an aquifer is defined as the water-level altitude in an imaginary well that is filled sufficiently with freshwater such that the weight of the column of freshwater exactly balances the fluid pressure in the aquifer (Luszczynski, 1961, p. 4248; DeWiest, 1965, p. 307). In other words, equivalent-freshwater head is a mechanism for normalizing water-level measurements and direct-pressure measurements relative to a constant fluid density so that they are related to fluid pressure in a given aquifer in a consistent manner. Luszczynski (1961) and DeWiest (1965) have shown analytically that strictly horizontal flow is driven by gradients of equivalent-freshwater head. If there is a vertical component of flow, however, equivalent-freshwater head does not account for the density-related gravity forces that may contribute to driving fluid flow.

An aquifer is considered approximately horizontal if its dip does not exceed a few degrees. If such an aquifer contains substantial spatial variation in fluid density, the assumption is commonly made that because fluid flow is approximately horizontal, density-related gravity effects are very small and can be ignored. All of the previous ground-water flow models of the WIPP region use equivalent-freshwater head based on the assumption that because the dip of the Culebra Dolomite Member in the Rustler Formation and other water-bearing units in the WIPP region is very small (generally less than 2 degrees), flow is approximately horizontal, and therefore, density-related gravity effects are insignificant (U.S. Department of Energy, 1980a; Cole and Bond, 1980; D'Appolonia Consulting Engineers, 1981; Barr and others, 1983).

The objective of this segment of the WIPP regional ground-water flow analysis was to examine the equivalent-freshwater-head assumption in detail and assess whether density-related gravity effects are significant anywhere in the ground-water flow system in the WIPP region. This assessment was considered a prerequisite to the development of any new ground-water flow models of the WIPP region.

The approach to evaluating density-related gravity effects in the WIPP region was to use the most recent of the previous freshwater-head models (Barr and others, 1983) as a framework for the analysis. This model was chosen because it is a well-documented model that provided a readily adaptable framework for analyzing density effects. The analysis consisted of an analytic determination of the relative magnitudes of density-related and pressure-related driving forces in the Barr and others (1983) model area (fig. 3), complemented by a direct comparison of equivalent-freshwater-head and variable-density simulations.

The remainder of this section describes the theory behind the analytic determination of the relative magnitude of density-related and pressure-related driving forces, an analysis of the relative magnitude of density-related driving forces in the Barr and others (1983) model area, and direct comparisons of equivalent-freshwater-head and variable-density simulations of the Barr and others (1983) model area.

Driving-Force Theory

The relative importance of density-related gravity effects can be examined by expanding the gravity term in Darcy's Law and separating an equivalent-freshwater-head term, which represents the pressure-driven component of flow, from a density-related term, which represents the gravity-driven component of flow. The following derivation is adapted from Davies (1987, p. 889-893). The starting point for this derivation is Darcy's Law for an isotropic medium:

$$\bar{v} = - \frac{k}{\mu} [\nabla p - \rho \bar{g}] \quad (1)$$

where

- \bar{v} = Darcy velocity vector [L/T];
- k = intrinsic permeability [L²];
- μ = fluid viscosity [M/LT];
- ∇p = gradient of fluid pressure [1/L•M/LT²];
- ρ = fluid density [M/L³]; and
- \bar{g} = gravitational-acceleration vector [L/T²].

The gravitational-acceleration vector can be defined in terms of elevation measured relative to a specified datum as follows:

$$\bar{g} = - |g| \nabla E \quad (2)$$

where

- $|g|$ = magnitude of gravitational acceleration [L/T²]; and
- ∇E = gradient of elevation [1/L•L].

Substituting equation 2 into equation 1 yields:

$$\bar{v} = - \frac{k}{\mu} [\nabla p + \rho |g| \nabla E] \quad (3)$$

The relation between fluid density and solute concentration can be described by an equation of state, which is a first-order Taylor expansion about a reference density:

$$\rho = \rho_0 (1 + \alpha (c - c_0)) \quad (4.1)$$

or

$$\rho = \rho_0 + \Delta\rho \quad (4.2)$$

where

- ρ_0 = reference fluid density [M/L³];
- c = solute concentration [M/L³];
- c_0 = reference solute concentration [M/L³];
- α = volumetric-expansion coefficient [L³/M]; and
- $\Delta\rho$ = difference between actual fluid density and reference-fluid density [M/L³].

Equivalent-freshwater head at a given point within an aquifer containing fluid-density variations is defined as the water-level elevation, measured relative to a standard datum, in a well sufficiently filled with freshwater to balance the pressure at the given point. This can be expressed analytically as follows:

$$H_f = \frac{p}{\rho_f |g|} + E \quad (5)$$

where

- H_f = freshwater head [L];
- p = pressure [M/LT²];
- ρ_f = density of freshwater [M/L³]; and
- E = elevation relative to datum [L].

In order to quantify the assumptions inherent in the use of equivalent-freshwater head, equations 3, 4, and 5 are combined to produce an expression that contains an explicit, equivalent-freshwater-head term and a density-related error term that is implicitly assumed to be insignificant

when equivalent-freshwater heads are used. For this analysis, the reference-fluid density is equal to the density of freshwater, and the reference-solute concentration is zero:

$$\rho_0 = \rho_f \quad (6.1)$$

and

$$c_0 = 0 \quad (6.2)$$

Substituting equations 4.1, 6.1, and 6.2 into equation 3 yields:

$$\bar{v} = - \frac{k}{\mu} [\nabla p + \rho_f (1 + \alpha c) |g| \nabla E] \quad (7)$$

Because ρ_f and $|g|$ are constant, equation 7 can be rearranged as follows:

$$\bar{v} = - \frac{k |g| \rho_f}{\mu} \left[\nabla \left(\frac{p}{\rho_f |g|} + E \right) + \alpha c \nabla E \right] \quad (8)$$

Finally, substitution of equation 5 into equation 8 yields:

$$\bar{v} = - \frac{k |g| \rho_f}{\mu} [\nabla H_f + \alpha c \nabla E] \quad (9.1)$$

or, by substituting equation 4.2 for equation 4.1:

$$\bar{v} = - K \left[\nabla H_f + \frac{\Delta \rho}{\rho_f} \nabla E \right] \quad (9.2)$$

where

$$K = \frac{k |g| \rho_f}{\mu} = \text{hydraulic conductivity [L/T].}$$

The first term inside the brackets in equations 9.1 and 9.2 is the gradient of equivalent-freshwater head, whereas the second term in the brackets is a density-related error term. In situations where solute concentrations are small or where changes in elevation within the flow domain are small, the density-related error terms in equations 9.1 and 9.2 are small. However, if the gradient of equivalent-freshwater head is small as well, then density-related gravity effects may be significant. In other words, it is not the absolute magnitude of the density-related error term that controls its significance in a given flow situation, but rather, its magnitude relative to the magnitude of the gradient of equivalent-freshwater head.

Equations 9.1 and 9.2 can also be viewed in terms of the separate forces that drive fluid flow (fig. 9). The gradient of equivalent-freshwater head represents the component of flow that is driven by fluid-pressure differentials. The density-related error term represents the component of flow that is driven by gravity. Under most conditions, these two flow components differ in both magnitude and direction. The actual flow direction is the resultant of the pressure-driven and gravity-driven flow components. Significant errors in the direction and magnitude of flow predicted by equivalent-freshwater heads can occur if the gravity-driven component of flow, which is ignored in calculations based on equivalent-freshwater head, is of approximately equal or greater magnitude than the pressure-driven flow component.

A useful measure of the relative importance of the gravity-driven flow component is the dimensionless ratio of the magnitude of the gravity term to the magnitude of the pressure term, which is referred to as the driving-force ratio. This ratio can be expressed either in terms of solute concentration (eq. 10.1) or in terms of fluid density (eq. 10.2):

$$DFR = \frac{\alpha c |\nabla E|}{|\nabla H_f|} \quad (10.1)$$

or

$$DFR = \frac{\Delta \rho |\nabla E|}{\rho_f |\nabla H_f|} \quad (10.2)$$

where

- DFR = driving-force ratio [dimensionless];
- $|\nabla E|$ = magnitude of the gradient of elevation [dimensionless]; and
- $|\nabla H_f|$ = magnitude of the equivalent-freshwater-head gradient [dimensionless].

The driving-force ratio provides a convenient parameter for determining the potential for significant density-related gravity effects in field situations, as the properties required to evaluate equation 10.1 or equation 10.2 are readily measured. For the example driving-force plot shown in figure 9, the driving-force ratio is 0.5, and the error in predicted flow direction is 30 degrees, assuming an isotopic medium. A driving-force ratio of 0.5 can be considered an approximate threshold at which density-related gravity effects may become significant. This threshold may vary

Driving-Force Vector Components

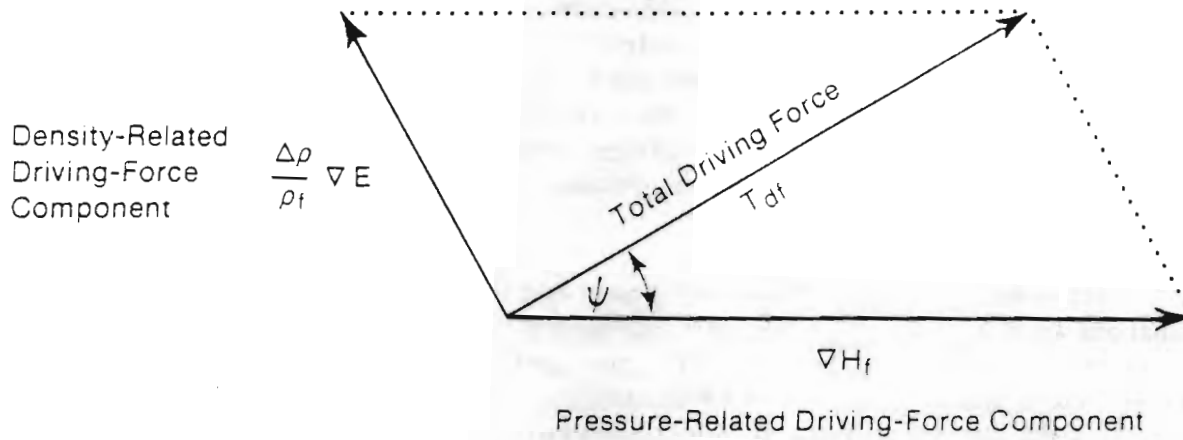


Figure 9.-- Relation between pressure-related driving-force component, density-related driving-force component, and the total driving force.

somewhat depending on the actual flow conditions and on the accuracy requirements of a particular study.

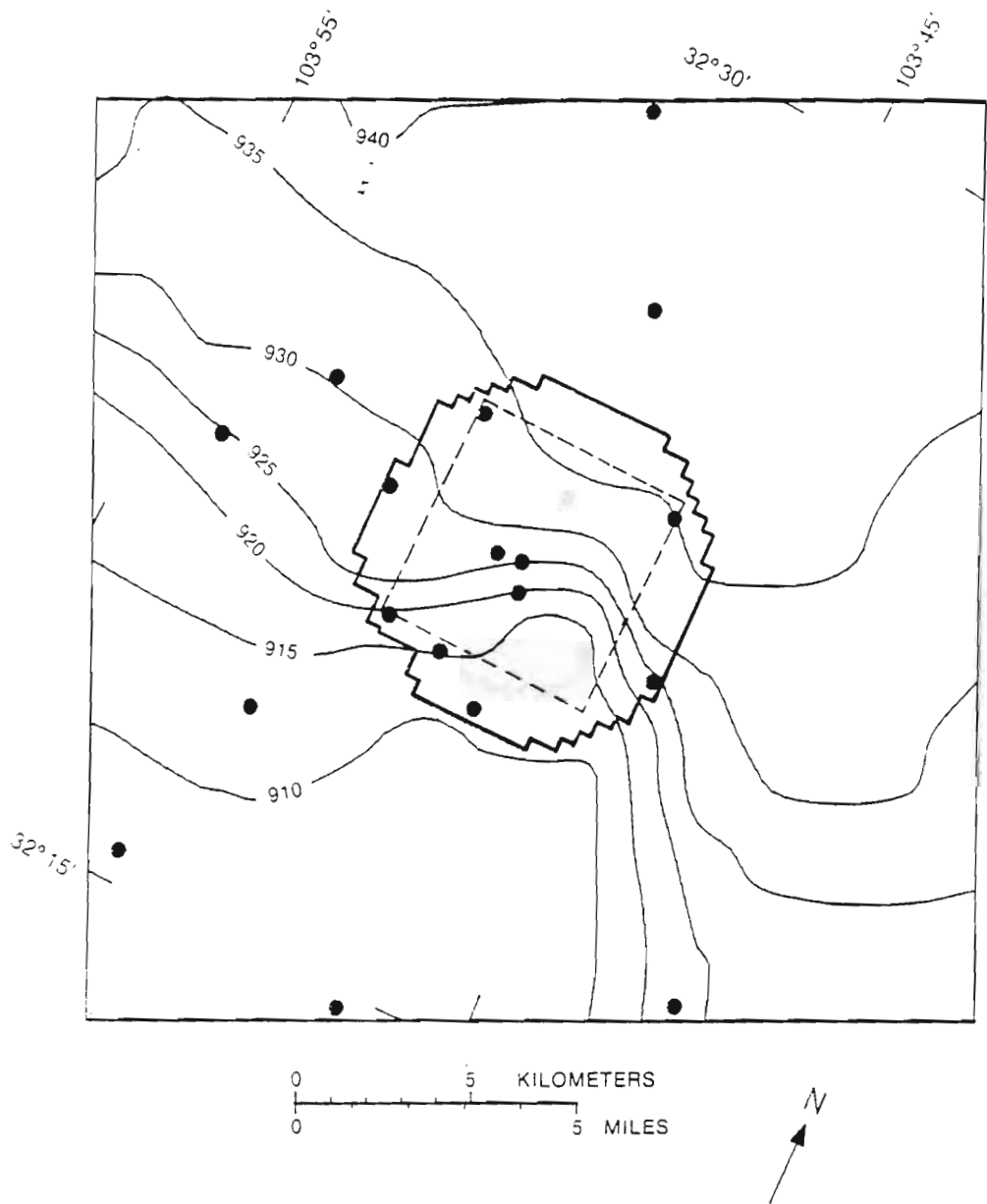
Driving-Force Analysis of the Model Area of Barr and Others (1983)

For the case of a relatively thin aquifer in which flow parallels the upper and lower bounding surfaces, the data required to compute the driving-force ratio are equivalent-freshwater head, fluid density, and aquifer elevation (structure). Equivalent-freshwater head in the Culebra Dolomite Member for the Barr and others (1983) model area is shown in figure 10. Head gradients range from a maximum of 7 meters per kilometer (37 feet per mile) in the vicinity of the WIPP site to a minimum of approximately 4 centimeters per kilometer (0.2 foot per mile) in areas north and south of the site. The fluid-density distribution of the Culebra in the Barr and others (1983) model area is shown in figure 11. Measured densities range from 1.000 to 1.104 grams per cubic centimeter. Freshwater is present in the southwest, whereas brine is present in the east and northwest.

Because the variable-density modeling code used in this study for the ground-water flow simulations was constrained to modeling a planar aquifer, a best-fit, first-order trend surface was used to characterize aquifer structure. This constraint was imposed to facilitate comparisons between flow simulations and the driving-force analysis of density-related gravity effects. The trend-surface fit yields a regional strike of 4 degrees east of north and a regional dip of 0.44 degree to the east.

Driving-force ratio (DFR) values for the Barr and others (1983) model area were computed by discretizing the equivalent-freshwater-head and fluid-density maps into 1.6- by 1.6-kilometer cells, computing a local equivalent-freshwater-head gradient for each grid cell and a regional aquifer-elevation gradient, and computing a DFR value for each grid cell using equation 10.2. In addition to computing the driving-force ratio for each cell, the density-related and pressure-related driving-force components (illustrated in fig. 9) also were computed. The results of these computations are shown on a contour map of the magnitude of the driving-force ratio (fig. 12) and a vector plot of the relative magnitude and direction of the driving-force components (fig. 13).

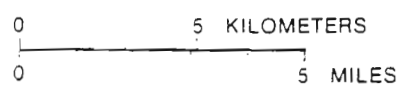
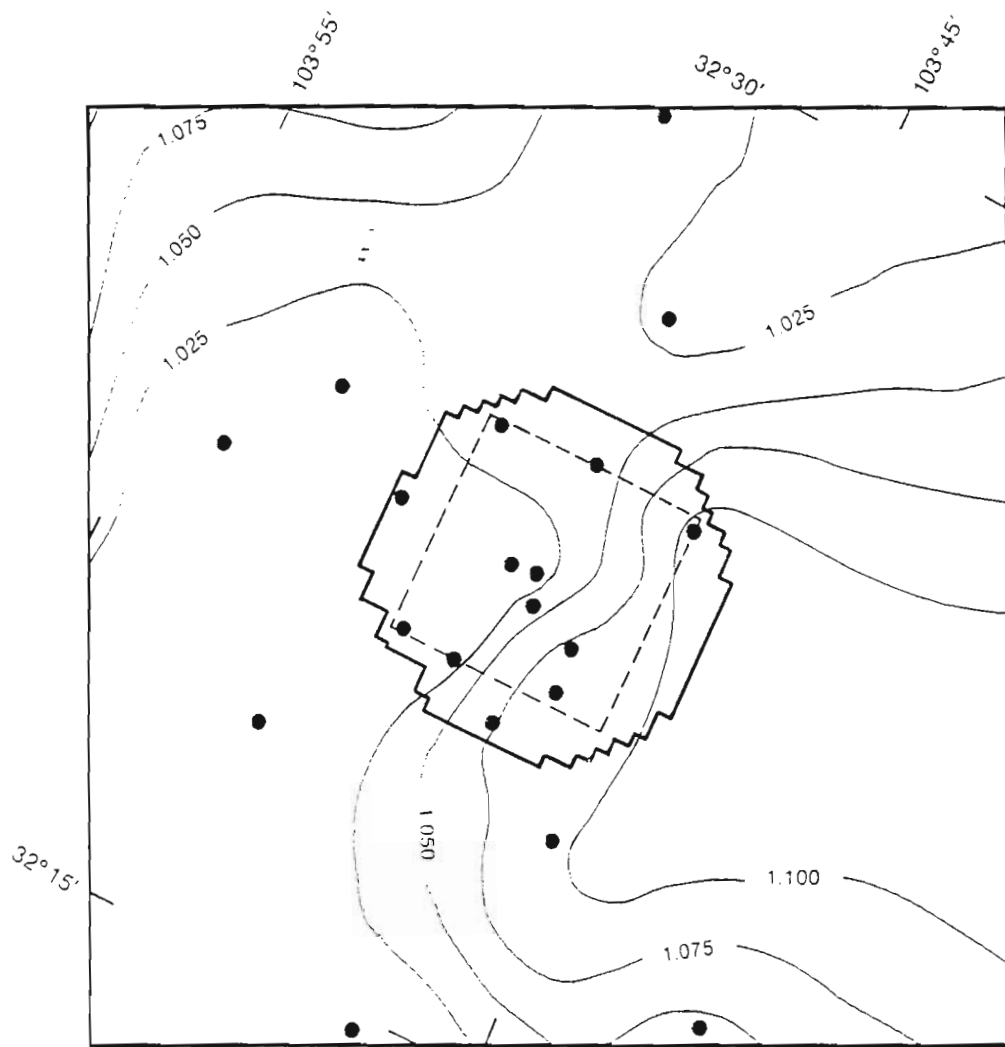
The contour plot of the magnitude of the driving-force ratio (fig. 12) clearly shows where density-related gravity effects are significant and where they are not. As mentioned previously, the approximate threshold above which density-related gravity forces exert a significant influence on ground-water flow is $DFR = 0.5$. In figure 12, this line separates the stippled and nonstippled areas. There are two areas in which DFR values greater than this threshold indicate that density-related gravity effects are significant. One area is to the east and northeast of the WIPP site (fig. 12), where DFR values reach a maximum of 3. The other area is south of the WIPP site (fig. 12), where DFR values reach a maximum of 31. The large DFR values south of the WIPP site indicate that the gravity-driven component of flow in this area is completely dominant. There are also large areas where DFR values are less than the 0.5 threshold, including the WIPP site and most of the area to the west.



EXPLANATION

- 910 — FRESHWATER HEAD CONTOUR— Shows altitude at which water having a density of 1.00 gram per cubic centimeter would have stood in a tightly cased well. Contour interval 5 meters. Datum is sea level
- WIPP ZONE IV BOUNDARY
- WIPP SITE BOUNDARY
- WELL

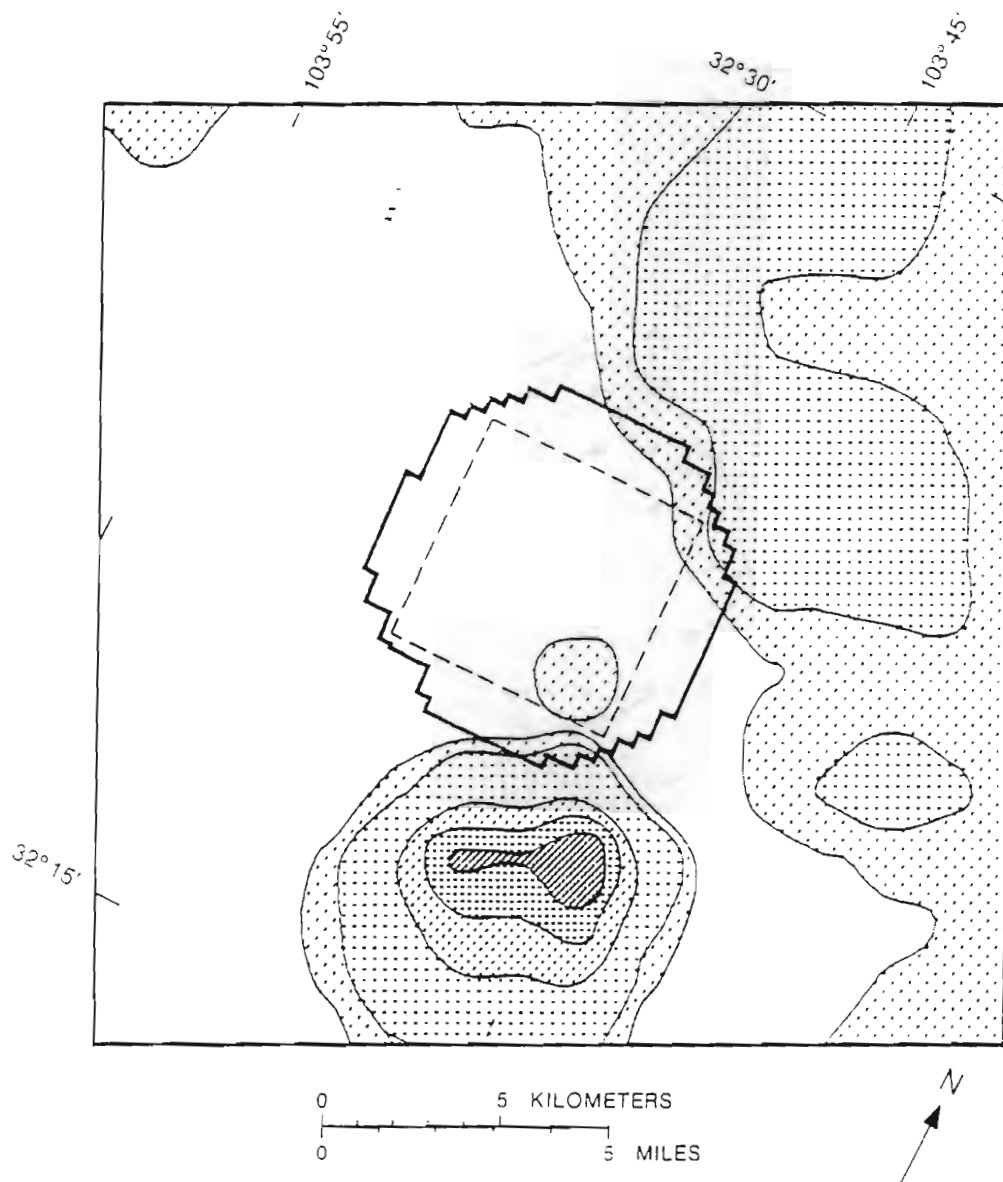
Figure 10.-- Equivalent-freshwater head for wells completed in the Culebra Dolomite Member of the Rustler Formation. Head distribution from Barr and others (1983, fig. 5).



EXPLANATION

- 1.100 — LINE OF EQUAL FLUID DENSITY--Interval 0.025 gram per cubic centimeter
- WIPP ZONE IV BOUNDARY
- - - - - WIPP SITE BOUNDARY
- WELL

Figure 11.-- Fluid density in wells completed in the Culebra Dolomite Member of the Rustler Formation. Data from Mercer (1983), Lambert and Robinson (1984), Westinghouse Electric Corp. (1985), Intera Technologies Inc. and Hydro Geochem Inc. (1985), and Intera Technologies Inc. (1986).



EXPLANATION

DRIVING FORCE RATIO
MAGNITUDE (DIMENSIONLESS)

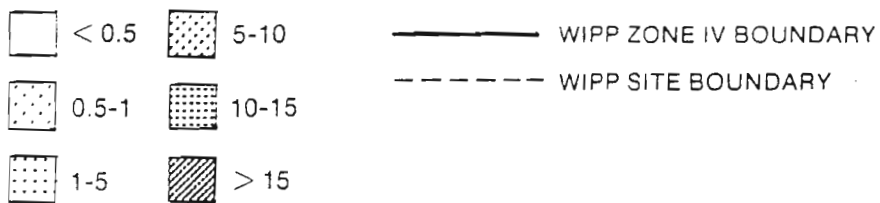


Figure 12.-- Areal distribution of the dimensionless driving-force ratio in the model area of Barr and others (1983).

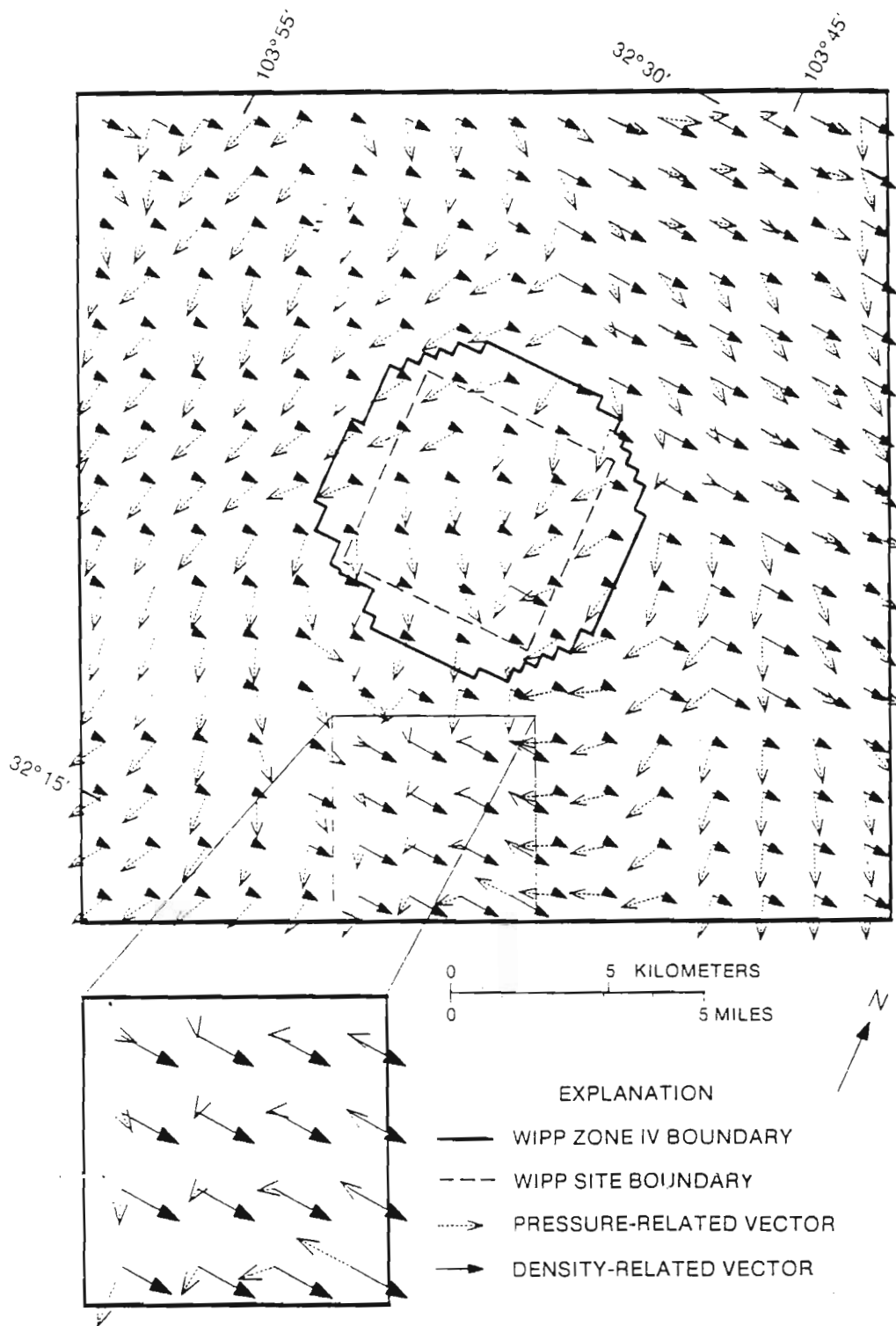


Figure 13.-- Relative magnitude and direction of density-related and pressure-related driving-force vector components in the model area of Barr and others (1983). Vector lengths are scaled locally at each position to show relative magnitude of driving-force components at that single location.

The vector plot of the relative magnitude and direction of the density-related and pressure-related driving-force components (fig. 13) is useful in determining whether fluid densities have an effect on ground-water flow directions. In areas where the driving-force ratio is small, in the vicinity of the WIPP site and to the west (fig. 12), the magnitude of the density-related driving-force component is negligible, and pressure-related driving forces control ground-water flow (fig. 13). Because density effects are insignificant, equivalent-freshwater head adequately characterizes ground-water flow in these areas.

North and northeast of the WIPP site, driving-force ratios are greater than the 0.5 threshold (fig. 12), indicating that the density-related driving-force component will make a significant contribution to driving fluid flow. To the north, the angle between the two driving-force components is large (fig. 13), indicating that equivalent-freshwater-head simulations, which ignore the density-related driving-force component, will produce misleading flow directions in this area. To the northeast, the angle between the two driving-force components is small (fig. 13). Therefore, density-related driving forces in this area will increase the magnitude of the total driving force, thereby increasing velocity magnitudes. However, because of the small angle, density-related driving forces will not cause a large deviation from the flow directions predicted by equivalent-freshwater-head simulations.

South of the WIPP site, density-related driving-force components are as much as an order of magnitude larger than the pressure-related driving-force components (fig. 13). The density-related driving-force components are not only much greater in magnitude, but the angle between the two driving-force components is very large, almost 180 degrees in some areas. Because flow simulations based on equivalent-freshwater head ignore the density-related driving forces, such simulations will produce large errors in predicted flow direction in this area. Flow directions in this area south of the site are important because this area may include flow paths for potential contaminant transport away from the site.

Comparison of Freshwater-Head and Variable-Density Flow Simulations

A second approach to evaluating the relative importance of density-related flow effects is to construct both equivalent-freshwater-head and variable-density simulations and then compare the results. The strategy for making this comparison for the WIPP study was to reconstruct the equivalent-freshwater-head solution presented in Barr and others (1983) and then construct a similar model using a variable-density solution that accounts for density-related gravity effects.

The original model presented by Barr and others (1983) used ISOQUAD, a finite-element flow and transport code written by Pinder (1974). The model consisted of a steady-state solution using specified-head boundary conditions around the perimeter of the area and incorporating an anisotropic hydraulic-conductivity distribution determined from aquifer tests. Anisotropy was characterized with a major-to-minor axis ratio of 2.3:1, with the major axis oriented 25 degrees west of north. After the flow model was constructed, a number of contaminant transport scenarios

were examined. Additional information about this model is contained in the report by Barr and others (1983).

The procedure for reworking the equivalent-freshwater-head model using a variable-density flow code was to convert hydraulic conductivity to permeability, convert specified freshwater-head boundary conditions to specified-pressure boundary conditions, and incorporate the fluid-density distribution (fig. 11) using a corresponding dimensionless solute distribution. For this model, the x-y coordinate plane was tilted to coincide with the slope of the Culebra, and the regional strike and dip were used to compute the magnitude of the gravitational vector acting in the plane of the aquifer. The variable-density, finite-element code SUTRA (Voss, 1984) was used for these simulations.

The variable-density simulation was used to produce a steady-state pressure distribution consistent with the measured density (solute) distribution. The basic assumption behind this approach is that there is no significant solute redistribution over the time frame of interest, which is similar to the rationale behind the steady-state variable-density flow codes by Weiss (1982) and Kuiper (1983, 1985). This assumption was tested for the variable-density rework of the Barr and others (1983) model using transient simulations to determine the length of time required for significant solute redistribution to occur.

An effective means of characterizing the results of this variable-density simulation is to plot a direct comparison of the flow fields produced by this simulation and by the equivalent-freshwater-head simulation (fig. 14). In the vicinity of the WIPP site and to the west, where driving-force ratios are less than the 0.5 threshold, there are no significant differences between the equivalent-freshwater-head and variable-density simulations. This occurs because the pressure-related driving-force component, which is adequately characterized by equivalent-freshwater head, is dominant in these areas. To the northeast, where driving-force ratios are greater than the 0.5 threshold and the angle between the two driving-force components is small, the equivalent-freshwater-head simulation predicts the correct flow direction; however, it underestimates velocity magnitudes by as much as a factor of 2.

South and north of the WIPP site, where driving-force ratios are greater than the 0.5 threshold and the angle between the two flow-driving components is large, the equivalent-freshwater-head simulation produces large errors in both flow direction and velocity magnitude. In the important area south of the WIPP site, flow-direction errors produced by the equivalent-freshwater-head simulation are as large as 170 degrees. Also, the equivalent-freshwater-head simulation underestimates velocity magnitudes by an order of magnitude or more.

After the steady-state simulations were completed, a series of transient simulations was made to determine the length of time required for flow to change the solute distribution enough to cause significant changes in the flow pattern. Because of the relatively low permeability of rocks in the vicinity of the WIPP site, flow velocities are slow and solute redistribution takes place slowly. The transient simulations indicate that flow patterns remain approximately constant over a 100-year time period, but after 1,000 years, enough solute redistribution would occur that flow patterns would begin to deviate from the steady-state configuration.

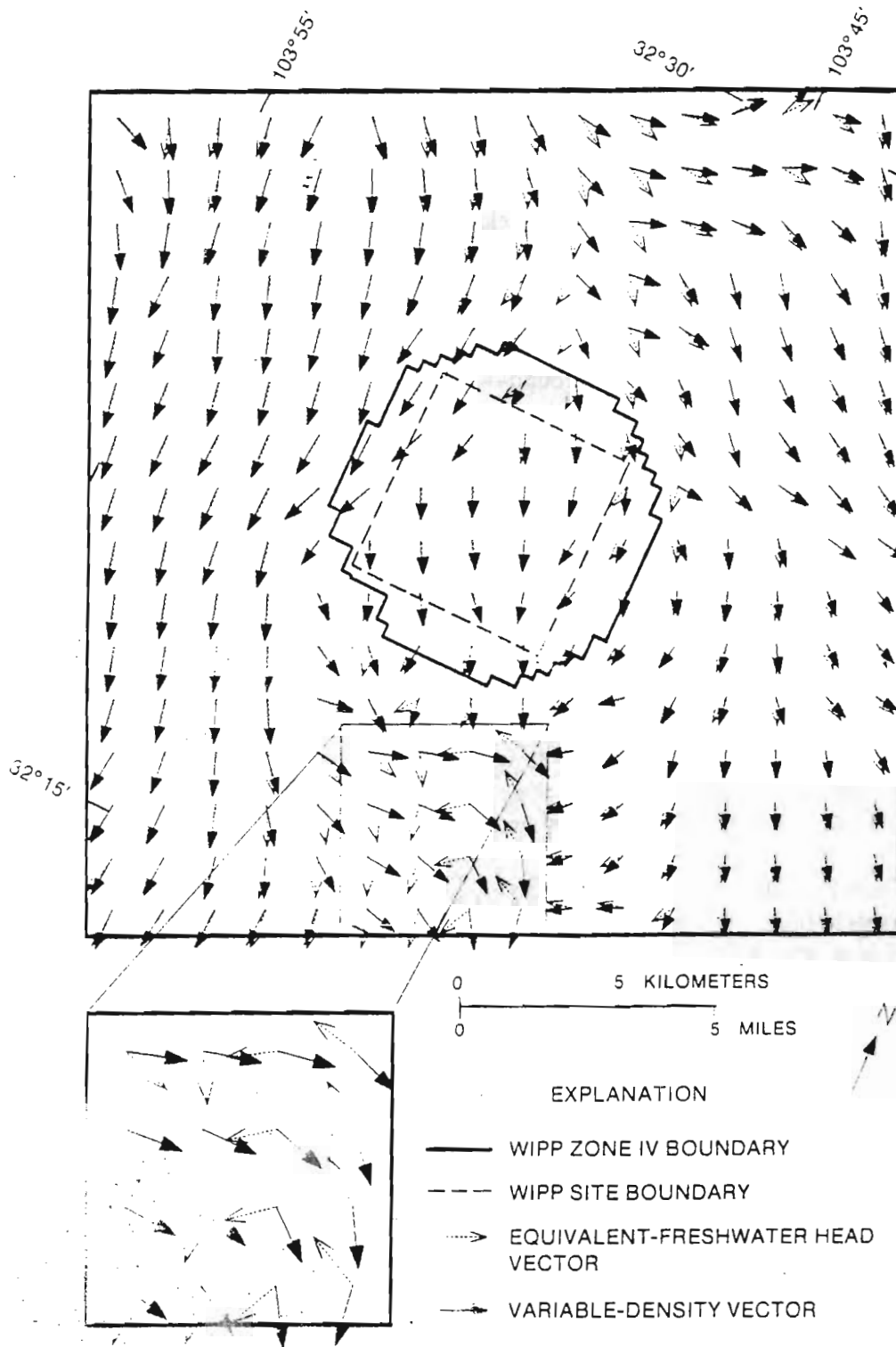


Figure 14.-- Comparison of flow velocities and directions computed by the equivalent freshwater-head simulation and by the variable-density simulation in the model area of Barr and others (1983). Vector length is proportional to log of velocity with the maximum velocity of 2×10^{-6} m/s having a vector length of 0.3 inch.

Summary and Conclusions

The objective of the driving-force analysis and comparative modeling study described in this section was to determine whether or not density-related gravity effects have a significant impact on flow patterns in the WIPP region. If density-related gravity effects are insignificant, then the equivalent-freshwater-head concept can be utilized in modeling studies and other hydrologic analyses. However, if density-related gravity effects are significant, then analyses based on equivalent-freshwater head may produce misleading results. In this case, density effects must be explicitly accounted for by using variable-density simulation codes or other appropriate analytic techniques.

The driving-force analysis of ground-water flow in the Culebra Dolomite Member in the WIPP region indicates that although density-related gravity effects are not significant at the WIPP site and to the west, they are significant in areas to the north, northeast, and south of the site. The area where density effects appear to be most significant is to the south, where the combination of a gently dipping Culebra, moderate fluid densities, and very flat freshwater-head gradients create flow conditions in which the density-related flow component is dominant. This area is important because it contains flow paths that extend southward from the WIPP site, which are potential contaminant-transport pathways.

A direct comparison of equivalent-freshwater-head and variable-density flow simulations has shown that at the WIPP site and to the west, where density-related gravity effects are insignificant, equivalent-freshwater heads adequately characterize the flow-driving forces. In contrast, in the area south of the WIPP site where the density-related flow component appears to dominate, simulations based on equivalent-freshwater head produce very misleading information on predicted flow directions and velocity magnitudes.

The combination of the driving-force analysis and comparative simulations described in this section clearly demonstrates that density effects can be quite significant in the WIPP region. Thus, density effects need to be explicitly addressed in some rigorous manner in future modeling studies and other hydrologic analyses.

ANALYSIS OF THE REGIONAL-SCALE FLOW SYSTEM IN THE CULEBRA DOLOMITE MEMBER OF THE RUSTLER FORMATION

The primary objective of the analysis of the flow system in the Culebra Dolomite Member of the Rustler Formation on a regional scale was to develop a more thorough understanding of the relation between ground-water flow in the vicinity of the WIPP site and flow in the larger regional system. This analysis was designed to provide information on questions such as what impact, if any, do distant stresses have on flow in the site area? If radionuclides were transported beyond the site, where would these contaminants be transported? What are the implications of the regional flow system for the boundary conditions that are used for more detailed site-scale modeling?

Simulating at a regional versus local scale involves tradeoffs. Although examination of a given flow system on a regional scale may provide important information about regional-scale phenomena that are difficult to recognize or characterize in a small area, the coarser resolution of the regional-scale data limits the degree of detail in conclusions that can be drawn concerning localized flow behavior. Comprehensive, high-density, and good-quality data that are available for a thoroughly characterized site are usually not available at the regional scale. Regional- and local-scale analyses have different data requirements and they are used to address different types of questions. These analyses serve complementary functions of providing an understanding of the overall controls and behavior of flow on a regional scale, and the occurrence and character of localized flow phenomena.

The first step in the construction of the WIPP regional ground-water flow model was to assemble the available regional hydrologic and geologic data from the literature and from existing U.S. Geological Survey data bases, and to merge this information with published data from WIPP-related field studies. The strengths and weaknesses of the WIPP regional data set are a direct function of the primary data sources, which include limited drilling for water supplies; extensive drilling for oil, gas, and potash exploration; and a few locally focused hydrogeologic studies. Although the Culebra Dolomite Member appears to be a relatively significant water-bearing unit throughout much of the WIPP region, there are few wells beyond the vicinity of the WIPP site that have been carefully tested or completed in this unit. Therefore, water-level and water-quality information from wells completed over some larger, unspecified part of the Rustler have been used as a first approximation of conditions in the Culebra in the regional-scale analysis. During the calibration process, more weight was given to WIPP-related wells completed in only the Culebra than was given to distant wells with uncertain completion. Fluid density has rarely been directly measured in wells not related to the WIPP project. However, a reliable surrogate for fluid density such as dissolved-solids concentration or specific conductance commonly is available. Due to extensive drilling for oil, gas, and potash exploration, there is excellent control on elevation (structure) and thickness of the Culebra. The most significant weakness in the regional data is in the area east of WIPP, where no water-level or water-quality data are available. This absence of hydrologic data to the east was the primary motivation for analyzing model sensitivity to a variety of boundary conditions in the eastern part of the flow system.

The next step in the construction of the model was to define the boundaries of the model region. Most of the previous WIPP ground-water models incorporate a single set of rectangular-

shaped, specified-head (pressure) boundary conditions. The use of this type of boundary assumes that the head distribution is known along all boundaries and that this distribution does not change over the time period of interest. In order to improve the characterization of the flow-system boundaries, boundaries for the regional model were selected to coincide wherever possible with hydrologically significant features. Specifying model boundaries that coincide with hydrologic features that are likely to remain constant over long periods of time is an important step in characterizing the long-term behavior of a flow system. As part of the boundary selection process, a driving-force analysis was carried out for the WIPP region to aid in the selection of model boundaries that are not strongly influenced by density-related gravity effects.

Following the selection of model boundaries, a combination of aquifer-test data and geologic information on halite dissolution and burial depth was used to map regional hydraulic-conductivity trends. A more detailed hydraulic-conductivity distribution in the vicinity of the WIPP site, based on a model analysis of large-scale pumping tests and hydraulic response to shaft construction (Haug and others, 1987), then was merged with the regional hydraulic-conductivity distribution to produce the distribution used in the regional model.

The simulation analysis began with the calibration of a baseline, steady-state pressure solution that was consistent with the specified (observed) density distribution, the specified boundary conditions, and the equivalent-freshwater-head distribution before the test shaft was completed. Calibration was accomplished by making small changes in the hydraulic-conductivity distribution that were consistent with regional hydraulic-conductivity trends. This baseline, steady-state simulation was then used as a reference point to examine (1) sensitivity of the flow system to fluid-density effects, (2) assumptions underlying the use of a specified density distribution in a steady-state solution, (3) boundary-condition uncertainty, (4) sensitivity of the flow system to water levels in the Pecos River, and (5) the possibility of vertical flux as a source of recharge.

Regional Driving-Force Analysis

A preliminary look at regional system boundaries indicated that a no-flow boundary coincident with a well-defined flow line would be useful for one or more boundaries in the WIPP regional model. However, a significant problem with this type of boundary in a variable-density environment like the WIPP region is that "flow lines" identified on the basis of an equivalent-freshwater-head map may bear no resemblance to a flow line in the real system because equivalent-freshwater head does not account for the influence of density-related gravity effects on flow directions. Therefore, after the assembly of the regional hydrogeologic data base, a driving-force analysis of the WIPP region was carried out to identify areas where density effects are not significant or where the direction of density-related driving forces is nearly coincident with the direction of pressure-related driving forces. In these areas, the equivalent-freshwater-head map can be used to determine accurate flow lines, which can be used for model boundaries.

The theoretical background and analytic procedure for assessing the relative magnitude of pressure-related and density-related driving forces were presented in the section titled "Analysis

of Fluid-Density Effects on Ground-Water Flow." The data required to complete this assessment are aquifer structure (elevation), fluid-density distribution, and equivalent-freshwater-head distribution. The data for each of these parameters are described in the following sections, followed by a description of the regional driving-force analysis and its implications for the selection of regional boundaries.

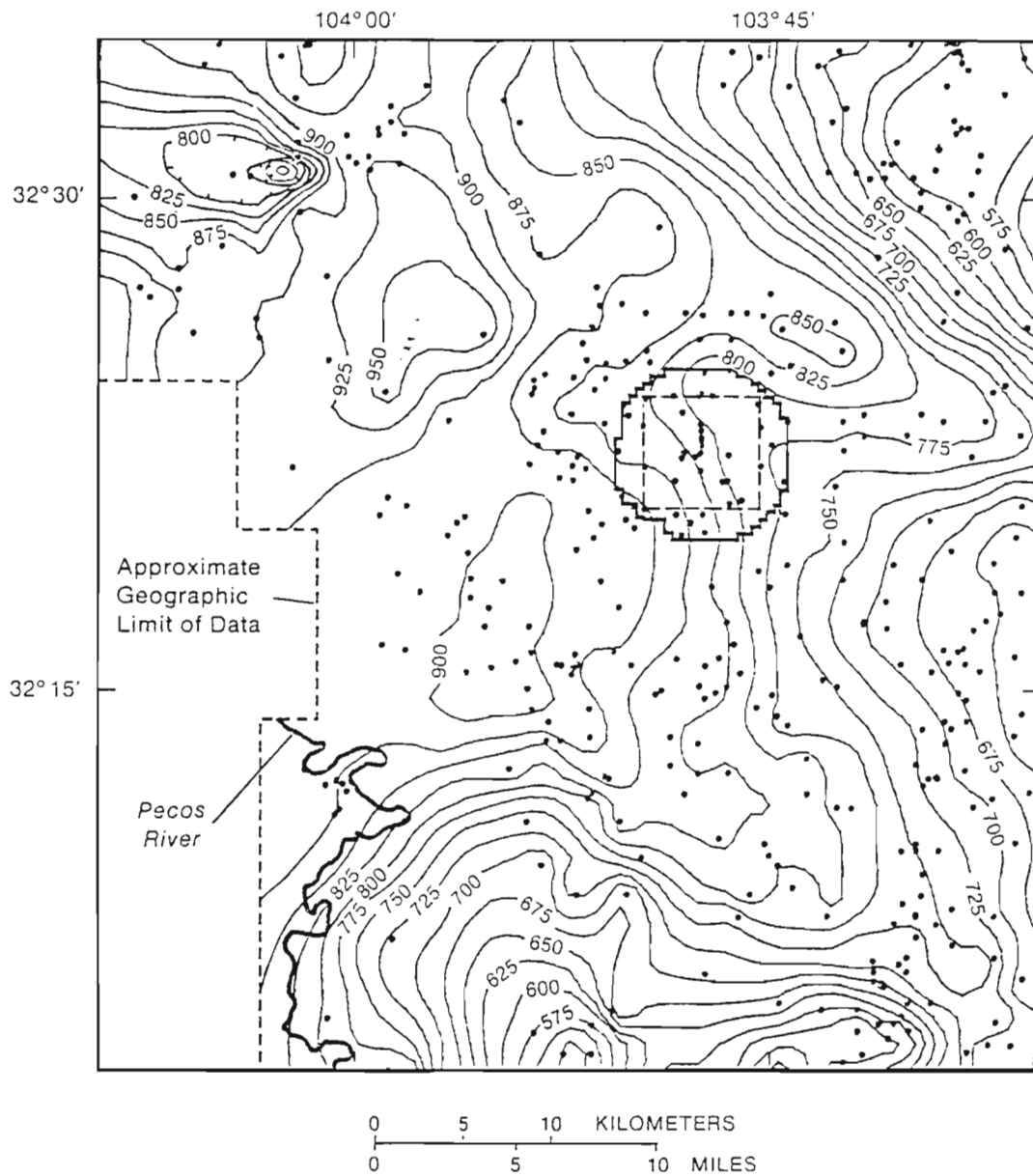
Regional Structure of the Culebra Dolomite Member of the Rustler Formation

Data from WIPP-related drill holes in the vicinity of the site and oil, gas, and potash exploration drill holes in the region were used to produce a structure contour map of the Culebra (fig. 15). The regional strike is approximately north-south, and the regional dip is 1 1/2 degrees to the east. Smaller scale variations are superimposed on the regional trend, and locally the dip is as large as 3 1/2 degrees. Northeast of the WIPP site is a local high that is underlain by a large anticlinal structure in the Castile Formation (Borns and others, 1983). Along the southern margin of the region is the northern part of a large irregularly shaped depression referred to as the Balmorhea-Loving Trough (Maley and Huffington, 1953; Anderson, 1981; Lambert, 1983; Bachman, 1987). This depression, which is filled with Cenozoic alluvial materials, is the by-product of extensive dissolution of the evaporites beneath the Culebra. A small closed depression in the northwest and a linear monoclinical feature in the northeast are underlain by the Capitan reef and also may be related to evaporite dissolution.

Regional Fluid-Density Distribution

The first step in assessing the fluid-density distribution on a regional scale was to gather fluid-density, specific-conductance, and dissolved-solids data for distant wells so that these data could be merged with the WIPP-project data. Data from many of the distant wells in the Rustler were discarded because a given well was not deep enough to penetrate the Culebra Member of the Rustler Formation or because the well depth was unknown.

As discussed previously, density data of the relatively high quality available in the immediate vicinity of the WIPP site were not available over the entire regional study area, and therefore, data of somewhat lesser quality have been used in the regional analysis. With the exception of data from well P-18, the same data have been used in the immediate WIPP site area for the regional analysis that were used for the preliminary analysis of density effects in the immediate vicinity of the WIPP site (see section titled "Analysis of Fluid-Density Effects on Ground-Water Flow"). The Culebra at well P-18 has a very low permeability and difficulties in sampling resulted in some uncertainty in how representative the samples are of formation fluid. In the preliminary analysis of density effects in the immediate site area, only data known to be of relatively high quality were used and P-18 data were excluded. Because water-quality data from P-18 were consistent with the somewhat reduced standards used for the regional analysis, these data were included in the regional analysis.



EXPLANATION

- WIPP ZONE IV BOUNDARY
- - - - WIPP SITE BOUNDARY
- 900 — STRUCTURE CONTOUR--Shows altitude of base of the Culebra Dolomite Member of the Rustler Formation. Contour interval 25 meters. Datum is sea level
- WELL OR TEST HOLE

Figure 15.-- Structure contour map of the base of the Culebra Dolomite Member of the Rustler Formation. Data from Richey (1989).

For wells with only specific conductance or dissolved-solids concentration available, linear and curvilinear regressions were used to estimate fluid density. These analyses revealed that the specific-conductance-based regressions had more available data and less scatter than the dissolved-solids-based regressions. Also, specific conductance was available for many of the distant wells that lacked dissolved-solids concentration. Therefore, specific conductance was used to estimate fluid density in all cases where direct density measurements were unavailable. The regression analysis that was chosen for making density estimates was a second-order curve that was constrained to pass through the y-axis at a fluid density of 1.0 gram per cubic centimeter (fig. 16). The constraint of requiring that a specific conductance of zero correspond with a fluid density of 1.0 was imposed to improve the estimates of fluid density at the low end of the range.

The target date for the regional freshwater-head and fluid-density distributions was approximately 1980, prior to the introduction of large hydraulic stresses associated with the excavation of the WIPP shafts. Therefore, a priority was placed on using fluid-density data from samples that were taken close to that time. However, as the preliminary simulations showed (see section titled "Analysis of Fluid-Density Effects on Ground-Water Flow") and the regional simulations later confirmed, solute redistribution in the WIPP region takes place very slowly. Therefore, although most of the fluid-density data used in constructing the regional density distribution were from samples collected in the 1970's and early 1980's, a few data from samples collected in the 1950's also were used. The fluid-density data are summarized in table 1. Wells from which those data were obtained are shown in figure 17.

In the WIPP region, fluids in the Culebra range from freshwater to brine that is close to sodium chloride saturation (density equal to approximately 1.2 grams per cubic centimeter) (fig. 18). Fluid densities are relatively high in the eastern part of the WIPP region and in the vicinity of Malaga Bend. Local density highs occur at WIPP-29 and WIPP-27 in central and northern Nash Draw, respectively. Both of these highs are downgradient of potash-mine tailings ponds. The geochemistry of samples from these wells confirms that these local highs are a by-product of local inflow of brine from the potash-mine operations (M.W. Bodine and B.F. Jones, U.S. Geological Survey, written commun., 1988). Fluid densities are relatively low, and many wells contain nearly fresh water throughout the central and southeastern parts of the region.

Regional Equivalent-Freshwater-Head Distribution

Equivalent-freshwater head is a mechanism for normalizing water-level measurements relative to a constant density fluid (freshwater) so that these measurements are related in a consistent manner to fluid pressure in a given aquifer. The objective in constructing an equivalent-freshwater-head distribution in the WIPP region was to produce a tool for assessing the pressure-related component of flow-driving forces in the WIPP region prior to the introduction of large pressure changes associated with the excavation of the WIPP shafts. Therefore, like the density data, the target date for the equivalent-freshwater-head distribution was approximately 1980. Because fluid-pressure changes propagate through a system much more readily than solutes, the selection criteria for an acceptable measurement date were more restrictive for water-level data than those used for fluid density. For the distant wells, no water-level data prior to 1975 were included

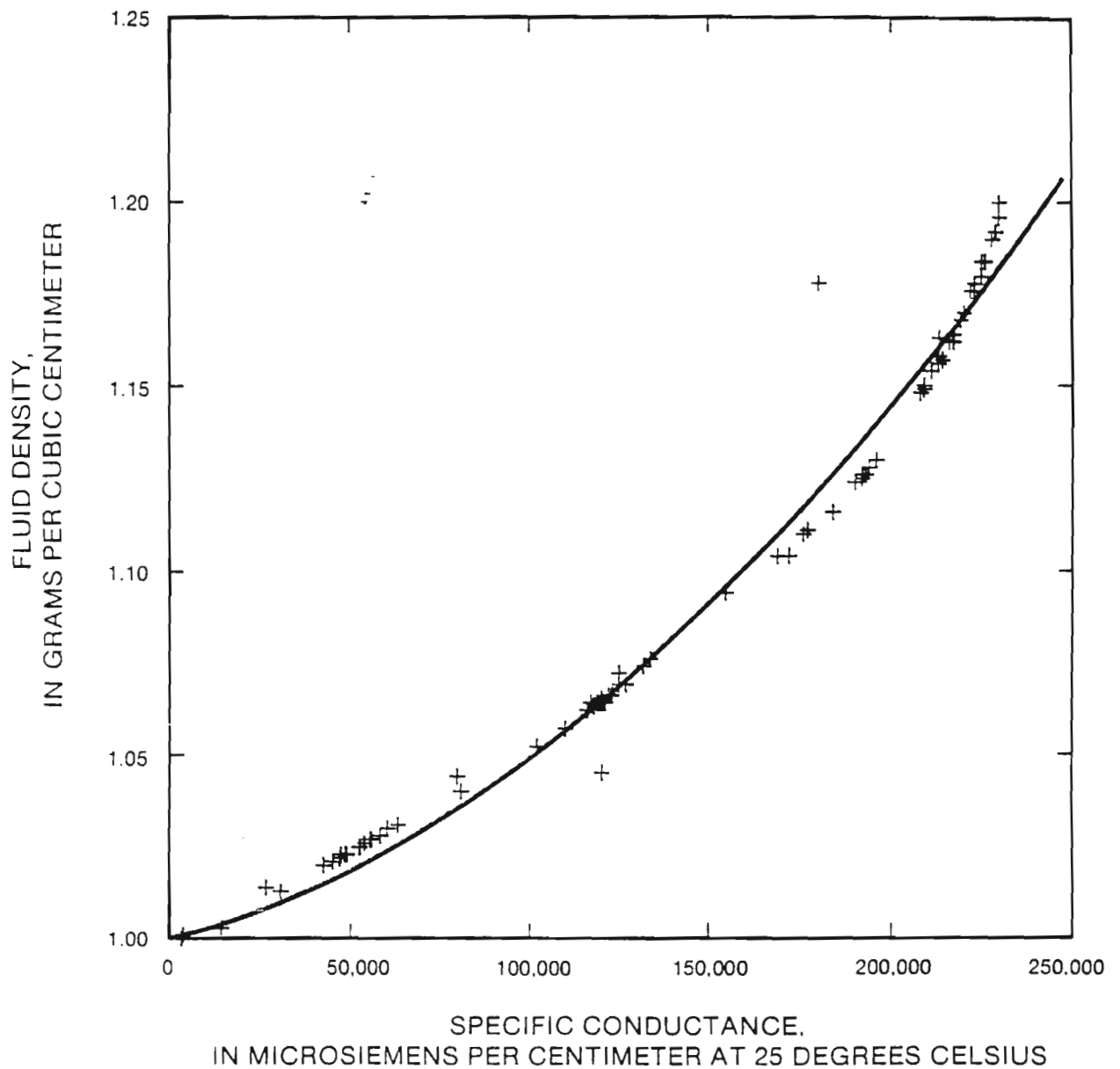
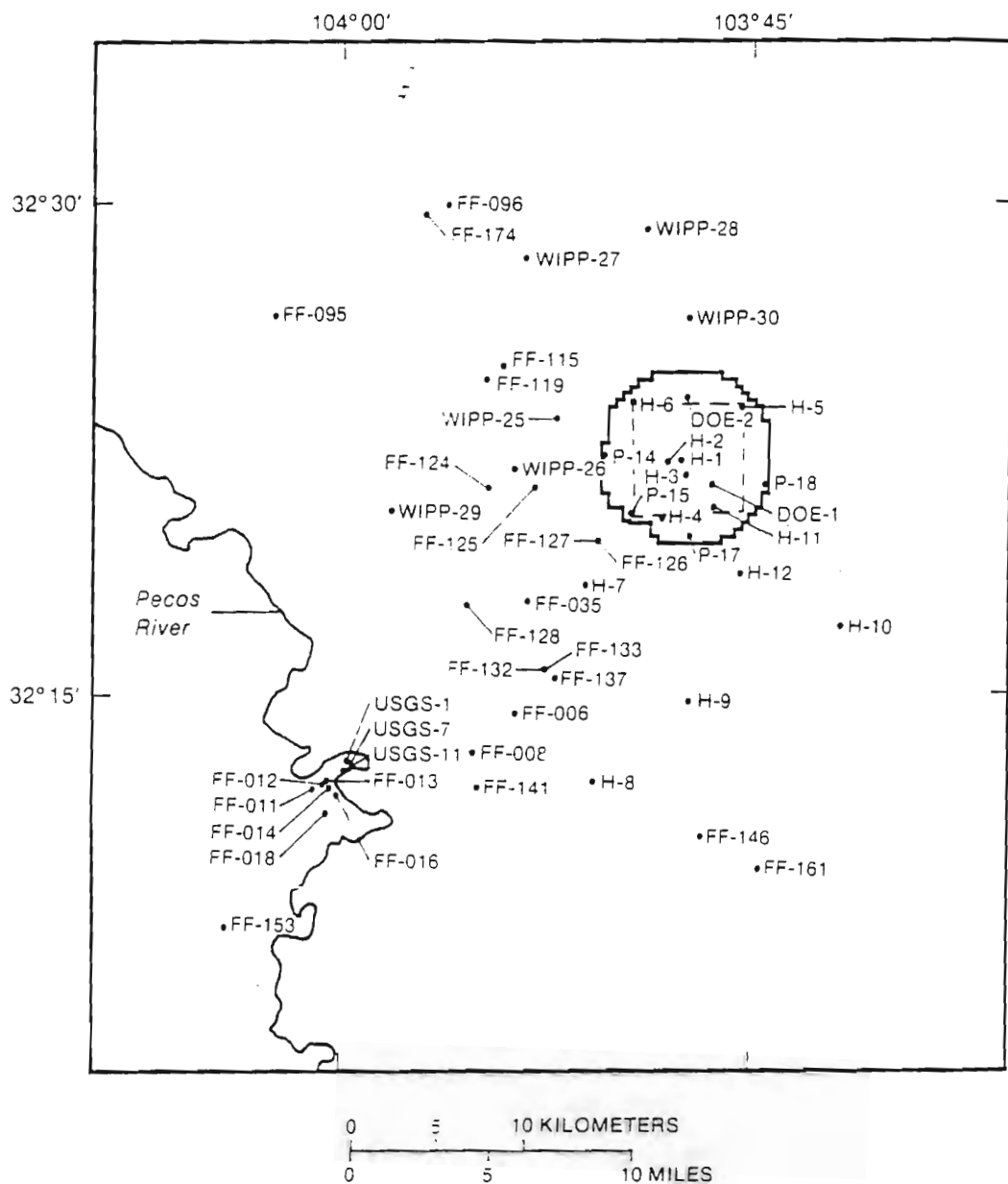


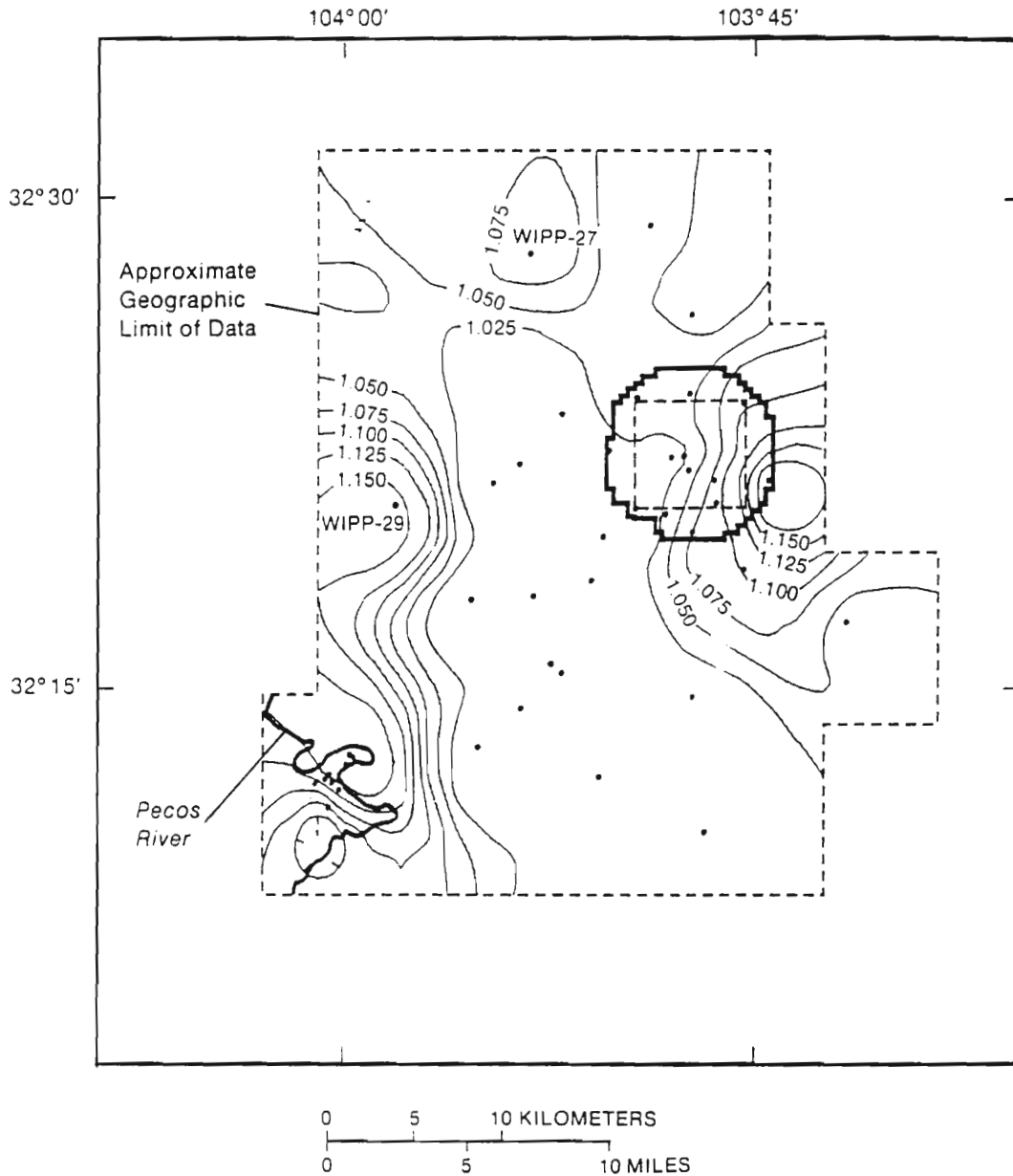
Figure 16.-- Curvilinear regression of relation between fluid density and specific conductance for ground water in the Rustler Formation in the WIPP region. Data from Mercer (1983), Hale and others (1954), and U.S. Geological Survey Water Data Storage and Retrieval System (WATSTORE).



EXPLANATION

- WIPP ZONE IV BOUNDARY
- - - WIPP SITE BOUNDARY
- H-1 WELL OR HYDROLOGIC TEST PAD AND WELL DESIGNATION

Figure 17.-- Location of wells with hydrologic data in the WIPP region.



EXPLANATION

- WIPP ZONE IV BOUNDARY
- - - - - WIPP SITE BOUNDARY
- 1.025— LINE OF EQUAL FLUID DENSITY--Interval 0.025 gram per cubic centimeter
- WELL OR TEST HOLE

Figure 18.-- Distribution of approximate fluid density in the Culebra Dolomite Member of the Rustler Formation.

in the data set. For WIPP-related wells, no data from wells drilled after the excavation of the WIPP shafts were used.

Measured water levels were converted to equivalent-freshwater heads using the following equation, which expresses fluid pressure in an observation well as a function of the height of the fluid column in the well bore. The result is then substituted into equation 5 (page 26):

$$p = (WL - E) \rho |g| \quad (11)$$

where

- p = fluid pressure at zone of completion in an observation well [M/LT²];
- WL = measured water level [L];
- E = elevation of zone of completion in an observation well [L];
- ρ = density of fluid filling the well bore [M/L³]; and
- |g| = magnitude of gravitational acceleration [L/T²].

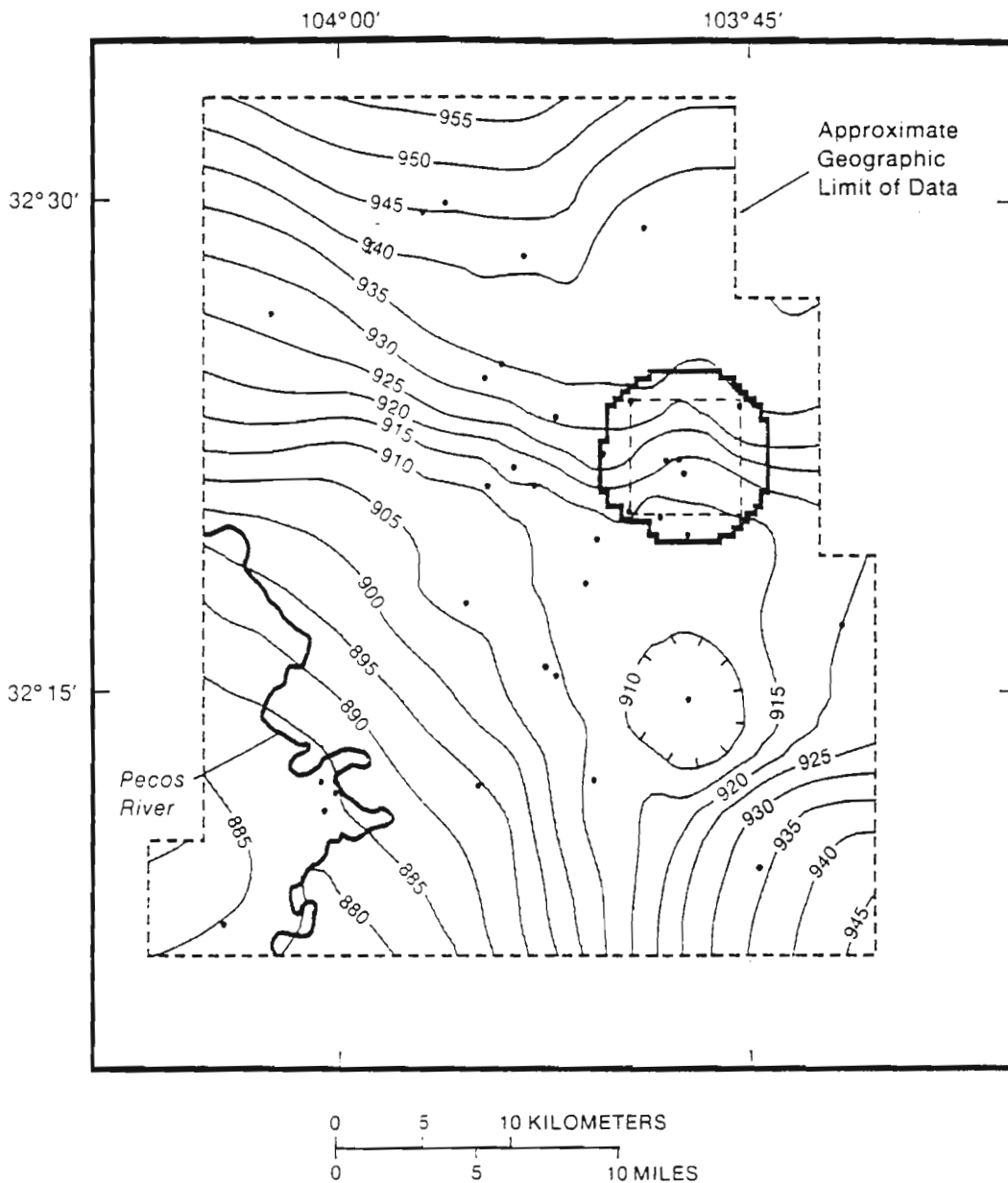
Substituting equation 11 into equation 5 yields:

$$H_f = \frac{(WL - E) \rho}{\rho_f} + E \quad (12)$$

where

- H_f = equivalent-freshwater head [L]; and
- ρ_f = density of freshwater [M/L³].

Equivalent-freshwater heads and the parameters from which they were computed are summarized in table 1. The distribution of freshwater heads is shown in figure 19. Equivalent-freshwater heads are highest in the north and lowest in the southwest. Head gradients range from a maximum of 6 meters per kilometer (32 feet per mile) in the vicinity of the WIPP site to a minimum of approximately 7 centimeters per kilometer (0.4 foot per mile) in areas to the north and south of the site. Gradients elsewhere in the WIPP region generally fall between these two extremes.



EXPLANATION

- WIPP ZONE IV BOUNDARY
- - - - - WIPP SITE BOUNDARY
- 900 — FRESHWATER HEAD CONTOUR—Shows altitude at which water having a density of 1.00 gram per cubic centimeter would have stood in a tightly cased well. Contour interval 5 meters. Datum is sea level.
- WELL OR TEST HOLE

Figure 19.-- Estimated equivalent-freshwater head in the Culebra Dolomite Member of the Rustler Formation prior to shaft excavation at the WIPP site in 1981.

Evaluation of Potential Errors in the Estimation of Equivalent-Freshwater Head

The use of equation 12 to compute equivalent-freshwater head contains an assumption that is a source of error under certain conditions. The assumption implicit in equation 12 is that the entire well bore of the observation well is filled with formation fluid, which has a constant density equal to that found in the formation. A water level meeting this criterion is sometimes referred to as "point-water head" (Luszczynski, 1961, p. 4247). Under actual field conditions, however, the fluid in the well bore of an observation well may have density stratification as a result of the introduction of less dense foreign fluids into the well bore during testing and sampling, or as a result of incomplete sealing of the well from precipitation or runoff. The use of equation 12 to compute equivalent-freshwater head results in an overestimate of the value if the introduction of less dense fluids has created density stratification. In this case, an accurate equivalent-freshwater head can be computed by measuring the fluid-density profile and integrating density over the height of the fluid column to obtain an accurate value for fluid pressure at the zone of completion. An alternative approach is to measure absolute pressure in the zone of completion. Either of these approaches is time consuming and expensive; therefore, neither density-profile nor absolute fluid-pressure data are commonly available.

Recognition of the data-quality problems associated with density stratification prompted the development of a program by International Technologies to carefully measure density profiles and compute more accurate freshwater heads in WIPP-related observation wells starting in 1986. However, due to the extensive aquifer testing and water-quality sampling activities through the years and to the absence of extensive field data on the transient behavior of well-bore density stratification, it is difficult to reconstruct a set of density profiles from which accurate equivalent-freshwater heads could be computed for "undisturbed conditions" prior to the large hydraulic stresses associated with the excavation of the WIPP shafts. An effort to reconstruct density-profile histories at each of the WIPP wells is currently being carried out by INTERA Technologies in order to improve estimates of undisturbed freshwater heads. Neither density-stratification nor absolute-pressure data are available for any of the distant wells.

One measure of the sensitivity of a given well to potential errors associated with density stratification can be derived by examining the density of the formation fluid and the height of the fluid column in the well bore. For example, if the formation fluid is very dense, but the fluid column is relatively short, errors associated with borehole stratification may be small. Likewise, if the formation fluid is not very dense, density-stratification effects may not be very pronounced, even in situations where the fluid column is relatively long. The situation that is most sensitive to density-stratification errors is the case where formation-fluid density is high and the fluid column in the well bore is large. The relative sensitivity of a well to density-stratification effects can be quantified by examining the extreme case in which the well bore is completely filled with freshwater, and therefore, the measured water level is equal to the equivalent-freshwater head. The difference between this extreme and the ideal, in which the well bore is filled completely with formation fluid, provides a measure of the maximum possible error associated with density stratification. Although the occurrence of the extreme case is highly unlikely, this type of computation provides a useful measure of the sensitivity of a given well to density-stratification errors. This error measure does not account for the less common situation of the well-bore fluid density being higher than the formation-fluid density as a result of the higher density drilling fluids

being left in the well bore or from the presence of halite beds in perforated or uncased parts of the well.

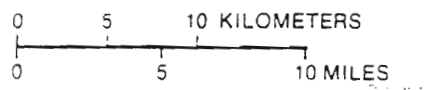
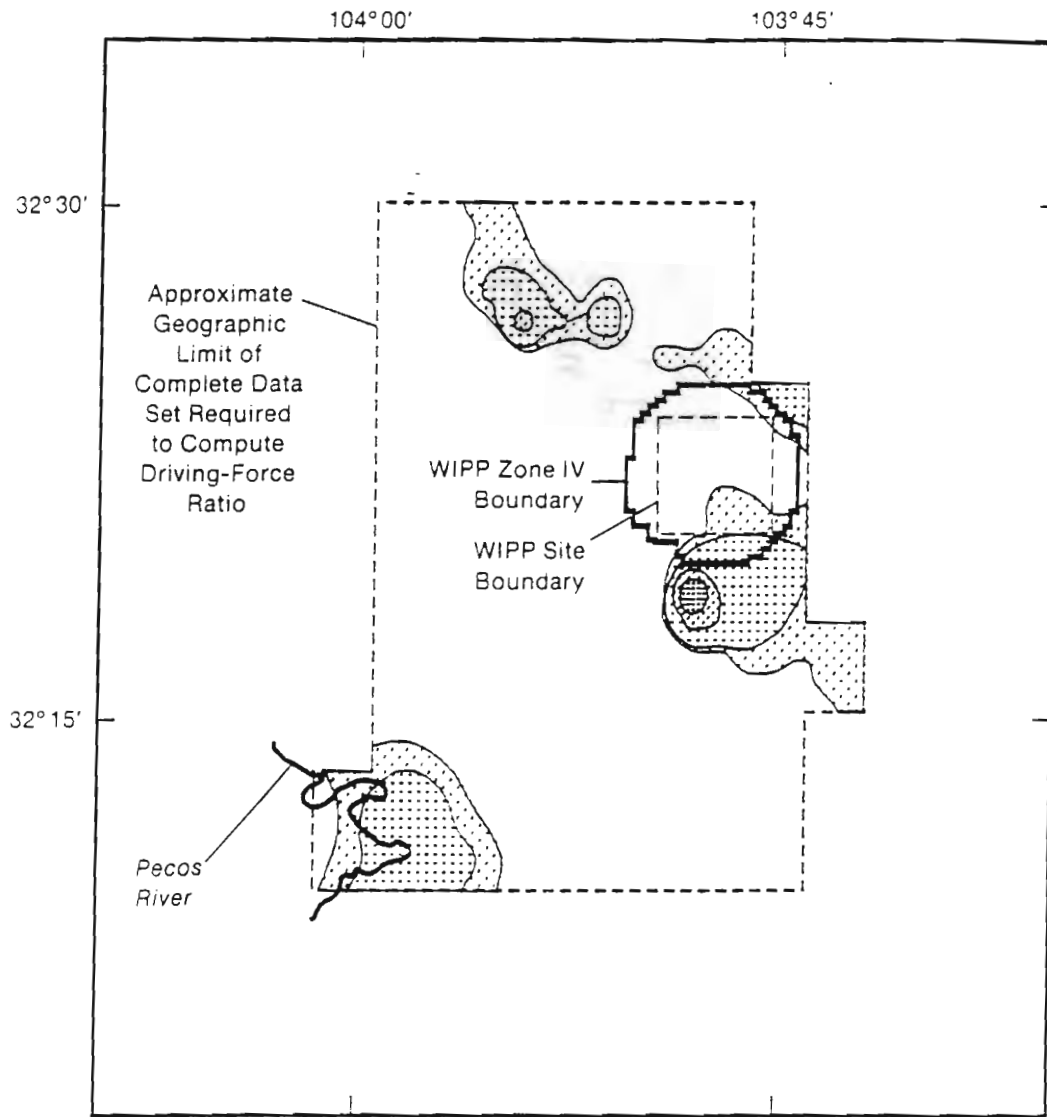
The sensitivity of wells in the WIPP region to density stratification has been computed using the method described above, and the results are presented in table 1. In 75 percent of the wells, the maximum possible error in equivalent-freshwater head is 1 meter or less. The most sensitive well is H-5-B, in which the combination of a high formation-fluid density (1.104 g/cm^3) and a long fluid column in the well bore (130 meters), produces a maximum possible freshwater-head error of 13.5 meters. The computed potential freshwater-head error is a measure of the sensitivity of the well to error associated with density stratification, not a computation of actual error. Actual errors in most cases are substantially smaller. For example, the results of a recent pressure-density survey for the H-5 well on April 15, 1987 (Crawley, 1987) show the actual error in computing equivalent-freshwater head using equation 12 compared to using measured density-profile data is approximately 0.8 meter.

Results of the Regional Driving-Force Analysis

The aquifer-structure, fluid-density, and equivalent-freshwater-head distributions were discretized into a regularly spaced grid using a quadrant-search and distance-weighted interpolation routine from the SURFACE II spatial analysis package (Sampson, 1978). The grid consisted of 1.6- x 1.6-kilometer cells. The driving-force components and the dimensionless driving-force ratio were then calculated as described in the section titled "Analysis of Fluid-Density Effects on Ground-Water Flow."

The areal distribution of the dimensionless driving-force ratio in the WIPP region is shown in figure 20. The dashed line around the perimeter of this plot shows the approximate geographic limits of the area for which there were sufficient data to compute this ratio. The large, unshaded zone in which the driving-force ratio is less than 0.5 indicates that throughout much of the WIPP region, density-related effects are relatively insignificant. In this area, equivalent-freshwater heads adequately characterize the flow-driving forces. There are four areas where driving-force ratios are larger than the 0.5 threshold value, and where, therefore, density-related effects may be significant. Relative to WIPP, the most important of these areas is just south of the site, where driving-force ratios are greater than the 0.5 threshold and reach a maximum value of 8. This area is important because it lies along potential transport pathways that extend southward from the site. Other areas where driving-force ratios are greater than the 0.5 threshold are an area in the north that is associated with the high-density fluids in the vicinity of borehole WIPP-27 and nearby potash mining operations, an area in the southwest where dense fluids from the Rustler-Salado contact zone are moving upward through the Rustler Formation to discharge into the Pecos River, and a relatively small area to the north and northeast of the WIPP site.

Because of its potential significance to WIPP, the area of high driving-force ratios just south of the site warrants closer examination. An enlargement of this area showing the relative magnitudes and directions of the pressure-related and density-related driving-force components is shown in figure 21. In the vicinity of the WIPP site, pressure-related driving forces dominate,



EXPLANATION






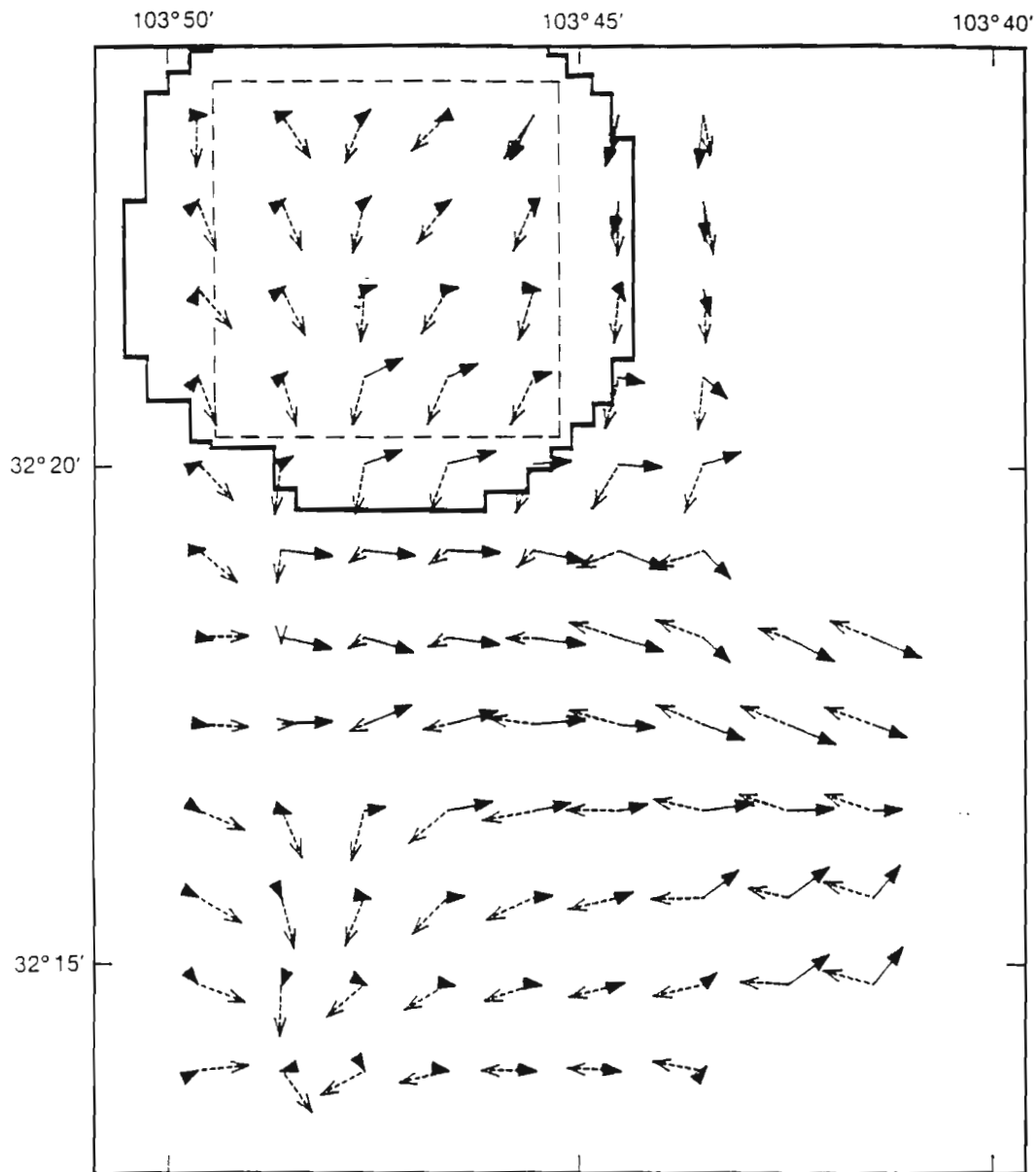
DRIVING-FORCE RATIO MAGNITUDE			
	< 0.5		3-5
	0.5-1		> 5
	1-3		

Figure 20.-- Areal distribution of the dimensionless driving-force ratio in the WIPP region.



0 1 2 3 KILOMETERS
 0 1 2 3 MILES

EXPLANATION

- WIPP ZONE IV BOUNDARY
- - - WIPP SITE BOUNDARY
- - - > PRESSURE-RELATED COMPONENT
- > DENSITY-RELATED COMPONENT

Figure 21.-- Relative magnitude and direction of density-related and pressure-related driving-force vector components at the WIPP site and in the area to the south. Vector lengths are scaled locally at each position to show relative magnitude of driving-force components at that single location.

and equivalent-freshwater heads adequately characterize the flow-driving forces. However, density-related forces become increasingly significant toward the south, and southeast of the Zone IV boundary, density-related forces are dominant and have a distinct easterly trend in direction. Thus, the effect of fluid density on flow patterns in this area is to drive fluid flow in a more easterly, downdip direction than would be predicted by an analysis based solely on equivalent-freshwater heads. Although there are some differences in the input data between this regional analysis and the driving-force analysis that was carried out for the Barr and others (1983) model area, these analyses produce similar-sized areas that have driving-force ratios greater than the 0.5 threshold just south of the WIPP site.

In addition to identifying this area just south of the WIPP site where density-related effects may be significant, the driving-force analysis of the WIPP region was used in the selection of boundaries for the regional ground-water flow model to assess the potential for density-related complications in the vicinity of model boundaries. This boundary selection process is discussed in the following section.

Regional Variable-Density Ground-Water Flow Model

The following sections describe the implementation and analysis of a numerical model used to simulate variable-density ground-water flow in the WIPP region. The first section covers model implementation details. The second section describes the calibration of an approximate steady-state solution that serves as a baseline for comparisons with subsequent sensitivity simulations. The third section describes a series of simulations that examine system sensitivity to factors such as fluid density, boundary conditions, and vertical flux.

Model Implementation

The following section describes the selection of boundary conditions; merging of regional-scale conductivity trends with more detailed conductivity information in the vicinity of the WIPP site; and other miscellaneous model-implementation details.

Boundary conditions

The primary objectives in the selection of model boundaries were to locate boundaries coincident with significant hydrologic features and in areas that are free of density-related effects wherever possible. The location of the regional model boundaries is shown in figure 22 on a map that also shows the location of significant hydrologic features and areas where the driving-force ratio is larger than the 0.5 threshold value. In the discussion that follows, the rationale behind each boundary is described, starting with the Nash Draw boundary and moving counterclockwise around the model area.

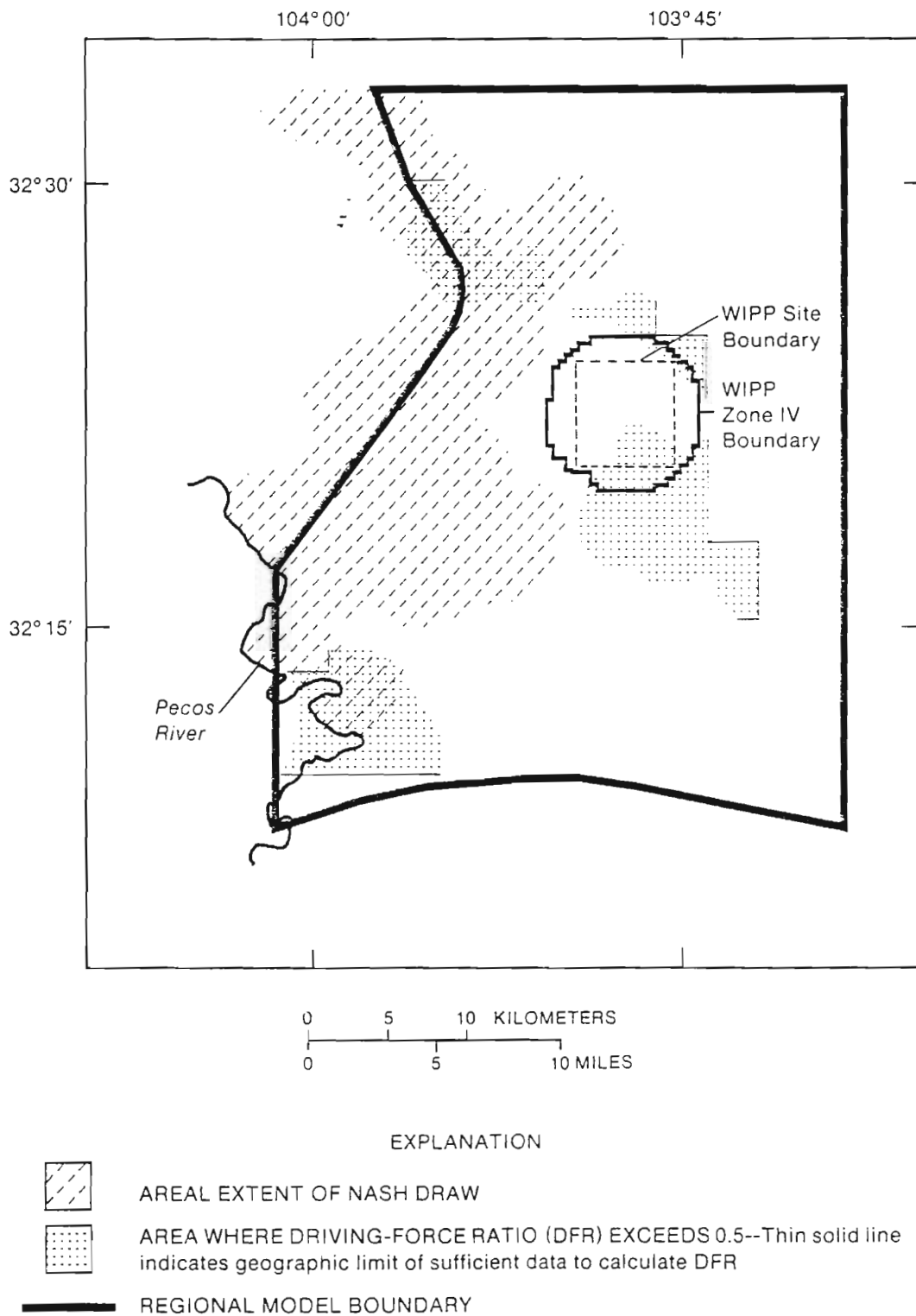


Figure 22.-- Location of regional model boundary and significant hydrologic features.

Two characteristics make Nash Draw a significant hydrologic feature. First, it is a topographic low (fig. 5); second, extensive halite dissolution, subsidence, and calcium sulfate hydration at the top of the evaporite section have produced extensive structural deformation accompanied by large increases in hydraulic conductivity. The combination of low topography and high conductivity causes Nash Draw to act as a drain in the regional flow system. Because this feature is well defined and is likely to continue to act as a drain under a wide variety of conditions, a flow line down the center of Nash Draw was selected as a no-flow boundary for the regional model. The results of the regional driving-force analysis show that over most of the path of this flow line, density-related flow-driving forces are relatively insignificant (fig. 22). At the northern end of this flow line is a small area in the vicinity of a potash-mining operation where the driving-force analysis indicates that density-related flow-driving forces are significant (fig. 22). The easterly direction of density-related driving forces in this area indicates that there may be a localized eastward deviation of the flow line in this area. Because the potash-mine effects are a relatively localized phenomenon and are not likely to have significant regional-scale impact, incorporation of this feature into the regional flow simulations was deemed unnecessary.

A second well-defined hydrologic feature in the WIPP region is the Pecos River. Streamflow data, along with the measured discharge of large quantities of dissolved salt, show that significant volumes of ground water discharge to the Pecos along this reach of the river (Haie and others, 1954; Havens and Wilkins, 1979; Hunter, 1985). Therefore, the Pecos River was selected as a discharge boundary for the model. Because detailed data for the Culebra were unavailable along the Pecos River, the Pecos discharge boundary was defined using the relatively simple straight-line geometry shown in figure 22.

The southern part of the WIPP region has no hydrologic features that are as well defined as the Pecos River or Nash Draw. However, there are flow lines based on the equivalent-freshwater-head map (fig. 19) along which the driving-force analysis shows that density-related effects are relatively insignificant (figs. 20 and 22). Therefore, an approximate flow line was selected as a no-flow boundary to the south. Although this boundary is not as well defined as the Nash Draw flow line or the Pecos River, this southern area is relatively free of major stresses on the regional flow system.

In the eastern part of the WIPP region, no data for the Rustler are available to define hydrologic features. To the north, limited data are available, but no well-defined features are present. Therefore, a sensitivity analysis was used to explore the influence of these boundaries on the flow system, examining a wide range of specified-pressure conditions. A specified-pressure distribution representing the middle of this range has been used for the baseline steady-state simulation.

For most of the regional simulations, no-flow boundaries have been assumed for the top and bottom of the Culebra, consistent with the conceptualization that the Culebra is relatively isolated from vertical flow (Mercer, 1983; Lambert, 1987; and Lambert and Harvey, 1988). In this conceptualization of the flow system, the primary source of recharge to the Culebra in the WIPP area is lateral flow from an unspecified recharge area to the north. Based on geochemical evidence, the concept of total vertical isolation of the Culebra has been questioned by Chapman (1986) and by M.W. Bodine and B.F. Jones (U.S. Geological Survey, written commun., 1988). Therefore, an aerially distributed, specified vertical flux has also been simulated to examine this alternative source

of recharge to the Culebra. The potential for vertical flux to the Culebra has been examined further using a vertical section model (see section titled "Analysis of Long-Term System Response to Paleohydrologic Conditions").

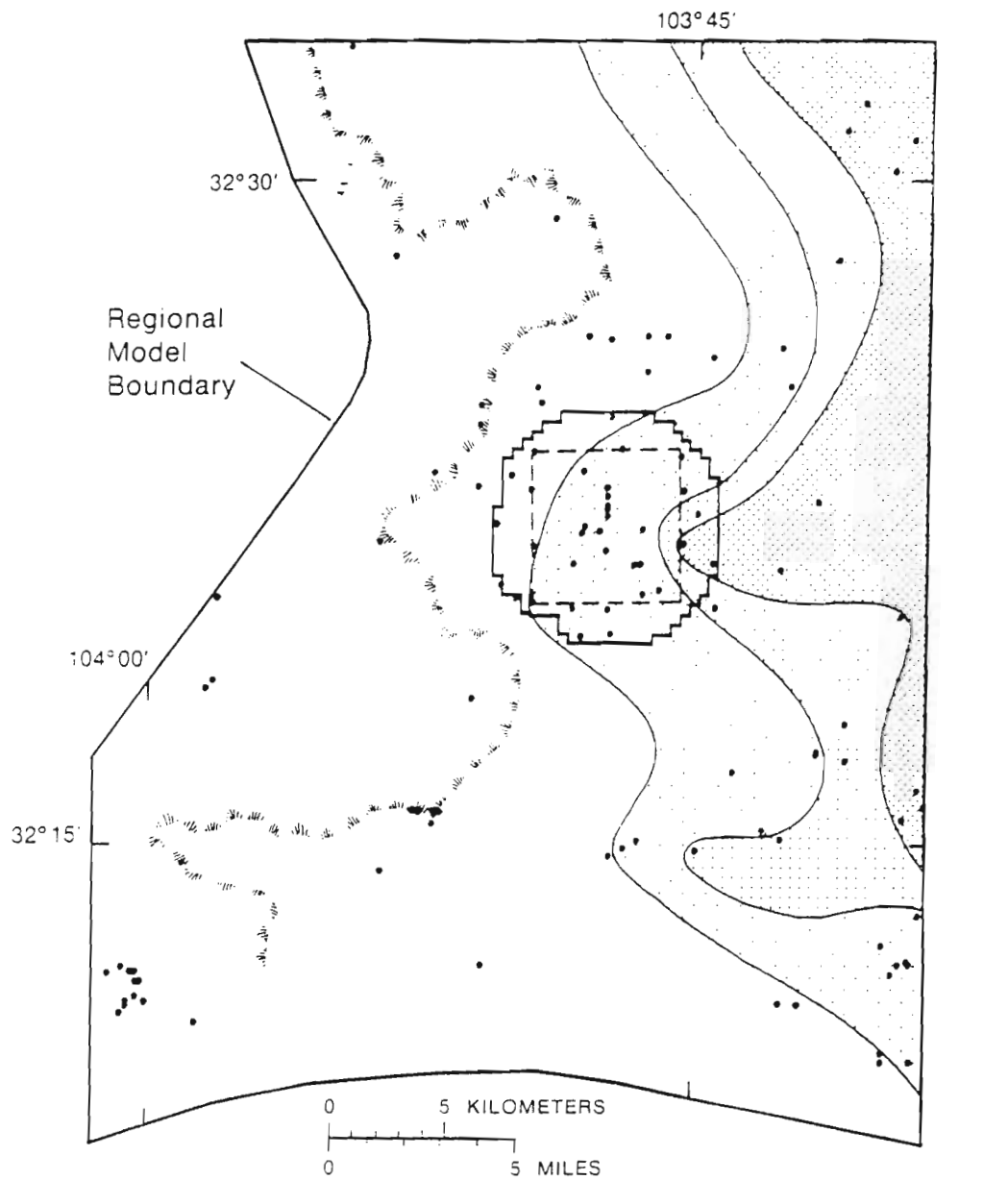
Hydraulic-conductivity distribution

Beyond the vicinity of the WIPP site, hydraulic-conductivity data are sparse. Therefore, the hydraulic-conductivity distribution in distant parts of the WIPP region were extrapolated from other types of geologic information. Because the lithology of the Culebra Dolomite Member is uniform, other geologic factors control hydraulic conductivity. The following paragraphs describe how the regional conductivity distribution was derived.

The primary controls on hydraulic conductivity of the Culebra are the secondary processes of halite dissolution, subsidence, and calcium sulfate hydration (see section titled "Halite Dissolution and Related Secondary Processes"). The results of aquifer tests in the Culebra Dolomite Member show a correlation between hydraulic conductivity and the degree of halite removal (Mercer, 1983, p. 56-60; Gonzalez, 1983a, p. 17-18; Chaturvedi and Channell, 1985, p. 46-51). This correlation, along with the mechanistic link between halite-dissolution processes and the generation of secondary permeability, indicates that the degree of halite removal within the Rustler provides a mappable, indirect measure of hydraulic conductivity. The areal distribution of halite in the Rustler Formation for the model region is shown in figure 23. Similar maps of the WIPP site vicinity have been published by Mercer (1983), Chaturvedi and Channell (1985), and Snyder (1985).

Although halite-removal patterns in the vicinity of the WIPP site have been discussed in the reports just cited, two characteristics of halite-removal patterns elsewhere in the model region are of significance in determining the regional hydraulic-conductivity trends. First, to the east and northeast of WIPP, the Rustler appears to be totally intact. This fact, in combination with the relatively large depth of the Culebra in this area, has led to the conclusion that the relatively impermeable conditions in the easternmost part of the WIPP site as at drill hole P-18 probably extend both eastward and northeastward. Second, the southern part of the model region is characterized by a large area in which most, if not all, of the halite in the Rustler has been removed (fig. 23). This area comprises the northern part of the large Balmorhea-Loving Trough depression (see section titled "Regional Structure of the Culebra Dolomite Member"). The absence of Rustler halite in this southern area indicates that halite dissolution probably has been active in the Rustler, which motivated the use of somewhat higher conductivities than would have been used if the Rustler in this area had contained intact halite beds.

Confining stress may exert a secondary influence on hydraulic conductivity of the Culebra because the secondary permeability induced by halite dissolution and related processes is primarily in the form of fractures and the depth of the Culebra over the model region ranges from a few meters in the west to more than 400 meters in the east. The depth of burial to the top of the Culebra (fig. 24) provides a mappable, indirect measure of confining stress. The Culebra is shallow, generally 0 to 100 meters, throughout most of Nash Draw and is characterized by relatively high hydraulic conductivity. In the east, the Culebra is buried at depths of as much as 450 meters. As noted previously, the Rustler has experienced minimal halite dissolution in this area, and it appears to be relatively impermeable.



EXPLANATION









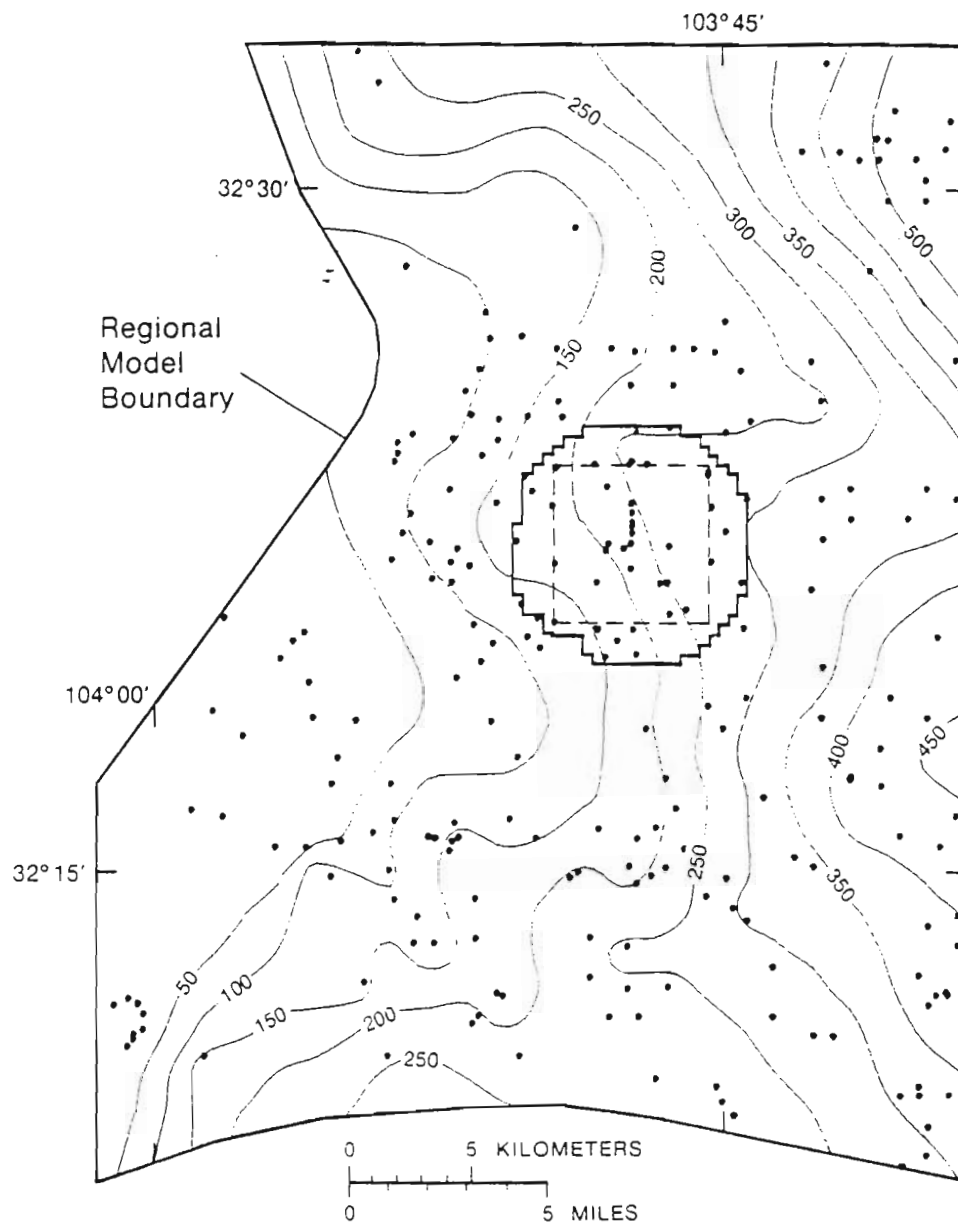
- | | | | |
|---|--|---|-------------------------------|
|  | NO HALITE IN RUSTLER FORMATION |  | WIPP ZONE IV BOUNDARY |
|  | HALITE MISSING ABOVE CULEBRA DOLOMITE MEMBER |  | WIPP SITE BOUNDARY |
|  | HALITE MISSING ABOVE MAGENTA DOLOMITE MEMBER |  | EASTERN BOUNDARY OF NASH DRAW |
|  | NO HALITE MISSING FROM RUSTLER FORMATION |  | WELL OR TEST HOLE |

Figure 23.-- Areal distribution of halite in the Rustler Formation in the model region.



EXPLANATION

- WIPP ZONE IV BOUNDARY
- - - - WIPP SITE BOUNDARY
- 200— LINE OF EQUAL DEPTH--Shows depth below land surface to top of the Culebra Dolomite Member of the Rustler Formation. Interval 50 meters
- WELL OR TEST HOLE

Figure 24.-- Depth to the top of the Culebra Dolomite Member of the Rustler Formation in the model region.

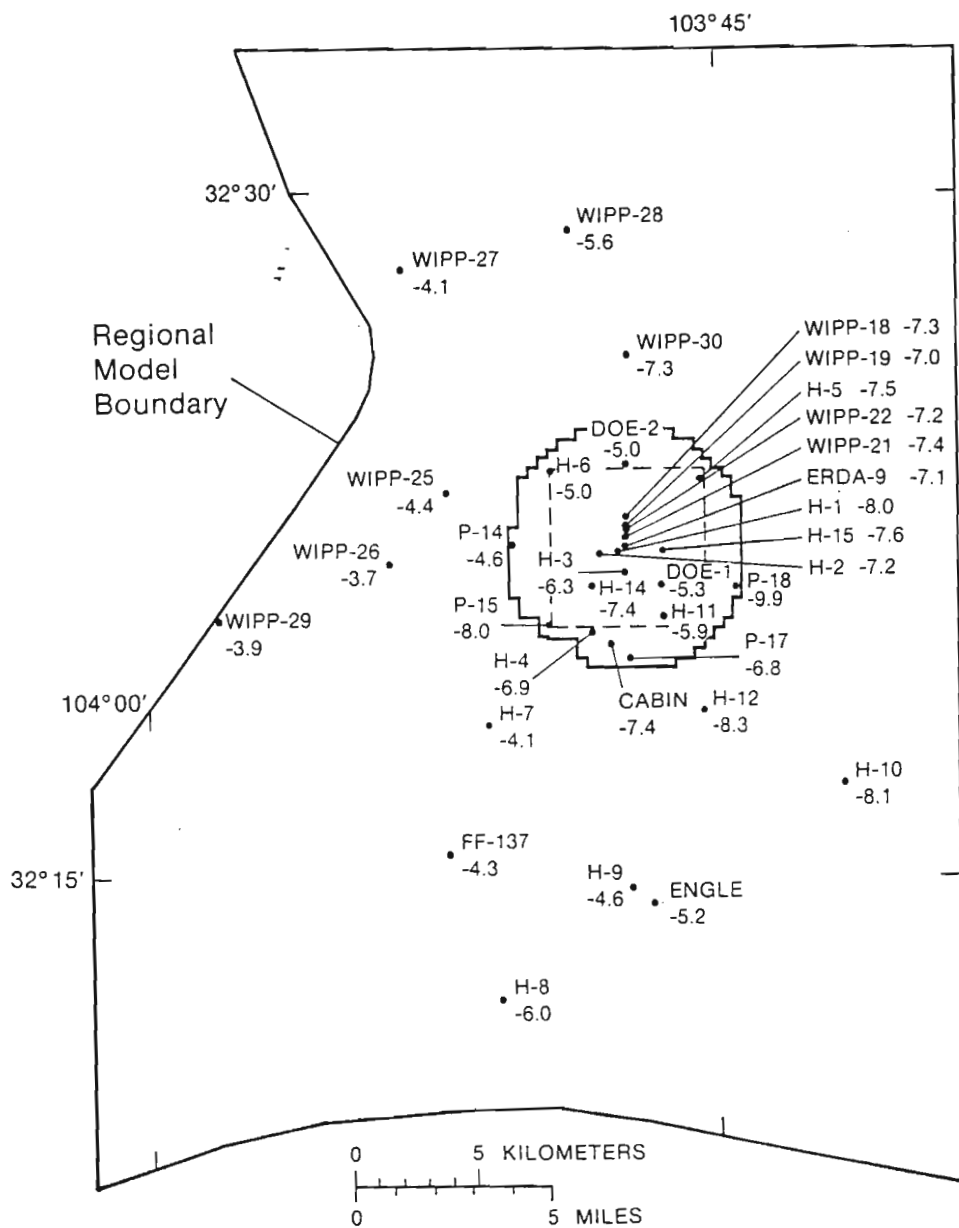
Nash Draw represents an extreme case in which extensive exposure to secondary processes has produced relatively high hydraulic conductivity. Because extreme exposure to secondary processes produces significant subsidence, topography provides a mappable measure of the areal extent of Nash Draw conditions. The schematic perspective diagram of vertically exaggerated topography of the model region (fig. 7) shows two well-developed reentrants that extend eastward from Nash Draw, one to the north of the WIPP site and one to the south. These reentrants indicate that higher conductivity associated with extensive exposure to secondary processes probably extends eastward from the main trend of Nash Draw in these two areas.

In addition to the indirect measures of hydraulic conductivity described in the previous paragraphs, direct measurements of hydraulic conductivity on a local scale are available from aquifer tests at many localities within the model region (Cooper, 1962; Cooper and Glanzman, 1971; Seward, 1982; Mercer, 1983; Gonzalez, 1983b; Beauheim, 1986, 1987a, 1987b; and Haug and others, 1987). Representative values for hydraulic conductivity at individual wells are shown in figure 25.

Integrating the information from these direct measurements with the indirect geologic information on degree of halite removal, depth of burial, and topography produced the regional hydraulic-conductivity trends shown in figure 26. Values of hydraulic conductivity are plotted in zones of one-half order of magnitude difference. Of the 33 measured values of local-scale conductivity from aquifer tests, 22 are located in the correct zone, 5 are located in zones that are one-half order of magnitude too high or low, and 6 are located in zones that are more than one-half order of magnitude too high or low. All 11 wells that do not precisely follow regional trends are located in the transition zone, in which local variations in halite removal have produced a large degree of spatial variability in hydraulic conductivity (see "Halite Dissolution and Related Secondary Processes").

In the vicinity of the WIPP site, the large number of single-well aquifer tests and multiple-well aquifer tests provides sufficient data to characterize the variability in hydraulic conductivity within the transition zone. This information has been analyzed in an integrated fashion in the multiple-well aquifer-test simulation of Haug and others (1987). The conductivity distribution of Haug and others (1987) is shown in figure 27 using the same one-half order of magnitude zones used in figure 26. A comparison of figures 26 and 27 indicates the extent of local variation within the regional-scale conductivity trends. Significant local variations from the regional trend in the Haug and others (1987) model include a postulated north-south high-conductivity zone in the south and low conductivity zones in the northeast and southwest.

The final step in defining a hydraulic-conductivity distribution for input into the regional ground-water model was to merge the information on detailed hydraulic-conductivity variations in the vicinity of the WIPP site from the Haug and others (1987) model (fig. 27) with the larger scale regional hydraulic-conductivity trends (fig. 26). Hydraulic conductivity in the Haug and others (1987) model varies from cell to cell on the basis of their Kriged value and on subsequent model calibration. Therefore, the Haug and others (1987) hydraulic-conductivity values were grouped into one-half order of magnitude zones, mapped into the coarser mesh of the regional model, and merged with the regional hydraulic-conductivity trends (fig. 28). This allowed the regional model to incorporate a hydraulic-conductivity distribution that contains not only regional



EXPLANATION

- WIPP ZONE IV BOUNDARY
- WIPP SITE BOUNDARY
- H-12
-8.3 WELL OR TEST HOLE AND NAME—Bottom number is the log of hydraulic conductivity in meters per second

Figure 25.-- Hydraulic conductivity at wells and test holes in the model region. Data from Mercer (1983), Gonzalez (1983b), Seward (1982), Beauheim (1986, 1987a, 1987b), Haug and others (1987), Cooper (1962), Cooper and Glanzman (1971).

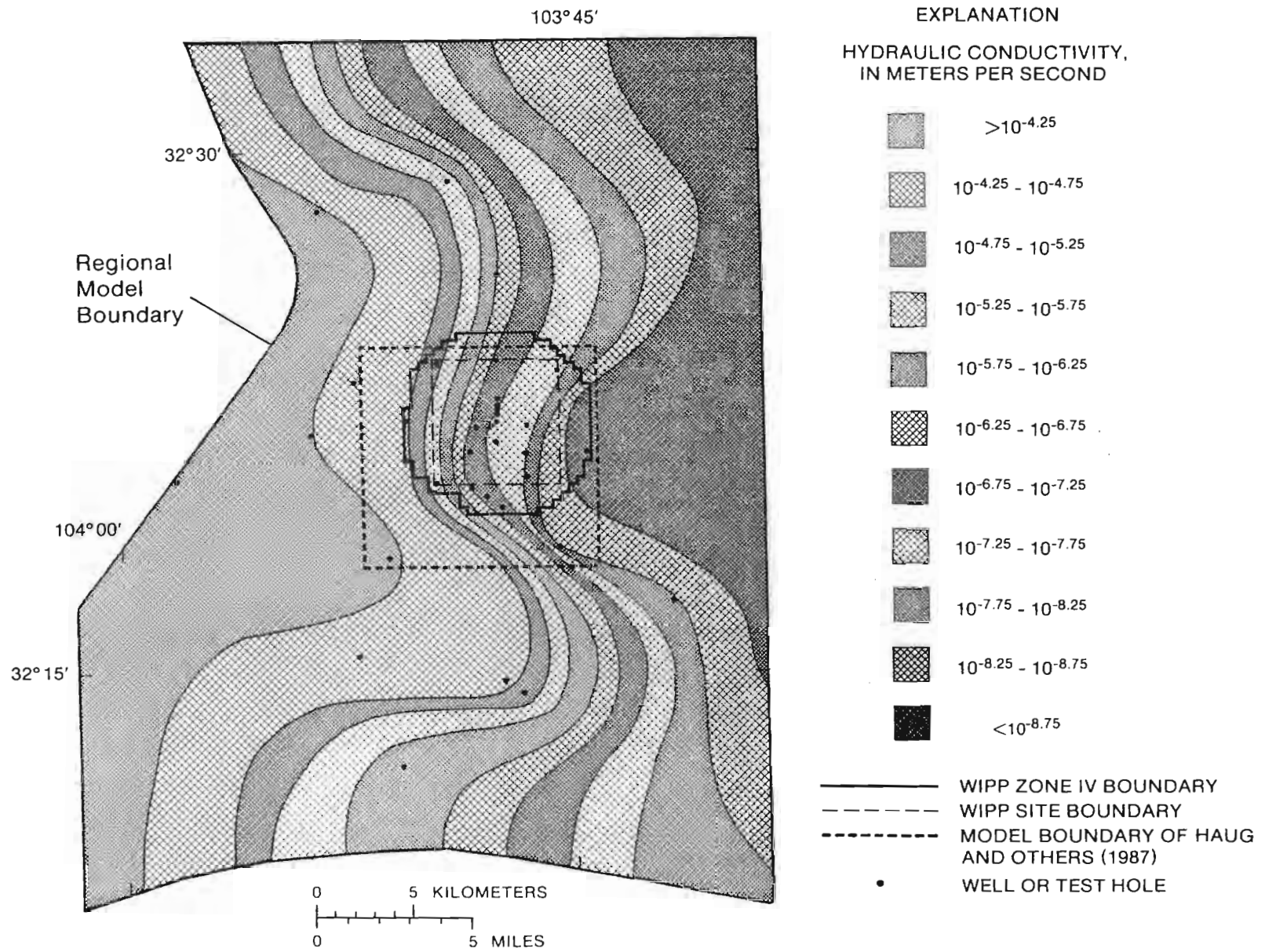


Figure 26.-- Regional hydraulic-conductivity trends and location of model area of Haug and others (1987).

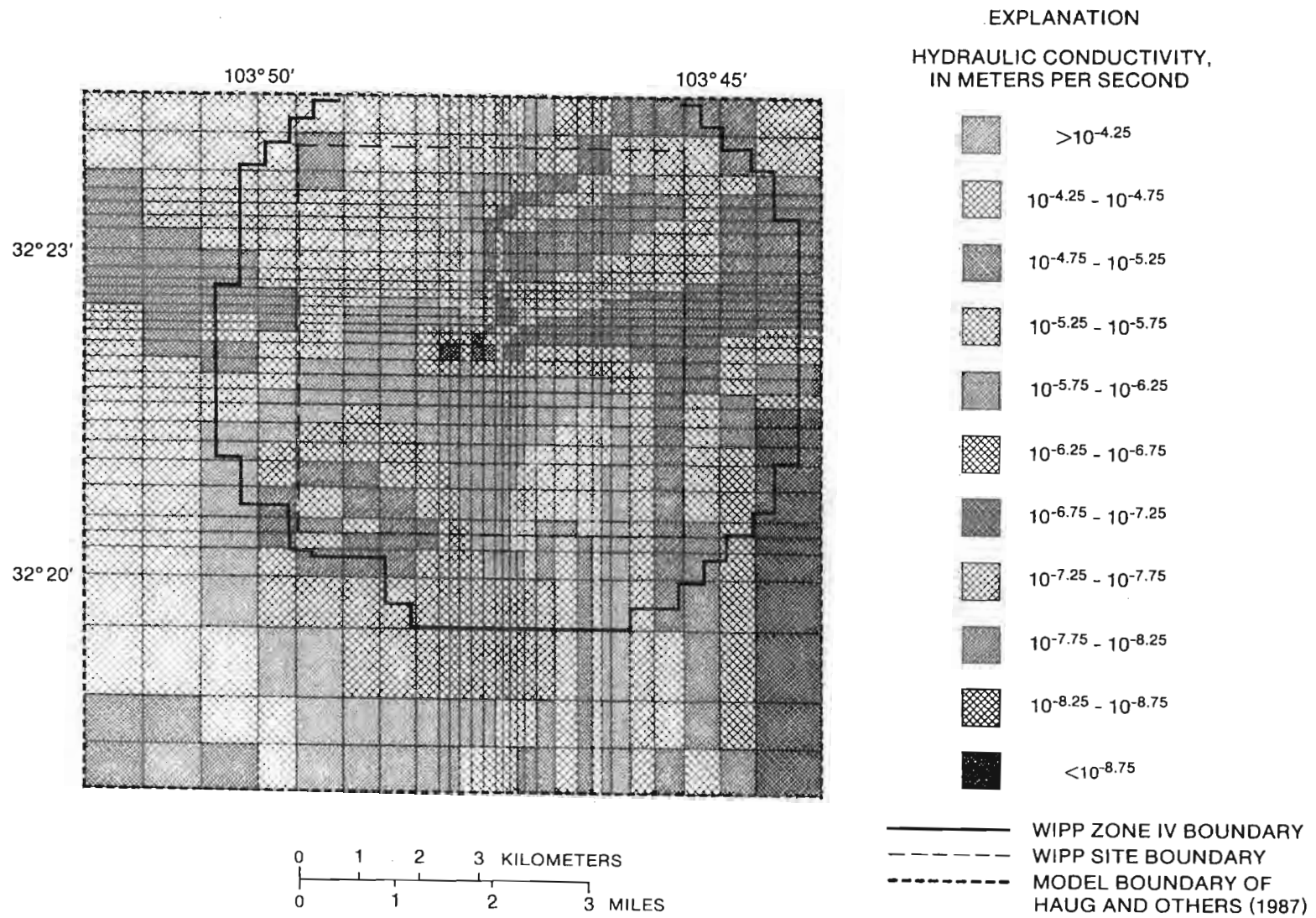


Figure 27.-- Hydraulic-conductivity distribution in model area of Haug and others (1987). Values have been grouped into 1/2 order of conductivity zones. See figure 26 for location of Haug and others (1987) model area.



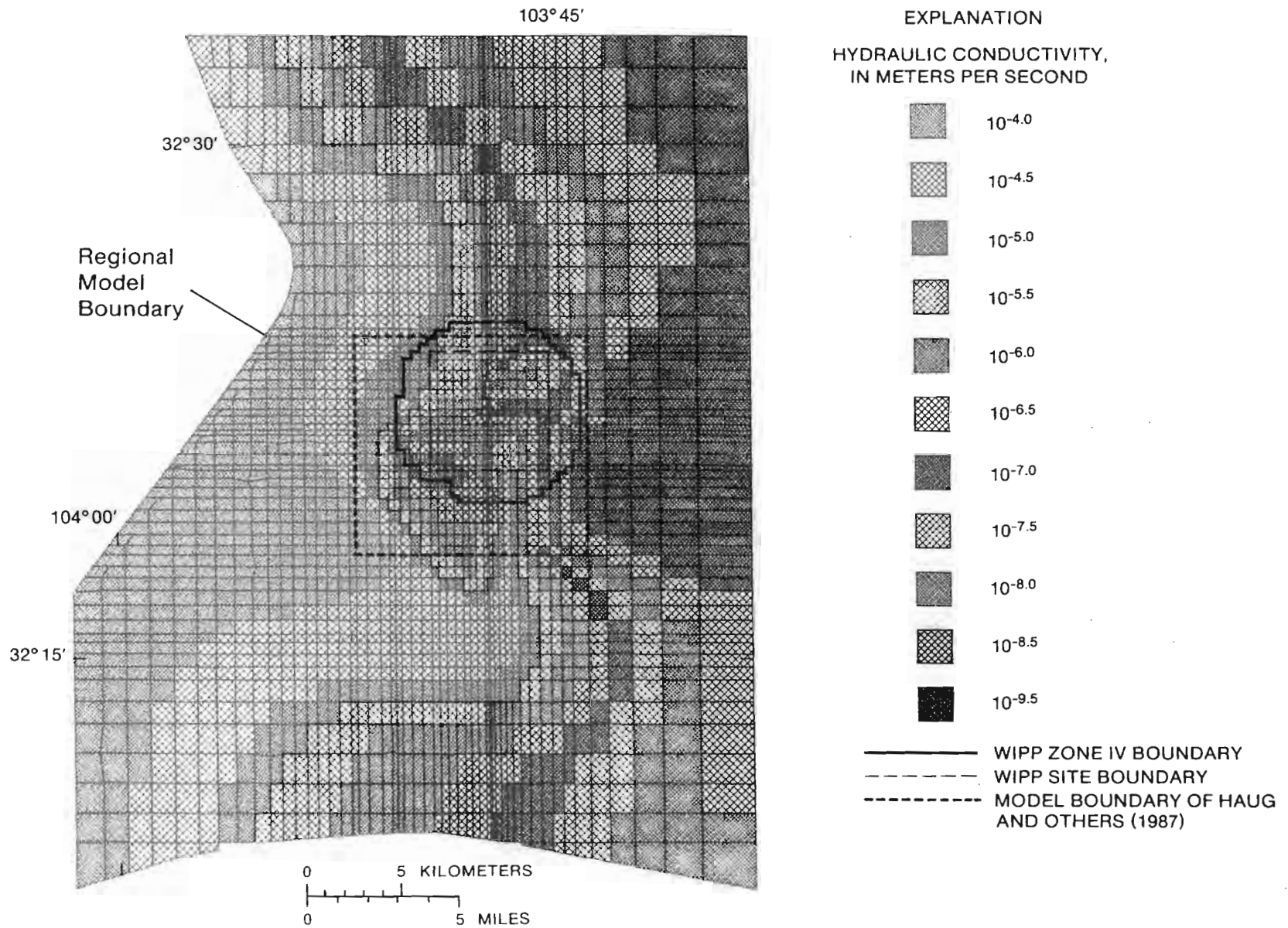


Figure 28.-- Hydraulic-conductivity distribution that incorporates both regional-scale trends and local-scale features.



trends, but also the general structure and most prominent features of the Haug and others (1987) site-scale model.

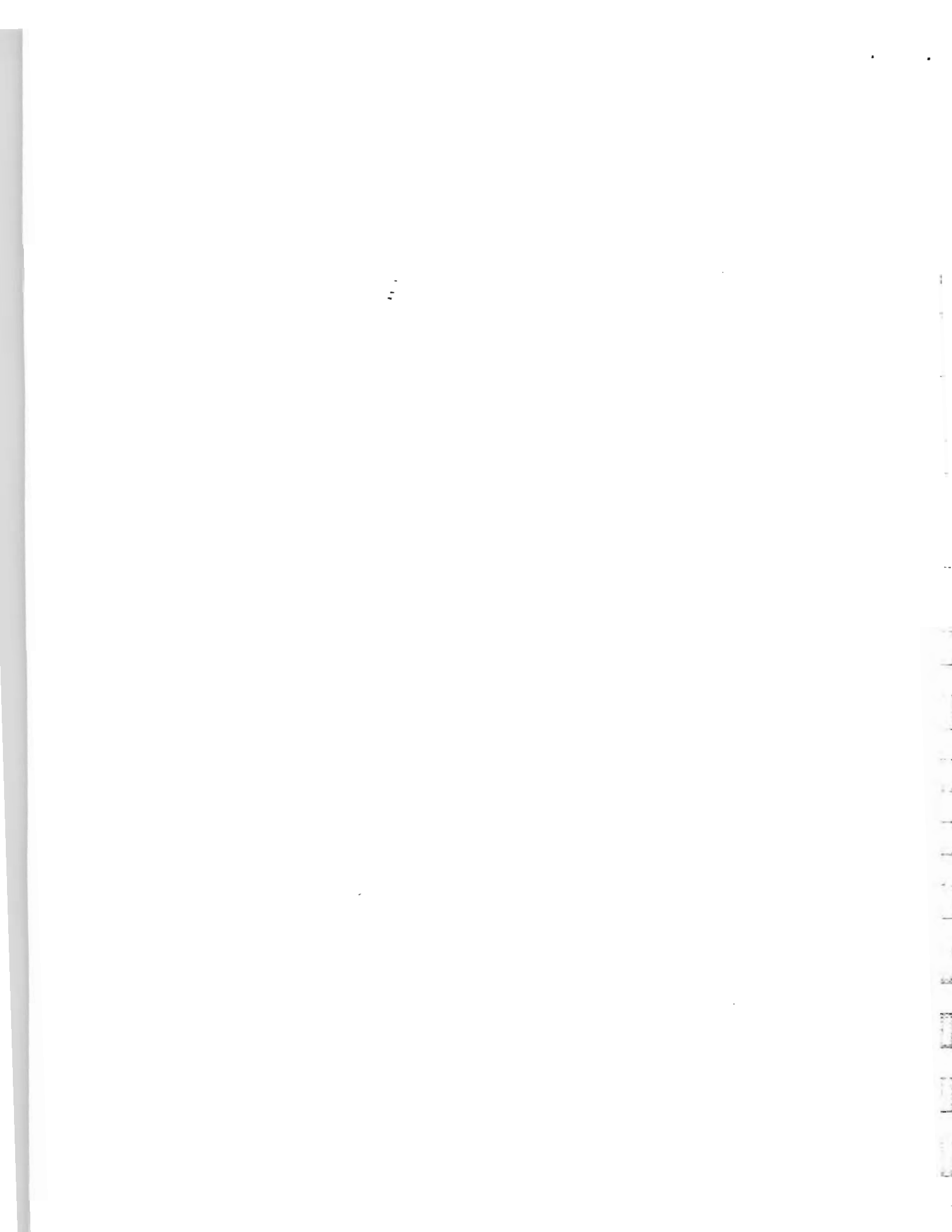
Other model input

The variable-density finite-element code SUTRA (Voss, 1984) was used for the numerical simulations. The finite-element mesh for the regional model contains 5,007 elements and 5,177 nodes (fig. 29). Element dimensions range from 120 to 800 meters. The mesh is finest in the vicinity of the WIPP site where detailed investigations and analyses provide sufficient control to define local-scale variability in hydraulic properties. The mesh also is relatively fine in the area directly south of WIPP where the driving-force analysis indicated that density-related gravity effects may be significant. The mesh is coarser elsewhere in the region. However, solving a variable-density flow problem requires solution of the transport equations; therefore, the mesh generally is much finer than would be required if only the flow equations were being solved. The mesh has been locally deformed so that observation-well and mine-shaft locations coincide with a specific node.

Thickness of the Culebra is relatively uniform throughout the WIPP region, having a mean of 7.7 meters with a standard deviation of 1.6 meters in a sample of 725 drill holes (fig. 30). Therefore, a constant thickness of 8 meters was specified for the regional model. The available data on porosity of the Culebra come primarily from the vicinity of the WIPP site, where a range of 0.07 to 0.30 from core analyses has been reported (Haug and others, 1987). On the basis of this information, a representative value of 0.20 was used for the regional model.

In SUTRA, the storage properties of an aquifer are characterized by specifying rock and fluid compressibility, which are used along with porosity to compute a specific pressure storativity (Voss, 1984, p. 24). For the regional model, a rock compressibility of $2 \times 10^{-10} \text{ [kg/m}\cdot\text{s}^2\text{]}^{-1}$ was specified. This value is within the range of typical values (10^{-8} to $10^{-10} \text{ [kg/m}\cdot\text{s}^2\text{]}^{-1}$) for fissured rock given by Freeze and Cherry (1979) and is similar to the value ($7.6 \times 10^{-10} \text{ [kg/m}\cdot\text{s}^2\text{]}^{-1}$) used by Haug and others (1987), which was calculated from the sparse storage data that are available from tests in the vicinity of the WIPP site. For fluid compressibility, a value of $4.6 \times 10^{-10} \text{ [kg/m}\cdot\text{s}^2\text{]}^{-1}$ was specified (Mercer and others, 1982). These compressibility values, along with a porosity of 0.20 and a thickness of 8 meters, translate to a storage coefficient of 2×10^{-5} .

Because of the absence of well-defined, sharp density contrasts, Haug and others (1987) found ground-water flow and brine transport in the Culebra to be relatively insensitive to dispersivity. In their analysis, a longitudinal dispersivity, α_L , of 50 meters and transverse dispersivity, α_T , of 2.5 meters were used. These values were based on measured thickness and transmissivity heterogeneities of the Culebra and on arguments concerning scale-dependent dispersion described by Pickens and Grisak (1981a, b). On the basis of the Haug and others (1987) results, these same values were used in the regional model. However, because the regional model covers a somewhat larger area and contains two somewhat localized bodies of high-density fluids located in the relatively fast flow-rate area of Nash Draw, a sensitivity analysis similar to that used in Haug and others (1987) also was performed.



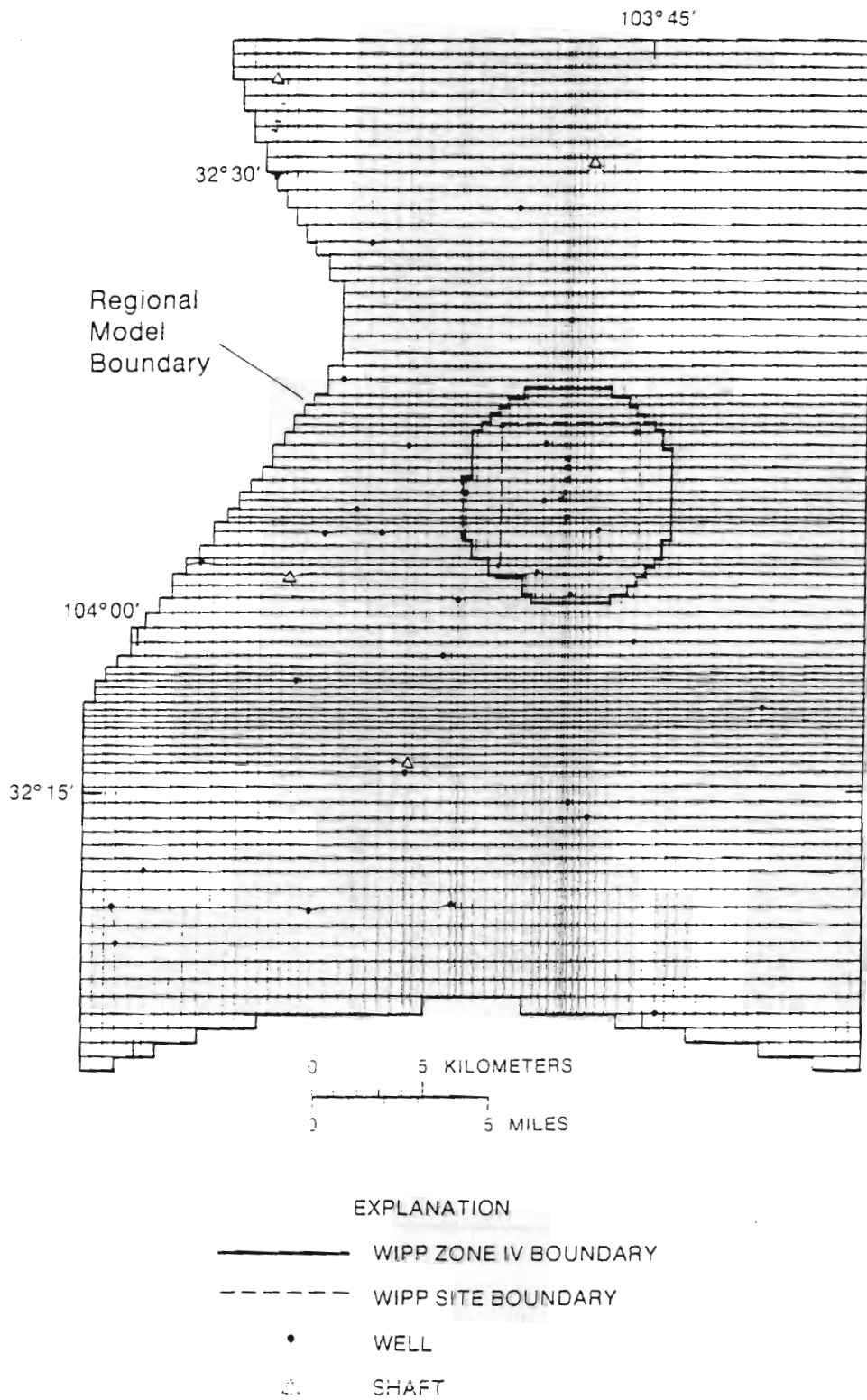


Figure 29.-- Finite-element mesh for the regional model.

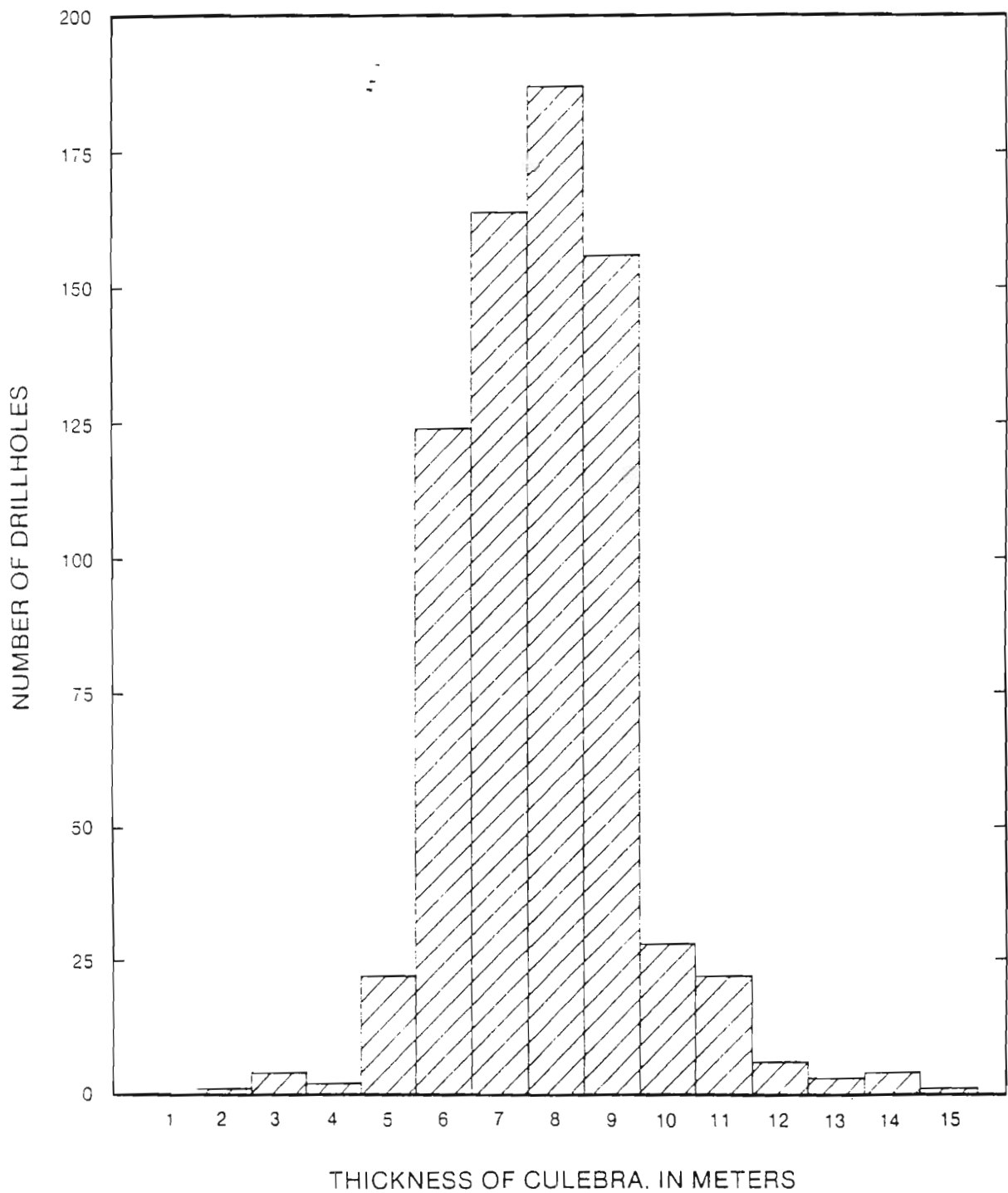


Figure 30.-- Thickness distribution of the Culebra Dolomite Member of the Rustler Formation in 725 drill holes in the northern Delaware Basin.

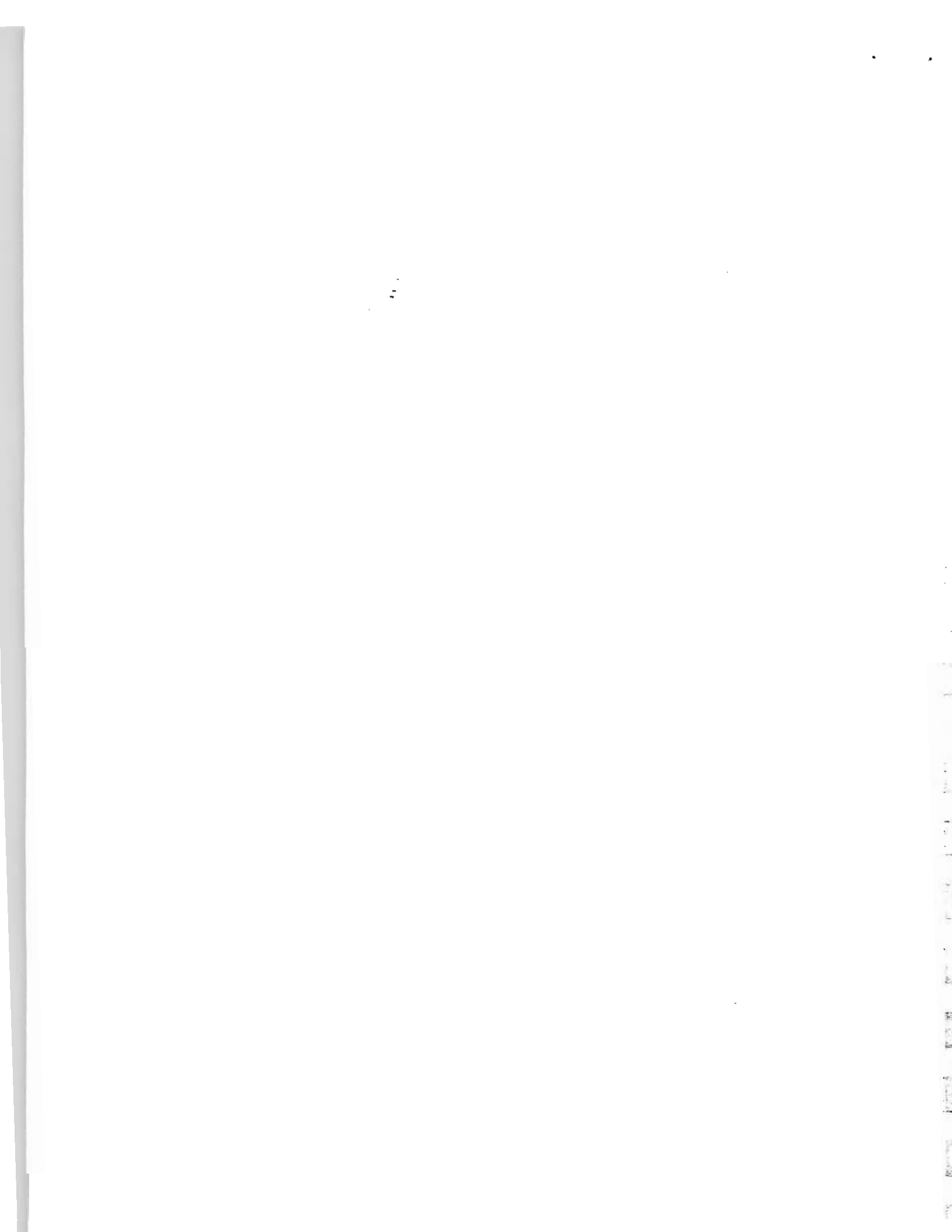
Gravity was incorporated into the model by specifying the magnitude of the gravitational acceleration acting in the plane of the mesh, on the basis of the regional strike and dip. In the model area, the regional strike is 6 degrees west of north and the regional dip is 0.4 degree to the east. This translates to gravitational acceleration components of 0.068764 m/s^2 in the x-direction (east) and 0.0071871 m/s^2 in the y-direction (north). Although this implementation of gravity adequately characterizes regional-scale gravity effects, it does not capture smaller scale effects that are associated with local variations in strike and dip.

Baseline Approximate Steady-State Simulation

The initial phase in the simulation process was to calibrate an approximate, steady-state simulation of the flow system prior to the excavation of the WIPP shafts. The objectives of this simulation were to provide information about the overall behavior of the flow system and to provide a baseline for comparing other system conceptualizations and for examining system sensitivity to various model parameters and underlying assumptions. This simulation is referred to as the "baseline" simulation in the remainder of this report.

In the baseline simulation, the fluid-density distribution was specified as a dimensionless solute distribution. The model then was solved to produce a steady-state pressure distribution. This type of solution is approximate because although the solute (density) distribution is held constant during the simulation, it is not necessarily at steady state. As noted in the section titled "Comparison of Freshwater-Head and Variable-Density Flow Simulations," this type of solution is based on the fact that the time required for significant solute redistribution is long compared to the time required for significant pressure redistribution (Weiss, 1982; Kuiper, 1983, 1985). In other words, this type of solution assumes that significant solute redistribution does not occur over the time period of interest. For the WIPP simulations, significant solute redistribution can be defined as a change in solute distribution that is large enough to cause significant changes in flow directions or flow magnitudes. The time required for significant solute redistribution can be determined by executing a transient simulation that allows solute transport to occur and monitoring velocity changes that are associated with the movement of solutes. This type of transient simulation has been carried out, and the results are described later in this report.

The baseline simulation was calibrated to the preshaft freshwater-head distribution by making changes in the initial hydraulic-conductivity distribution (fig. 28) that were consistent with the regional hydraulic-conductivity trends. The resulting hydraulic-conductivity distribution for the baseline simulation is shown in figure 31. Consistency with the regional trends was maintained by limiting changes to widening or narrowing the width of a given hydraulic-conductivity zone while maintaining a general west-to-east decrease in hydraulic conductivity. Following these constraints, no exotic features were introduced to locally improve calibration in the vicinity of a specific well. Very few changes were necessary in the vicinity of the WIPP site, indicating that the original hydraulic-conductivity distribution of Haug and others (1987) and the somewhat coarser adaptation of that distribution used in this model provide a reasonable fit to the preshaft equivalent-freshwater heads. The most significant changes made during the calibration process were extension of the zones of relatively high hydraulic conductivity associated with the two Nash



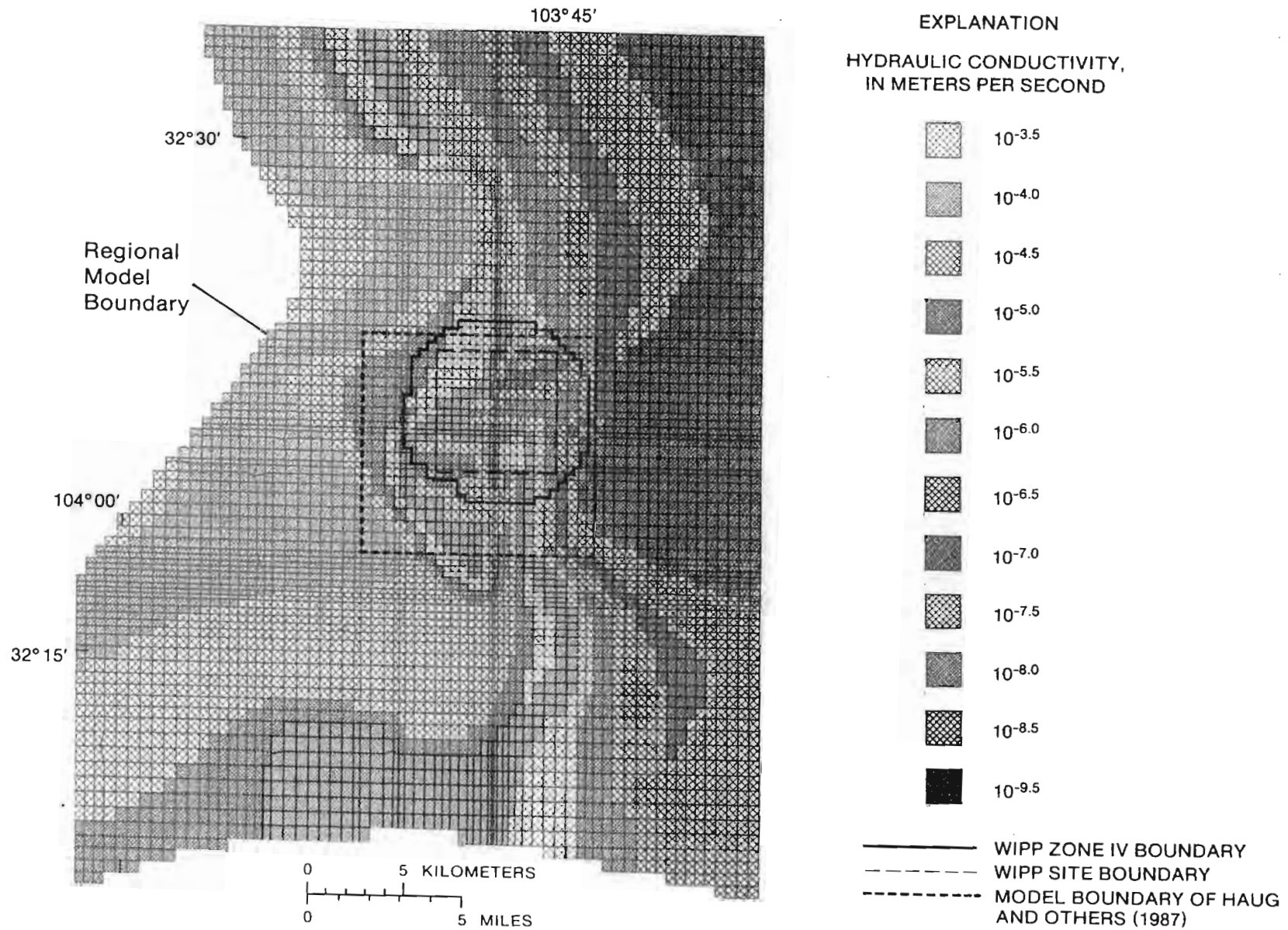


Figure 31.-- Hydraulic-conductivity distribution for the baseline simulation.



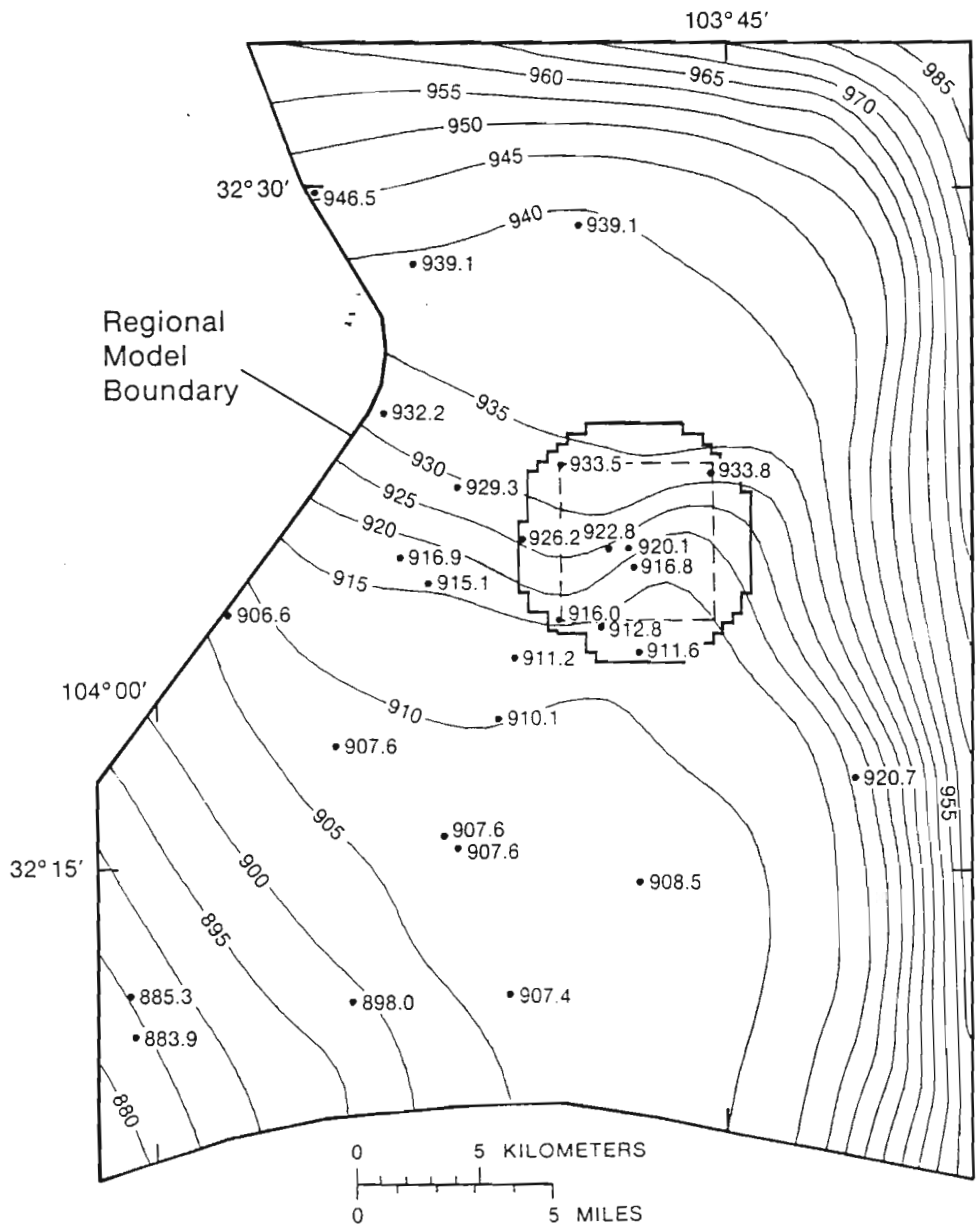
Draw reentrants somewhat further east. Other changes included a small increase in hydraulic conductivity at several places along the axis of Nash Draw and a moderate decrease in hydraulic conductivity along the southern part of the Pecos River discharge boundary.

The simulated equivalent-freshwater-head surface for the baseline simulation is shown in figure 32. The difference between the simulated equivalent-freshwater heads and the equivalent-freshwater heads calculated from field measurements at 28 wells is shown in figure 33. The mean absolute deviation from the field heads was 1.3 meters. Within the WIPP Zone IV boundary, the mean absolute deviation was 0.5 meter, with a maximum deviation of 1.2 meters. In the WIPP region, the largest deviations were along the southern margin, indicating the possibility of more complex conditions in this area. Additional analysis would require more extensive data than are currently available to fully characterize this area. The simulated equivalent-freshwater-head surface also contains the most prominent features in the observed equivalent-freshwater-head surface (fig. 19), including moderate gradients in the vicinity of the WIPP site and in the narrow part of Nash Draw west of the site and very flat gradients to the north and south of the site. The very low hydraulic conductivity that has been postulated to the east produces relatively steep head gradients in that area.

The Pecos River boundary was implemented by specifying heads along the boundary equal to the approximate river altitudes, which ranged from 893 meters at the north end of the boundary to 874 meters at the south end. Implementing the boundary in this fashion allows the model to compute discharge from the ground-water system to the Pecos River. This model-computed discharge can be compared with independent estimates of ground-water discharge to the Pecos River.

On the basis of water-budget calculations for an area that roughly corresponds with the model area, Hunter (1985) estimated that ground-water discharge to the Pecos River is between 300 and 4,500 acre-feet per year (1×10^{-2} to 2×10^{-1} m^3/s). This range includes discharge from the entire geologic section above the Salado salt, not just the Culebra. Havens and Wilkins (1979) reported an average river gain during low flow of approximately 1,300 acre-feet per year (5×10^{-2} m^3/s) for the reach of river between Malaga Bend and the Red Bluff streamflow-gaging station, which is a few miles south of the southern model boundary. Because these measurements were made during periods of low flow, this gain primarily reflects ground-water discharge to the Pecos River. This value represents discharge from the entire rock section above the Salado salt on both sides of the river. Hale and others (1954) reported an estimated ground-water discharge to the Pecos River at Malaga Bend of 1,740 acre-feet per year (7×10^{-2} m^3/s), 1,450 acre-feet per year (6×10^{-2} m^3/s) from irrigation-return flow and 290 acre-feet per year (1×10^{-2} m^3/s) from ground water.

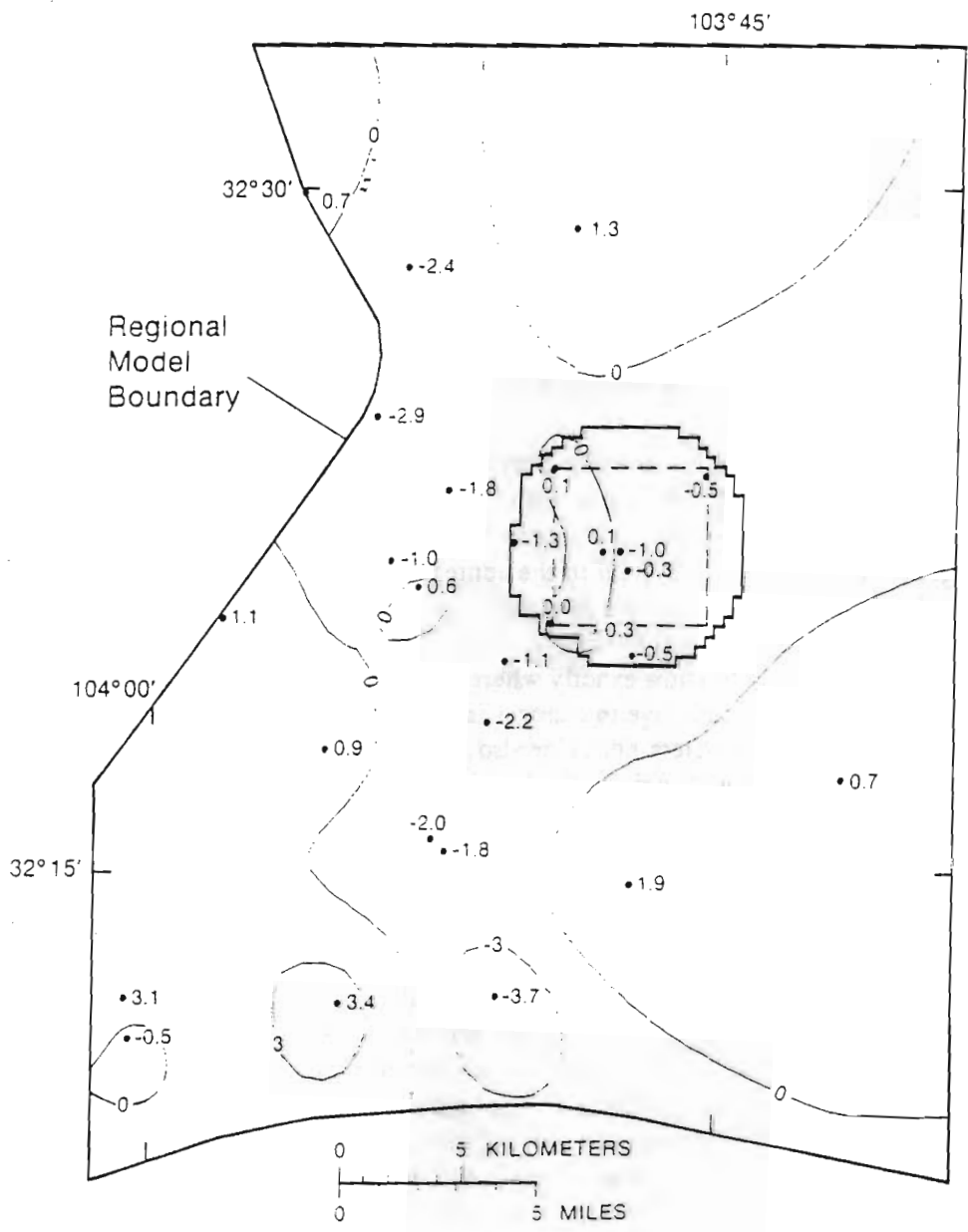
As discussed in the previous paragraph, the range of reported estimates of ground-water discharge to the Pecos is 290 to 4,500 acre-feet per year (1×10^{-2} to 2×10^{-1} m^3/s). Because all of these estimates include the entire rock section overlying the Salado salt, including the brine aquifer at the Rustler-Salado contact zone, and some include contributions from the west side of the river, discharge from the Culebra to the Pecos River from the model area probably is at the low end of this range or possibly somewhat less. The computed discharge to the Pecos River in the baseline simulation was approximately 225 acre-feet per year (9×10^{-3} m^3/s), which is of the correct order of magnitude.



EXPLANATION

- WIPP ZONE IV BOUNDARY
- - - - WIPP SITE BOUNDARY
- 900 — FRESHWATER HEAD CONTOUR—Shows altitude at which water having a density of 1.00 gram per cubic centimeter would have stood in a tightly cased well. Contour interval 5 meters. Datum is sea level
- 906.6 WELL OR TEST HOLE—Number is simulated equivalent—freshwater head at well, in meters. Datum is sea level

Figure 32.-- Simulated equivalent-freshwater-head surface from the baseline simulation.



EXPLANATION

- WIPP ZONE IV BOUNDARY
- - - WIPP SITE BOUNDARY
- 3 — LINE OF EQUAL DIFFERENCE BETWEEN HEADS—Interval 3 meters
- 1.9 WELL OR TEST HOLE—Number is the difference between simulated and calculated equivalent-freshwater heads at well, in meters

Figure 33.-- Difference between equivalent-freshwater heads from the baseline simulation and equivalent-freshwater heads calculated from field measurements.

Simulated flow directions and flow velocities from the baseline simulation are shown in figure 34. The highest flow rates are in Nash Draw, where velocities reach 10^{-6} m/s (approximately 30 m/yr). On the other extreme, velocities are 5 1/2 orders of magnitude lower in the area east of the WIPP site, approximately 1 mm/yr (millimeter per year). Because of the large local variations in conductivity, velocities are highly variable in the transition zone between these two extremes. Relative to WIPP, the most significant feature of the regional flow field is the relatively high velocities associated with the high conductivity zone that was postulated in the Haug and others (1987) model. Velocities in this zone range from 0.3 to 3 m/yr.

Sensitivity Analyses and Alternative System Conceptualizations

The approximate steady-state solution provided not only information about the overall behavior of the regional flow system but also a baseline for comparing other system conceptualizations and system sensitivity to various model parameters and underlying assumptions. Given that this study examined a flow system in the context of evaluating a potential point source of contamination, flow direction was selected as the primary parameter for making comparisons in the sensitivity analyses. Flow direction was chosen for two reasons. In a potential contaminant transport situation, it is important to know exactly where the water is flowing. In the WIPP regional flow model, flow direction is very sensitive to changes in model parameters. Comparisons of other parameters that characterize flow-system behavior also were made, including velocity magnitude, equivalent-freshwater head, solute (density) distribution, and driving-force ratio. These other comparisons also are described where pertinent in the following sections.

Density effects

In order to highlight the role of fluid density, a simulation based on equivalent-freshwater head was executed. In this simulation, fluid density was completely removed from the solution by specifying zero solute concentrations throughout the entire flow domain. The magnitude of the angle between the flow direction produced by the equivalent-freshwater-head simulation and the flow direction produced by the baseline simulation (which takes into account the effects of fluid density) is shown in figure 35. An angle of zero usually indicates that density effects are insignificant, but under some circumstances a zero angle indicates that the direction of the density-related driving-force component happens to exactly coincide with the direction of the pressure-related driving-force component. Conversely, a large angle indicates that density effects are quite significant and that analyses based on equivalent-freshwater head will produce misleading results.

Throughout most of the WIPP region, fluid-density variations have little impact on flow directions (fig. 35). There is a moderate-sized area south and southeast of the WIPP site where density effects are significant. This is the same area that displayed high driving-force ratio values in the regional driving-force analysis (fig. 20). In this area, the flow directions produced by the equivalent-freshwater-head simulation are in error by as much as 107 degrees. The equivalent-freshwater-head simulation also underestimates velocity magnitudes by as much as 80 percent. This

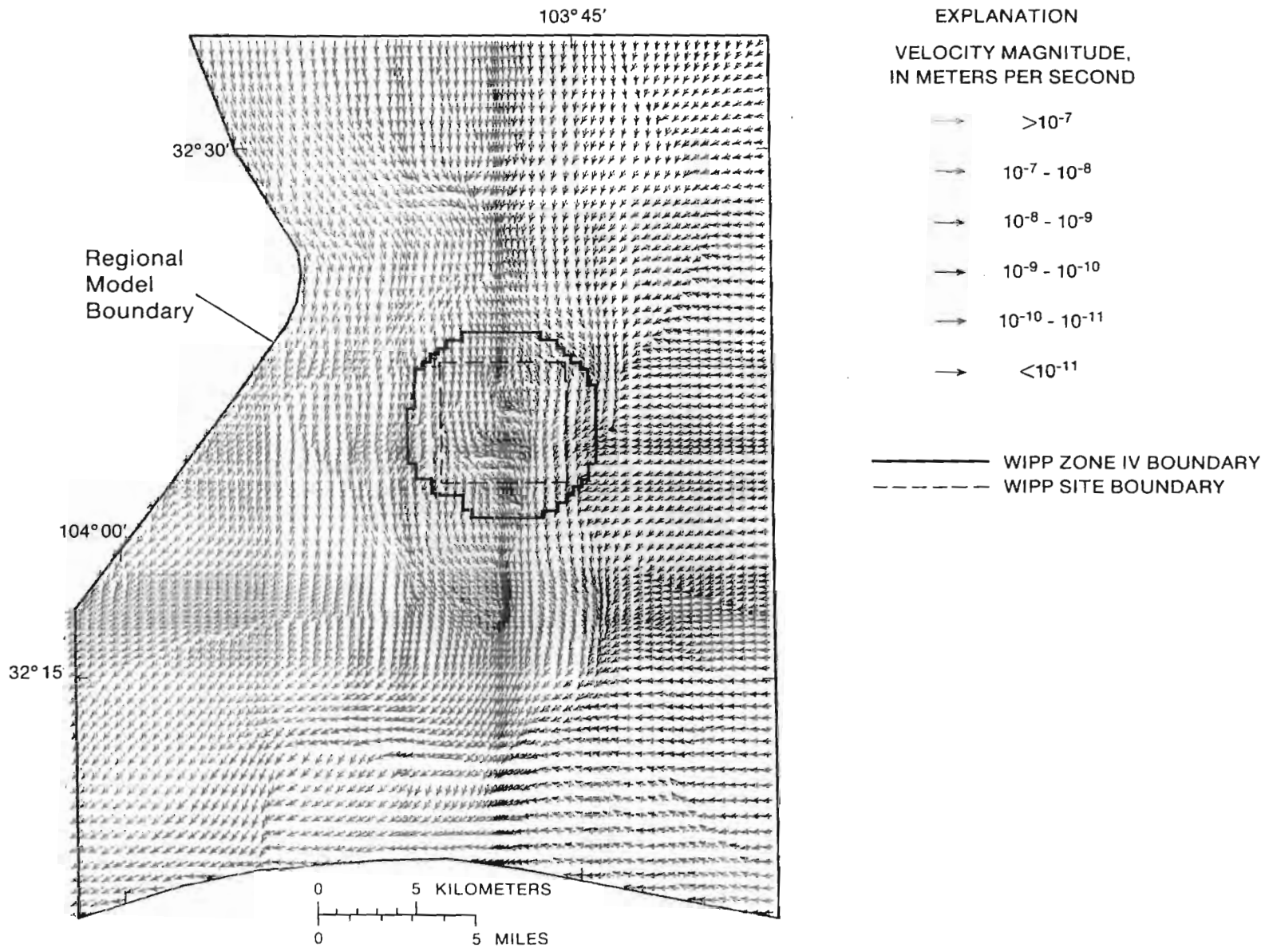
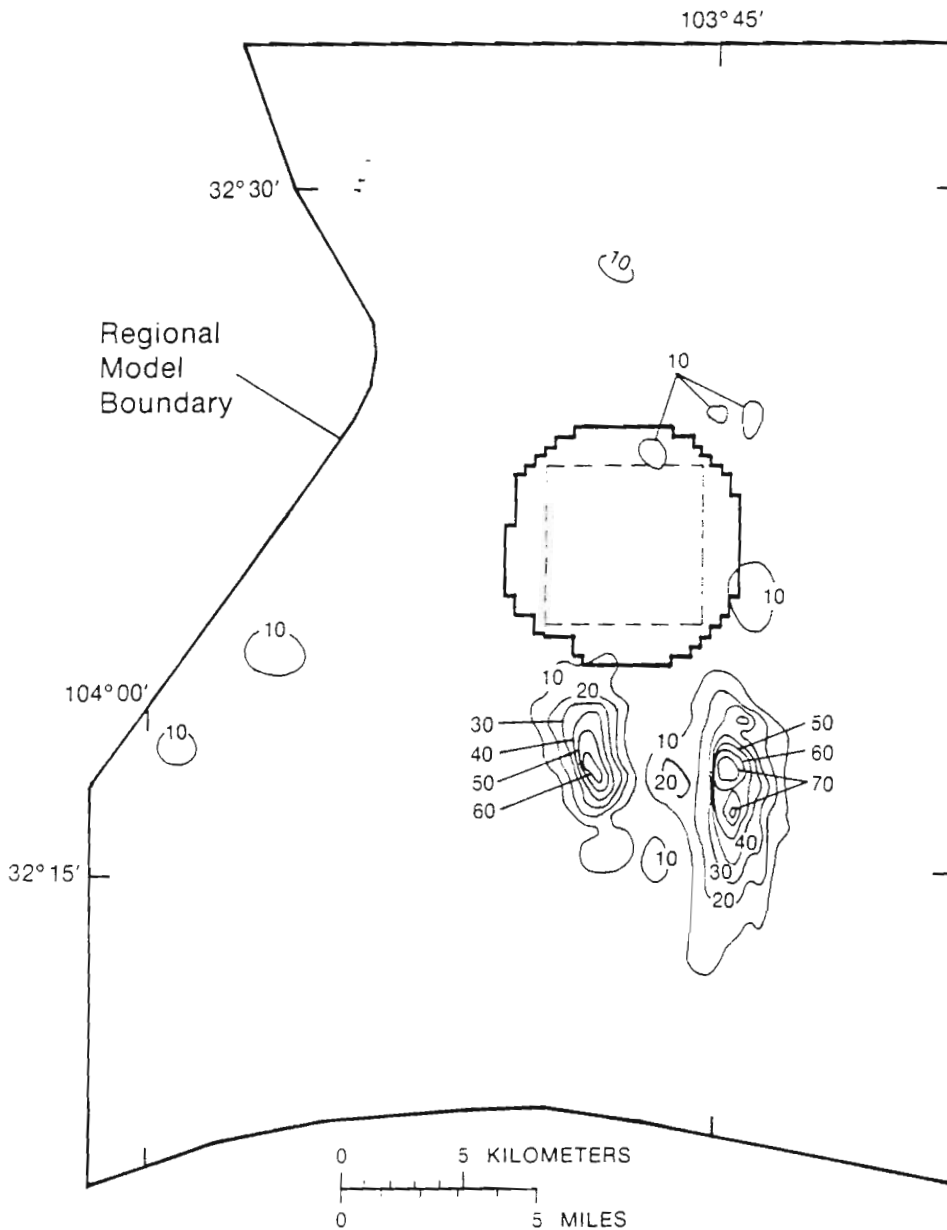


Figure 34.-- Simulated direction and magnitude of ground-water flow produced by the baseline simulation.





EXPLANATION

- WIPP ZONE IV BOUNDARY
- - - - WIPP SITE BOUNDARY
- 10— LINE OF EQUAL MAGNITUDE OF DEVIATION ANGLE —Interval 10 degrees

Figure 35.-- Magnitude of the deviation angle between the flow direction produced by the equivalent-freshwater-head simulation and the flow direction produced by the baseline (variable-density) simulation.

6 : 1000 1000 2

area is important relative to WIPP because it lies along potential transport pathways that extend southward from the site.

An enlargement of the area south of the WIPP site that is sensitive to fluid-density effects, comparing the velocity vectors for the two simulations, is shown in figure 36. The primary effect of fluid density is to drive fluid flow in a more easterly, downdip direction than predicted by the equivalent-freshwater-head-based simulation. This area has a very gentle dip and only moderate fluid densities. The major contributing factor to the dominance of fluid-density effects is the very flat head gradient in this area. The flat head gradients in this area and in a similar area to the north of the WIPP site make these two areas very sensitive not only to density effects but also to hydraulic stresses and other factors that influence system behavior.

Steady-state variable-density assumptions

An important assumption underlying the baseline simulation is that significant solute redistribution takes place slowly; therefore, over some length of time, the solute distribution can be considered constant relative to its effect on ground-water flow patterns. In order to determine the length of time over which this assumption is valid, the baseline simulation was used as the starting point for a transient simulation during which solute movement and associated changes in flow patterns were monitored.

For this transient simulation, a small change in the Nash Draw boundary was made. As noted in the sections describing the regional driving-force analysis and the selection of model boundaries, there is a local body of high-density fluid associated with a potash mining and milling operation that is located along the northern part of the Nash Draw boundary. The driving-force analysis indicates that ground-water flow in this area may experience a small eastward deviation from the main flow line down the axis of Nash Draw. Preliminary testing of the transient simulation revealed that in the immediate vicinity of this local body of high-density fluid, there is a slight tendency for the denser fluid to move away from the model boundary somewhat and flow in a more easterly downdip direction. This behavior, which is exactly what the driving-force analysis predicts for this locality, has one unrealistic side effect when the Nash Draw boundary is implemented as a true no-flow (impermeable) boundary. The process of a local dense body of fluid moving away from a no-flow boundary creates a localized pressure decrease between the no-flow boundary and the body of fluid. That pressure decrease is unrealistic because in the real system the local eastward deviation of flow would cause a small amount of eastward fluid movement from the area that is directly updip.

In order to implement a somewhat more flexible boundary, the Nash Draw boundary was changed from a no-flow to a specified-pressure boundary and pressure values along the boundary were determined from the baseline simulation. The new boundary not only maintains an approximate flow line along the axis of Nash Draw but also allows more realistic flow in the vicinity of the local body of dense fluid in the northern part of Nash Draw.

The magnitudes of the deviation angles between the flow direction produced by the baseline simulation and the flow direction after 10, 50, 100, and 1,000 years of simulated transient flow and transport show the impact of solute redistribution on flow direction. The flow direction comparison

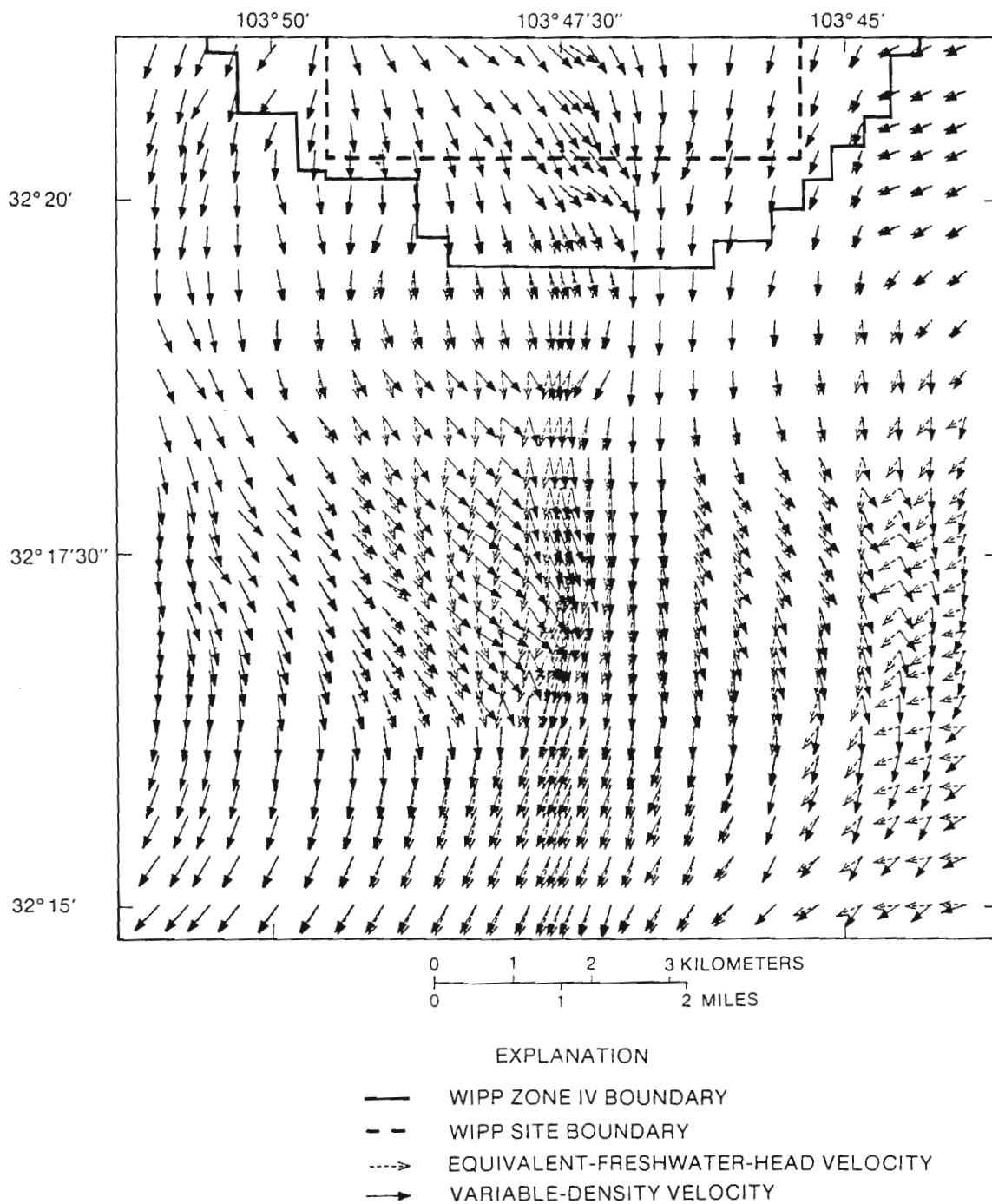


Figure 36.-- Comparison of the flow direction produced by the equivalent-freshwater-head simulation and the flow direction produced by the baseline (variable-density) simulation for the area just south of the WIPP site.

after 10 years of transient flow and transport indicates a small area with flow-direction differences of about 5 degrees, suggesting that the baseline and 10-year transient flow fields are essentially identical.

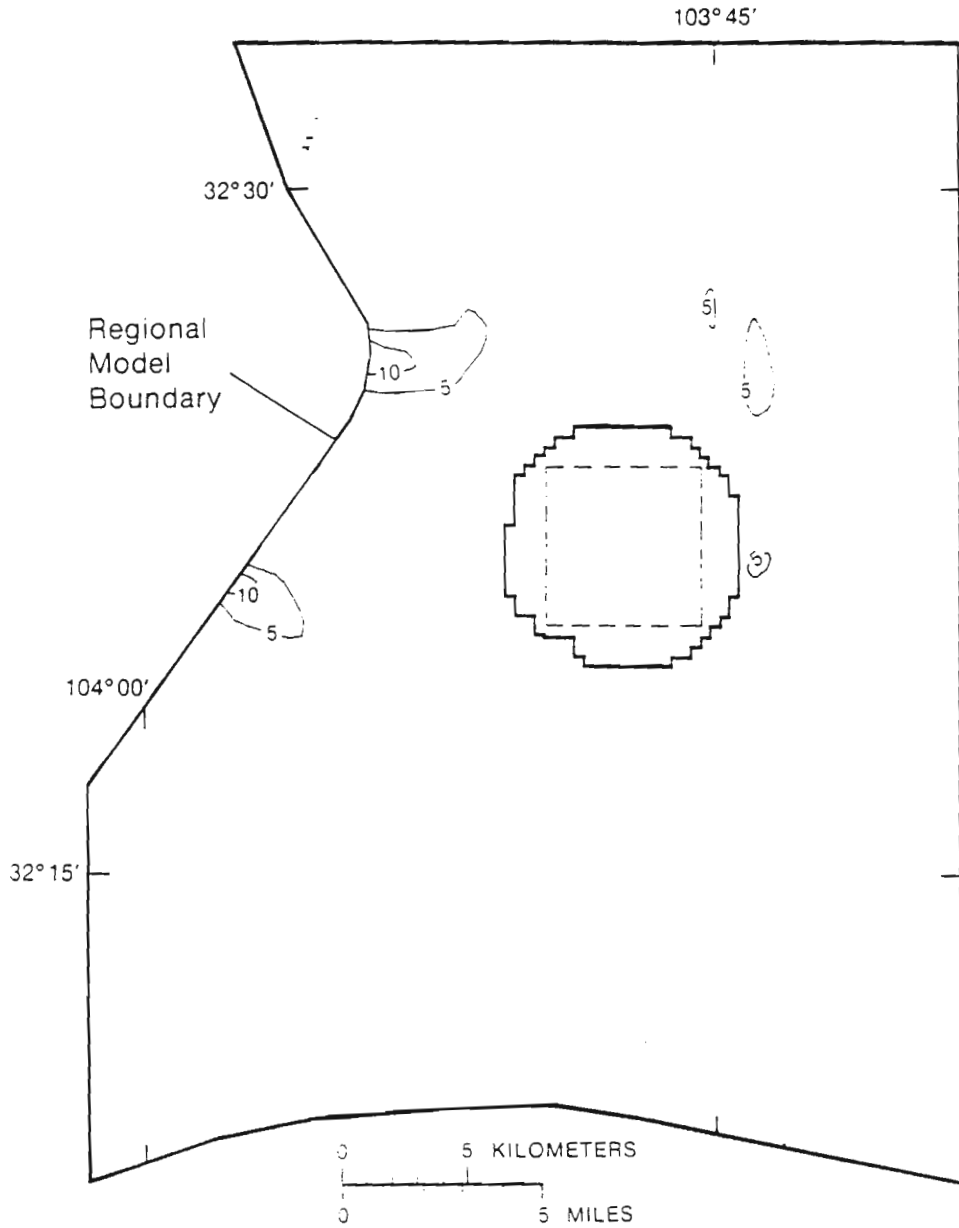
The differences between the baseline and 50-year transient flow fields are small (fig. 37). After 50 years, changes in flow direction of about 10 degrees begin to appear in two areas in Nash Draw. These changes are associated with the southward movement of local bodies of high-density fluids that are associated with potash-mining operations. Also, small changes in flow direction begin to occur in the area of flat head gradients northeast of the WIPP site. The flow-direction changes in this area are not a by-product of large fluid-density changes in this area, but rather, the result of the propagation of very small pressure changes associated with the updip passing of the dense body of fluid associated with the potash-mining operation to the west in Nash Draw. In most areas this small pressure change is not significant. However, because the head gradient in this area is so flat, this area is very sensitive to local pressure changes.

The differences between the baseline and 100-year transient flow fields are still fairly small (fig. 38). After 100 years, changes in flow directions have grown to approximately 15 degrees in the vicinity of the potash-related, dense-fluid bodies that are moving southward along Nash Draw. After 1,000 years of simulated transient flow and transport, the number and size of areas with changes in flow direction have increased, and the maximum change in flow direction has reached almost 25 degrees (fig. 39). However, the flow field at the WIPP site has remained fairly stable and has not been affected by solute redistribution, even after 1,000 years of flow and transport.

This transient simulation has shown that solute redistribution in the regional flow system takes place very slowly. This redistribution has very little impact on flow patterns over a 100-year time period and has small, but notable local impact over a 1,000-year time period. The first areas to experience changes in flow direction associated with solute redistribution are in the immediate vicinity of the two local bodies of potash mine-related, high-density fluids that move southward along the axis of Nash Draw at relatively fast velocities. The next areas to experience changes in flow directions are to the north and south of the WIPP site where head gradients are flat. These flat-gradient areas are very sensitive to small pressure changes. Solute redistribution has very little impact on flow directions in the vicinity of the WIPP site, even after 1,000 years of flow and transport.

Long-term brine transport patterns

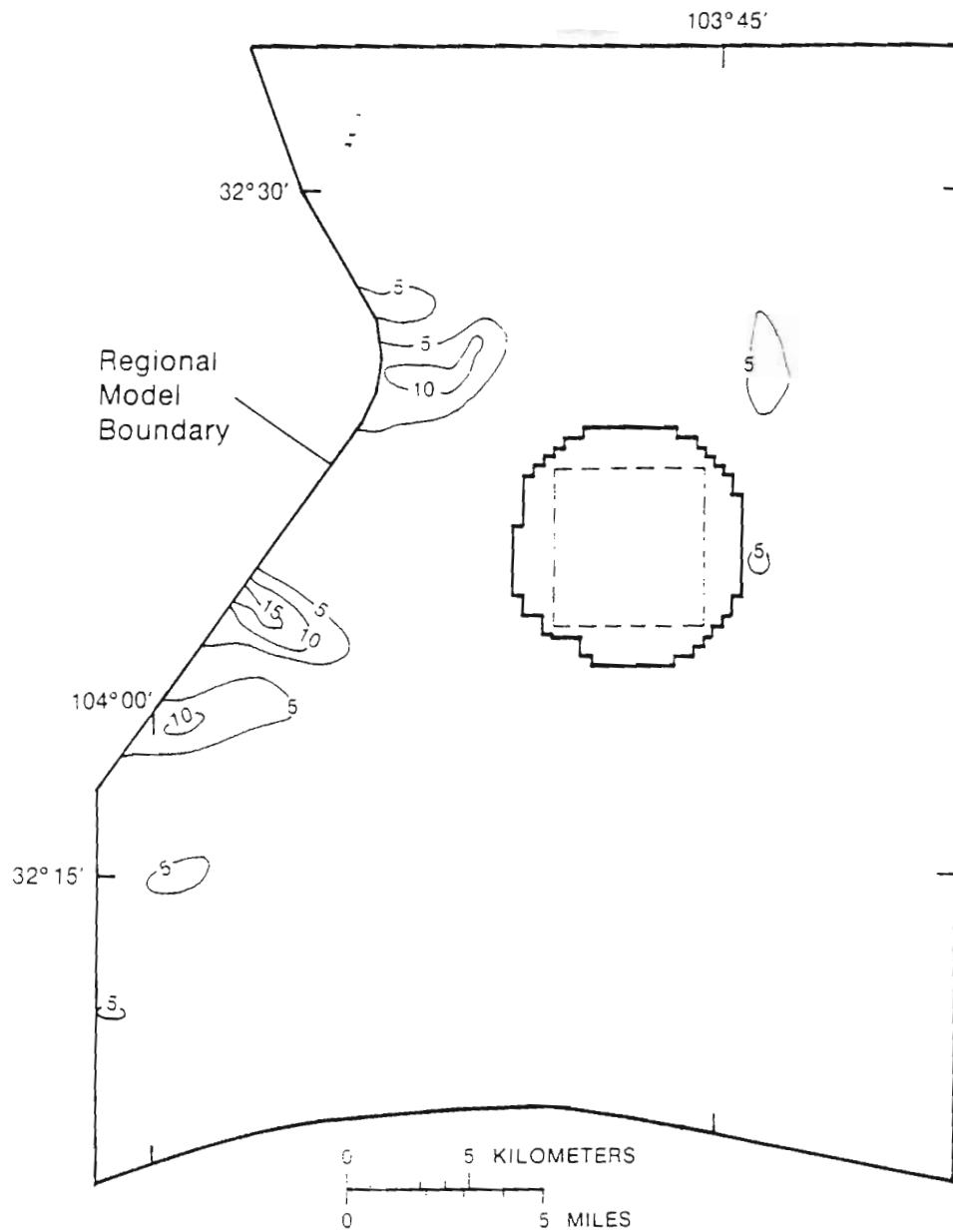
The pattern of brine transport over a 1,000-year time period gives a good qualitative indication of the transport behavior of the flow system on a regional scale for long time periods. The fluid-density distribution after 1,000 years of simulated transient flow is superimposed on the initial (present-day) fluid-density distribution in figure 40. After 1,000 years, Nash Draw has been almost entirely flushed, and the two localized bodies of high-density fluids associated with the potash mines have been completely removed. In contrast, to the east of WIPP there has been no significant movement of the high-density fluid. This area is characterized by low hydraulic conductivity and slow fluid velocity. Transport behavior in the vicinity of the WIPP site lies between these two extremes. At the western edge of the site, there have been small to moderate



EXPLANATION

- WIPP ZONE IV BOUNDARY
- - - - WIPP SITE BOUNDARY
- 5 — LINE OF EQUAL MAGNITUDE OF DEVIATION ANGLE — Interval 5 degrees

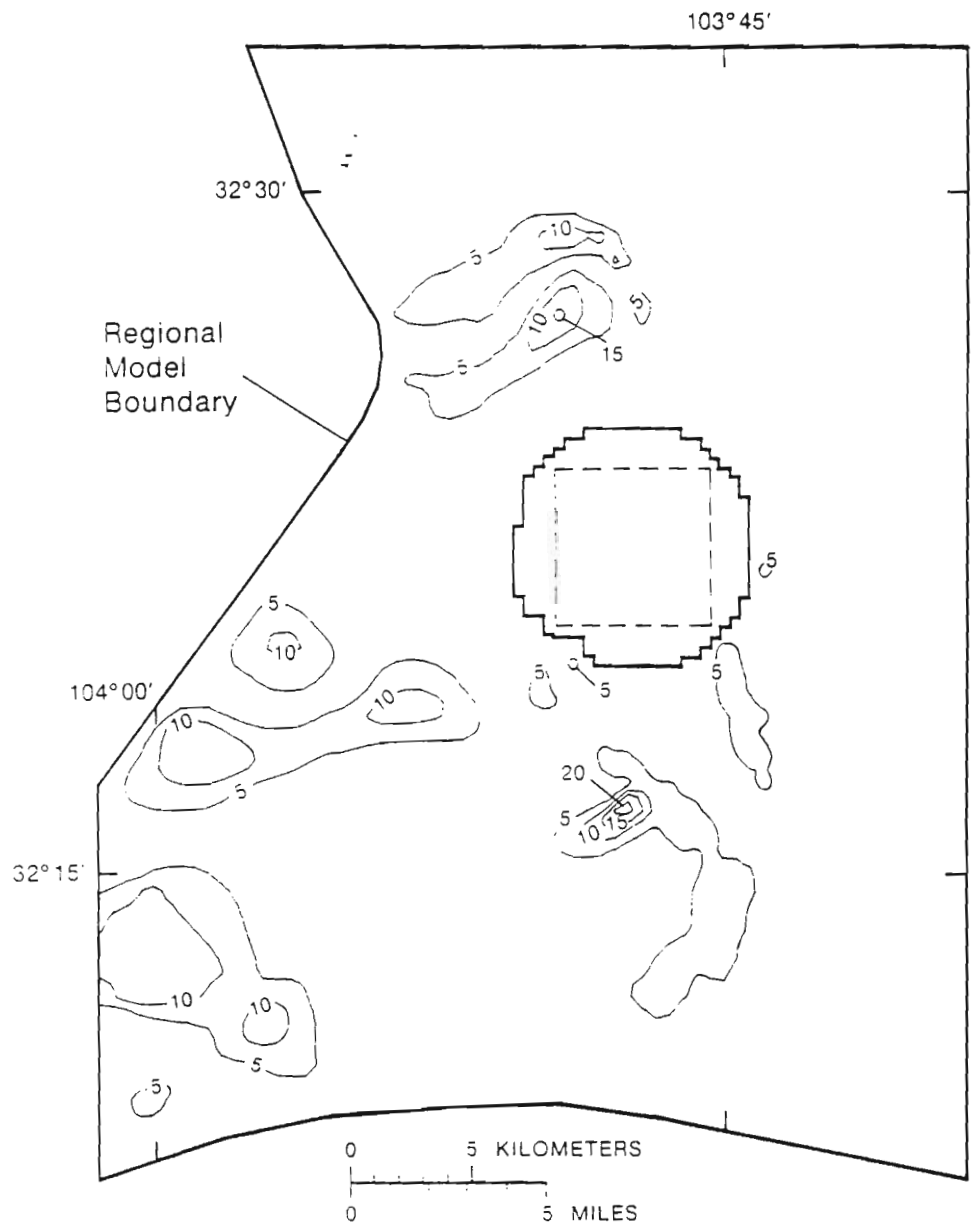
Figure 37.-- Magnitude of the deviation angle between the flow direction produced by the baseline simulation and the flow direction after 50 years of transient flow and transport.



EXPLANATION

- WIPP ZONE IV BOUNDARY
- - - - WIPP SITE BOUNDARY
- 5— LINE OF EQUAL MAGNITUDE OF DEVIATION ANGLE —Interval 5 degrees

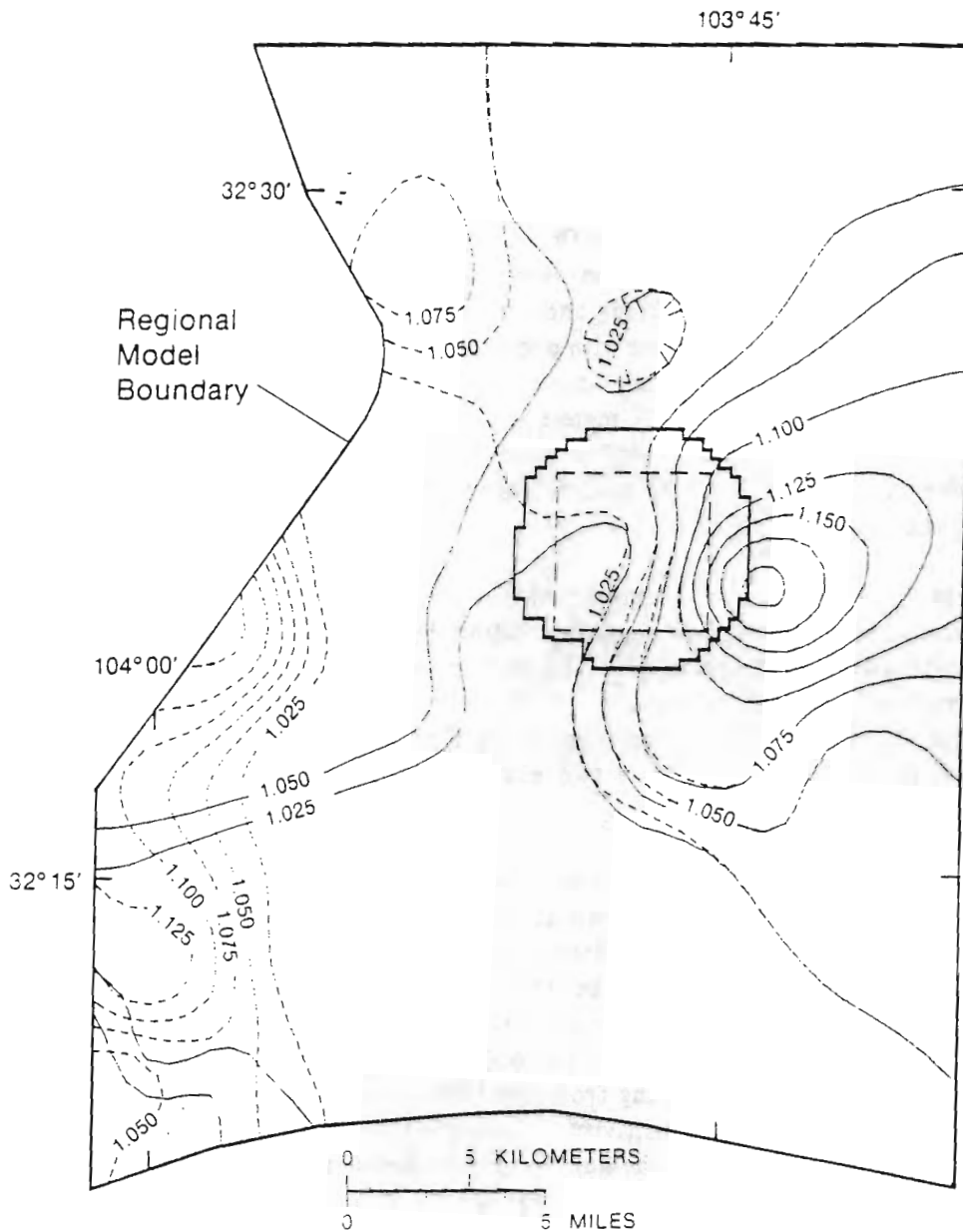
Figure 38.-- Magnitude of the deviation angle between the flow direction produced by the baseline simulation and the flow direction after 100 years of transient flow and transport.



EXPLANATION

- WIPP ZONE IV BOUNDARY
- - - - WIPP SITE BOUNDARY
- 5 — LINE OF EQUAL MAGNITUDE OF DEVIATION ANGLE — Interval 5 degrees

Figure 39.-- Magnitude of the deviation angle between the flow direction produced by the baseline simulation and the flow direction after 1,000 years of transient flow and transport.



EXPLANATION

- WIPP ZONE IV BOUNDARY
- WIPP SITE BOUNDARY
- 1.025 — LINE OF EQUAL FLUID DENSITY AFTER 1,000 YEARS OF TRANSIENT FLOW AND TRANSPORT—Interval 0.025 grams per cubic centimeter
- 1.050 --- LINE OF EQUAL INITIAL FLUID DENSITY—Interval 0.025 grams per cubic centimeter

Figure 40.-- Fluid-density distribution after 1,000 years of transient flow and transport superimposed on the initial (present-day) fluid-density distribution.

changes in the fluid-density distribution, whereas in the eastern part of the site, there has been very little change in the fluid-density distribution.

Sensitivity to dispersivity

As noted in the description of model implementation, Haug and others (1987) found ground-water flow and brine transport in the Culebra flow system to be relatively insensitive to dispersivity due to the absence of well-defined, sharp density contrasts. Because the regional model of the Culebra covers a larger area than the Haug and others (1987) model and because it contains two localized bodies of dense fluids associated with potash mining and milling operations in Nash Draw, model sensitivity to dispersivity was analyzed. The dispersivity values incorporated into this analysis were maximum values of $\alpha_L=200$ meters and $\alpha_T=10$ meters, and minimum values of $\alpha_L=20$ meters and $\alpha_T=1$ meter. Transient simulations were run for 100-year time periods. Comparisons with the baseline simulation ($\alpha_L=50$ and $\alpha_T=2.5$) were made by examining differences in the fluid-density distributions and flow fields.

Differences between the baseline, high-dispersivity, and low-dispersivity density distributions and flow fields were very small, indicating that flow and transport at the regional scale are relatively insensitive to dispersivity. The maximum local density difference between the extreme case and the baseline simulation was 0.01 g/cm^3 for both the high- and low-dispersivity cases. The impact of these small differences on the flow field was essentially insignificant; the maximum deviation angles between the two extreme cases and the baseline simulation were approximately 3 degrees.

The reason for negligible sensitivity to dispersivity is the general absence of sharp density (solute-concentration) gradients. The somewhat localized bodies of potash mine-related dense fluids are the most sensitive. These bodies of dense fluid may actually have relatively sharp density (concentration) gradients at their margins, but there are insufficient data to define these gradients. In terms of the regional objectives, precise definition of the margins of these bodies is much less important than characterizing the impact of the bodies on the flow system as a whole. The small to moderate transport distances resulting from the 100-year simulated transport period also may have contributed to the apparent insensitivity to dispersivity. The large computational demands of the transient simulations constrained the number and length of transient runs. Therefore, longer tests of sensitivity to dispersivity were not executed.

Northern and eastern boundaries

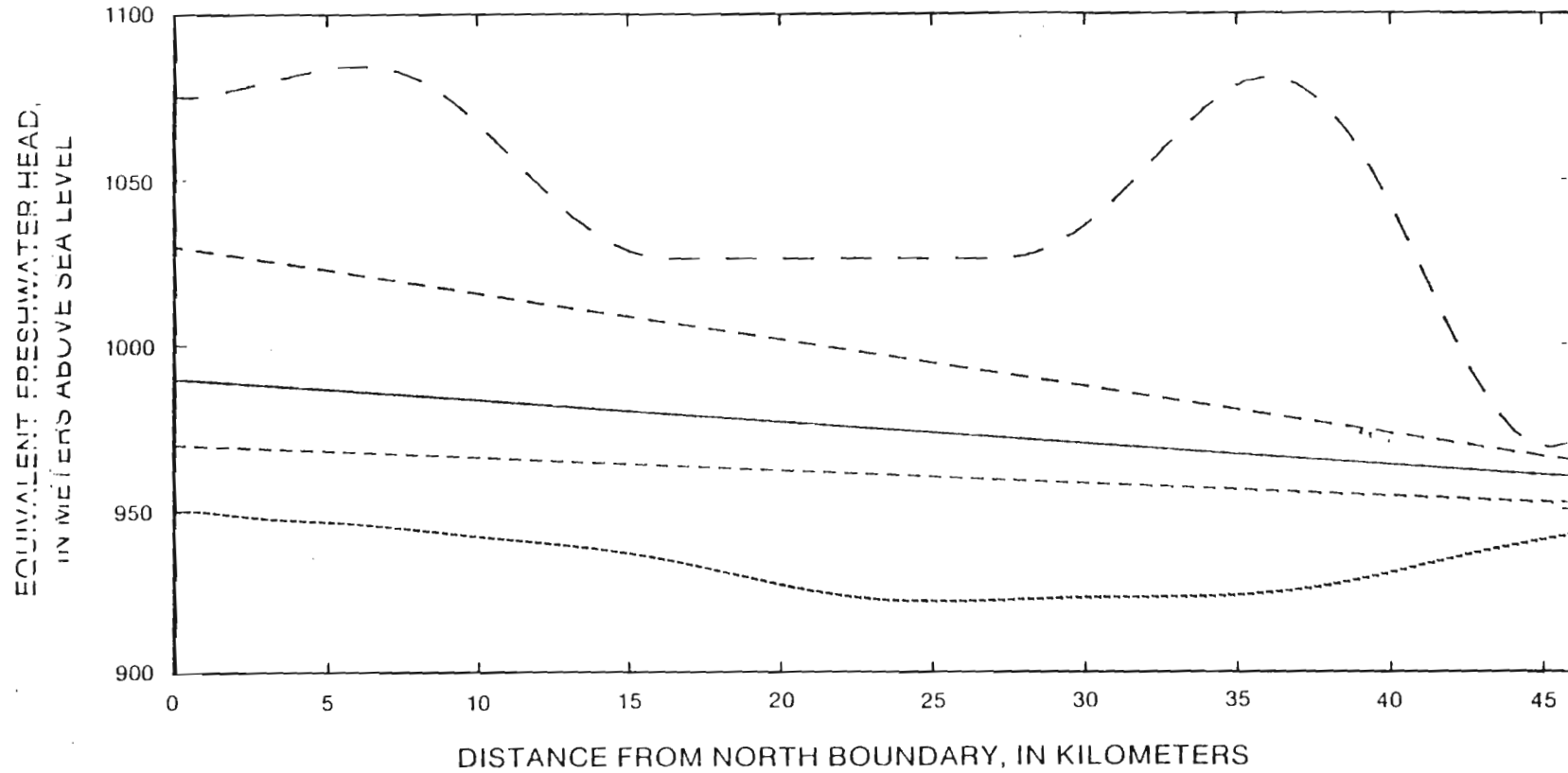
As noted in the section titled "Boundary Conditions," there are no hydrologic data in the Culebra or in any other part of the Rustler Formation in the area east of WIPP. To the north, data are sparse, and no well-defined hydrologic features are present. The absence of sufficient data to delineate well-constrained boundaries to the east and to the north motivated the execution of a series of sensitivity simulations that examined a broad range of possible head (pressure) conditions along these two boundaries.

The ranges of equivalent-freshwater-head distributions that have been used to specify fluid pressures along the eastern and northern boundaries are shown in figures 41 and 42. For an upper bound, a head distribution was estimated on the basis of Hunter's (1985, pl. 1) regional map of water levels in the stratigraphically highest water-bearing unit at any given locality. In the vicinity of the WIPP site, a pronounced decrease in head with depth occurs between the Culebra and Magenta Dolomite Members (Mercer, 1983, figs. 17 and 20). This pattern is what generally would be expected in an area that underlies a regional topographic high and in the immediate vicinity of a thin, relatively high transmissivity layer (Toth, 1963, 1979; Freeze and Witherspoon, 1966, 1967). Although it is very unlikely that Culebra heads are as high as the water levels in Hunter's (1985, pl. 1) regional map, this distribution does provide an extreme upper-bound case. For a lower bound, head distributions along the northern and eastern boundaries were projected eastward and northward from the relatively flat head gradients in the general vicinity of the WIPP site. A pronounced decrease in hydraulic conductivity to the east and northeast would require a substantial increase in head gradients in order to drive fluid flow in this area. Therefore, it is very unlikely that heads in the east and northeast are as low as this projection would indicate. This projection does, however, provide an extreme lower bound. The boundary heads specified for the baseline simulation fall in the midrange between the upper and lower bounds. In addition to the two extreme cases, intermediate-high and intermediate-low head distributions also were simulated.

The magnitude of the deviation angle between the flow direction produced by the baseline simulation and the flow direction produced by simulations with the intermediate-high and the intermediate-low boundary conditions is shown in figures 43 and 44. Throughout most of the WIPP region, there is essentially no difference between the flow fields produced by the baseline simulation and the intermediate-high and intermediate-low simulations. Although there are a few areas where the differences in flow directions range from 5 to 20 degrees, these differences are considered relatively minor.

The magnitude of the deviation angle between the flow direction produced by the baseline simulation and the flow direction produced by the simulation with the extreme-high northern and eastern boundary condition is shown in figure 45. This simulation did produce significant changes in flow directions in local areas along the northern and eastern boundaries. The largest deviation angles, located in the northwest corner, are related to a steep east-west gradient (fig. 42) in the Hunter (1985) water-level map. Some flow-direction changes also were produced in the sensitive, flat-gradient area south of the WIPP site. In contrast to these local areas, large parts of the region, including the WIPP site, were relatively insensitive to the extreme-high northern and eastern boundaries.

The magnitude of the deviation angle between the flow direction produced by the baseline simulation and the flow direction produced by the simulation with the extreme-low northern and eastern boundary condition is shown in figure 46. Like the extreme-high simulation, the extreme-low simulation produced significant flow-direction deviations from the baseline simulation along the eastern and northern boundaries. The bounding heads were so low that the direction of flow was actually reversed and water flowed eastward out of the system along some parts of the eastern boundary. However, the WIPP site and the rest of the central and western parts of the region were relatively insensitive to this extreme case.



EXPLANATION

- — — — — HEAD DISTRIBUTION FOR EXTREME-HIGH BOUNDARY CONDITION
- - - - - HEAD DISTRIBUTION FOR INTERMEDIATE-HIGH BOUNDARY CONDITION
- HEAD DISTRIBUTION FOR BASELINE BOUNDARY CONDITION
- - - - - HEAD DISTRIBUTION FOR INTERMEDIATE-LOW BOUNDARY CONDITION
- HEAD DISTRIBUTION FOR EXTREME-LOW BOUNDARY CONDITION

Figure 41.-- Pressure distributions (expressed as equivalent-freshwater head) that were specified as boundary conditions along the eastern boundary.

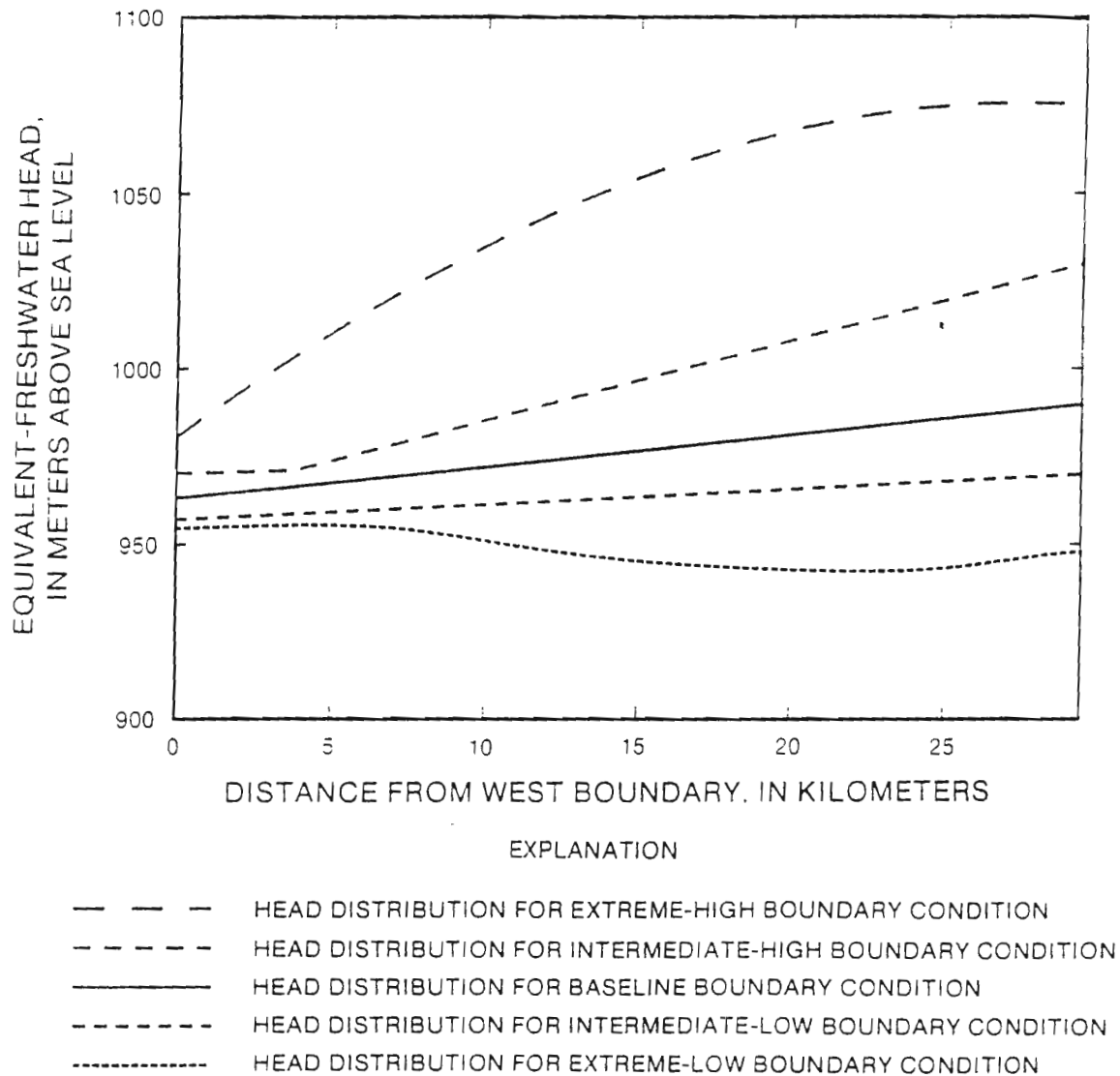


Figure 42.-- Pressure distributions (expressed as equivalent-freshwater head) that were specified as boundary conditions along the northern boundary.

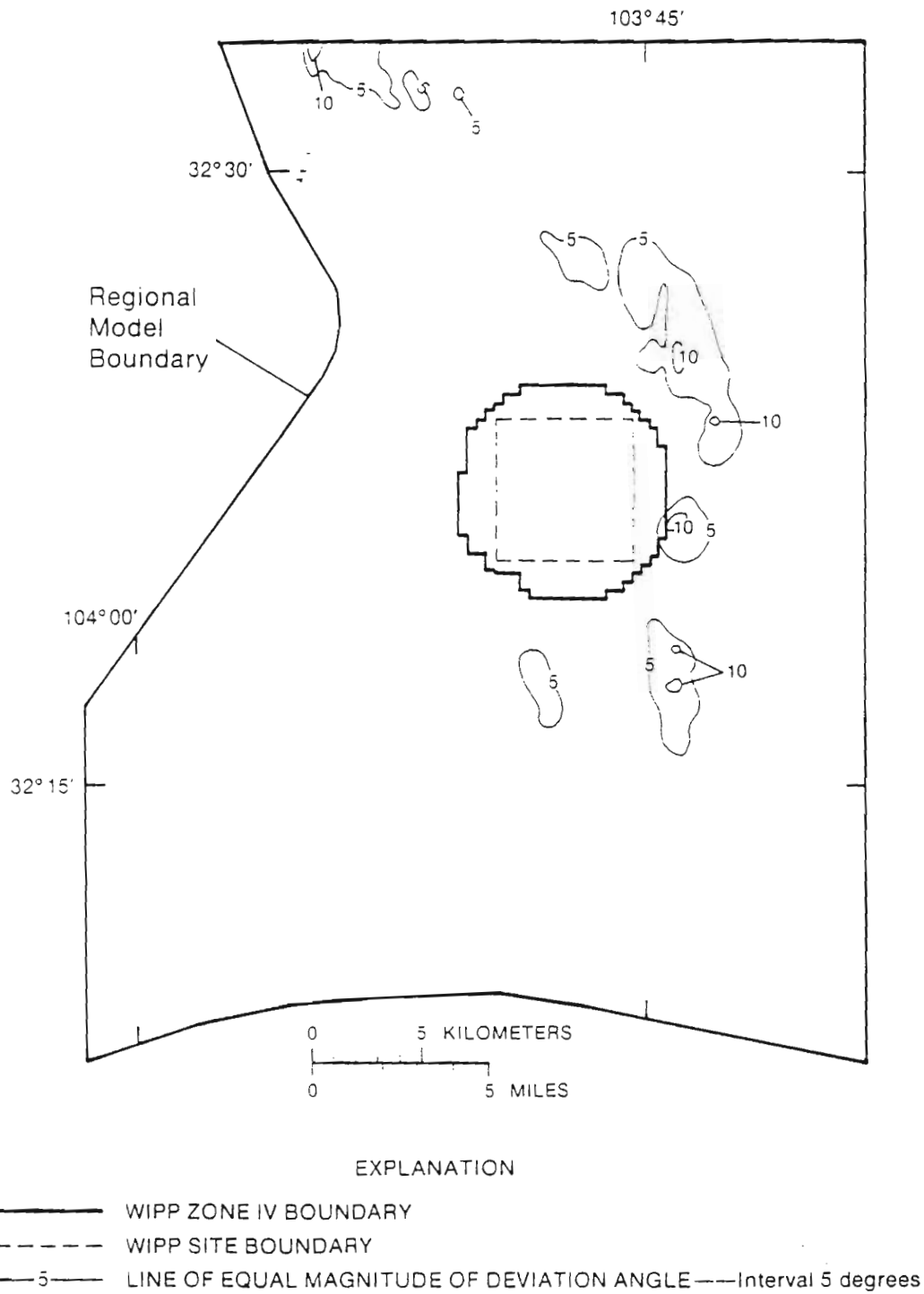
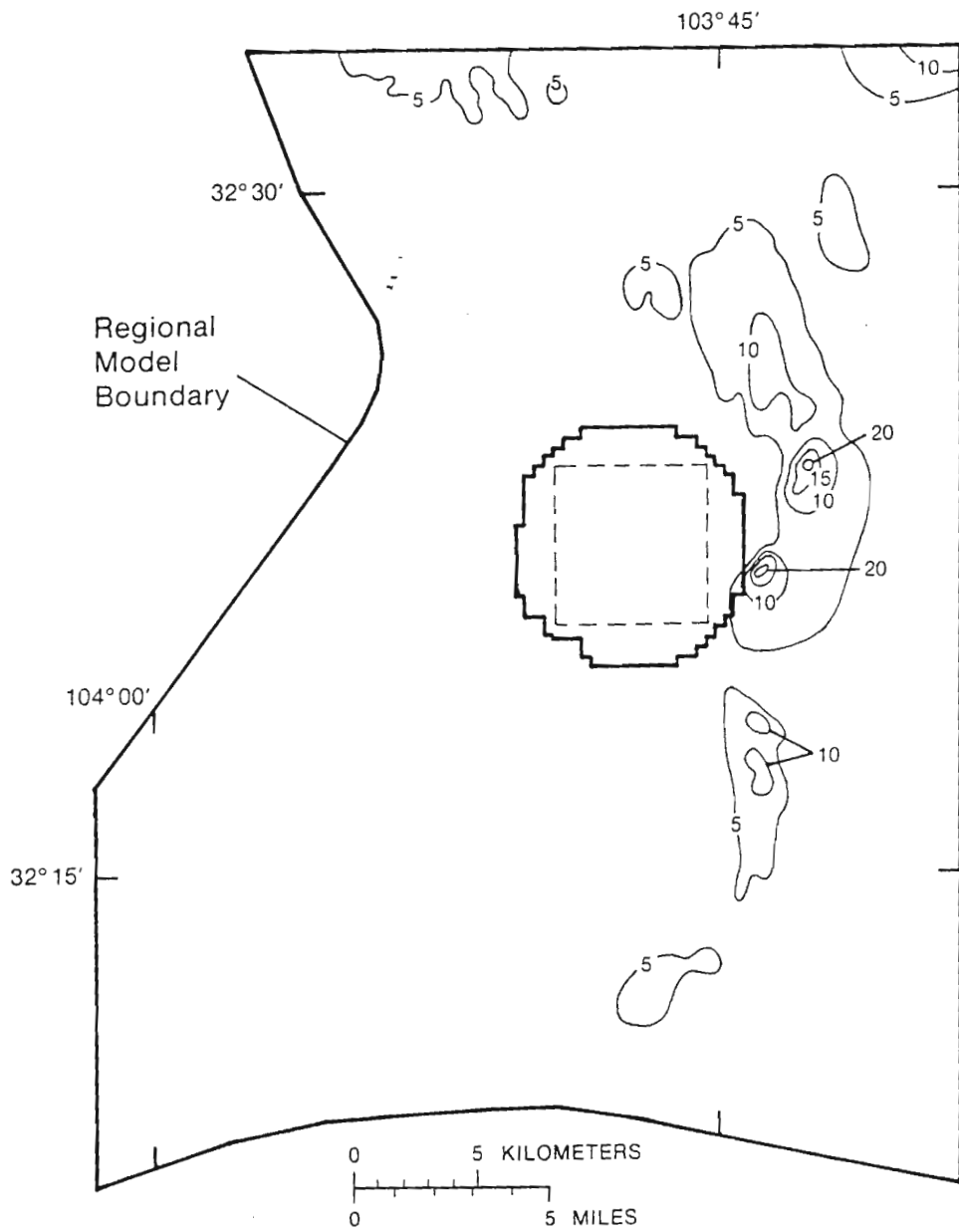


Figure 43.-- Magnitude of the deviation angle between the flow direction produced by the baseline simulation and the flow direction produced by the intermediate-high northern and eastern boundary simulation.



EXPLANATION

- WIPP ZONE IV BOUNDARY
- - - - WIPP SITE BOUNDARY
- 5—— LINE OF EQUAL MAGNITUDE OF DEVIATION ANGLE——Interval 5 degrees

Figure 44.-- Magnitude of the deviation angle between the flow direction produced by the baseline simulation and the flow direction produced by the intermediate-low northern and eastern boundary simulation.

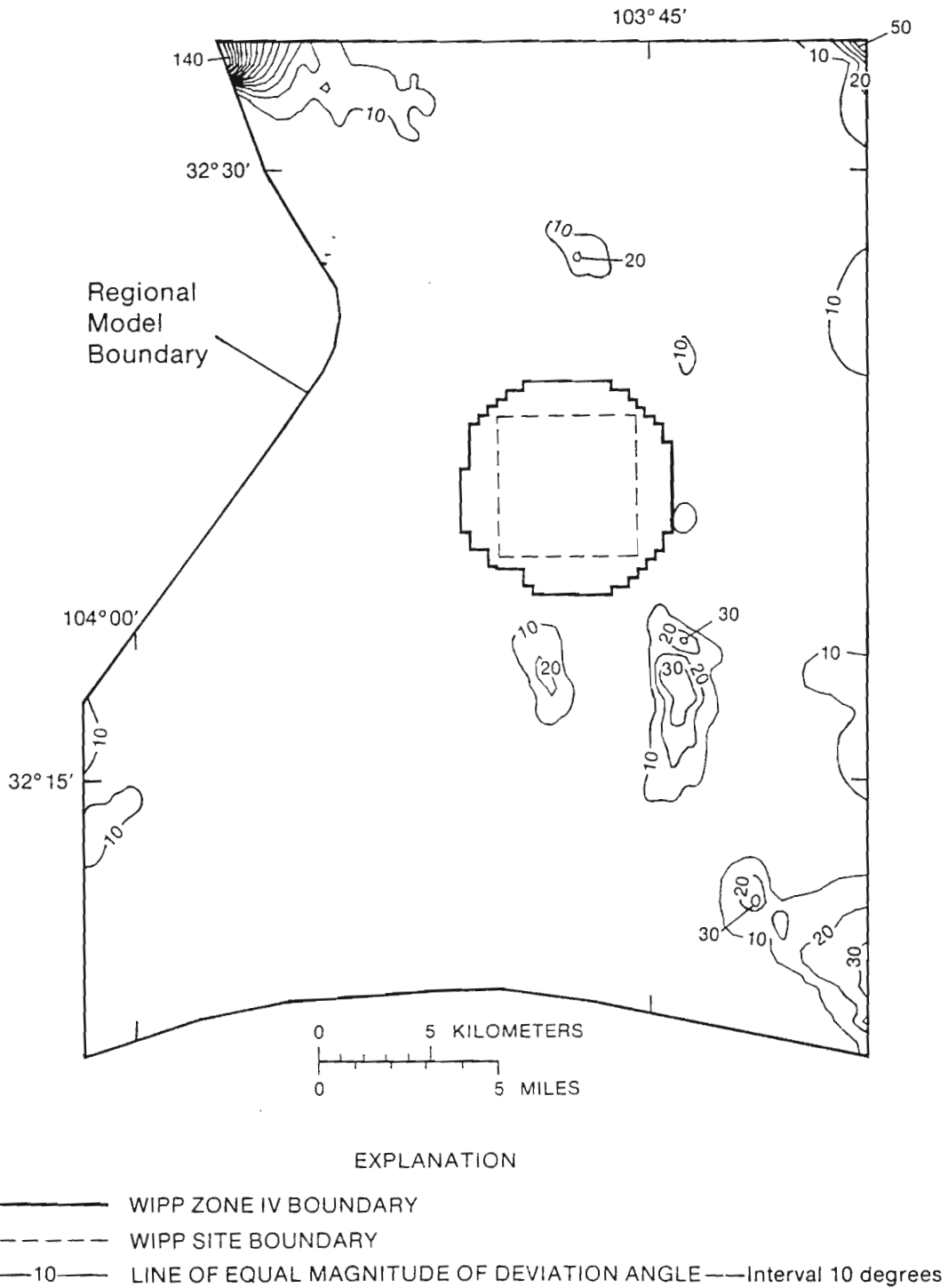
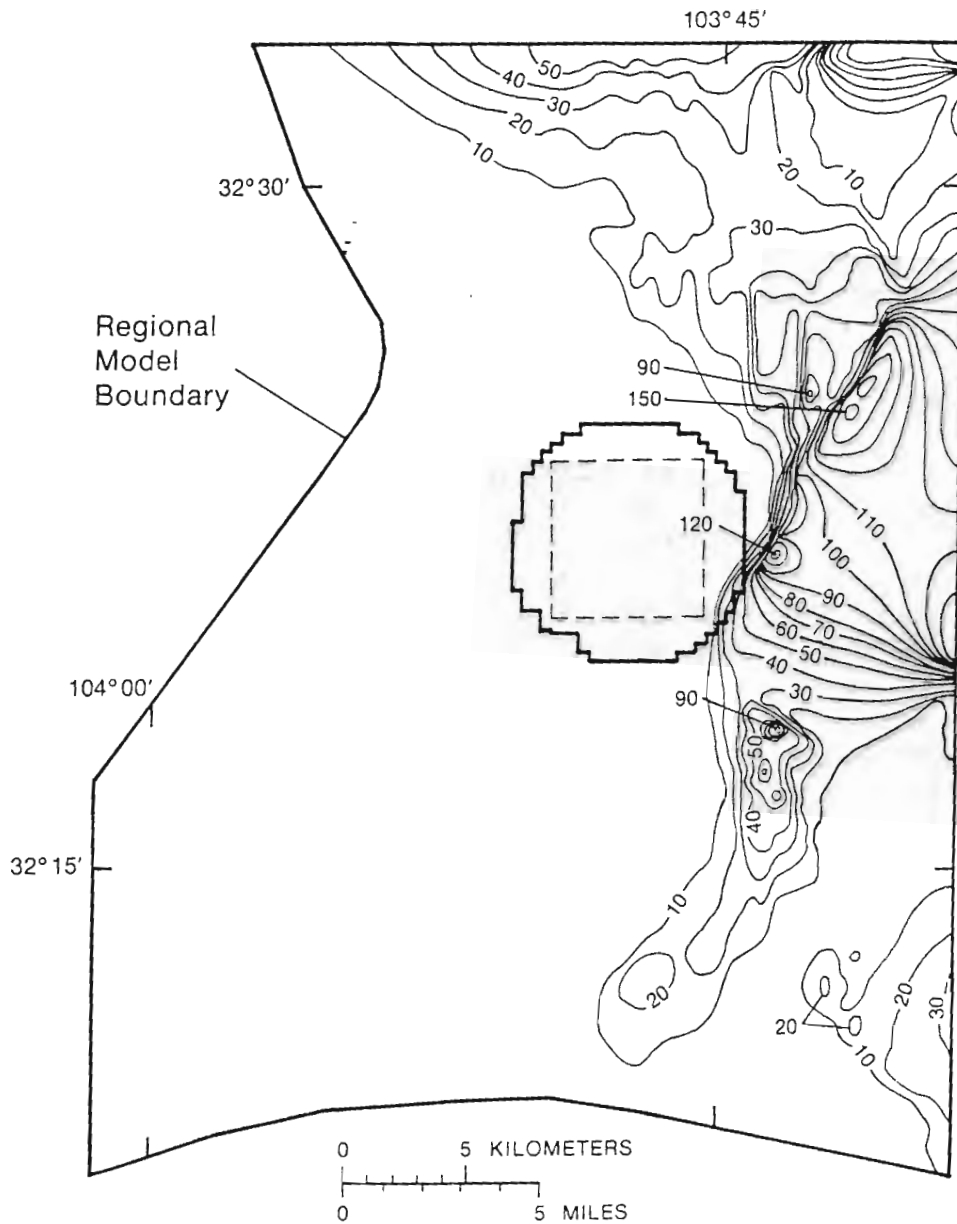


Figure 45.-- Magnitude of the deviation angle between the flow direction produced by the baseline simulation and the flow direction produced by the extreme-high northern and eastern boundary simulation.



EXPLANATION

- WIPP ZONE IV BOUNDARY
- WIPP SITE BOUNDARY
- 10—— LINE OF EQUAL MAGNITUDE OF DEVIATION ANGLE ———Interval 10 degrees

Figure 46.-- Magnitude of the deviation angle between the flow direction produced by the baseline simulation and the flow direction produced by the extreme-low northern and eastern boundary simulation.

The sensitivity analyses of northern and eastern boundary conditions revealed several significant aspects of ground-water flow behavior in the WIPP region. Like other sensitivity analyses, these analyses indicated that the area of very flat gradients south of the WIPP site is sensitive to changes in pressure conditions. These analyses also indicate that if the Culebra is as impermeable in the east and northeast as geologic conditions indicate, then ground-water flow patterns in the central and western part of the region, and at the WIPP site in particular, are insensitive to boundaries to the east and northeast. Flow patterns in the vicinity of the WIPP site may be fairly stable because the large hydraulic-conductivity variations in the site vicinity have produced a relatively strong fabric of high and low hydraulic-conductivity zones that dominates control of flow directions in this area.

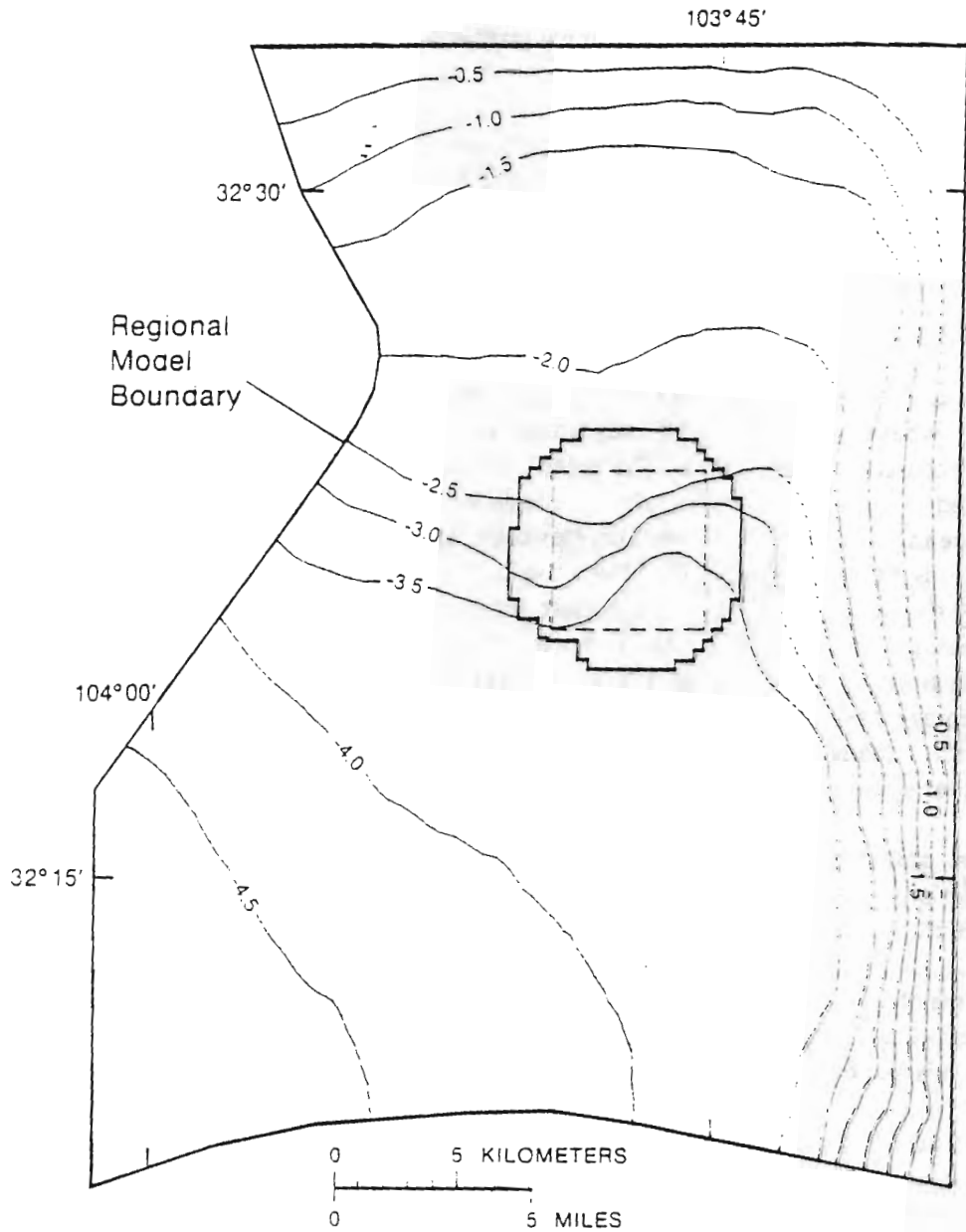
Pecos River boundary

The model boundary that could conceivably change the most in the future is the Pecos River. This boundary controls the elevation of discharge from the regional flow system. Changes to this boundary could be human-induced, such as the construction or removal of reservoirs or significant changes in irrigation practices in the vicinity of the river. River elevation also could change in response to major climatic shifts. If this type of change were to occur, it would take place more gradually than human-induced changes.

A series of steady-state and transient simulations was performed in order to examine the response of the flow system to a 5-meter increase in the Pecos River boundary elevation. In addition to the general regional-system response, the effect on ground-water flow in the vicinity of the WIPP site also was examined.

The difference between the equivalent-freshwater head produced by the baseline simulation and the equivalent-freshwater head produced by a steady-state simulation in which Pecos River boundary heads were increased by 5 meters is shown in figure 47. This figure indicates that slightly more than 50 percent of any change in Pecos River boundary elevation would eventually reach the center of the WIPP site. The difference between steady-state flow directions produced by the baseline simulation and by the simulation of the 5-meter increase was very small. The maximum deviation angle was only 6 degrees, and within the WIPP Zone IV boundary, deviations were all less than 1 degree. The largest deviation angles were located in the area of flat head gradients south of the WIPP site. As noted in previous sections, this area is sensitive in many respects due to its very flat head gradients.

In addition to how far changes in the boundary condition at the Pecos River propagate through the system, how fast and in what manner this stress propagation occurs were examined. A series of transient simulations was used to examine the response of the system to an instantaneous 5-meter head increase along the Pecos River boundary. The transient propagation of this stress then was tracked through a 100-year simulation period. In these transient simulations, the rate of stress propagation is a function not only of hydraulic conductivity but also of the storage characteristics of the water-bearing unit. The baseline storage coefficient (2×10^{-5}) was based primarily on sparse storage data from well tests in the vicinity of the WIPP site. In Nash Draw, however, the Culebra is more fractured and is closer to the land surface. Therefore, it is possible that storage coefficients are actually higher in the Nash Draw area. This possibility is significant in the examination of



EXPLANATION

- WIPP ZONE IV BOUNDARY
- - - - WIPP SITE BOUNDARY
- -3.0—— LINE OF EQUAL DIFFERENCE IN EQUIVALENT—FRESHWATER HEADS ———
Interval 0.5 meters

Figure 47.-- Difference between equivalent-freshwater heads produced by the baseline simulation and equivalent-freshwater heads produced by a steady-state simulation in which Pecos boundary heads were increased by 5 meters.

transient effects because Nash Draw is a primary conduit for the propagation of hydraulic stresses caused by changes in river elevation. Therefore, in addition to a simulation incorporating the baseline storage coefficient of 2×10^{-5} , two additional transient simulations with storage coefficients of 1×10^{-4} and 1×10^{-3} were performed.

The equivalent-freshwater head change at the center of the WIPP site normalized by the total head change after steady state is reached is shown in figure 48. About 50 percent of the head increase at this location was reached at approximately 1, 9, and 84 years for storage coefficient values of 2×10^{-5} , 1×10^{-4} , and 1×10^{-3} , respectively. Accurate prediction of the actual rate of stress propagation will be difficult without more detailed information on regional variation of storage characteristics.

Another question concerning the propagation of stresses associated with changes in the Pecos River boundary is whether there are significant temporary changes in flow patterns associated with the passage of transient stress gradients. The magnitude of the deviation angle between the flow direction produced by the baseline simulation and the flow direction produced by a simulation with a 5-meter increase in the Pecos River boundary elevation (storage coefficient = 10^{-4}) after 10 years of transient stress is shown in figure 49. The flow-deviation angles are quite large, reaching a maximum of 160 degrees. The areas that are most sensitive to Pecos River-related stress are the flat gradient areas to the north and south of the WIPP site. The WIPP site vicinity is relatively insensitive in this simulation and in other simulations at different time periods and using different values for the storage coefficient. A sudden 5-meter change in Pecos River boundary heads is a fairly extreme case. Changes in head along the Pecos River probably would take place much more slowly, and smaller pressure gradients would be produced.

One final observation concerning the sensitivity analyses needs to be made. In all the preceding simulations, the Culebra Dolomite Member has been treated as a totally confined water-bearing unit, which implies that there is absolutely no vertical flux. Although this assumption may be reasonable for some types of analyses, there is geologic, hydrologic, and geochemical evidence that small amounts of vertical flux may occur in some parts of the regional system (see section titled "Analysis of Long-Term System Response to Paleohydrologic Conditions"). Therefore, it is useful to consider how this assumption may affect the interpretation of the preceding Pecos River analyses.

The presence of limited communication between the Culebra flow system and units that are higher or lower in the section would dampen stress propagation associated with changes in boundary heads at the Pecos River or with any other transient source or sink in the system. Changes in fluid pressure would not be wholly accommodated by changes in storage in the Culebra, but rather, would be accommodated in part by changes in the amount of vertical flux into or out of the Culebra at any given location. In terms of the possible role of vertical flux on the flow system as a whole, the following section is an examination of volumetric and geographic constraints on vertical flux. The vertical cross-sectional model described in the final segment of this report provides additional information on plausible vertical-flow patterns.

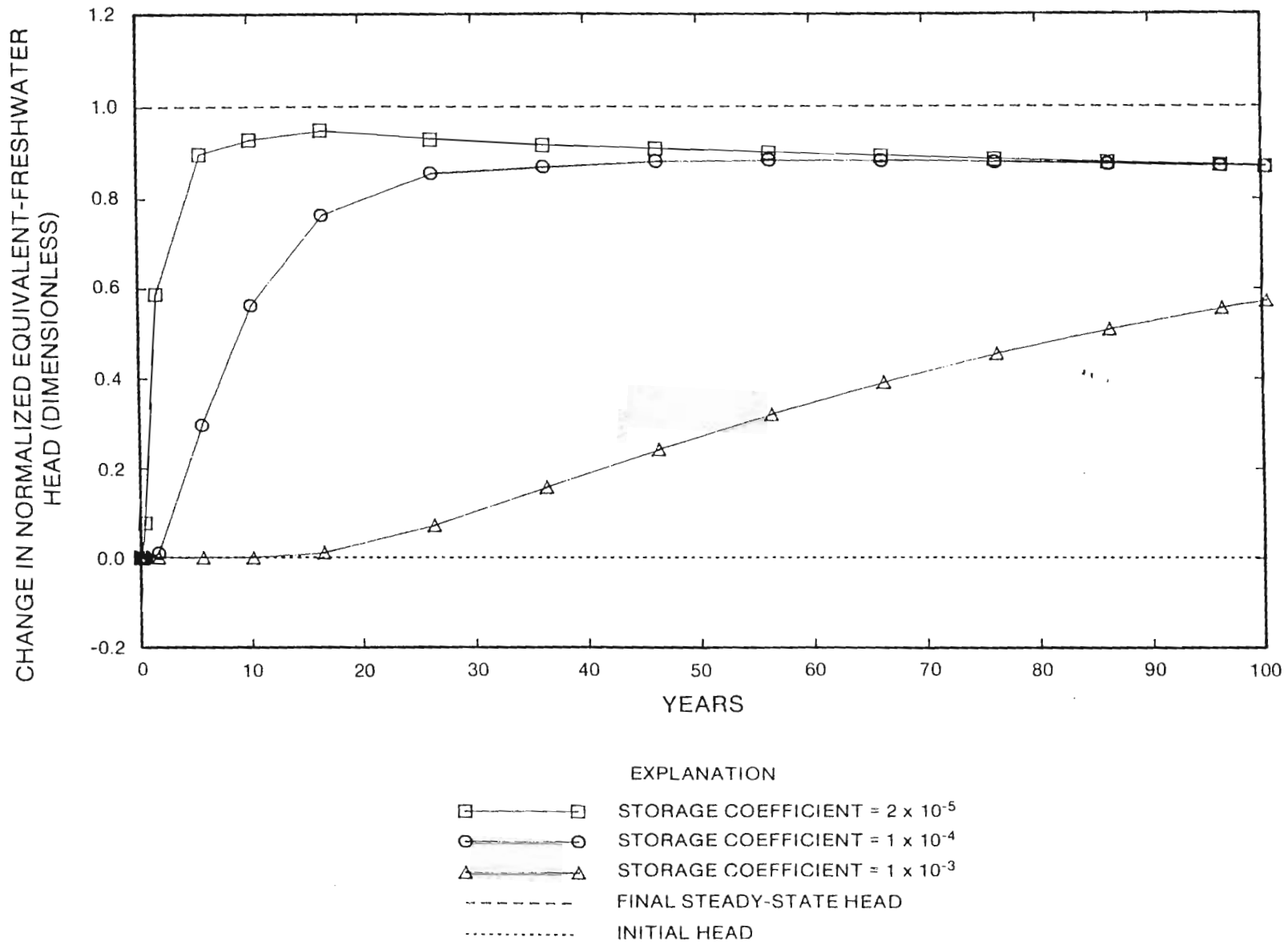


Figure 48.-- Change in equivalent-freshwater head at the center of the WIPP site caused by a 5-meter head increase at the Pecos River boundary. Heads are normalized with respect to total head change at steady state.

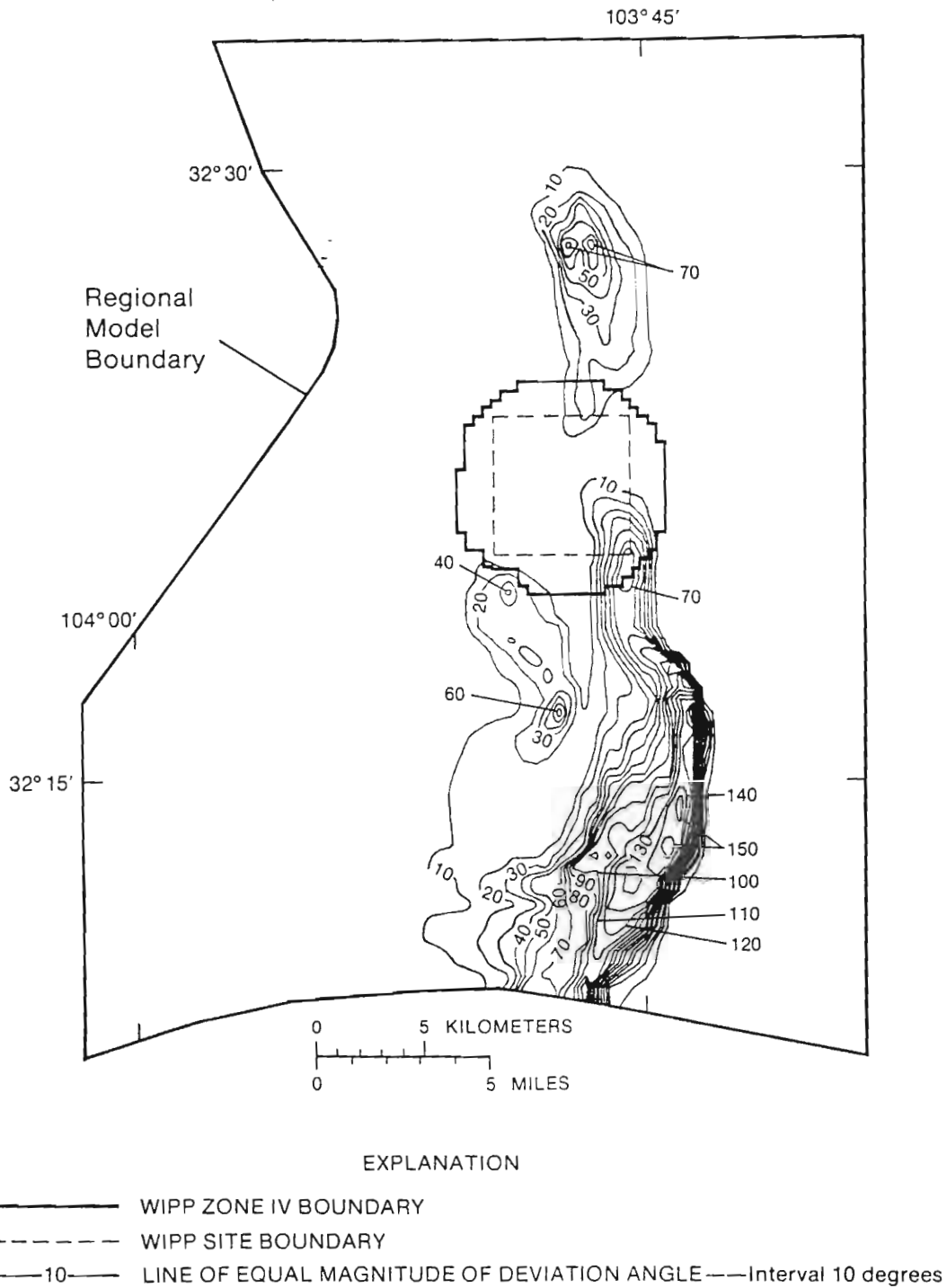


Figure 49.-- Magnitude of the deviation angle between the flow direction produced by the baseline simulation and the flow direction produced by a simulation of conditions 10 years after an instantaneous 5-meter head increase at the Pecos River boundary. Storage coefficient for this simulation was 10^{-4} .

Vertical flux

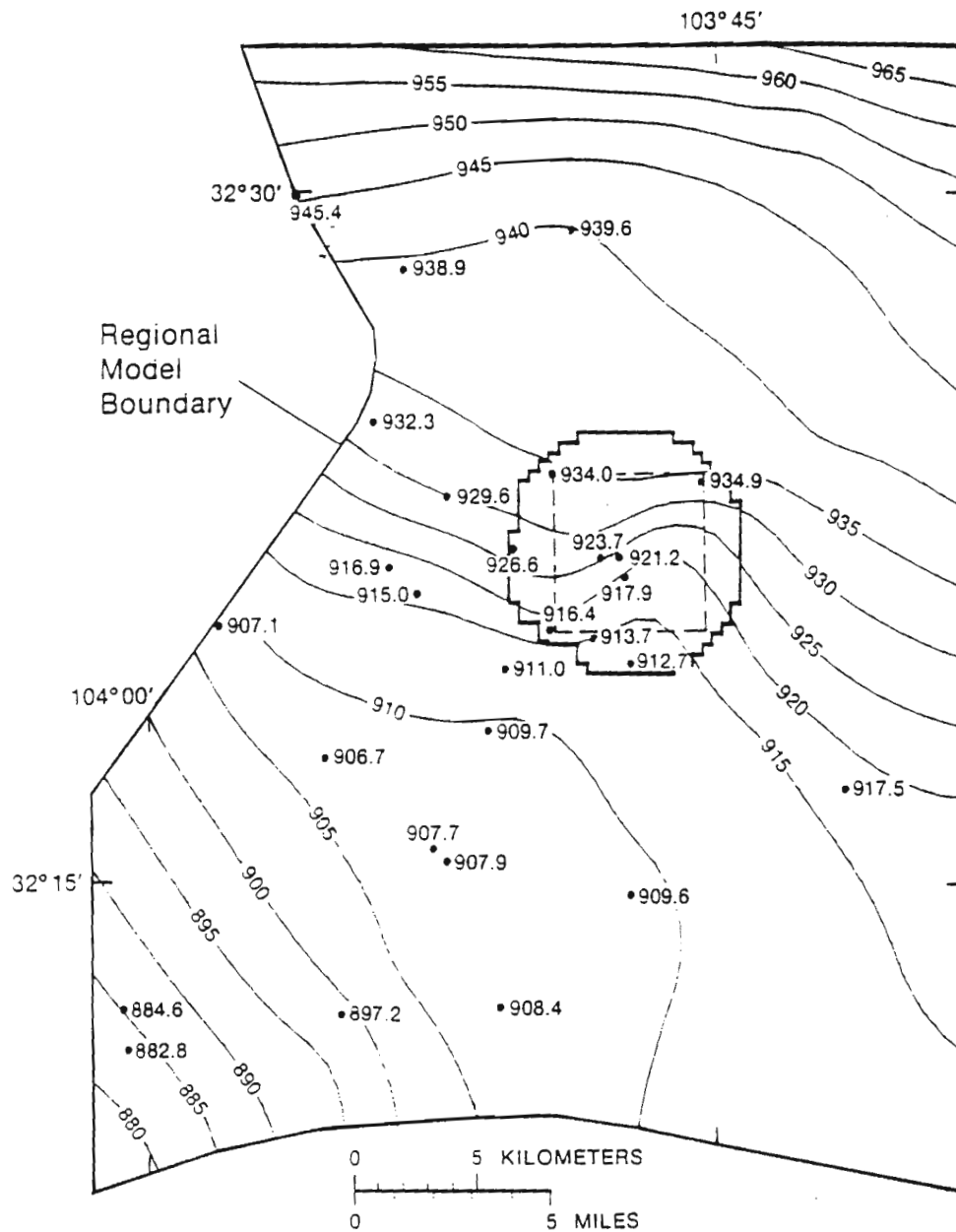
This section describes a series of simulations examining the possible role of vertical flux as a source of recharge fluids to the Culebra flow system. The primary objectives of these simulations were to determine what proportion of total flow through the system could be coming in vertically and the geologic and geographic limitations on where such vertical flow could occur. Another objective of these simulations was to determine what impact vertical flux may have on ground-water flow patterns.

The approach in analyzing vertical fluxes using the regional model was to calibrate a steady-state simulation in which a significant proportion of the total water inflow to the system entered by means of a specified fluid source at nodes within the interior of the model region. On the basis of the field evidence and cross-sectional model results that are discussed later in the report, it was anticipated that the largest quantities of vertical flux would enter the Culebra flow system along the westernmost part of the transition zone adjacent to Nash Draw and that smaller amounts of vertical flux could be entering the Culebra further to the east.

In the vertical-flux simulations, the Nash Draw, Pecos River, and southern boundaries were the same as in the baseline simulation. In order to reduce the amount of lateral flow entering the system through the northern and eastern boundaries in a realistic fashion, the northern boundary utilized the specified-pressure (specified-head) boundary from the intermediate-low case shown in figure 42, and the eastern boundary was specified as a no-flow boundary. This eastern no-flow boundary may be more realistic than the specified-pressure conditions used for this boundary in the baseline simulation. No flow along the eastern boundary is more realistic because it approximately underlies both a regional topographic divide and an apparent ground-water divide in the shallowest water-bearing units (U.S. Geological Survey, 1954; Hunter, 1985, pl. 1). Most likely there is a divide in the Culebra flow system in this area as well, separating an area in which ground water flows west and southwest toward the Pecos River from an area in which ground water flows toward topographic lows in the east.

The vertical-flux model was calibrated to the distribution of equivalent-freshwater heads prior to shaft construction by varying the amount and distribution of vertical flux. During calibration, a few changes were made to the baseline hydraulic-conductivity distribution. The most significant of these changes consisted of respecifying hydraulic conductivity in the southern Nash Draw and Pecos River areas to approximately the distribution that was derived from the original mapping of regional conductivity trends shown in figure 26.

A series of calibration simulations resulted in a steady-state simulation in which approximately 25 percent of inflow to the system enters by means of specified vertical flux. The equivalent-freshwater-head distribution for this simulation is shown in figure 50. The mean absolute deviation from equivalent-freshwater heads calculated from field measurements at 28 observation wells for this simulation was 1.4 meters, which is nearly the same as the degree of match (1.3 meters) achieved in the baseline simulation. Calibration was not achieved for vertical-flux proportions significantly larger than 25 percent, indicating that 25 percent represents an approximate upper bound on the proportion of fluid entering the Culebra flow system as vertical flux.



EXPLANATION

- WIPP ZONE IV BOUNDARY
- - - - WIPP SITE BOUNDARY
- 900 — FRESHWATER HEAD CONTOUR—Shows altitude at which water having a density of 1.00 gram per cubic centimeter would have stood in a tightly cased well. Contour interval 5 meters. Datum is sea level
- 906.7 WELL OR TEST HOLE—Number is simulated equivalent—freshwater head at well, in meters. Datum is sea level

Figure 50.-- Equivalent-freshwater-head surface from the vertical-flux simulation.

The calibration process also revealed geologic and geographic constraints on the distribution of vertical flux. Spatial variations in hydraulic conductivity of the Culebra through the transition zone adjacent to Nash Draw control the upper limits on how much fluid can enter the Culebra as vertical flux in any given location. If significant amounts of fluid enter the Culebra as vertical flux, then most of this influx must be occurring in the westernmost part of the transition zone, where hydraulic conductivity of the Culebra is relatively high (fig. 51). The marked decrease in hydraulic conductivity to the east strictly limits the amount of fluid that can enter the Culebra without raising heads to anomalously high levels. This eastward decrease in vertical flux is similar to the eastward decrease in flux observed in the cross-sectional simulations described later in this report.

The flow field generated by the vertical-flux simulation is shown in figure 52. Comparison of this flow field with the flow field generated by the baseline simulation (fig. 34) reveals two general areas where flow directions differ. One area is along the eastern boundary, where the change from a specified-pressure boundary to a no-flow boundary caused flow directions in the vertical-flux simulation to trend more toward the south and southwest rather than due west as produced by the baseline simulation. The other area is south-southwest of the WIPP site, in the northern part of the southern Nash Draw reentrant. In this area, flow directions in the baseline simulation follow the northern margin of the reentrant, trending southeastward. In the vertical-flux simulation flow directions in this area trend due south and southwestward. In the vicinity of the WIPP site, the introduction of vertical fluxes has very little impact on flow directions.

Summary and Conclusions

The primary objective of the analysis of the flow system in the Culebra Dolomite Member of the Rustler Formation on a regional scale was to enhance understanding of ground-water flow in the vicinity of the WIPP site by examining this area in the broader context of the regional flow system. Boundaries for the regional model were selected to coincide with significant hydrologic features wherever possible because this is an important factor in the assessment of long-term flow system behavior. The process of selecting boundaries in a variable-density environment is complicated by the fact that flow lines or other features that might be identified on the basis of equivalent-freshwater heads may not accurately reflect the real system because equivalent-freshwater heads do not account for the density-related gravity forces that may also contribute to driving fluid flow. Therefore, a driving-force analysis of the WIPP region was used to identify where density-related effects are significant. The information from this analysis was used to guide selection of model boundaries so that these boundaries were located in areas that are largely free of density-related effects.

The hydraulic-conductivity distribution for the regional model was produced by mapping regional conductivity trends and then merging these trends with more detailed information on hydraulic-conductivity variations in the vicinity of the WIPP site from a site-scale model by Haug and others (1987). Regional trends were mapped by integrating local-scale well-test data with indirect geologic measures of hydraulic conductivity. These indirect measures included the degree of halite removal from the Rustler Formation as an indirect measure of the degree of deformation

1. 2. 3. 4. 5. 6. 7. 8. 9. 10. 11. 12. 13. 14. 15. 16. 17. 18. 19. 20. 21. 22. 23. 24. 25. 26. 27. 28. 29. 30. 31. 32. 33. 34. 35. 36. 37. 38. 39. 40. 41. 42. 43. 44. 45. 46. 47. 48. 49. 50. 51. 52. 53. 54. 55. 56. 57. 58. 59. 60. 61. 62. 63. 64. 65. 66. 67. 68. 69. 70. 71. 72. 73. 74. 75. 76. 77. 78. 79. 80. 81. 82. 83. 84. 85. 86. 87. 88. 89. 90. 91. 92. 93. 94. 95. 96. 97. 98. 99. 100.

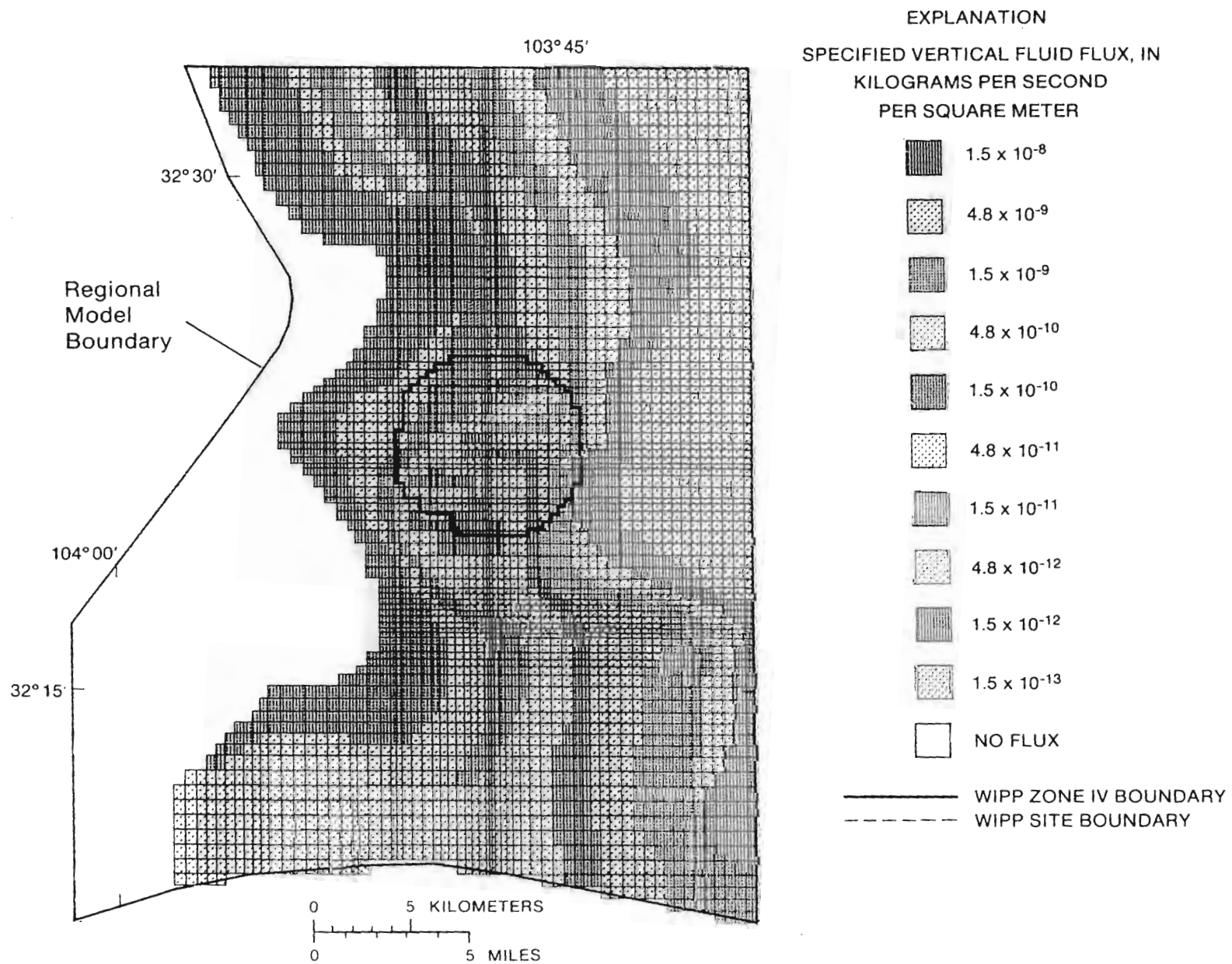


Figure 51.-- Distribution of specified vertical flux used in the vertical-flux simulation.



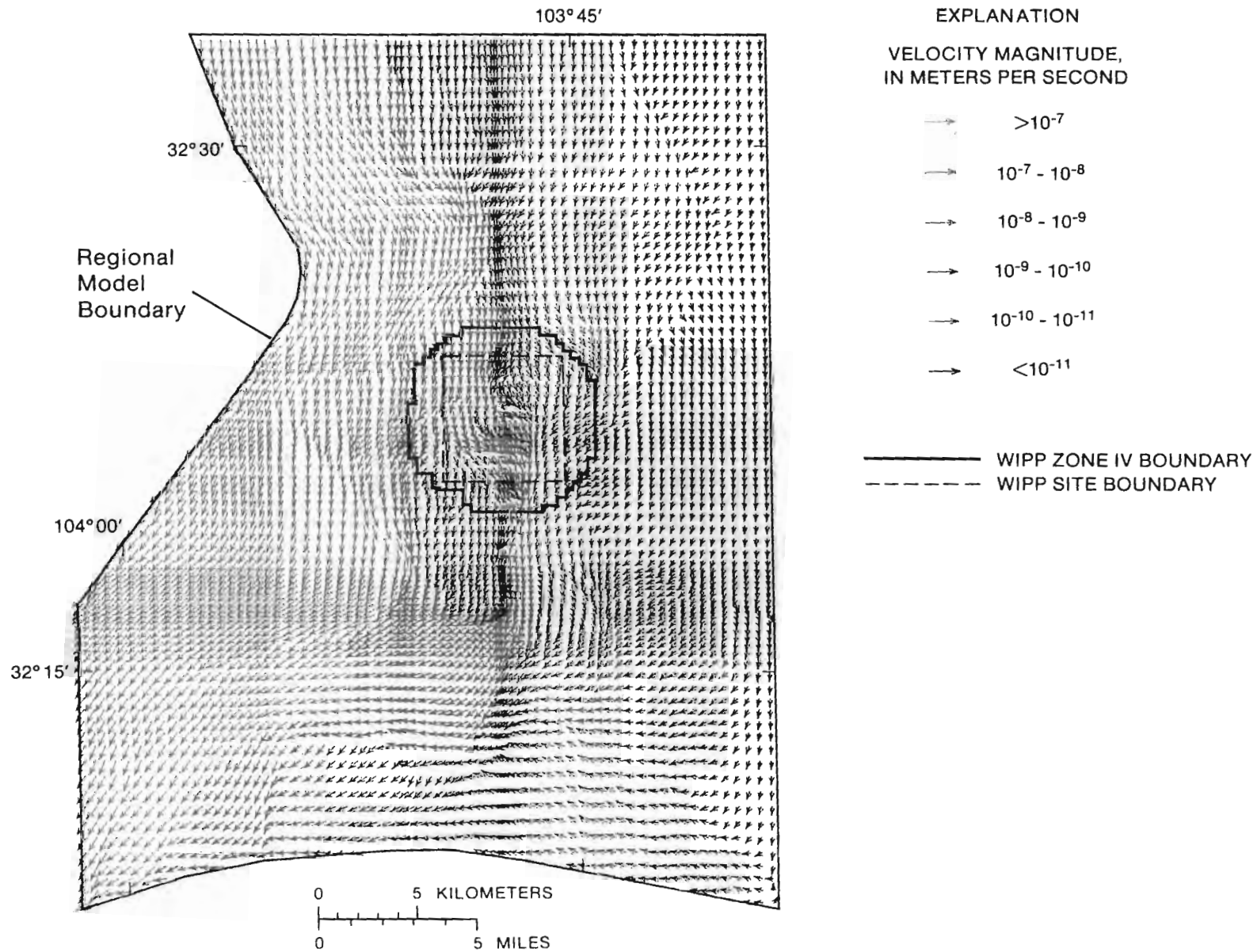


Figure 52.-- Simulated direction and magnitude of ground-water flow produced by the vertical-flux simulation.



induced by halite dissolution and related secondary processes, depth of burial as an indirect measure of confining stress, and topography as an indirect measure of the areal extent of extreme Nash Draw-type conditions.

A baseline, approximate steady-state simulation was calibrated to the preshaft distribution of equivalent-freshwater heads by making changes in the regional hydraulic-conductivity distribution that were consistent with the regional trends. Fluid density was specified in the baseline simulation on the basis of the measured fluid-density distribution. This approach assumes that solute redistribution takes place slowly, and can, therefore, be treated as a constant. This assumption was later examined using a transient simulation in which solutes were allowed to move with the flow, and the effect of solute redistribution on flow patterns was monitored. This transient simulation showed that solute redistribution occurs very slowly in the WIPP region and that redistribution has very little impact over a 100-year period. Over a 1,000-year period, solute redistribution does have a small impact on flow patterns in several local areas. In the vicinity of the WIPP site, solute redistribution has very little impact on flow directions, even over a 1,000-year time period.

The flow field from the baseline simulation and the brine transport pattern during a 1,000-year simulation period indicate that flow velocities are relatively fast in Nash Draw and extremely slow in the eastern and northeastern parts of the region. In the transition zone between these two extremes, velocities are highly variable. Relative to WIPP, the most significant feature of the regional flow field is the relatively fast velocities associated with the high conductivity zone just south of the WIPP site that was postulated in the Haug and others (1987) site-scale model.

Comparison of the baseline simulation with a similar simulation based on equivalent-freshwater heads indicates that throughout much of the WIPP region, and at the WIPP site proper, fluid density has very little impact on flow directions. However, in an area south of the site, the combination of the gentle dip in the Culebra, moderate fluid densities, and very flat head gradients produce flow conditions in which density-related forces dominate over pressure-related forces in driving fluid flow. In this area, higher fluid densities cause the water to flow in a more easterly, downdip direction than would be predicted by a simulation based on equivalent-freshwater heads. Understanding flow patterns in this area is important because it contains flow paths that extend southward from the WIPP site, which are potential contaminant-transport pathways.

A lack of hydrologic data to the east and to a lesser extent to the north creates a large degree of uncertainty in the specification of boundary conditions along these margins. This circumstance motivated the simulation of a wide range of specified conditions along these boundaries. These simulations revealed that if the Culebra is as impermeable to the east and northeast as geologic conditions indicate, then ground-water flow patterns in the central and western parts of the region, including the WIPP site, are fairly insensitive to whatever conditions are assumed to be present along these boundaries. Flow patterns in the vicinity of the WIPP site appear to be well established because the large conductivity variations in this area produce a configuration of high- and low-conductivity zones that controls flow directions.

The Pecos River boundary is the boundary that could conceivably change the most in the future due to human activities or to climatic change. A steady-state simulation of a 5-meter head increase in the Pecos River boundary indicated that if the Culebra flow system is truly confined

1
2
3
4
5
6
7
8
9
10
11
12
13
14
15
16
17
18
19
20
21
22
23
24
25
26
27
28
29
30
31
32
33
34
35
36
37
38
39
40
41
42
43
44
45
46
47
48
49
50
51
52
53
54
55
56
57
58
59
60
61
62
63
64
65
66
67
68
69
70
71
72
73
74
75
76
77
78
79
80
81
82
83
84
85
86
87
88
89
90
91
92
93
94
95
96
97
98
99
100

throughout the entire region, then approximately 50 percent of any change in river elevation would eventually reach the WIPP site. Uncertainty in the regional distribution of storage characteristics in the Culebra makes it difficult to predict how long it would take for Pecos River-related stresses to propagate through the WIPP region. Some geologic and hydrologic evidence indicates that the Culebra is not completely confined, particularly in Nash Draw and the westernmost part of the transition zone. The presence of vertical communication between the Culebra and other water-bearing horizons may significantly dampen the propagation of Pecos River (or other) stresses through the region.

In order to examine the potential for vertical flux as a source of recharge to the Culebra flow system, a series of simulations was carried out in which varying amounts of flux were introduced to the Culebra within the interior of the model. A calibrated steady-state simulation was achieved in which 25 percent of the total flux through the system entered the Culebra as vertical flux. Calibration of simulations with significantly larger proportions of vertical flux was not possible, which indicates that 25 percent is an approximate upper bound on the proportion of influx that can be entering the system as vertical flow. The calibration process also revealed geologic and geographic constraints on the distribution of vertical flux. If significant volumes of water enter the Culebra vertically, most of the influx must be occurring in the westernmost part of the transition zone, where hydraulic conductivity in the Culebra is relatively high. The marked decrease in hydraulic conductivity to the east strictly limits the amount of water that can enter the Culebra without raising heads to anomalously high levels.

The simulations described in the previous paragraphs cover the sensitivity analyses and alternative system conceptualizations considered to be the highest priority and most likely to yield useful information about flow-system behavior. A number of other somewhat lower priority simulations that might yield additional useful information were not examined because of time constraints. Longer transient simulations may be warranted. Most of the transient simulations carried out for this study were limited to 100 years, due to extremely long computation times (on the order of 200,000 CPU seconds for a 100-year simulation). Given that the one simulation for 1,000 years did show some changes in flow patterns related to solute redistribution that did not appear in the 100-year simulation and that repository interactions with the environment may take place over thousands of years, it may be useful to carry out additional long-term simulations.

Examination of the influence of the southern boundary on flow-system behavior may provide additional useful information. Data available to define this boundary are limited to a single WIPP-project well (H-8) and a few non-WIPP wells that are completed over some unspecified interval of the Rustler Formation. As noted in the description of the baseline simulation, this southern area was the most difficult area to calibrate. This area also may be fairly complex geologically. As noted in the description of regional hydraulic-conductivity trends, this area has been subject to extensive evaporite dissolution below the Culebra. Therefore, it may be useful to examine an alternative set of boundary conditions that allows a limited amount of southward flow along this boundary. Relative to assessing WIPP repository performance, the southern no-flow boundary specified in the regional model provides a conservative scenario that causes all southward-directed flow to eventually turn westward and discharge at the Pecos River.

In addition to the large stresses created by the excavation of the WIPP shafts and by hydrologic testing and sampling, the Culebra flow system has experienced other hydraulic stresses

in the region related to potash-mining operations. The excavation of potash-mine shafts and disposal of process water may have an impact on the Culebra. What the effects are and how large an area is affected are unknown. Simulations of other stresses and boundary conditions indicate that ground-water flow patterns in the vicinity of the WIPP site are fairly insensitive to stresses. Therefore, the relatively small stresses associated with potash-mining activities are unlikely to affect flow directions in the vicinity of the site. Examination of potash mine-related, point-source stresses may be useful in delineating the geographic limits of the area affected by these activities.

The source of detailed information on hydraulic conductivity in the vicinity of the WIPP site was a recent modeling study by Haug and others (1987). This site-scale model currently is being revised to incorporate a large amount of new aquifer-test data and to simulate additional multiple-well pumping tests. Once the results of this new study are available, revision of the hydraulic-conductivity distribution in the WIPP site part of the regional model may be warranted.

As mentioned in the section titled "Halite Dissolution and Related Secondary Processes," a recently completed study (Holt and Powers, 1988) indicates that extensive halite dissolution may not have occurred in the Rustler Formation. This study concludes that the present-day distribution of halite beds in the Rustler Formation is a by-product of facies changes and syndepositional dissolution. The hydrologic implications of this hypothesis are not clear. No mechanistic explanation has been given for the variation of permeability in the Culebra, which ranges over several orders of magnitude. If at some point the hydrologic ramifications of this alternative hypothesis are assessed and indicate a different interpretation of regional hydraulic-conductivity trends, then construction of additional regional simulations that explore this alternative system conceptualization would be useful.

The final and most complex topic about which additional effort may yield useful information about the flow system is assessment of the nature and limitations of vertical interactions between the Culebra and other water-bearing units. Although the vertical-flux simulation of the regional model and the vertical cross-sectional model described in the following section provide useful information, further progress in understanding vertical interactions will require additional data on the other rock units in the section and more detailed, possibly three-dimensional, simulation analyses. Furthering the understanding of the three-dimensional characteristics of the system may help resolve questions concerning the nature of recharge to the Culebra and the origins of lateral geochemical variations that appear to be inconsistent with two-dimensional, horizontal flow patterns in the Culebra (Hunter, 1985; Ramey, 1985; Chapman, 1986; Lambert and Harvey, 1988; M.W. Bodine and B.F. Jones, U.S. Geological Survey, written commun., 1988). The construction and analysis of three-dimensional simulations will be a time consuming and computationally demanding task.

ANALYSIS OF LONG-TERM SYSTEM RESPONSE TO PALEOHYDROLOGIC CONDITIONS

The generally accepted flow-system conceptualization for the WIPP region envisions the water-bearing units of the Rustler Formation as receiving recharge somewhere to the north and as being isolated vertically (Mercer, 1983). In recent years, however, isotopic data from Rustler Formation ground water and other geochemical analyses have raised questions regarding the nature of recharge to and vertical flow within the Rustler Formation. Chapman (1986) concluded that the Rustler is receiving modern recharge from precipitation in the vicinity of the WIPP site. This conclusion was based on similarities in isotopic composition between water in the Rustler from the WIPP vicinity and shallow ground waters in the nearby Roswell Basin and on the fact that some of these other shallow ground waters have tritium concentrations large enough to imply a recent meteoric origin for the water.

Lambert (1987) and Lambert and Harvey (1988) have presented a different interpretation of the WIPP isotope data. On the basis of the presence of isotopically distinct water from the Rustler compared to modern water from Carlsbad Caverns and other areas in the Delaware Basin and on radiocarbon and tritium data from the WIPP site vicinity, Lambert concluded that there is no significant modern meteoric recharge to the Rustler at or near the WIPP site. In addition, Lambert indicated that the Rustler flow system probably last received significant recharge during the last glacial pluvial period, 10,000 to 30,000 years ago, and that the system has been draining since that time.

M.W. Bodine and B.F. Jones (U.S. Geological Survey, written commun., 1988) have computed and analyzed normative salt assemblages in ground-water samples from the Rustler. These analyses indicate that vertical infiltration of recharge into the water-bearing units of the Rustler has had identifiable geochemical impact in some areas.

Presentation of the differing isotope interpretations to the National Academy of Sciences WIPP review panel by Lambert in November 1984 and by Chapman in February 1985 motivated the development of a transient, cross-sectional model. The primary objective of this modeling effort was to examine the physical feasibility of Lambert's geochemically based hypothesis of long-term drainage.

Geohydrology and Paleohydrology of the Model Section

The section selected to be modeled was a 30-kilometer, east-west geologic section through the WIPP site and vicinity (figs. 3 and 53). The base of the section is the top of salt in the Salado Formation, and the top of the section is land surface. The section was oriented east-west in order to provide the shortest possible flow path for drainage. Because the Rustler-Salado contact zone probably had very little influence on the drainage process, it was not included as a distinct unit in this analysis. **The west end of the section** is approximately at the low point in the center of Nash Draw. The east end of the section is at a topographic divide approximately 11 kilometers east of

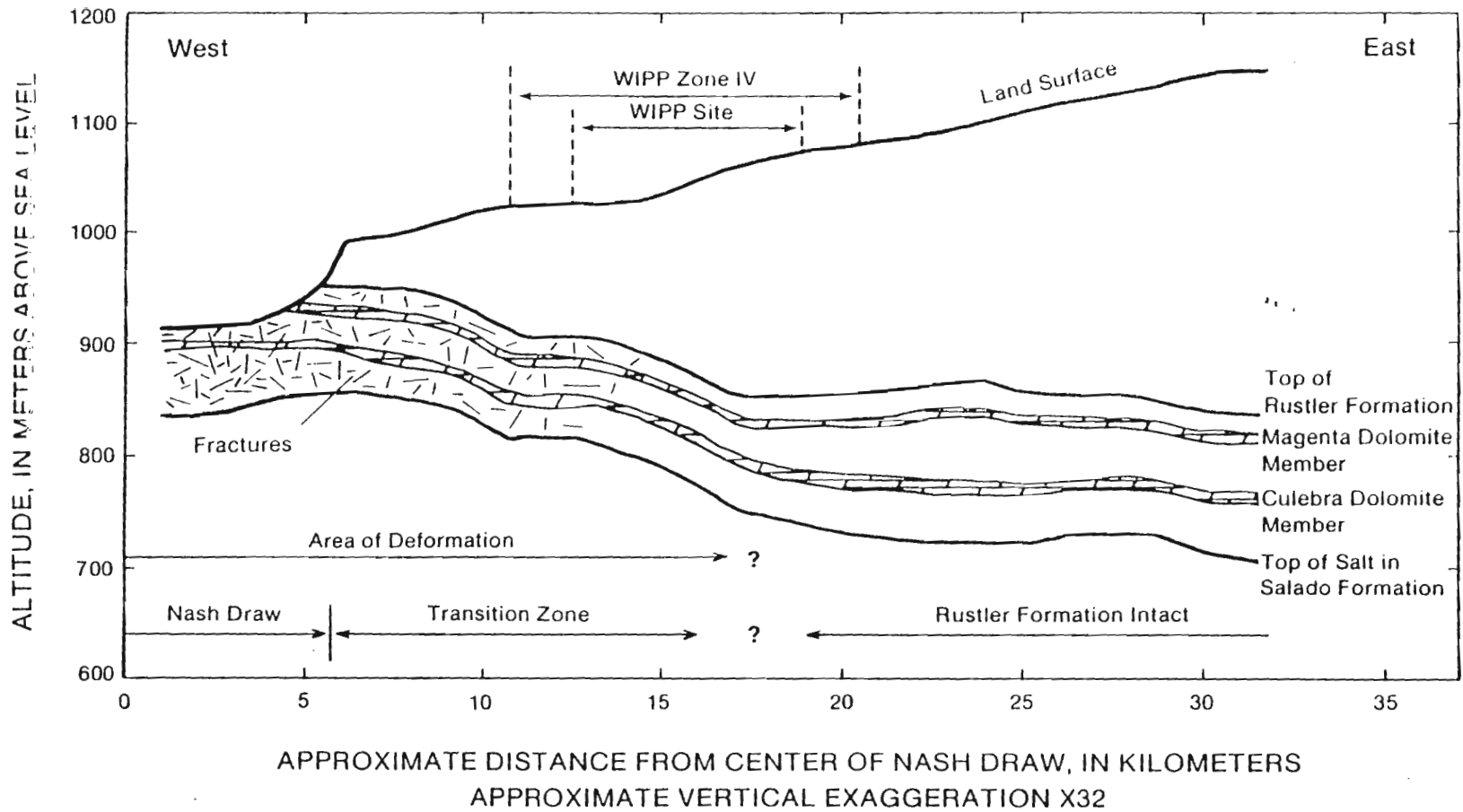


Figure 53.-- Geologic section used in the cross-sectional model showing approximate distribution of deformation associated with halite dissolution and other secondary processes.

the WIPP site. This topographic divide roughly coincides with an apparent ground-water divide in the shallowest aquifers (Hunter, 1985, pl. 1).

Halite dissolution and other related secondary processes have had a significant impact on the Rustler Formation. The effect of these secondary processes is depicted schematically in figure 53. At the west end of the section, the Rustler Formation is at or near land surface. Halite in the upper part of the Salado Formation and in all of the Rustler Formation has been completely removed. Subsidence associated with this dissolution and volumetric changes associated with the hydration of anhydrite to gypsum have produced extensive deformation. These secondary processes have created relatively high hydraulic conductivity at the west end of the section. At the east end of the section, the Rustler Formation is a few hundred meters below land surface. In this area, the Rustler is completely intact and approximately 50 percent of its thickness is comprised of thick, clayey halite beds. The Rustler is relatively impermeable in this area. Between these two extremes is a transition zone. From east to west, the Rustler becomes progressively shallower and thinner, and progressively more halite has been removed from stratigraphically deeper horizons. The westward increase in secondary process activity has created significant local variations in hydraulic conductivity and a distinct regional trend of increasing hydraulic conductivity toward Nash Draw.

The paleohydrology of the area can be reconstructed using a variety of evidence. Lambert and Harvey (1988) cited paleoplant-community evidence of moist climatic conditions during past glacial pluvial periods in southeastern New Mexico as indicators that the ground-water flow system contained more water in the past than it does at present. Several types of geologic evidence support that conclusion.

The calcium sulfate spring deposits mapped by Bachman (1981, 1985) are perhaps the most striking evidence of paleoclimate and paleoground-water conditions. These deposits are products of ancient springs along the east side of Nash Draw (fig. 54). Bones of extinct species of horses and camels found in these deposits indicate that the springs were active during late Pleistocene. The paleohydrologic significance of these spring deposits is that they indicate that the late Pleistocene ground-water flow system contained more water than the system contains at present and that the water table was located in the upper part of the Dewey Lake Red Beds.

A second line of geologic evidence of higher ground-water levels in the past is the presence of gypsum-filled fractures in the Dewey Lake Red Beds, which have been described by Bachman (1985) and Snyder (1985). These fractures indicate that at some time in the past, sulfate-bearing water was circulating through the sandstones of the Dewey Lake Red Beds. Although this gypsum has not been dated, the similarity in composition with the nearby spring deposits indicates the possibility that these two deposits are similar in age.

Surficial geologic mapping and exploratory drill holes have provided direct evidence of significant quantities of surface water during past glacial pluvial periods. As described in the section titled "Halite Dissolution and Related Secondary Processes," Bachman's (1985) mapping of middle Pleistocene stream gravel (fig. 8) has shown that Nash Draw was the location of a major stream during the middle Pleistocene. The distribution of these deposits also indicates the presence of a secondary east-west stream channel north of the WIPP site and a possible second channel across the central and southern parts of the site. The presence of these Pleistocene streams indicates that significant quantities of surface water were available to recharge the ground-water system. The

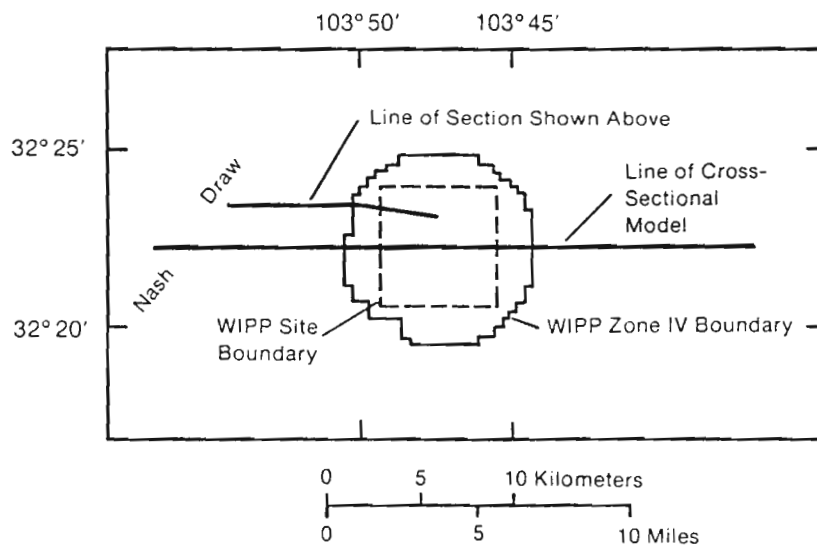
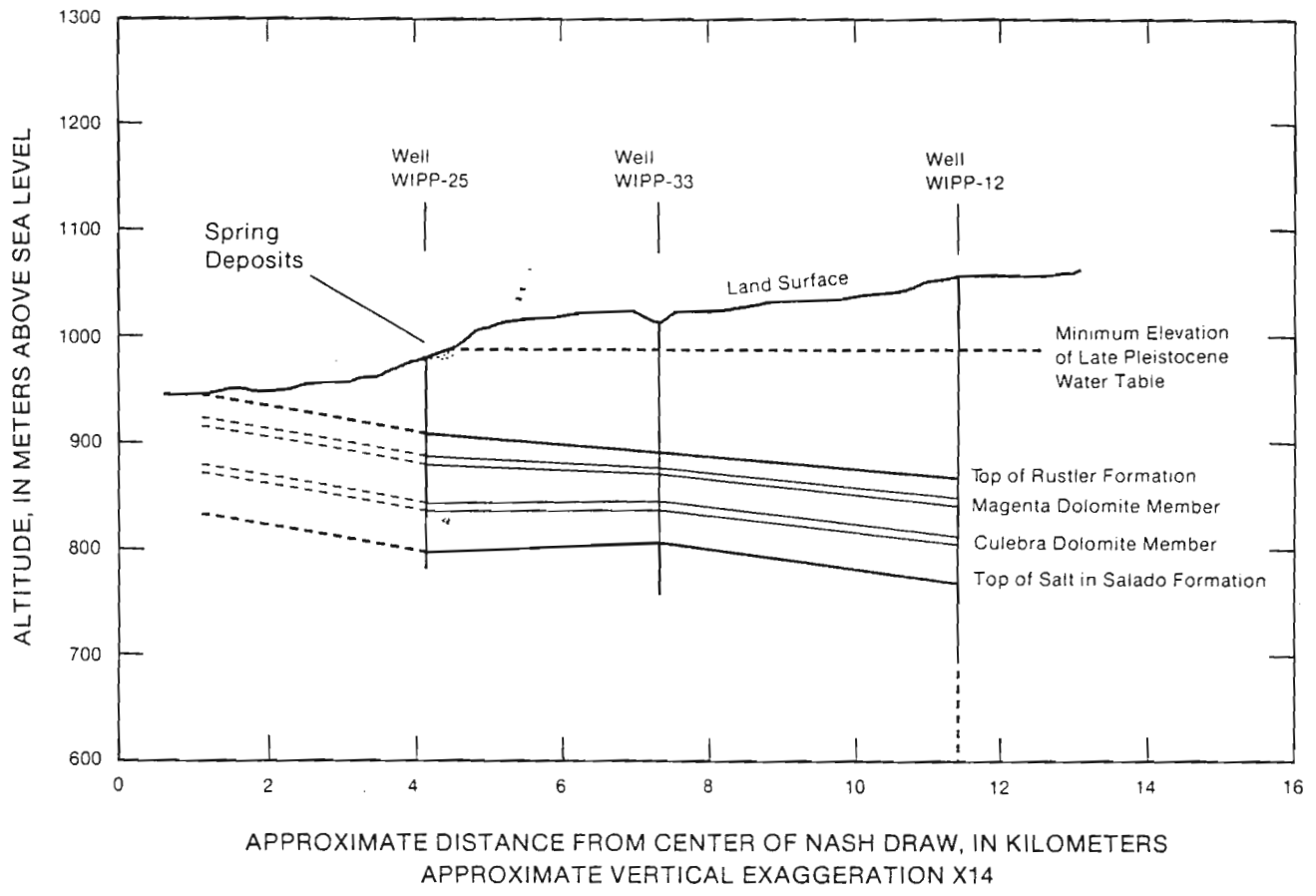


Figure 54.-- Spring deposits of late Pleistocene age on the eastern margin of Nash Draw and inferred water table.

combination of spring deposits along the eastern margin of Nash Draw, gypsum-filled fractures in the Dewey Lake Red Beds, and Pleistocene stream gravels indicates that during past glacial pluvial periods, surface water was more abundant, the ground-water flow system contained more water than at present, and the water table was in the units that overlie the Rustler Formation.

The current head distributions in the Magenta and Culebra Dolomite Members of the Rustler Formation also are pertinent to the cross-sectional model described in the next section. Equivalent-freshwater-head profiles of the Magenta and Culebra Members along the section are shown in figure 55. In the vicinity of the WIPP site, heads in the Culebra are more than 30 meters lower than heads in the Magenta, which lies only 30 meters higher in the section. This difference implies a vertical gradient greater than one, an unusually large vertical gradient for a natural flow system. Because fluid densities in the Magenta and Culebra are fairly similar in this area, this large head differential is not an artifact of the conversion from water-level measurements to equivalent-freshwater heads. In addition, the head difference between the Magenta and Culebra decreases westward toward Nash Draw. The dissipation of large head differentials with increasing proximity to Nash Draw also has been noted elsewhere in the WIPP site vicinity by Chaturvedi and Channell (1985, p. 39-43).

Transient Cross-Sectional Flow Model

The primary objective of this modeling effort was to construct a simple, physically based conceptual model of the flow system as it drains through time following an initially recharged state that corresponds with the last glacial pluvial period. The model was designed to examine the rate at which drainage occurs and whether or not there could be enough water following late Pleistocene recharge to sustain flow over thousands of years without draining the system down to static water levels, assuming no further recharge. A secondary objective of this modeling effort was to examine vertical-flow relations between the Culebra Dolomite Member of the Rustler Formation and other units of the stratigraphic section overlying the Salado Formation.

Model Implementation

The two-dimensional, finite-difference, ground-water flow code by Trescott and others (1976) was used for numerical simulations. The model grid (fig. 56) dips to the east approximately coincident with the regional dip of the post-Salado rock units. Grid cells ranged in length from 100 meters in the west to 500 meters in the east. Cell height was 8 meters. The smaller grid-cell size in the west was required to accommodate the transition to higher hydraulic conductivity in the vicinity of Nash Draw. In order to avoid confusion with the baseline simulation of the regional flow model, the simulation of the cross-sectional model to which other simulations are compared is referred to as the "standard" simulation.

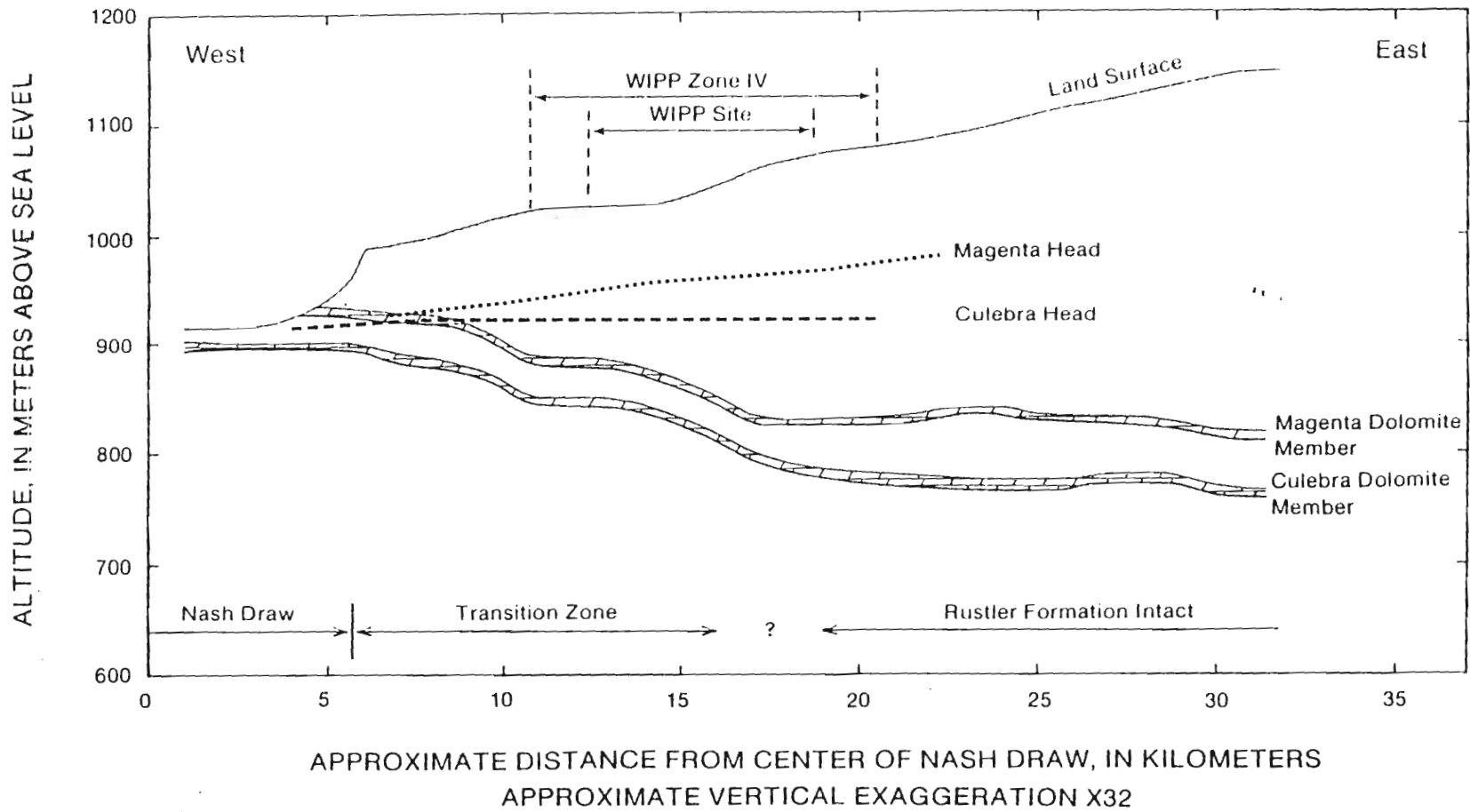


Figure 55.-- Equivalent-freshwater heads of the Magenta and Culebra Dolomite Members of the Rustler Formation.

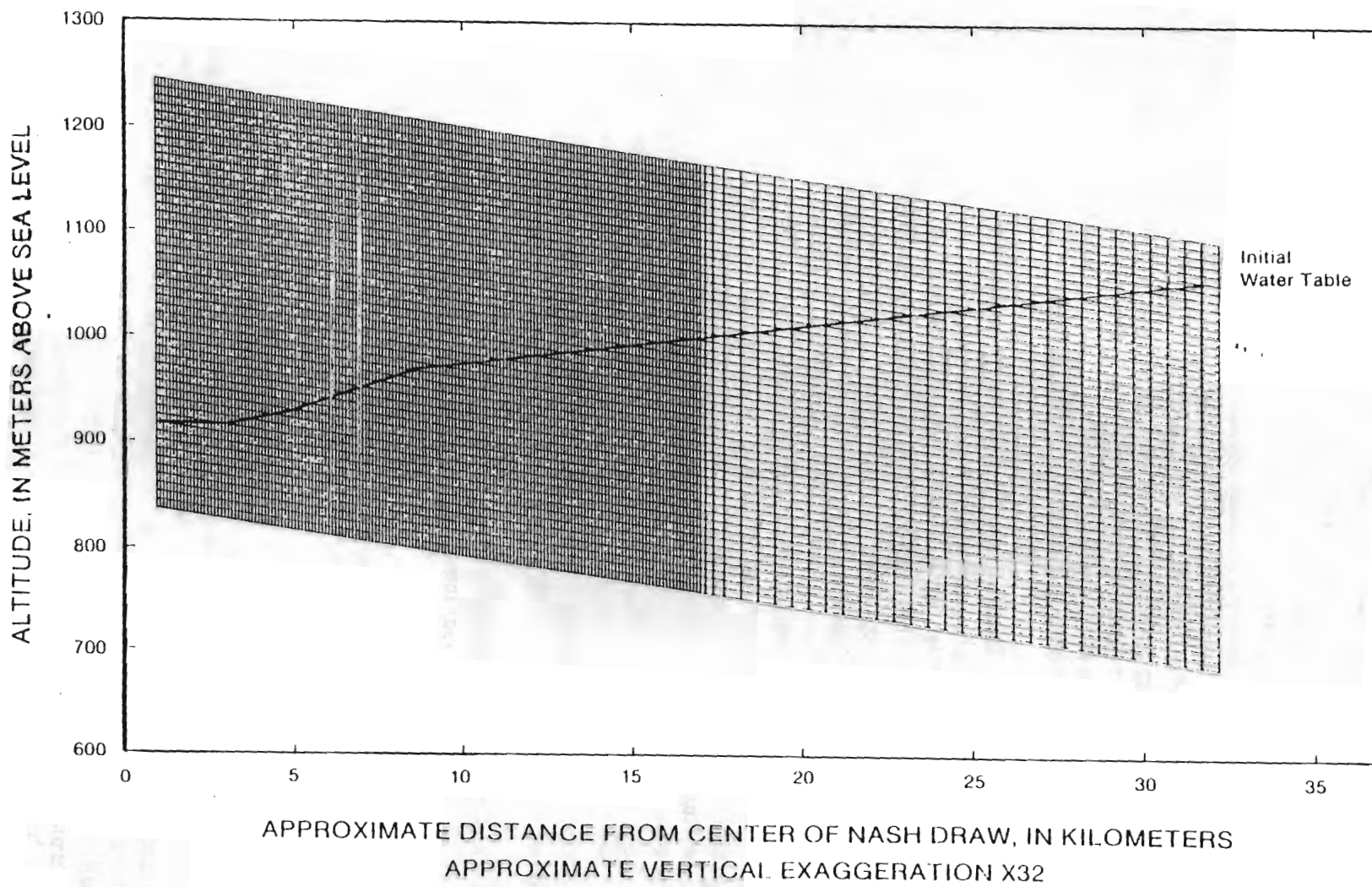


Figure 56.-- Finite-difference grid for cross-sectional flow model.

Hydraulic-conductivity distribution

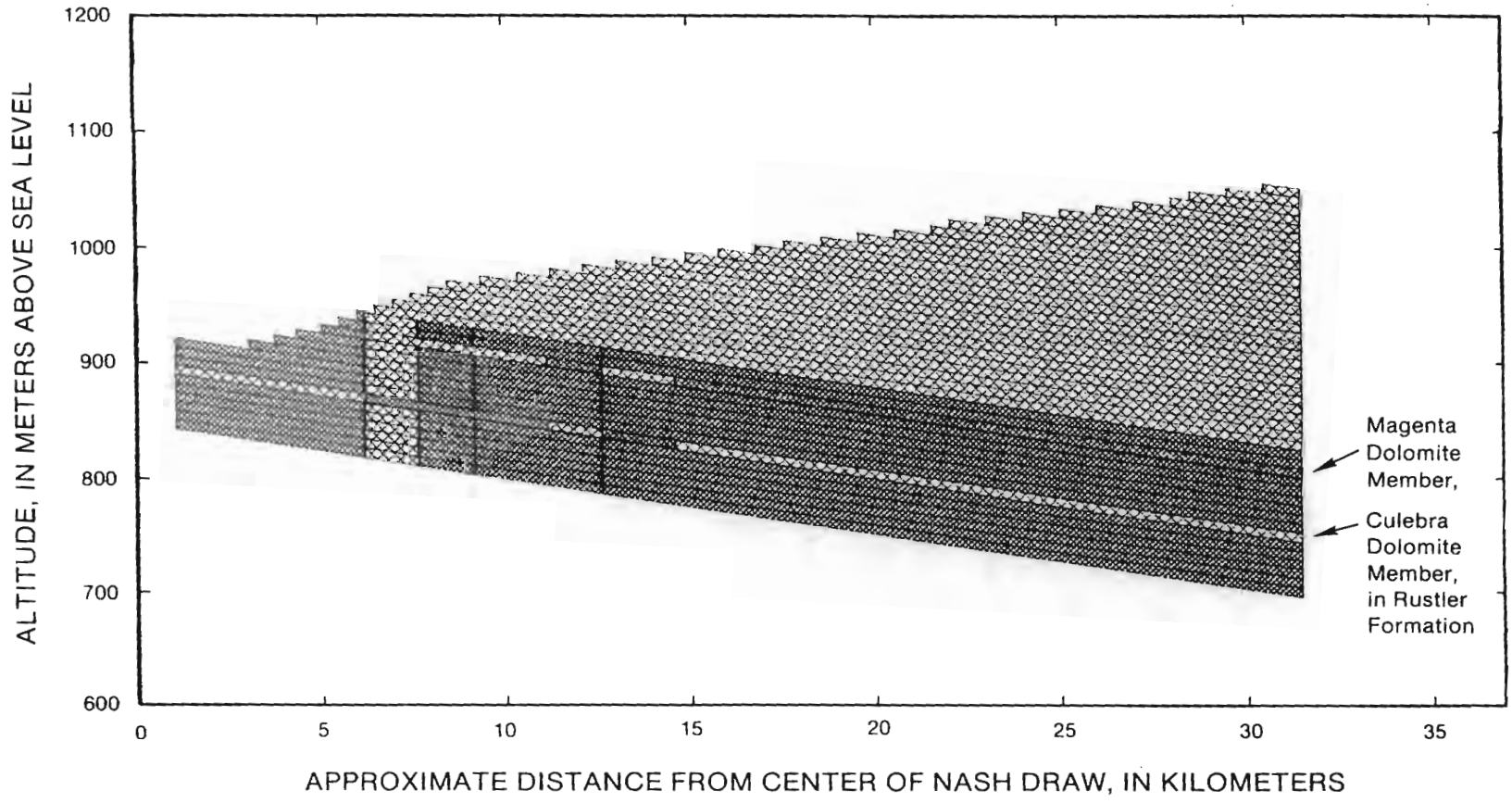
Hydraulic conductivity for the standard simulation (fig. 57) was assigned on the basis of regional trends in test data and on lithology and degree of deformation where no data were available. Hydraulic conductivity of the Culebra Dolomite Member ranged from 10^{-8} m/s in the eastern part of the section, increasing through the transition zone to 10^{-4} m/s in Nash Draw at the west end of the section. Fewer data were available for defining regional trends in the Magenta Dolomite Member. The available data for the Magenta (Mercer, 1983) indicate that hydraulic conductivity in the Magenta is lower than that in the Culebra but that the pattern is similar: low conductivity in the east, increasing through the transition zone to higher conductivity in the vicinity of Nash Draw. For the standard simulation, the Magenta was assigned hydraulic conductivity ranging from 10^{-9} to 10^{-5} m/s, with the hydraulic conductivity at any given location being one order of magnitude less than the corresponding conductivity in the Culebra.

The Forty-niner Member, Tamarisk Member, and lower unnamed member of the Rustler Formation, which consist of anhydrite and clayey halite in the east, and gypsum and mudstone in the west, are relatively impermeable. With the exception of a few tests in the Forty-niner, the hydraulic conductivity of these units has been too low to measure using standard testing techniques (Beauheim, 1987a). Although the large head differentials between the Magenta and Culebra in the vicinity of the WIPP site indicate that the 30 meters of Tamarisk between these two units has a relatively low hydraulic conductivity, this head differential dissipates westward toward Nash Draw. Thus, the Tamarisk probably follows a pattern, similar to that in the Culebra and Magenta, of increasing hydraulic conductivity in the vicinity of Nash Draw as a result of increased exposure to secondary processes. Given the similarities in lithology, the Forty-niner and lower unnamed members of the Rustler probably follow hydraulic-conductivity patterns similar to that in the Tamarisk. For these three units, hydraulic conductivity used in the standard simulation ranges from 10^{-11} m/s in the eastern part of the section, increasing through the transition zone to 10^{-7} m/s in Nash Draw. For comparison, this range of hydraulic conductivity roughly corresponds to an impermeable marine shale at the low end to a moderately impermeable, but fractured, rock at the high end (Freeze and Cherry, 1979, p. 29).

No hydraulic-conductivity data were available for the Dewey Lake Red Beds, which overlie the Rustler Formation. Mercer (1983) indicated that these fine-grained sandstones and siltstones have relatively low hydraulic conductivity. Therefore, a hydraulic conductivity of 10^{-8} m/s, which falls at the low end of the range of typical values for fine-grained sandstones (Morris and Johnson, 1967, p. D18), was used in the standard simulation.

Storage Parameters

Two types of storage provide water as the flow system is drained. The first type (specific yield) is the drainage of water from rock pores as the water table is lowered. The second type (specific storage) is the production of water that occurs when fluid pressure drops and in response, water expands and the porous medium contracts. During drainage of the vertical section, the water table primarily is in the Dewey Lake Red Beds. Therefore, a value of 0.2 was specified for specific yield, which is an average value of specific yield for a fine-grained sandstone (Morris and Johnson, 1967, p. D18). For specific storage, a value of 10^{-4} m⁻¹ was used, which roughly falls at the lower



EXPLANATION
HYDRAULIC CONDUCTIVITY, IN METERS PER SECOND









| | | | |
|---|---|---|--|
|  10^{-4} |  10^{-6} |  10^{-8} |  10^{-10} |
|  10^{-5} |  10^{-7} |  10^{-9} |  10^{-11} |

Figure 57.-- Hydraulic-conductivity distribution for the standard simulation.



end of the range for dense sand and at the upper end of the range for jointed rock (Domenico, 1972, p. 231).

Boundary and initial conditions

The boundary and initial conditions for the standard simulation are shown in figure 58. The boundary conditions consisted of a water table at the top of the section and a no-flow boundary coincident with the top of salt in the Salado Formation at the base. Topographic and underlying ground-water divides at the east end of the section were assumed to be long-term features; therefore, a no-flow boundary similar to the eastern boundary in the vertical-flux simulation of the regional model was used for the eastern boundary of the cross-sectional model. Also similar to the regional model, a no-flow boundary at the axis of Nash Draw was used for the western boundary of the cross-sectional model. Discharge in Nash Draw was simulated using specified-head nodes located approximately at land surface. Physically this boundary is representative of ground water leaving the system by springs, evapotranspiration, or discharge to a stream.

The initial conditions for this simulation were designed to represent the possible head configuration at the end of the last glacial pluvial period, which had presumably fully recharged the system. The initial conditions were implemented by specifying the location of a water table based on the elevation of the spring deposits, with a small upward slope toward the east. This slope was a subdued replica of the topography, which is a common configuration for the water table (Bredehoeft and others, 1982, p. 302-305). Beneath the water table, a vertical hydrostatic head distribution was specified.

Model Results

The standard simulation used the previously described model properties to examine transient behavior of the system over 20,000 years. This simulation then was compared with a series of simulations in which alternative distributions of hydraulic conductivity were simulated.

Standard simulation

Given the boundary conditions, initial conditions, and parameters characterizing the system, the model was run for a 20,000-year simulation period. This simulation provided not only a first look at transient system behavior over a long time period, but also, it provided a standard for comparing other simulations in which alternative hydraulic-conductivity distributions and other parameter variations were examined.

The initial water-table configuration and the response of the water table after 1,000, 4,000, 10,000, and 20,000 years of drainage are shown in figure 59. The steady-state level that the water table would eventually reach if the system were to drain to completely static conditions also is shown. Two features of the water-table response are significant. First, drawdown is concentrated

11 12 13 14 15 16 17 18 19 20 21 22 23 24 25 26 27 28 29 30 31 32 33 34 35 36 37 38 39 40 41 42 43 44 45 46 47 48 49 50 51 52 53 54 55 56 57 58 59 60 61 62 63 64 65 66 67 68 69 70 71 72 73 74 75 76 77 78 79 80 81 82 83 84 85 86 87 88 89 90 91 92 93 94 95 96 97 98 99 100

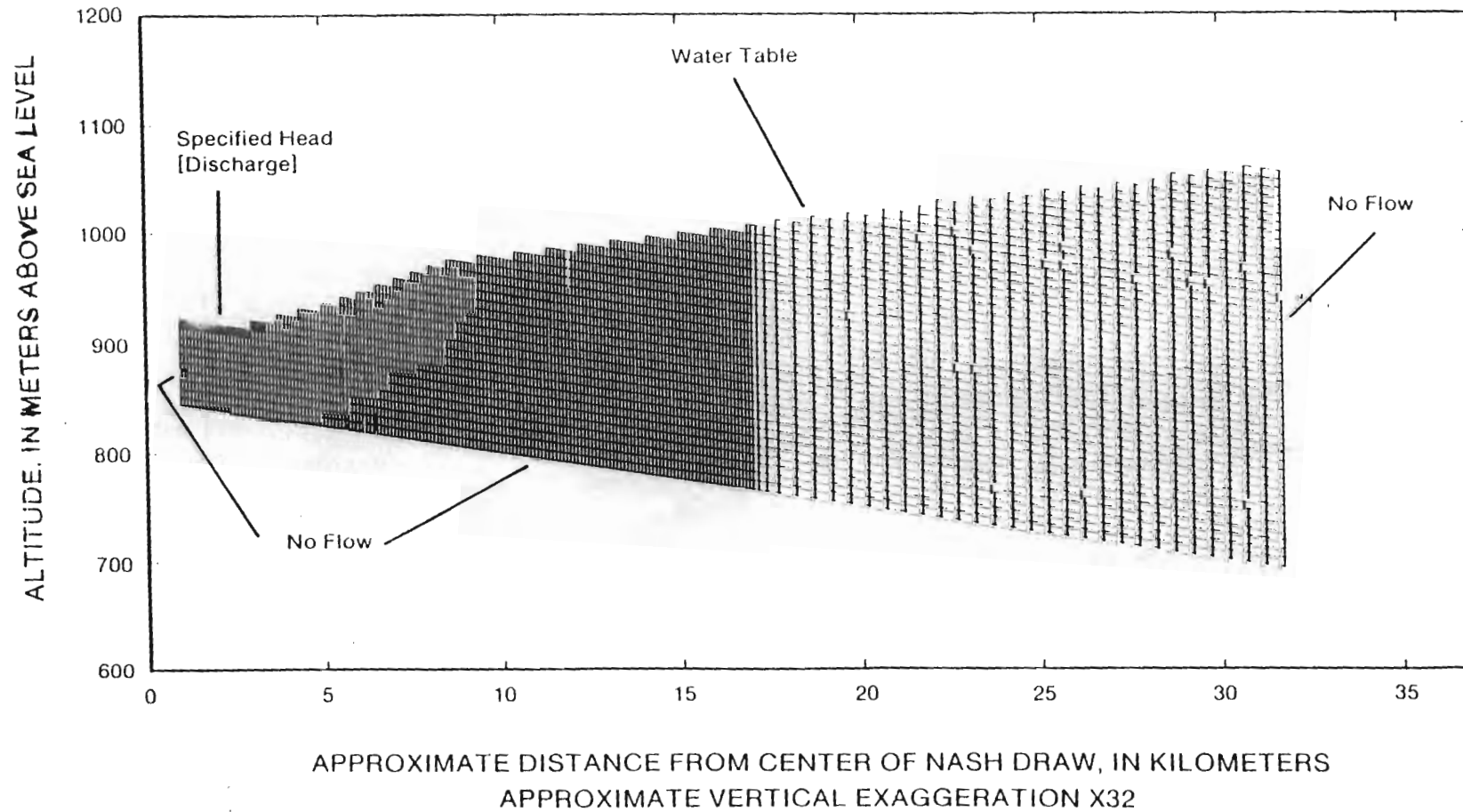


Figure 58.-- Boundary and initial conditions for the cross-sectional model.

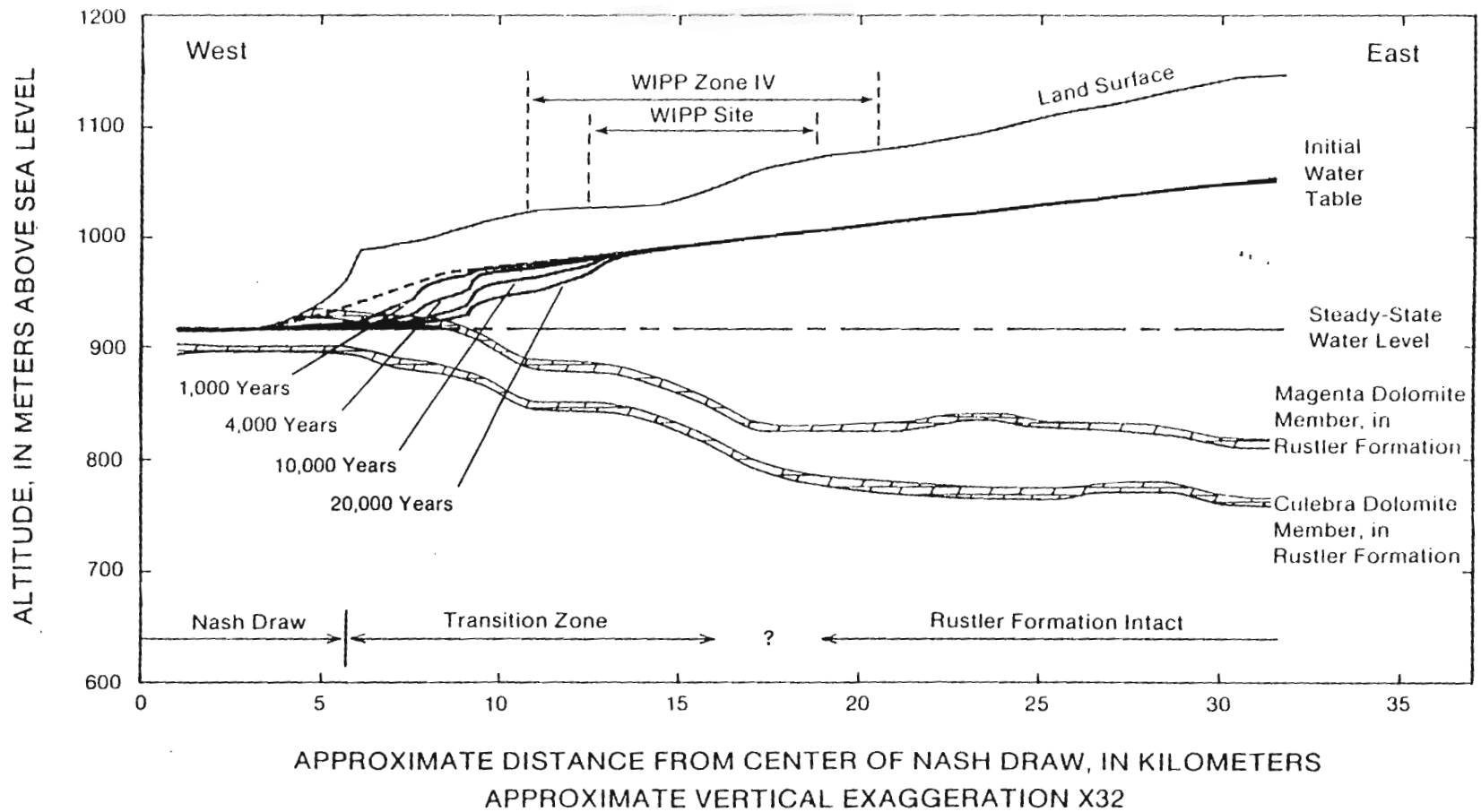


Figure 59.-- Initial water table and the configuration of the water table produced by the standard simulation after 1,000, 4,000, 10,000, and 20,000 years of drainage.

in the higher conductivity area of the transition zone adjacent to Nash Draw. Second, even after 20,000 years of drainage there is a very large volume of water remaining in storage, much of it in the thick sandstone that overlies the Rustler Formation in the central and eastern parts of the section.

Heads in the Magenta and Culebra Members over the same 20,000-year simulation are shown in figure 60. In the westernmost part of the transition zone, Culebra and Magenta heads have declined from their initial values but are quite similar to each other. In this area, dissolution, subsidence, and gypsum hydration have increased the hydraulic conductivity of the Tamarisk confining unit such that it no longer is fully effective in hydraulically isolating the Magenta from the Culebra. Therefore, Magenta head declines closely follow those in the Culebra. The hydraulic conductivity of the Tamarisk confining unit in this subregion was 10^{-8} to 10^{-9} m/s.

Further east to about the middle of the WIPP site, heads in the Culebra have declined much further than heads in the Magenta. In this area, hydraulic conductivity in the Tamarisk confining unit has decreased to about 10^{-9} to 10^{-11} m/s, which largely isolates the Magenta from the underlying Culebra. The differential between simulated Magenta and Culebra heads is about 10 to 20 meters, which is similar to the head differentials that were reported by Mercer (1983).

East from the middle of the WIPP site, both Culebra and Magenta heads are still at their initial values. In this area, heads in the Magenta and Culebra have not yet been affected by drainage because of the relatively large distance from Nash Draw and the lower hydraulic conductivity throughout the entire section.

The flow velocities at selected nodes throughout the model grid after 1,000 years of drainage are shown in figure 61. The vectors, which show the direction (corrected for vertical exaggeration) and magnitude of ground-water flow, illustrate the general flow patterns within the section as the system drains. In the sandstone units that occupy the upper part of the section, water flows westward toward Nash Draw until it reaches a point in the transition zone adjacent to Nash Draw where the hydraulic conductivity of the Forty-niner confining unit is high enough to allow significant downward leakage into the underlying Magenta. Closer to Nash Draw, hydraulic conductivity of the Tamarisk confining unit increases and increased quantities of water can drain downward from the Magenta to the Culebra. Ground water in the Culebra moves westward, collecting progressively larger amounts of downward leakage, finally discharging into Nash Draw.

Alternative hydraulic-conductivity distributions

A number of alternative hydraulic-conductivity distributions were simulated to further examine the relation between the Culebra Dolomite Member and other parts of the flow system. All simulations were for the same 20,000-year period as the standard simulation.

A comparison of heads in the Magenta and Culebra Members produced by a simulation in which hydraulic conductivity of the Tamarisk confining unit was increased by one order of magnitude along all but the western end of the cross section is shown in figure 62. The head differential between the Magenta and Culebra is much smaller than the head differential in both the standard simulation and in the field. This simulation indicates that in order to maintain the

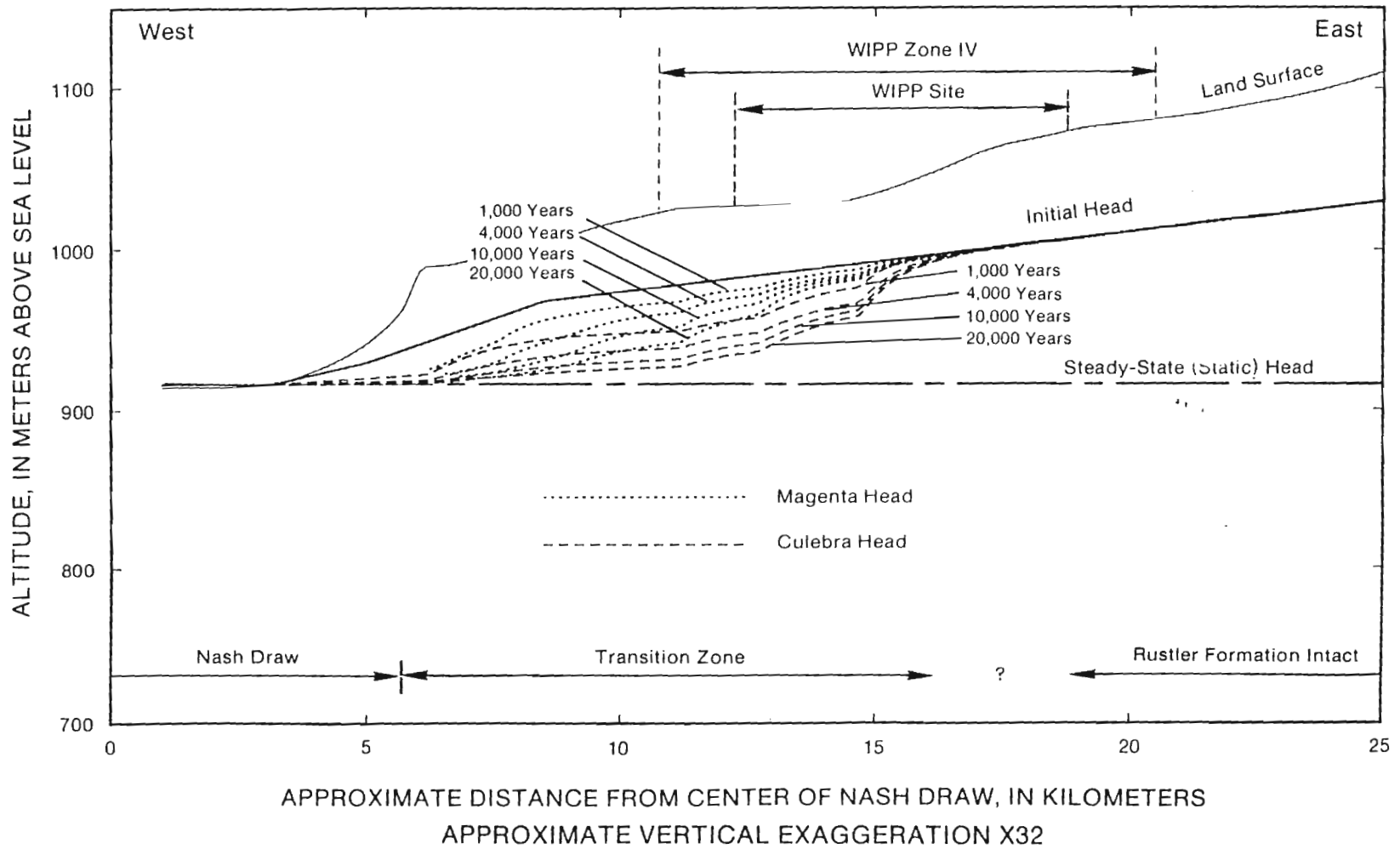


Figure 60.-- Comparison of simulated heads in the Magenta and Culebra Dolomite Members of the Rustler Formation produced by the standard simulation after 1,000, 4,000, 10,000, and 20,000 years of drainage.

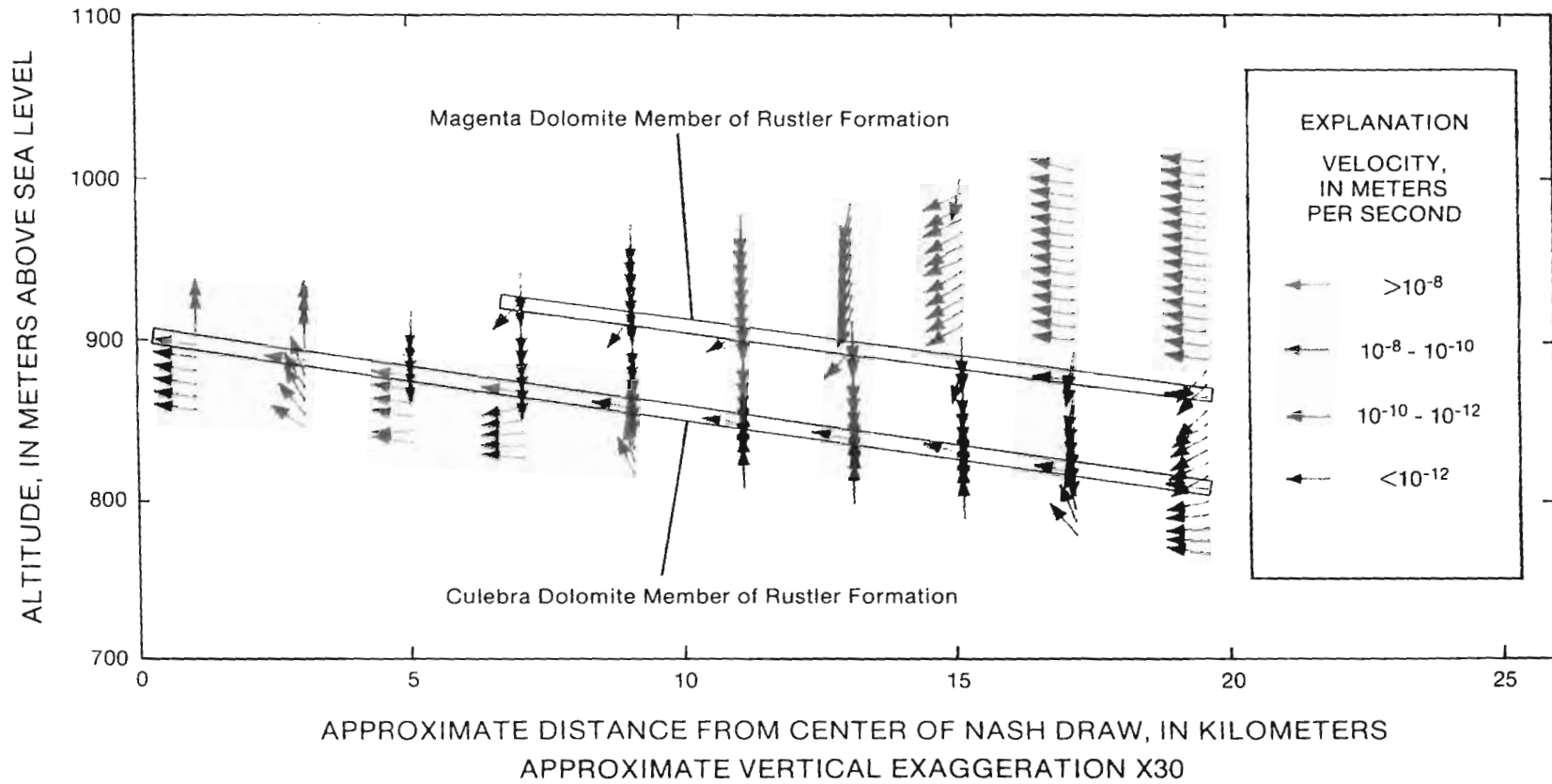


Figure 61.-- Direction (corrected for vertical exaggeration) and magnitude of ground-water flow produced by the standard simulation after 1,000 years of drainage.



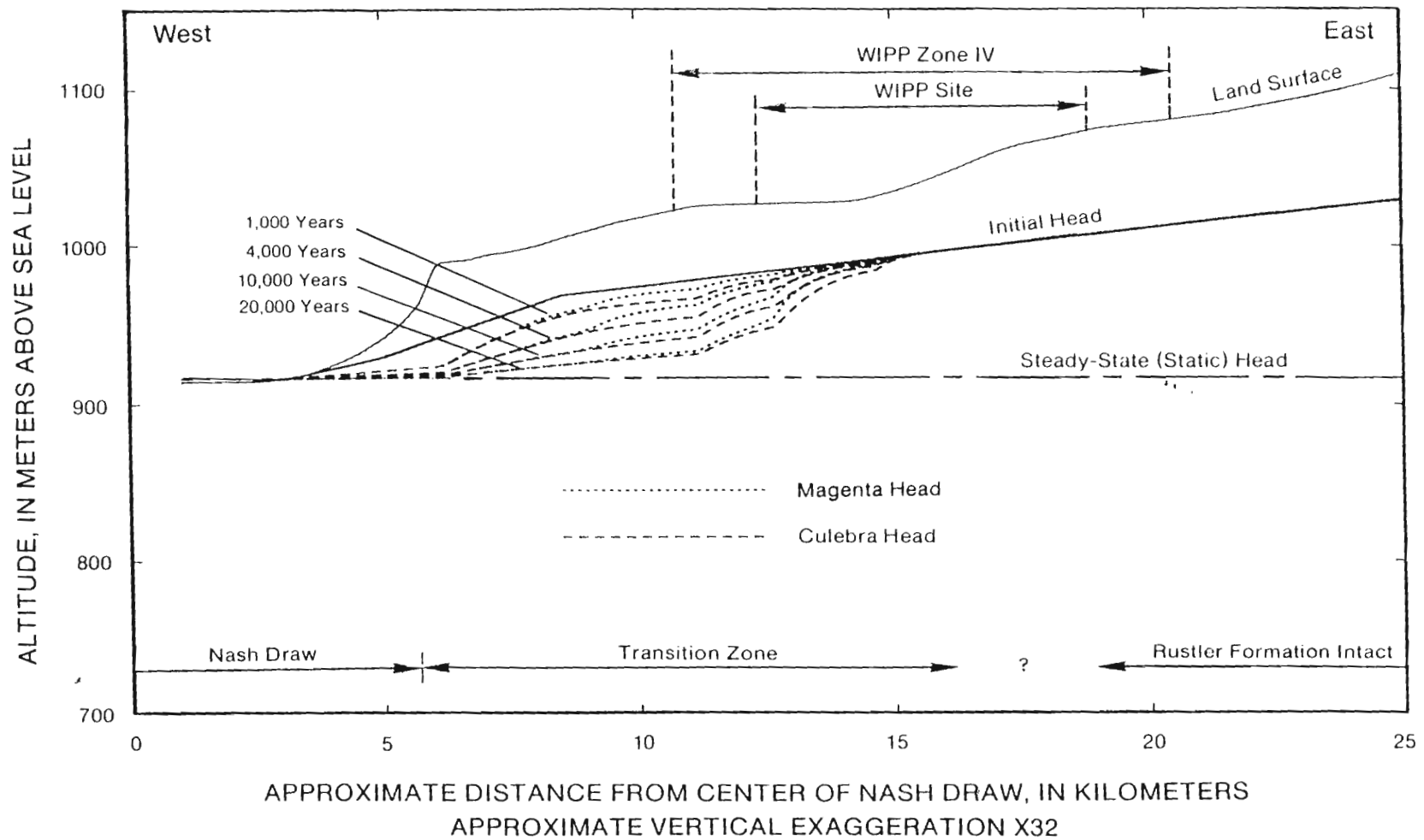


Figure 62.-- Comparison of heads in the Magenta and Culebra Dolomite Members of the Rustler Formation (after 1,000, 4,000, 10,000, and 20,000 years of drainage) produced by a simulation in which the hydraulic conductivity of the Tamarisk confining unit was one order of magnitude greater than that used in the standard simulation.

2 1 1 1 1 1 1 1 1 1 1 1 1 1

large head differential between the Magenta and Culebra that is present in the vicinity of the WIPP site, the effective vertical hydraulic conductivity of the Tamarisk confining unit must be on the order of 10^{-10} m/s or less.

In order to examine the extreme low end of the conductivity spectrum in the Tamarisk confining unit, a simulation was executed in which the hydraulic conductivity of the Tamarisk was set equal to zero. This totally isolates the Culebra from any source of vertical infiltration from above. The resulting Culebra head distribution is shown in figure 63. Head in the Culebra declines much more rapidly because it is not receiving any recharge from higher units. Over the western part of the transition zone, the Culebra head profile declines to a near-horizontal position, which is similar to the near-horizontal profile present in the field (fig. 55).

Discharge from the total system in this simulation is less than 1 percent of the discharge from the total system in the standard simulation in which the Culebra is not isolated from overlying units. Thus most of the discharge in the standard simulation is water that flowed downward into the Culebra from overlying units.

The simulation in which the Culebra is isolated from overlying units is unrealistic in two respects. First, even if hydraulic conductivity of the Tamarisk confining unit in the east is very small, it is unlikely that it is actually equal to zero. Second, the geology of the transition zone just east of Nash Draw indicates that this area has experienced halite dissolution and related secondary processes, which would increase the hydraulic conductivity of the Tamarisk. In addition, the dissipation of the head differential between the Magenta and Culebra in this area is direct hydraulic evidence of higher conductivity in the Tamarisk.

The results of a simulation in which vertical flow through the Tamarisk confining unit was allowed only in the westernmost part of the transition zone just east of Nash Draw are shown in figure 64. The hydraulic conductivity of the Tamarisk in this area was the same as in the standard simulation; to the east, it was zero. Head in the Culebra draws down somewhat more slowly. In the Magenta, water flows westward toward Nash Draw, then drains downward into the Culebra in the westernmost part of the transition zone. In this simulation, the total discharge was 96 percent of that in the standard simulation. Comparison of this total discharge with the discharge in the previous simulation (less than 1 percent of the standard) indicates that most of the discharge in the standard simulation is from vertical infiltration into the Culebra in the westernmost part of the transition zone, just east of Nash Draw. This result is quite similar to the geographic constraint on the spatial distribution of vertical flux that was determined during the analysis of vertical flux in the regional flow model.

Summary and Conclusions

Motivated by recent isotopic and geochemical analyses, the primary objective of the cross-sectional model was to construct a simple, physically based model of the flow system as it drains following late Pleistocene recharge. A secondary objective was to examine vertical flow and the

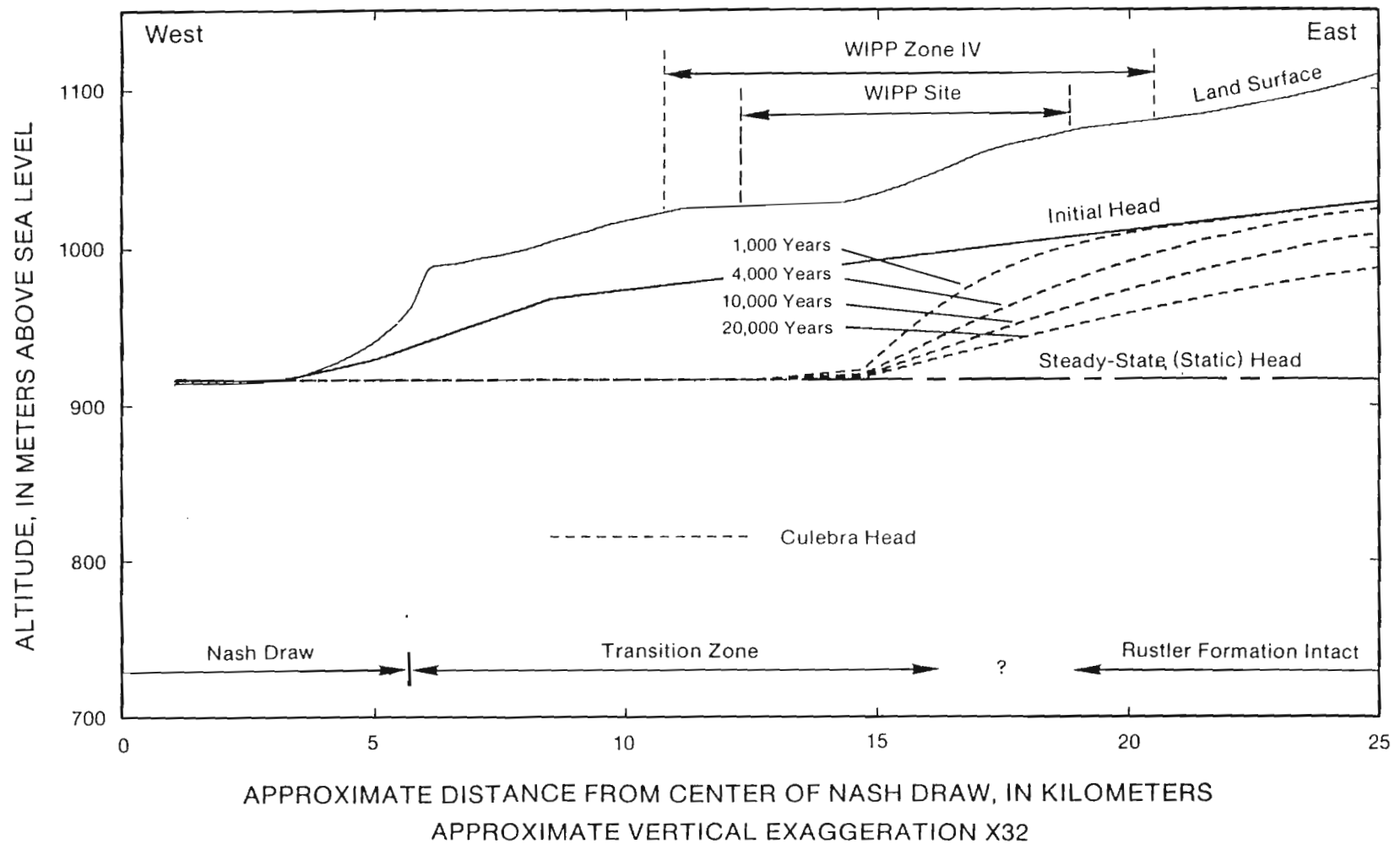


Figure 63.-- Head in the Culebra Dolomite Member of the Rustler Formation (after 1,000, 4,000, 10,000, and 20,000 years of drainage) produced by a simulation in which the hydraulic conductivity of the Tamarisk confining unit was set equal to zero, effectively isolating the Culebra from recharge from overlying units.

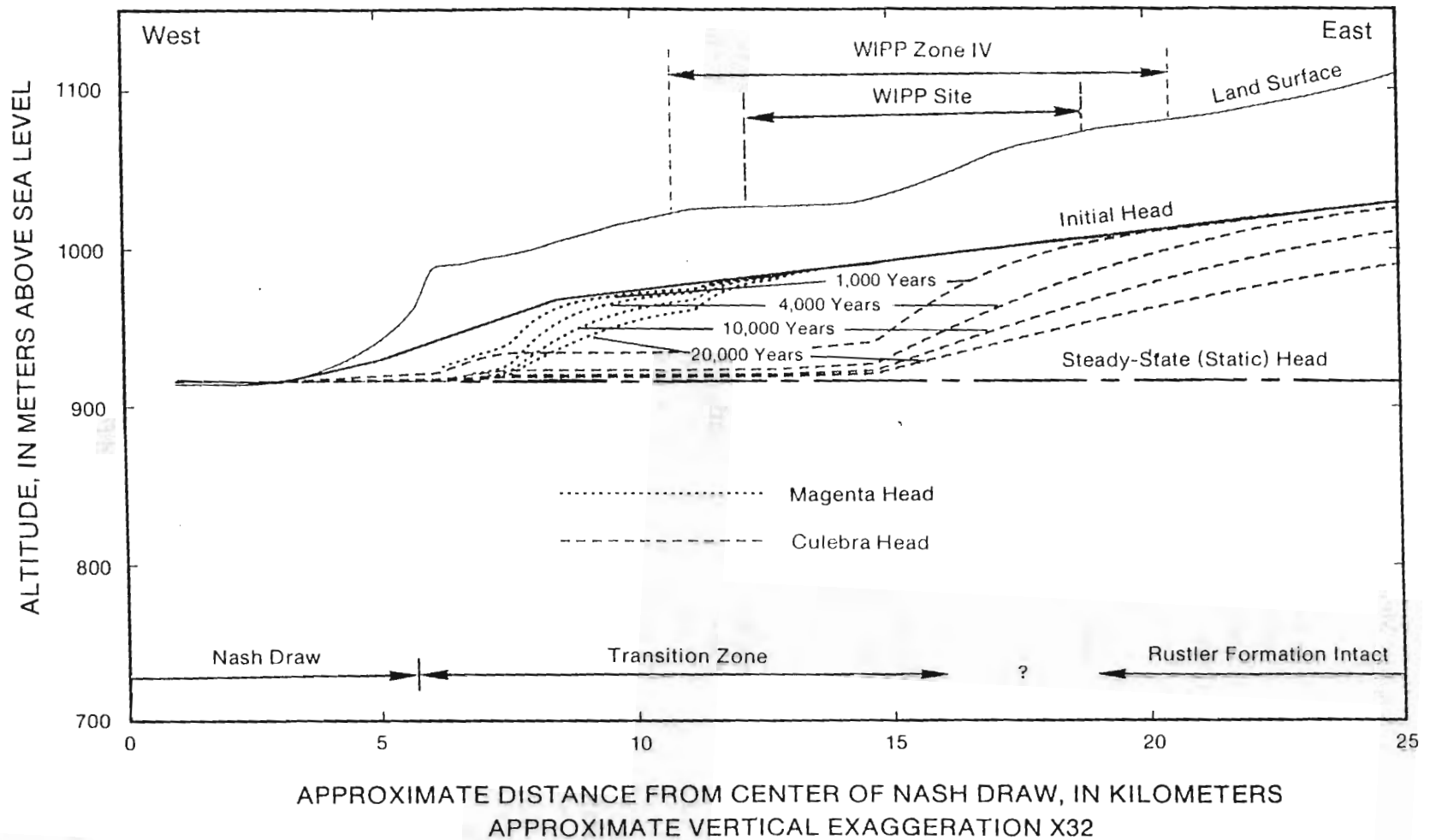


Figure 64.-- Comparison of heads in the Magenta and Culebra Dolomite Members of the Rustler Formation (after 1,000, 4,000, 10,000, and 20,000 years of drainage) produced by a simulation in which vertical flow through the Tamarisk confining unit was allowed only in the westernmost part of the transition zone.

relation between the Culebra Dolomite Member and other water-bearing units overlying the Salado Formation.

The model configuration was based on an east-west geologic section through the WIPP region. Values of storage and hydraulic conductivity used in the model were based on field data where available and on values for similar rock types where no data exist. The initial water-table configuration was based on the elevation of spring deposits of late Pleistocene age on the eastern margin of Nash Draw.

A variety of simulations over 20,000-year time periods indicates that the system drains very slowly. Even at the highest discharge rates, the system drains slowly enough that it apparently could sustain transient flow from the Pleistocene to the present without additional recharge. Conclusions drawn from the model need to be viewed in terms of the quality of input data. The geology of the section, the regional trends in hydraulic conductivity of the Culebra and Magenta Dolomite Members, and the elevation of the late Pleistocene water table are well documented. However, the model was limited to using representative values for hydraulic conductivity of other units and for the storage characteristics of the system as a whole. Therefore, the model can neither definitively prove nor disprove the drainage hypothesis proposed by Lambert (1987) and Lambert and Harvey (1988). The results of the model do indicate, however, that long-term transient drainage is physically reasonable.

The process of constructing and analyzing the cross-sectional model called attention to the underpressured state of the Culebra Dolomite Member relative to the overlying Magenta Dolomite Member in the vicinity of the WIPP site. Simulations showing the development of this underpressuring through time and the critical role of the hydraulic conductivity of the intervening Tamarisk confining unit indicate that underpressuring is the hydrodynamic result of the Culebra being a relatively high conductivity unit that is well connected to its discharge area but poorly connected to sources of recharge. This type of underpressuring has been observed in other groundwater flow systems (Toth, 1978; Orr and others, 1985; Belitz and Bredehoeft, in press). The dissipation of the large pressure differential between the Magenta and Culebra in the westernmost part of the transition zone adjacent to Nash Draw is the result of increased conductivity in the Tamarisk caused by more extensive exposure to secondary processes. The dissipation of pressure differentials is accompanied by a distinct increase in the downward vertical flux through the Tamarisk to the Culebra. The overall distribution of vertical flux in the cross-sectional model is similar to that of the vertical-flux simulations of the regional flow model; the largest fluxes occur adjacent to Nash Draw and flux decreases to the east.

Although the cross-sectional model simulations met the objectives of this study, the analysis could be expanded by the incorporation of additional data on the hydraulic characteristics of the non-dolomite units, by the execution of more extensive sensitivity analyses, and possibly by examining the problem using a fully three-dimensional approach. Although the presence of long-term transients may have only small impact on short-term flow system behavior, such transients may be important to calibrating a model that is to be used for projecting the behavior of the current flow system for thousands of years into the future. These transients, if present, introduce uncertainty in the use of steady-state models for predictions over extended time periods. Given the time period of thousands of years that is pertinent to assessing the long-term performance of the WIPP repository, further work on the effects of long-term transients is warranted.

SUMMARY AND CONCLUSIONS

The primary objective of the model analyses described in this report is to enhance understanding of ground-water flow in the vicinity of the WIPP site by examining this area in the broader context of the regional flow system. This study primarily focused on the Culebra Dolomite Member of the Rustler Formation, which is considered an important potential pathway for the transport of radionuclides to the biosphere in the event of a breach of the WIPP repository.

Halite dissolution and related secondary processes are the primary factors controlling spatial variations in the hydraulic conductivity of the Culebra and of other units in the stratigraphic section. These processes have been most active and hydraulic conductivity is highest (10^{-4} m/s) in Nash Draw, a north-south valley located west of the WIPP site. The combination of low topography and high hydraulic conductivity causes Nash Draw to act as a drain in the regional flow system. Two eastward-trending reentrants locally extend these conditions to areas located north and south of the WIPP site. East of the WIPP site, the Rustler Formation is completely intact, and the Culebra is more than 400 meters below land surface. Sparse data indicate that the Culebra probably is relatively impermeable in this area, with hydraulic conductivity on the order of 10^{-9} m/s. Between Nash Draw and the totally intact Rustler to the east is a transition zone, which is characterized by strong spatial variability in hydraulic conductivity and a general trend of increasing hydraulic conductivity to the west. The WIPP site is located in this transition zone.

The initial phase of the study consisted of a driving-force analysis and comparative simulations in order to determine whether density-related gravity effects have a significant impact on flow behavior in the WIPP region. These analyses revealed that density-related gravity effects are not significant at the WIPP site and to the west, but are significant in areas to the north, northeast, and south of the site. The area to the south is important because it lies along potential contaminant transport pathways that extend southward from the WIPP site. In this area, a combination of a gentle dip in the Culebra, moderate fluid densities, and very flat equivalent-freshwater-head gradients create flow conditions in which the density-related flow component is the dominant flow-driving force. Simulations based on equivalent-freshwater head produce very misleading information on flow directions and velocity magnitudes in this area.

Following the determination of the significance of fluid-density effects, a regional-scale, variable-density model of ground-water flow in the Culebra was constructed. Boundaries for the regional model were selected to coincide with significant hydrologic features wherever possible because boundary conditions are an important factor in the assessment of long-term flow system behavior. A regional-scale, driving-force analysis was used to locate boundaries in areas that are largely free of density-related effects. The hydraulic-conductivity distribution for the regional model was produced by merging regional trends with more detailed hydraulic-conductivity variations in the vicinity of the WIPP site from a previously published site-scale model.

A baseline, approximate steady-state simulation was calibrated to the equivalent-freshwater-head distribution present prior to WIPP shaft construction, with fluid density implemented as a specified parameter on the basis of the observed fluid-density distribution. Subsequent transient simulations showed that solute redistribution takes place very slowly. This redistribution has very

little effect on flow patterns over a 100-year period and small effect in localized areas over a 1,000-year period. The flow field produced by the baseline simulation, along with long-term brine transport patterns, indicates that flow velocities are relatively fast in Nash Draw and extremely slow in the eastern and northeastern parts of the region. Relative to WIPP, the most significant feature of the regional flow field is the relatively fast velocities associated with a high conductivity zone just south of the site that was postulated in the previously published site-scale model.

A series of sensitivity simulations was used to examine the effect of uncertainty in the specification of conditions along the eastern and northern model boundaries. These simulations indicate that if the Culebra is as impermeable to the east and northeast of the WIPP site as geologic conditions indicate, the central and western parts of the region, including the WIPP site, are fairly well insulated from these boundaries and are insensitive to whatever conditions are assumed to be present along these boundaries. A simulation of a 5-meter head increase along the Pecos River boundary indicates that if the Culebra were tightly confined throughout the entire region, approximately 50 percent of any change in river elevation would eventually reach the WIPP site. Uncertainty in the regional distribution of storage characteristics in the Culebra makes it difficult to accurately predict how long it would take for stresses related to the Pecos River to propagate through the WIPP region. The presence of vertical communication between the Culebra and other water-bearing horizons may significantly dampen the propagation of Pecos River (or other) stresses through the region.

In order to examine the potential for vertical flux as a source of recharge to the Culebra, a series of simulations was carried out in which varying specified fluxes were introduced to the Culebra within the interior of the model. These simulations indicate that as much as 25 percent of total inflow to the Culebra could be entering as vertical flux. The calibration also indicated that if significant volumes of water enter the Culebra vertically, then most of the influx must be occurring in the westernmost part of the transition zone adjacent to Nash Draw. The marked eastward decrease in hydraulic conductivity of the Culebra strictly limits the amount of water that can enter the Culebra without raising heads to anomalously high levels.

Motivated by recent isotopic and geochemical analyses, a simple cross-sectional model was developed to provide a physically based analysis of the flow system as it drains through time following recharge during a past glacial pluvial. A secondary objective of the cross-sectional model was to examine vertical-flow behavior and the relation between the Culebra and other water-bearing units. The model configuration was based on an east-west geologic section through the WIPP region. Values of storage and hydraulic conductivity used in the model were based on field data where available and on values for similar rock types where no data exist. The initial water-table configuration was based on the elevation of spring deposits of late Pleistocene age on the eastern margin of Nash Draw.

Twenty thousand years of drainage were simulated using a variety of hydraulic-conductivity distributions for rock units overlying the Culebra. These simulations indicate that the system as a whole drains very slowly and that it apparently could sustain flow from purely transient drainage following recharge of the system during the Pleistocene. Although these simulations do not prove that this has been the case, they do show that such long-term transient drainage is physically possible. The simulations also indicate that the observed underpressuring of the Culebra in the vicinity of the WIPP site is most likely the hydrodynamic result of the Culebra being a relatively

high conductivity unit that is well connected to its discharge area but poorly connected to sources of recharge. Underpressuring in the Culebra apparently is dissipated in the westernmost part of the transition zone as a result of increased hydraulic conductivity in the overlying Tamarisk confining unit, which allows an increase in downward vertical flow from the Magenta to the Culebra.

REFERENCES

- Anderson, R.Y., 1981, Deep-seated salt dissolution in the Delaware Basin, Texas and New Mexico: New Mexico Geological Society Special Publication no. 10, p. 133-145.
- Bachman, G.O., 1980, Regional geology and Cenozoic history of Pecos region, southeastern New Mexico: U.S. Geological Survey Open-File Report 80-1099, 116 p.
- 1981, Geology of Nash Draw, Eddy County, New Mexico: U.S. Geological Survey Open-File Report 81-31, 8 p.
- 1985, Assessment of near-surface dissolution at and near the Waste Isolation Pilot Plant (WIPP), southeastern New Mexico: Albuquerque, N. Mex., Sandia National Laboratories Report SAND 84-7178, 33 p.
- 1987, Karst in evaporites in southeastern New Mexico: Albuquerque, N. Mex., Sandia National Laboratories Report SAND 86-7078, 82 p.
- Barr, G.E., Miller, W.B., and Gonzalez, D.D., 1983, Interim report on the modeling of the regional hydraulics of the Rustler Formation: Albuquerque, N. Mex., Sandia National Laboratories Report SAND 83-0391, 58 p.
- Beauheim, R.L., 1986, Hydraulic-test interpretations for well DOE-2 at the Waste Isolation Pilot Plant (WIPP) site: Albuquerque, N. Mex., Sandia National Laboratories Report SAND 86-1364, 89 p.
- 1987a, Interpretations of single-well hydraulic tests conducted at and near the Waste Isolation Pilot Plant (WIPP) site, 1983-1987: Albuquerque, N. Mex., Sandia National Laboratories Report SAND 87-0039, 169 p.
- 1987b, Analysis of pumping tests of the Culebra Dolomite conducted at the H-3 hydropad at the Waste Isolation Pilot Plant (WIPP) site: Albuquerque, N. Mex., Sandia National Laboratories Report SAND 86-2311, 154 p.
- Belitz, K.R., and Bredehoeft, J.D., in press, Hydrodynamics of the Denver Basin, an explanation of subnormal fluid pressures: American Association of Petroleum Geologists Bulletin.
- Borns, D.J., Barrows, L.J., Powers, D.W., and Snyder, R.P., 1983, Deformation of evaporites near the Waste Isolation Pilot Plant (WIPP) site: Albuquerque, N. Mex., Sandia National Laboratories Report SAND 82-1069, 143 p.
- Bredehoeft, J.D., Back, W., and Hanshaw, B.B., 1982, Regional ground-water flow concepts in the United States--Historical perspectives, *in* Narasimhan, T.N., ed., Recent trends in hydrogeology: Geological Society of America Special Paper 189, p. 297-316.

- Brokaw, A.L., Jones, C.L., Cooley, M.E., and Hays, W.H., 1972, Geology and hydrology of the Carlsbad potash area, Eddy and Lea Counties, New Mexico: U.S. Geological Survey Open-File Report 4339-1, 86 p.
- Chapman, J.B., 1986, Stable isotopes in southeastern New Mexico groundwater--Implications for dating recharge in the WIPP area: Santa Fe, N. Mex., State of New Mexico Environmental Evaluation Group Report EEG-35, 76 p.
- Chaturvedi, Lokesh, and Channell, J.K., 1985, The Rustler Formation as a transport medium for contaminated groundwater: Santa Fe, N. Mex., State of New Mexico Environmental Evaluation Group Report EEG-32, var. pag.
- Cole, C.R., and Bond, F.W., 1980, Assessment of the effectiveness of geologic isolation systems --Comparison of INTERA and WISAP model application: Pacific Northwest Laboratory, PNL-3070, 50 p.
- Cooper, J.B., 1962, Ground-water investigations of the Project Gnome area, Eddy and Lea Counties, New Mexico: U.S. Geological Survey Trace Elements Investigations Report 802, 67 p.
- Cooper, J.B., and Glanzman, V.M., 1971, Geohydrology of Project Gnome site, Eddy County, New Mexico: U.S. Geological Survey Professional Paper 712-A, 24 p.
- Crawley, M.E., 1987, Second data release report for the pressure-density survey program: Consultant's report prepared by International Technologies Corporation and Westinghouse Electric Corporation, var. pag.
- D'Appolonia Consulting Engineers, 1981, Modeling verification studies long-term waste isolation assessment, Waste Isolation Pilot Plant (WIPP) project, southeastern New Mexico: Consultant's report prepared for U.S. Department of Energy, var. pag.
- Davies, P.B., 1984, Deep-seated dissolution and subsidence in bedded salt deposits: Stanford, Calif., Stanford University, unpublished Ph.D. thesis, 379 p.
- 1986, Pleistocene-to-present flow-system evolution in the northern Delaware Basin, southeastern New Mexico--Analysis using transient cross-sectional flow simulations: Geological Society of America, Abstracts with Programs, v. 18, no. 6, p. 580.
- 1987, Modeling areal, variable-density, ground-water flow using equivalent freshwater head --Analysis of potentially significant errors: Proceedings of the NWWA Conference on Solving Ground Water Problems with Models, Denver, Colorado, February 10-12, 1987, p. 888-903.
- DeWiest, R.J.M., 1965, Geohydrology: New York, John Wiley and Sons, 366 p.

- Dillon, R.T., Lantz, R.B., and Pahwa, S.B., 1978, Risk methodology for geologic disposal of radioactive waste--The Sandia waste isolation flow and transport (SWIFT) model: Albuquerque, N. Mex., Sandia National Laboratories Report SAND 78-1267.
- Domenico, P.A., 1972, Concepts and models in groundwater hydrology: New York, McGraw Hill, 405 p.
- Freeze, R.A., and Cherry, J.A., 1979, Groundwater: Englewood Cliffs, N.J., Prentice Hall, Inc., 604 p.
- Freeze, R.A., and Witherspoon, P.A., 1966, Theoretical analysis of regional groundwater flow: 1. Analytic and numerical solutions to the mathematical model: Water Resources Research, v. 2, no. 4, p. 641-656.
- 1967, Theoretical analysis of regional groundwater flow: 2. Effect of water-table configuration and subsurface permeability variation: Water Resources Research, v. 3, no. 2, p. 623-634.
- Geohydrology Associates, Inc., 1978, Collection of hydrologic data eastside Roswell range EIS area New Mexico: New Mexico Bureau of Mines and Mineral Resources Open-File Report 95, 98 p.
- Gonzalez, D.D., 1983a, Groundwater flow in the Rustler Formation, Waste Isolation Pilot Plant (WIPP), southeastern New Mexico (SENM), interim report: Albuquerque, N. Mex., Sandia National Laboratories Report SAND 82-1012, 39 p.
- 1983b, Hydrogeochemical parameters of fluid-bearing zones in the Rustler and Bell Canyon Formations: Waste Isolation Pilot Plant (WIPP), southeast New Mexico (SENM): Albuquerque, N. Mex., Sandia National Laboratories Report SAND 83-0210, 37 p.
- Hale, W.E., Hughes, L.S., and Cox, E.R., 1954, Possible improvement of quality of water of the Pecos River by diversion of brine at Malaga Bend, Eddy County, New Mexico: U.S. Geological Survey Open-File Report, 43 p.
- Haug, A., Kelley, V.A., LaVenue, A.M., and Pickens, J.F., 1987, Modeling of ground-water flow in the Culebra Dolomite at the Waste Isolation Pilot Plant (WIPP) site: Albuquerque, N. Mex., Sandia National Laboratories Report SAND 86-7167, var. pag.
- Havens, J.S., and Wilkins, D.W., 1979, Experimental salinity alleviation at Malaga Bend of the Pecos River, Eddy County, New Mexico: U.S. Geological Survey Water-Resources Investigations 80-4, 65 p.
- Hendrickson, G.E., and Jones, R.S., 1952, Geology and ground-water resources of Eddy County, New Mexico: New Mexico Bureau of Mines and Mineral Resources Ground-Water Report 3, 169 p.

- Holt, R.M., and Powers, D.W., 1988. Facies variability and post-depositional alteration within the Rustler Formation in the vicinity of the Waste Isolation Pilot Plant, southeastern New Mexico: U.S. Dept. of Energy Report DOE/WIPP-88-004, var. pag.
- Hunter, R.L., 1985, A regional water balance for the Waste Isolation Pilot Plant (WIPP) site and surrounding area: Albuquerque, N. Mex., Sandia National Laboratories Report SAND 84-2233, 83 p.
- Hydro Geo Chem, Inc., 1985, WIPP hydrology program, Waste Isolation Pilot Plant, SENM, hydrologic data report #1: Albuquerque, N. Mex., Sandia National Laboratories Report SAND 85-7206, 710 p.
- INTERA Technologies, Inc., 1986, WIPP hydrology program. Waste Isolation Pilot Plant, southeastern New Mexico, hydrologic data report #3: Albuquerque, N. Mex., Sandia National Laboratories Report SAND 86-7109, var. pag.
- INTERA Technologies, Inc., and Hydro Geo Chem, Inc., 1985, WIPP hydrology program. Waste Isolation Pilot Plant, southeastern New Mexico, hydrologic data report #2: Albuquerque, N. Mex., Sandia National Laboratories Report SAND 85-7263, var. pag.
- Jones, C.L., 1959, Thickness, character, and structure of Upper Permian evaporites in part of Eddy County, New Mexico: U.S. Geological Survey Trace Elements Memorandum Report 1033, 19 p.
- 1973, Salt deposits of Los Medaños area, Eddy and Lea Counties. New Mexico: U.S. Geological Survey Open-File Report 4339-7, 67 p.
- Kuiper, L.K., 1983, A numerical procedure for the solution of the steady state variable density groundwater flow equation: Water Resources Research, v. 19, no. 1, p. 234-240.
- 1985, Documentation of a numerical code for the simulation of variable density ground-water flow in three dimensions: U.S. Geological Survey Water-Resources Investigations Report 84-4302, var. pag.
- Lambert, S.J., 1983, Dissolution of evaporites in and around the Delaware Basin, southeastern New Mexico and west Texas: Albuquerque, N. Mex., Sandia National Laboratories Report SAND 82-0461, 96 p.
- 1987, Stable-isotope studies of groundwaters in southeastern New Mexico, in Chaturvedi, Lokesh, ed., The Rustler Formation at the WIPP site: Santa Fe, N. Mex., State of New Mexico Environmental Evaluation Group Report EEG-34, p. 36-57.
- Lambert, S.J., and Harvey, D.M., 1988, Stable-isotope geochemistry of groundwaters in the Delaware Basin of southeastern New Mexico: Albuquerque, N. Mex., Sandia National Laboratories Report SAND 87-0138, 258 p.

- Lambert, S.J., and Robinson, K.L., 1984, Field geochemical studies of groundwaters in Nash Draw, southeastern New Mexico: Albuquerque, N. Mex., Sandia National Laboratories Report SAND 83-1122, 38 p.
- Lowenstein, T.K., 1987, Post burial alteration of the Permian Rustler Formation evaporites, WIPP site, New Mexico--Textural, stratigraphic and chemical evidence: Santa Fe, N. Mex., State of New Mexico Environmental Evaluation Group Report EEG-36, 54 p.
- Luszczynski, N.J., 1961, Head and flow of ground water of variable density: Journal of Geophysical Research, v. 66, no. 12, p. 4247-4256.
- Maley, V.C., and Huffington, R.M., 1953, Cenozoic fill and evaporite solution in the Delaware Basin, Texas and New Mexico: Geological Society of America Bulletin, v. 64, p. 539-546.
- Mercer, J.W., 1983, Geohydrology of the proposed Waste Isolation Pilot Plant Site, Los Medaños Area, southeastern New Mexico: U.S. Geological Survey Water-Resources Investigations Report 83-4016, 113 p.
- 1987, Compilation of hydrologic data from drilling the Salado and Castile Formations near the Waste Isolation Pilot Plant (WIPP) site in southeastern New Mexico: Albuquerque, N. Mex., Sandia National Laboratories Report SAND 86-0954, 39 p.
- Mercer, J.W., Thomas, S.D., and Ross, B., 1982, Parameters and variables appearing in repository siting models: U.S. Nuclear Regulatory Commission, NUREG/CR-3066, 221 p.
- Morris, D.A., and Johnson, A.I., 1967, Summary of hydrologic and physical properties of rock and soil materials, as analyzed by the hydrologic laboratory of the U.S. Geological Survey 1948-1960: U.S. Geological Survey Water-Supply Paper 1839-D, 41 p.
- National Academy of Sciences, 1984, Review of the scientific and technical criteria for the Waste Isolation Pilot Plant (WIPP): Washington, D.C., National Academy Press, 130 p.
- Neill, R.H., Channell, J.K., Chaturvedi, Lokesh, Little, M.S., Rehfeldt, Kenneth, and Spiegler, Peter, 1983, Evaluation of the suitability of the WIPP site: Santa Fe, N. Mex., State of New Mexico Environmental Evaluation Group Report EEG-23, 157 p.
- Nicholson, Alexander, and Clebsch, Alfred, 1961, Geology and ground-water conditions in southern Lea County, New Mexico: New Mexico Bureau of Mines and Mineral Resources Ground-Water Report 6, 123 p.
- Niou, S., and Pietz, J., 1987, A statistical inverse analysis of the H-3 hydropad pumping test: Consultant's report prepared by International Technologies Corp., var. pag.
- Nowak, E.J., 1986, Preliminary results of brine migration studies in the Waste Isolation Pilot Plant (WIPP): Albuquerque, N. Mex., Sandia National Laboratories Report SAND 86-0720, 64 p.

- Nowak, E.J., and McTigue, D.F., 1987, Interim results of brine transport studies in the Waste Isolation Pilot Plant (WIPP): Albuquerque, N. Mex., Sandia National Laboratories Report SAND 87-0880, 78 p.
- Orr, E.D., Kreitler, C.W., and Senger, R.K., 1985, Investigation of underpressuring in the deep-basin brine aquifer, Palo Duro Basin, Texas: University of Texas at Austin, Bureau of Economic Geology, Geological Circular 85-1, 44 p.
- Pickens, J.F., and Grisak, G.E., 1981a, Scale-dependent dispersion in a stratified granular aquifer: Water Resources Research, v. 17, no. 4, p. 1191-1211.
- 1981b, Modeling of scale-dependent dispersion in hydrologic systems: Water Resources Research, v. 17, no. 6, p. 1701-1711.
- Pinder, G.F., 1974, Galerkin-finite element models for aquifer simulation: Princeton, N.J., Princeton University Water Resources Program, Department of Civil Engineering, Department of Geological and Geophysical Science.
- Powers, D.W., Lambert, S.J., Shaffer, S.E., Hill, L.R., and Weart, W.D., eds., 1978, Geological characterization report, Waste Isolation Pilot Plant (WIPP) site, southeastern New Mexico: Albuquerque, N. Mex., Sandia National Laboratories Report SAND 78-1596, v. 1-2, var. pag.
- Ramey, D.S., 1985, Chemistry of Rustler fluids: Santa Fe, N. Mex., State of New Mexico Environmental Evaluation Group Report EEG-31, 61 p.
- Reisenauer, A.E., 1979, Variable thickness transient groundwater flow model (VTT), formulation, user's manual and program listings: Pacific Northwest Laboratory Report PNL 3160-1, PNL 3160-2, PNL 3160-3, var. pag.
- Richey, S.F., 1987, Water-level data from wells in the vicinity of the Waste Isolation Pilot Plant, southeastern New Mexico: U.S. Geological Survey Open-File Report 87-120, 107 p.
- 1989, Geologic and hydrologic data for the Rustler Formation near the Waste Isolation Pilot Plant, southeastern New Mexico: U.S. Geological Survey Open-File Report 89-32, 72 p.
- Robinson, T.W., and Lang, W.B., 1938, Geology and ground-water conditions of the Pecos River valley in the vicinity of Laguna Grande de la Sal, New Mexico: 12th and 13th Biennial Reports of the State Engineer of New Mexico, p. 77-100.
- Sampson, R.J., 1978, SURFACE II graphics system: Kansas Geological Survey, Series on Spatial Analysis, no. 1, 240 p.
- Sandia Laboratories and United States Geological Survey, 1979a, Basic data report for drillhole WIPP 25 (Waste Isolation Pilot Plant Site - WIPP): Albuquerque, N. Mex., Sandia National Laboratories Report SAND 79-0279, var. pag.

- Sandia Laboratories and United States Geological Survey, 1979b, Basic data report for drillhole WIPP 26 (Waste Isolation Pilot Plant - WIPP): Albuquerque, N. Mex., Sandia National Laboratories Report SAND 79-0280, var. pag.
- 1979c, Basic data report for drillhole WIPP 27 (Waste Isolation Pilot Plant - WIPP): Albuquerque, N. Mex., Sandia National Laboratories Report SAND 79-0281, var. pag.
- 1979d, Basic data report for drillhole WIPP 28 (Waste Isolation Pilot Plant - WIPP): Albuquerque, N. Mex., Sandia National Laboratories Report SAND 79-0282, var. pag.
- 1980, Basic data report for drillhole WIPP 30 (Waste Isolation Pilot Plant - WIPP): Albuquerque, N. Mex., Sandia National Laboratories Report SAND 79-0284, var. pag.
- Seward, P.D., 1982, Abridged borehole histories for the Waste Isolation Pilot Plant (WIPP) studies: Albuquerque, N. Mex., Sandia National Laboratories Report SAND 82-0082, 80 p.
- Snyder, R.P., 1985, Dissolution of halite and gypsum, and hydration of anhydrite to gypsum, Rustler Formation, in the vicinity of the Waste Isolation Pilot Plant, southeastern New Mexico: U.S. Geological Survey Open-File Report 85-229, 11 p.
- Theis, C.V., and Sayre, A.N., 1942, Geology and ground water, in U.S. National Resources Planning Board, 1942, Pecos River Joint Investigation--Reports of the participating agencies: Washington, D.C., U.S. Government Printing Office, p. 27-75.
- Toth, J., 1963, A theoretical analysis of groundwater flow in small drainage basins: Water Resources Research, v. 68, no. 16, p. 4795-4812.
- 1978, Gravity-induced cross-formational flow of formation fluids, Red Earth region, Alberta, Canada--Analysis, patterns, and evolution: Water Resources Research, v. 14, no. 5, p. 805-843.
- 1979, Patterns of dynamic pressure increment of formation-fluid flow in large drainage basins, exemplified by the Red Earth region, Alberta, Canada: Bulletin of Canadian Petroleum Geology, v. 27, no. 1, p. 63-86.
- Trescott, P.C., Pinder, G.F., and Larson, S.P., 1976, Finite-difference model for aquifer simulation in two dimensions with results of numerical experiments: U.S. Geological Survey Techniques of Water-Resources Investigations, book 7, chap. C1, 116 p.
- U.S. Department of Energy, 1980a, Waste Isolation Pilot Plant safety analysis report: U.S. Department of Energy, v. 1-5, var. pag.
- 1980b, Final environmental impact statement - Waste Isolation Pilot Plant: U.S. Department of Energy, DOE/EIS-0026, v. 1-2, var. pag.
- U.S. Geological Survey, 1954, Hobbs, topographic map, scale 1:250,000.

- Vine, J.D., 1963, Surface geology of the Nash Draw Quadrangle, Eddy County, New Mexico: U.S. Geological Survey Bulletin 1141-B, 46 p.
- Voss, C.I., 1984, A finite-element simulation model for saturated-unsaturated, fluid-density-dependent ground-water flow with energy transport or chemically reactive single-species solute transport: U.S. Geological Survey Water-Resources Investigations Report 84-4369, 409 p.
- Weart, W.D., 1983, Summary evaluation of the Waste Isolation Pilot Plant (WIPP) site suitability: Albuquerque, N. Mex., Sandia National Laboratories Report SAND 83-0450, 34 p.
- Weiss, Emanuel, 1982, A model for the simulation of flow of variable-density ground water in three dimensions under steady-state conditions: U.S. Geological Survey Open-File Report 82-352, 59 p.
- Westinghouse Electric Corp., 1985, Ecological monitoring program at the Waste Isolation Pilot Plant --Second semiannual report covering data collected January to June 1985: Consultant's report prepared for U.S. Department of Energy, DOE/WIPP-85-002, 128 p.

SUPPLEMENTAL INFORMATION

Table 1. Hydrologic data for wells in the WIPP region

EXPLANATION

Well location: For WIPP-related wells, see figure 65. For non-WIPP wells, see figure 66.

Reported completion: Culebra, Culebra Dolomite Member of the Rustler Formation.
Rustler, Rustler Formation.

Source of Culebra altitude: Log, geologic or geophysical log. Est. estimated from structure contour map.

Source of fluid density: Direct, direct measurement. Indirect, computed from specific conductance using relation shown in figure 16.

Sources of data:

1. Mercer, 1983
2. Lambert and Robinson, 1984
3. Westinghouse Electric Corp., 1985
4. INTERA Technologies, Inc., and Hydro Geo Chem, Inc., 1985
5. INTERA Technologies, Inc., 1986
6. U.S. Geological Survey Water-Data Storage and Retrieval System (WATSTORE)
7. Cooper, 1962
8. Hendrickson and Jones, 1952
9. Hale and others, 1954
10. U.S. Environmental Protection Agency, Environmental Monitoring and Systems Laboratory, Project Gnome Data Base
11. Richey, 1987
12. Geohydrology Associates, Inc., 1978

Table 1. Hydrologic data for wells in the WIPP region

| Well name | Well location | Reported completion | Altitude of bottom of well (meters) | Altitude of middle of Culebra (meters) | Source of Culebra altitude | Fluid density (grams per cubic centimeter) | Source of fluid density | Measured water-level altitude (meters) | Equivalent freshwater head | | Sources of data | |
|--------------------|----------------------|---------------------|-------------------------------------|--|----------------------------|--|-------------------------|--|----------------------------|-------------------------|-----------------|----------------------|
| | | | | | | | | | Altitude (meters) | Possible error (meters) | Density | Measured water level |
| WIPP related wells | | | | | | | | | | | | |
| H-1 | 22.31.29.0623N.1083E | Culebra | 774.4 | 826.0 | log | 1.016 | Direct | 919.6 | 921.1 | 1.5 | 1 | 11 |
| H-2-B | 22.31.29.0696N.1661W | Culebra | 827.7 | 836.0 | log | 1.005 | Direct | 922.3 | 922.7 | 0.4 | 4 | 11 |
| H-3 | 22.31.29.2085S.0138E | Culebra | 760.6 | 824.0 | log | 1.037 | Direct | 913.8 | 917.1 | 3.3 | 5 | 11 |
| H-4-B | 23.31.05.0498N.0633W | Culebra | 854.0 | 860.0 | log | 1.016 | Direct | 911.7 | 912.5 | 0.8 | 3 | 11 |
| H-5-B | 22.31.15.1007N.0234E | Culebra | 786.6 | 791.0 | log | 1.104 | Direct | 920.8 | 934.3 | 13.5 | 3 | 11 |
| H-6-B | 22.31.18.0196N.0322W | Culebra | 824.8 | 832.0 | log | 1.042 | Direct | 929.3 | 933.4 | 4.1 | 3 | 11 |
| H-7-B | 23.30.14.2566N.2563W | Culebra | 876.8 | 884.0 | log | 1.000 | Direct | 912.3 | 912.3 | 0.0 | 5 | 11 |
| H-8-B | 24.30.23.1995N.1405E | Culebra | 856.4 | 863.0 | log | 1.002 | Direct | 911.0 | 911.1 | 0.1 | 5 | 11 |
| H-9-B | 24.31.04.2391N.0239W | Culebra | 822.0 | 836.0 | log | 1.002 | Direct | 906.5 | 906.6 | 0.1 | 1 | 11 |
| H-10-B | 23.32.20.0485S.1985E | Culebra | 697.7 | 704.0 | log | 1.045 | Direct | 910.7 | 920.0 | 9.3 | 1 | 11 |
| H-11-B-2 | 22.31.33.1500S.0130E | Culebra | 799.2 | 811.0 | log | 1.092 | Direct | 0.0 | 0.0 | 0.0 | 3 | - |
| H-12 | 23.31.15.0100N.0100E | Culebra | 738.4 | 788.0 | log | 1.096 | Direct | 0.0 | 0.0 | 0.0 | 3 | - |
| DOE-1 | 22.31.28.0180S.0608E | Culebra | -180.8 | 802.0 | log | 1.092 | Direct | 0.0 | 0.0 | 0.0 | 3 | - |
| DOE-2 | 22.31.08.0698S.0122E | Culebra | -906.6 | 787.0 | log | 1.042 | Direct | 0.0 | 0.0 | 0.0 | 3 | - |
| P-14 | 22.30.24.0309S.0613W | Culebra | 553.3 | 845.0 | log | 1.018 | Direct | 926.0 | 927.5 | 1.5 | 1 | 11 |
| P-15 | 22.31.31.0411S.0190W | Culebra | 562.2 | 879.0 | log | 1.012 | Indirect | 915.6 | 916.0 | 0.4 | 1 | 11 |
| P-17 | 23.31.04.1356S.0398W | Culebra | 510.1 | 842.0 | log | 1.082 | Direct | 906.8 | 912.1 | 5.3 | 1 | 11 |
| P-18 | 22.31.26.0139S.0733E | Culebra | 449.7 | 778.0 | log | 1.217 | Indirect | 0.0 | 0.0 | 0.0 | 1 | 11 |
| WIPP-25 | 22.30.15.1853S.2838E | Culebra | 779.3 | 839.0 | log | 1.010 | Direct | 930.2 | 931.1 | 0.9 | 2 | 11 |
| WIPP-26 | 22.30.29.2232N.0012E | Culebra | 807.3 | 900.0 | log | 1.005 | Direct | 917.8 | 917.9 | 0.1 | 2 | 11 |
| WIPP-27 | 21.30.21.0090N.1485W | Culebra | 787.1 | 875.0 | log | 1.090 | Direct | 936.0 | 941.5 | 5.5 | 2 | 11 |
| WIPP-28 | 21.31.18.0099N.2401E | Culebra | 776.0 | 887.0 | log | 1.030 | Direct | 936.3 | 937.8 | 1.5 | 2 | 11 |
| WIPP-29 | 22.29.34.0407S.1828E | Culebra | 792.8 | 899.0 | log | 1.160 | Direct | 904.6 | 905.5 | 0.9 | 2 | 11 |
| WIPP-30 | 21.31.33.0668N.0177W | Culebra | 765.6 | 848.0 | log | 1.020 | Direct | 0.0 | 0.0 | 0.0 | 2 | 11 |

136

Table 1. Hydrologic Data for wells in the WIPP region Concluded

| Well name | Well location | Reported completion | Altitude of bottom of well (meters) | Altitude of middle of Culebra (meters) | Source of Culebra altitude | Fluid density (grams per cubic centimeter) | Source of fluid density | Measured water-level altitude (meters) | Equivalent-freshwater head | | Sources of data | |
|----------------|-----------------|---------------------|-------------------------------------|--|----------------------------|--|-------------------------|--|----------------------------|-------------------------|-----------------|----------------------|
| | | | | | | | | | Altitude (meters) | Possible error (meters) | Density | Measured water level |
| Non-WIPP wells | | | | | | | | | | | | |
| FF-006 | 24.30.04.333 | Culebra | 851.9 | 918.0 | log | 1.004 | Indirect | 0.0 | 0.0 | 0.0 | 6 | - |
| FF-008 | 24.30.18.231 | Rustler | 837.7 | 876.0 | Est | 1.003 | Indirect | 0.0 | 0.0 | 0.0 | 7 | - |
| FF-011 | 24.29.19.421 | Culebra | 877.2 | 880.0 | log | 1.074 | Direct | 0.0 | 0.0 | 0.0 | 6 | - |
| FF-012 | 24.29.20.134 | Culebra | 871.7 | 876.0 | log | 1.184 | Direct | 881.2 | 882.2 | 1.0 | 6 | 6 |
| FF-013 | 24.29.20.141 | Rustler | 849.5 | 876.0 | Est | 1.184 | Direct | 0.0 | 0.0 | 0.0 | 6 | - |
| FF-014 | 24.29.20.322 | Culebra | 870.5 | 874.0 | log | 1.168 | Direct | 0.0 | 0.0 | 0.0 | 6 | - |
| FF-016 | 24.29.20.432 | Rustler | 855.9 | 865.0 | Est | 1.126 | Direct | 882.4 | 884.6 | 2.2 | 6 | 6 |
| FF-018 | 24.29.29.143 | Culebra | 872.9 | 877.0 | log | 1.022 | Direct | 884.2 | 884.4 | 0.2 | 6 | 6 |
| FF-035 | 23.30.21.122 | Rustler | 902.5 | 910.0 | Est | 1.001 | Indirect | 0.0 | 0.0 | 0.0 | 8 | - |
| FF-095 | 21.28.36.12321 | Rustler | 901.8 | 909.0 | Est | 1.039 | Est | 926.2 | 926.9 | 0.7 | - | 6 |
| FF-096 | 21.29.12.21344 | Rustler | 895.2 | 918.0 | Est | 1.061 | Est | 944.2 | 945.8 | 1.6 | - | 6 |
| FF-115 | 22.30.05.43114 | Rustler | 879.9 | 894.0 | Est | 1.013 | Est | 934.7 | 935.2 | 0.5 | - | 6 |
| FF-119 | 22.30.07.242224 | Rustler | 896.5 | 896.0 | Est | 1.012 | Est | 931.7 | 932.1 | 0.4 | - | 6 |
| FF-124 | 22.30.32.11144 | Rustler | 886.9 | 903.0 | Est | 1.001 | Indirect | 910.7 | 910.7 | 0.0 | 7 | 6 |
| FF-125 | 22.30.33.212243 | Rustler | 888.1 | 899.0 | Est | 1.002 | Est | 914.5 | 914.5 | 0.0 | - | 6 |
| FF-126 | 23.30.02.44414 | Rustler | 893.1 | 895.0 | Est | 1.001 | Indirect | 0.0 | 0.0 | 0.0 | 7 | - |
| FF-127 | 23.30.02.44414 | Rustler | 894.0 | 895.0 | Est | 1.001 | Indirect | 912.3 | 912.3 | 0.0 | 6 | 6 |
| FF-128 | 23.30.19.123421 | Rustler | 897.0 | 906.0 | Est | 1.001 | Indirect | 906.7 | 906.7 | 0.0 | 7 | 6 |
| FF-132 | 23.30.34.133144 | Culebra | 882.4 | 889.0 | log | 1.002 | Indirect | 908.2 | 908.2 | 0.0 | 10 | 10 |
| FF-133 | 23.30.34.13323 | Culebra | 819.6 | 893.0 | log | 1.001 | Indirect | 909.6 | 909.6 | 0.0 | 10 | 10 |
| FF-137 | 23.30.34.32400 | Culebra | 823.7 | 881.0 | log | 1.001 | Indirect | 909.4 | 909.4 | 0.0 | 10 | 10 |
| FF-141 | 24.30.19.42113 | Rustler | 827.5 | 825.0 | Est | 1.017 | Est | 893.4 | 894.6 | 1.2 | - | 6 |
| FF-146 | 24.31.33.231113 | Rustler | 829.4 | 833.0 | Est | 1.002 | Indirect | 0.0 | 0.0 | 0.0 | 7 | - |
| FF-153 | 25.28.15.23000 | Rustler | 877.6 | 886.0 | Est | 1.022 | Est | 884.7 | 884.7 | 0.0 | - | 6 |
| FF-161 | 25.31.02.23441 | Rustler | 743.1 | 800.0 | Est | 1.000 | Est | 933.8 | 933.8 | 0.0 | - | 6 |
| FF-174 | 21.29.11.421 | Rustler | 934.8 | 934.0 | Est | 1.059 | Est | 944.2 | 944.8 | 0.6 | - | 12 |
| USGS-1 | 24.29.16.311 | Rustler | 819.2 | 872.0 | Est | 1.207 | Direct | 0.0 | 0.0 | 0.0 | 9 | - |
| USGS-7 | 24.29.16.314 | Rustler | 821.1 | 868.0 | Est | 1.203 | Direct | 0.0 | 0.0 | 0.0 | 9 | - |
| USGS-11 | 24.29.17.444 | Rustler | 810.3 | 870.0 | Est | 1.209 | Direct | 0.0 | 0.0 | 0.0 | 9 | - |

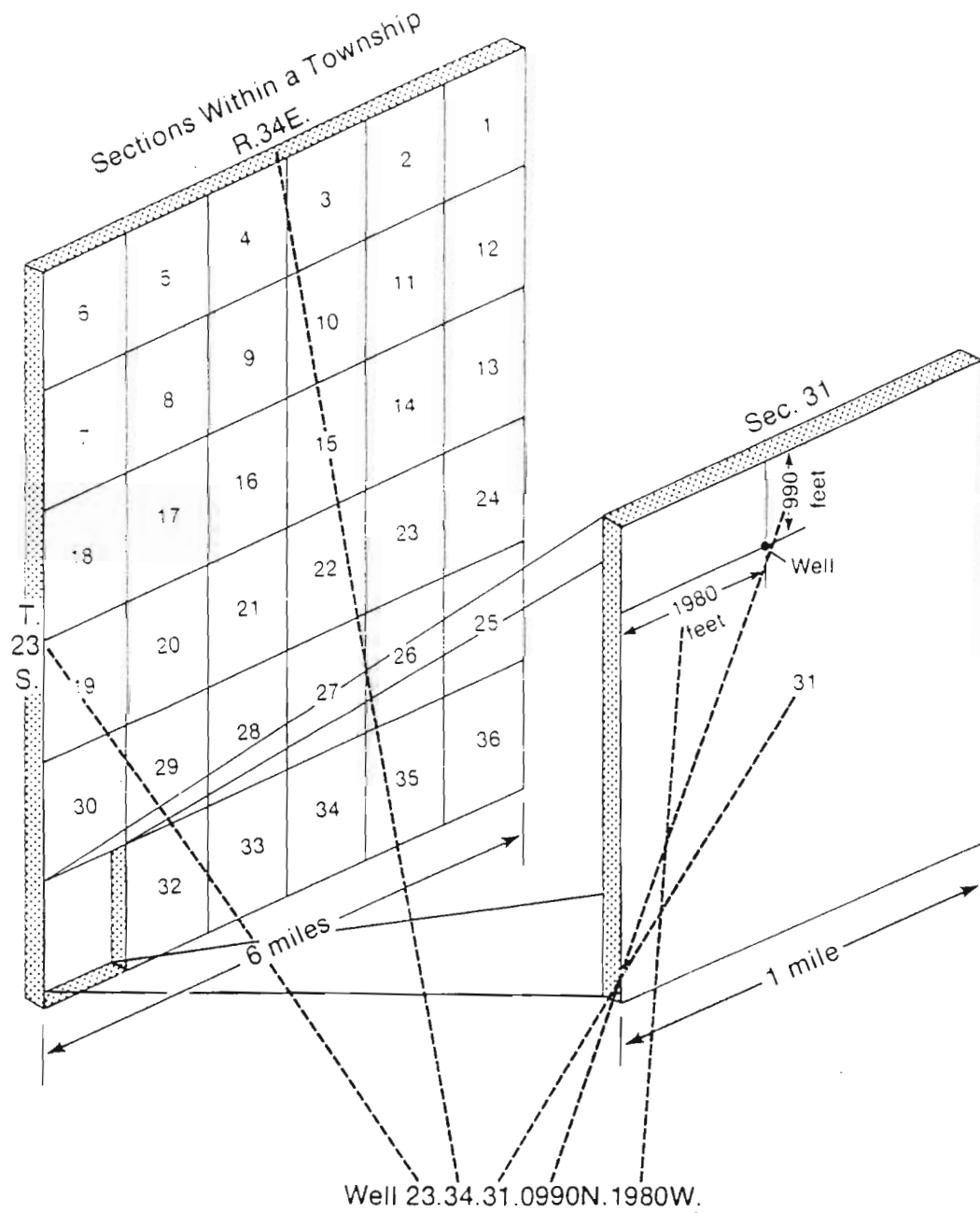


Figure 65.-- System for locating WIPP-related wells.

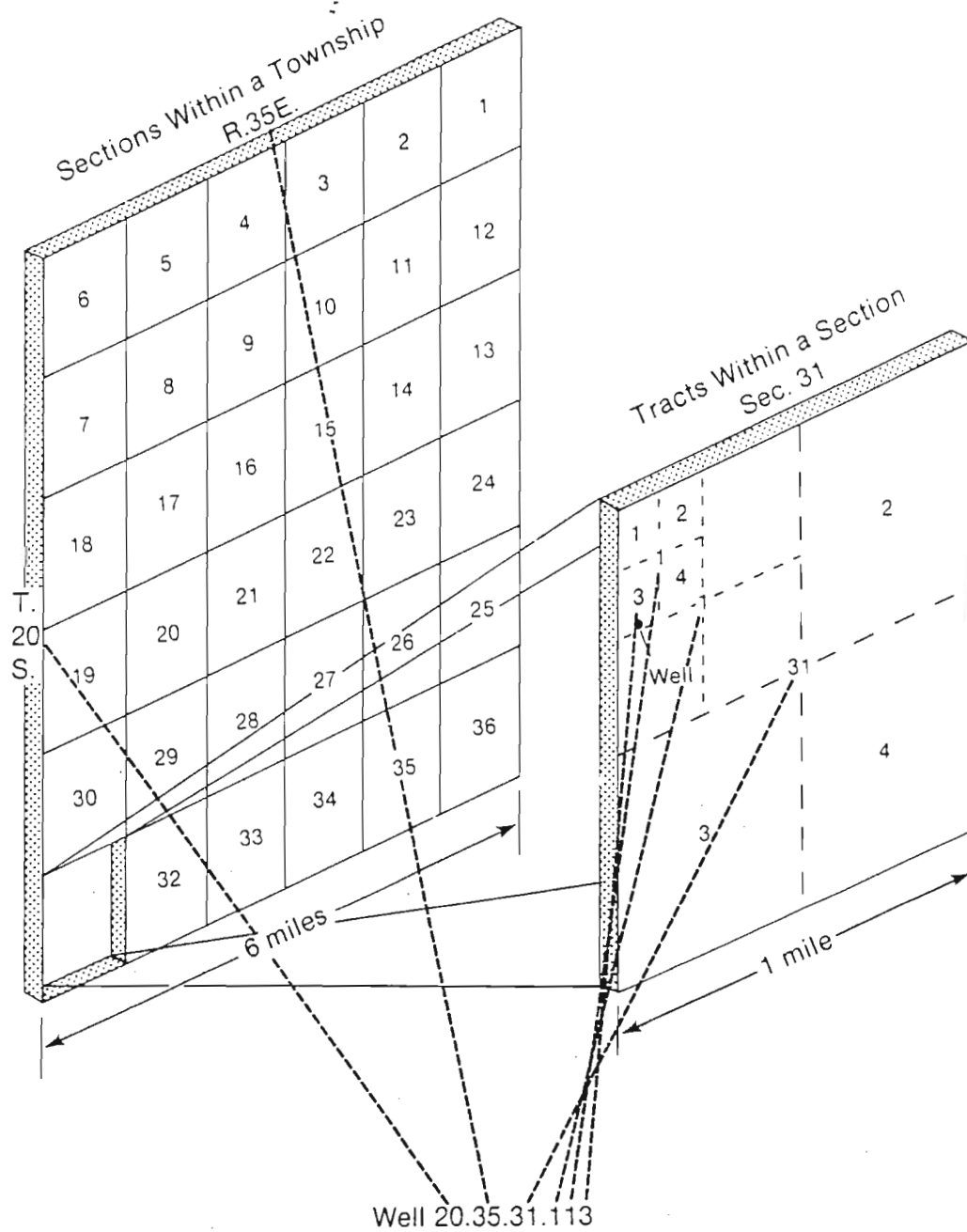


Figure 66.-- System for locating non-WIPP wells.

